ON SINGLE AMPLIFIER IMMITTANCE INVERTERS AND THEIR USE IN ACTIVE FILTER DESIGN

BY

W.T.RAMSEY

Thesis submitted in fulfilment of the requirements for the Degree of Doctor of Philosophy of the University of London, and Diploma of membership of the Imperial College.

January 1985

Department of Electrical Engineering,
Imperial College of Science and Technology,
University of London, Exhibition Road,
South Kensington, London SW7.

ABSTRACT

Classically, low frequency filters have been realised as a network of lumped element inductors and capacitors inserted between resistive source and load impedances. These LC filters, however, are unsuited to modern microelectronic technology as inductors of suitable value and quality factor cannot be realised in this way. Since microelectronic circuits have very desirable features such as small size and weight, and potential low cost, alternative designs using active units, resistors and capacitors have been advanced. Some important objectives in the design of active-RC filters are to produce circuits whose responses are relatively insensitive to changes in component values, and to reduce the DC power consumption caused by the inclusion of active units. Another objective might be to compensate for the effects of imperfections in the active units used. In this thesis we investigate active-RC filters which achieve the above objects in the following way.

The active-RC filter is designed to simulate a suitably designed LC filter, in such a way that the inherently low sensitivity of the LC network is retained. This is achieved by replacing the inductors in the LC filter by active-RC networks which simulate the inductive impedances. To minimise power consumption in the filter we are concerned with simulated inductance circuits which use a minimum number of active units. Some new networks for simulating a grounded inductance are proposed which contain only a single operational amplifier. A novel way of compensating the active-RC filter for the effects of non-ideal amplifier gain is also presented.

ACKNOWLEDGEMENTS

In particular, I would like to thank the late Dr Saraga for his patient guidance and encouragement during the course of this work, and for his considerable help in the preparation of this thesis. Special mention is also due to Dr D G Haigh for many helpful suggestions and for helping with the completion of the manuscript. Finally, I would like to thank my friends and associates at Imperial College for their advice and guidance.

<u>ABBREVIATIONS</u>

S.I.	-	Simulated Inductor
N.I.C.	-	Negative Impedance Converter
P.I.C.	-	Positive Impedance Converter
F.D.N.R.	-	Frequency Dependent Negative Resistor
S.B.I.	-	Simulated Biquadratic Impedance
S.A.	-	Single Amplifier
S.C.	-	Single Capacitor
C/L	-	Cheng/Lim
O/W	-	Orchard/Wilson
S/L	-	Schmidt/Lee
$L_{(\omega)}$	-	Inductance (frequency dependent)
$Q_{(\omega)}$	-	Quality factor (frequency dependent)
$R_{E(\omega)}$	-	Real Part of Impedance
$I_{M(\omega)}$	-	Imaginary Part of Impedance
w.c.	-	Worst Case
R.H.S.	-	Right Hand Side
F	-	Farads
H	-	Henries
Ω	-	Ohms
$\mho$	-	Mhos
D.C.	-	Direct Current
p	-	Laplace transform
f_T	-	Gain/Bandwidth Product for Amplifier
α	-	Inverse of D.C. gain of Amplifier
μ	-	Amplifier Gain
r.m.s.	-	Root Mean Square
w.r.t.	-	With Respect to

$\frac{dY}{dX}$	-	Derivative of Y w.r.t. X
S_X^Y	-	Relative Sensitivity $\frac{dY}{dX} \cdot \frac{X}{Y}$
f	-	frequency (Hz)
ω	-	frequency (r/s)
Z	-	Impedance
min	-	Minimum Value
max	-	Maximum Value
G_i	-	Conductance Value
R_i	-	Resistance Value
C_i	-	Capacitance Value
L_i	-	Inductance Value

CONTENTS

CHAPTER 1

INTRODUCTION

CHAPTER 2

ACTIVE-RC SIMULATION NETWORKS

CHAPTER 3

SOME NOVEL SIMULATED INDUCTOR CIRCUITS

CHAPTER 4

A STUDY OF SIMULATED INDUCTOR CIRCUIT B

4.1 INTRODUCTION

4.2 EFFECTS OF PASSIVE COMPONENT TOLERANCES

4.2.1 Typical effects of passive component tolerances

4.2.2 Reducing the effects of component tolerances

4.3 EFFECTS OF NON-IDEAL AMPLIFIER GAIN

4.3.1 Typical effects of non-ideal amplifier gain

4.3.2 Expressions for $L(\omega)$

4.3.2.1 Exact expression for $L(\omega)$

4.3.2.2 Approximation for $L(\omega)$

4.3.3 Expressions for $Q(\omega)$

4.3.3.1 Exact expression for $Q(\omega)$

4.3.3.2 Approximation for $Q(\omega)$

4.3.4 Design for improving $Q(\omega)$

4.3.5 Design for obtaining $Q(\omega)_{max}$ at a specified frequency

4.3.5.1 Initial assumptions

4.3.5.2 Outline of design procedure

4.3.6 Some design examples

4.3.6.1 Initial design

4.3.6.2 Improving $L(\omega)$ and $Q(\omega)$ by introducing a larger resistance spread

4.3.6.3 Design for different operating frequencies

4.4 COMBINED EFFECTS OF NON-IDEAL AMPLIFIER GAIN AND COMPONENT TOLERANCES

CHAPTER 5

FILTER DESIGN USING SIMULATED BIQUADRATIC IMPEDANCES

CHAPTER 6

SOME SENSITIVITY FEATURES FOR ACTIVE-RC FILTERS THAT USE SIMULATED BIQUADRATIC IMPEDANCES

CHAPTER 7

EXPERIMENTAL INVESTIGATIONS

CHAPTER I

INTRODUCTION

1.1 PRELIMINARY CONSIDERATIONS

An electrical filter is best defined using the frequency domain description for electrical signals and networks. In this domain a 2-port network is described by its transfer function $T(p)$ which is defined as the ratio of the response of the network measured at one port, and the input excitation at the other port. The response and input excitation can be either current or voltage signals $I(p)$ and $V(p)$ where p is the complex frequency variable. A filter can now be defined as a 2-port network which passes electrical signals in a certain portion of the frequency spectrum and blocks signals in the remainder of the spectrum. By "blocking" we mean that the magnitude response $|T(j\omega)|$ of the filter is approximately zero for that frequency range. In applications that require frequency selective networks, it is usual to first of all determine the transfer function $T(p)$ which meets the particular requirements. The problem, then, is to find a suitable practical filter network that can realise this function.

The classical approach to filter design is to realise the transfer function $T(p)$ by a passive circuit consisting of a network of inductors and capacitors inserted between a resistive source and a resistive load. This type of filter is generally referred to as an LC filter. Due to manufactoring tolerances and ageing , the values of the components in an LC filter will not be exactly equal to the nominal values and this causes the response of the filter to deviate from the required characteristic. LC filters have the feature that the sensitivity of their response to changes in the component values can be low (1) and this makes these circuits particularly attractive in practice.

LC filters, however, are not suited to modern microelectronic technology. Although resistors and capacitors can easily be realised in microelectronic form, inductors of sufficiently high quality factor and inductance value cannot be realised in this way. It is not possible to use networks having resistors and capacitors only because the transfer function of an RC network can have poles only on the negative real p axis, whereas for efficient filter design transfer functions with complex conjugate poles are required. Since microelectronic circuits have very desirable features such as small size and weight, potentially low cost, and increased reliability, alternative approaches to the synthesis of filters have been advanced.

A modern approach to filter design is to realise the transfer function T(p) by an active -RC network; i.e. a network consisting of resistors, capacitors, and active units, namely, operational amplifiers and/or transistors (recently another active unit has been proposed , i.e. , the current conveyor (2,3)). These components are all suited to miniaturisation and microelectronic realisation becomes possible.

Unfortunately, filters realised using active- RC networks were soon found not to possess the good sensitivity properties of their LC predecessors and the sensitivity aspects of the various synthesis methods became a major consideration in deciding the merits of the different methods.

Also, unlike LC filters, active -RC filters require power supplies for the correct operation of the active units. Not only are the active units generally the most expensive components in the filter but the cost of the power supplies can also be an important factor. To reduce these costs it is desirable that the number of active units in the filters is as small as possible.

Another reason for reducing the number of active units is that less heat is dissipated in the filters. The active units generate most of the heat in the active filters and this can affect the response. When the filter is built as a discrete component model the heat generated can easily be dissipated into the surroundings and the behaviour of the filter is not much affected. However, when the filter is realised microelectronically, and many of these filters are grouped together, the dissipation of heat becomes a problem. Fans to cool the filters may be required and this increases the overall cost and size.

Many synthesis methods for active -RC filters have appeared in the literature over the years, and a short survey of some of these methods will be presented in sections 1.2 and 1.3. The sensitivity aspects of the various methods, and the number of amplifiers that are required, are considered to be particularly important and will be outlined in the survey. After the survey we will then discuss in detail the approach to filter design taken in this thesis; this is done in Section 1.4. Finally, in Section 1.5, we state our specific aims and give an outline of the thesis.

1.2 SURVEY OF ACTIVE -RC FILTERS

The first general methods proposed for the realisation of active -RC filters were based on the use of only one active unit. Linvill in 1954 (4) showed that any arbitrary transfer function can be realsied using a negative impedance converter (N.I.C.)*, the active unit, embedded between two passive RC two-ports as shown in Fig.1.1. Other synthesis methods using a single active unit have also appeared in the literature, for instance,the methods proposed by Yanagisawa (5) and Mitra (6).

It was soon found, however, that these single active-unit networks were unsuitable for the realisation of high order filters (i.e., of degree > 2 or 3) as the sensitivity of the response of the filter to changes in the component values was found to be very large (7), and the

*An N.I.C. is a 2-port which when terminated at one of the ports in an impedance z gives rise to an impedance -KZ at the other port, where K is a positive constant.

circuits were totally unsuited to practical application. The inability of the single active unit networks to realise practical filters led to the exploration of alternative methods for the synthesis of active-RC filters.

Perhaps the earliest successful approach to the design of active-RC filters that produced filters with acceptable sensitivities was the "cascade method". In this method the required transfer function T(p) is factorised into 2nd order factors which have complex conjugate poles, and a factor containing any real poles that may occur. Each 2nd order factor is realised as the voltage transfer function of an active-RC 2-port, and the factor containing the real poles can in general be realised by a passive RC 2-port. The active -RC filter is then obtained by cascading the individual 2-ports as shown in Fig.1.2. Many active -RC circuits, using a single amplifier, that realise 2nd order sections have been proposed (8) and extensive study has shown that filters can be realised that have sensitivity features acceptable for many applications (9,10,11). Some two-amplifier networks for realising 2nd order sections have also been proposed (12).

Although filters with cascaded sections can have acceptable sensitivity properties, they suffer from the inherent disadvantage that the sensitivity of the filters' responses, to changes in the resonance frequencies of the sections, can be very large, particularly when the required

Q-values for the sections are large. For some specifications the cascade approach to filter design can therefore be unacceptable.

In 1966 Orchard (1) suggested a possible solution to the sensitivity problem in active-RC filter design that has since been found to be very satisfactory. Rather than directly designing the active-RC filter to realise the transfer function T(p) Orchard proposes, instead, designing the active filter from a low sensitivity LC filter having that transfer function. The active filter is obtained by retaining the capacitors and terminating resistors of the LC filter, and using active-RC networks to simulate the inductors. In this way he suggests that it might be possible to obtain an active filter that retains the low sensitivity properties of the original LC filter. Orchard also points out that a suitable LC filter to start from is one whose loss/frequency response, in the passband, contains points at which maximum possible transfer of power takes place from source to load. He shows that, at these frequencies, the 1st order differential sensitivities of the loss to the reactive component values are zero, and he also suggests that these sensitivities are low throughout the passband. Various other simulations methods stemming from Orchard's approach have since been proposed and intensively studied in recent years; a short survey of these simulation methods will be given later in Section 1.3.

Another approach to filter design , which has recently recieved some attention , is the multifeedback method (14,15). In this approach the active - RC filter once again consists of a cascade of 2nd order sections but in addition feedback , and sometimes also feed forward , is applied to the network. In this way it was hoped to overcome the sensitivity problem arising in the cascade method. Multifeedback filters have been intensively studied and the results seem to show that active-RC filters with sensitivities comparable to LC filters can be obtained (16,17,18). The active-RC networks used in the cascade approach for the realisation of the 2nd order sections can be used in this method , however , additional active units may be required to achieve the correct feedback or feedforward although in some cases this is not necessary (18).

One type of multifeedback filter , called the leapfrog feedback filter (14) , has the feature that it can be designed from the signal flow graph of an LC filter. This particular circuit will be discussed in more detail in section 1.3 which deals with the simulation of LC filters.

1.3 SIMULATION OF DOUBLY TERMINATED LC LADDER FILTERS

Many of the simulation methods make use of positive immittance inverter and converter circuits. The properties and definitions of these circuits are first of all described in section 1.3.1 The various simulation methods are then outlined in sections 1.3.2 , 1.3.3 , and 1.3.4.

1.3.1 Positive Immittance Inverters and Converters

1.3.1.1 The positive immittance inverter

The positive immittance inverter (P.I.I.) is a 2-port network which, when terminated at one port in an impedance Z,presents at the other port an impedance K/Z where K is a positive constant and depends only on the 2-port (19). Thus if port 1 is grounded (by "grounded" we mean where one terminal of the port is connected to ground) and port 2 is terminated in a capacitor , the network can simulate a grounded inductor as shown in Fig. 1.3 (a). When both ports 1 and 2 are grounded , two P.I.I.s and a single capacitor may be used to form a floating inductor in the way indicated in Fig. 1.3 (b).

An interesting feature of a P.I.I. network is that its ports 1 and 2 can be relabelled as ports 2 and 1 and a P.I.I. network still results.

1.3.1.2 The positive immittance converter

The positive immittance converter (P.I.C.) is a 2-port network which, when terminated at port 2 in an impedance Z, presents at port 1 and impedance KZ where K depends only on the 2-port network (19). If K is equal to Np, where N is a positive constant and p is the complex frequency variable, and if port 1 is grounded and port 2 is terminated in a resistor, then a grounded inductor is realised as shown in Fig.1.3 (c). When both ports 1 and 2 are grounded, two P.I.C.s (having $K=Np$) and a resistor may be used to form a floating inductor in the way shown in Fig.1.3(d).

P.I.C.s can also be used to obtain frequency dependent negative resistors (F.D.N.R.s) having impedances of the forms D/p^2 and Mp^2 where D and M are positive constants. The D/p^2 type F.D.N.R. is obtained if a resistor is used to terminate port 2 of a P.I.C. having $K = N/p^2$. Alternatively, one can use a P.I.C. having $K = N/p$, which is terminated in a capacitor. To obtain the Mp^2 type F.D.N.R. we can terminate port 2 of a P.I.C.,with $K= Np^2$, in a resistor.

As in the P.I.I. case, ports 1 and 2 of a P.I.C. network can be relabelled as ports 2 and 1 to give a P.I.C. network. This time, however, the parameter K associated with the new network is equal to the inverse of that of the original network.

1.3.2 Filter Design by Inductor Simulation

The first methods proposed for the simulation of LC filters by active RC networks may be classified as inductor simulating methods. This approach consists of simply retaining the resistors and capacitors in the LC filter and using active-RC circuits to simulate the inductors (1,20,21)

Grounded inductors may be simulated by terminating a P.I.I. or a P.I.C. circuit in the ways shown in Figs.1.3(a) and (c). Some simulated inductor circuits of this type, which use P.I.I and P.I.C. networks consisting of two amplifiers and a number of resistors, have been published by

Riordan (22) and Antoniou (23). Some single-amplifier RC circuits for the simulation of grounded inductors have also appeared in the literature (24,25,26,27). Two of these single-amplifier circuits, i.e., the Orchard/Willson circuit (26) and the Schmidt/Lee circuit (27), make use of single-amplifier P.I.I. networks.

To simulate a floating inductor we can again make use of P.I.I. and P.I.C. networks, i.e., in the ways shown in Figs. 1.3(b) and (d)(30). M. Silva ,however , has shown that ports 1 and 2 of a single-amplifier P.I.I. network cannot both be grounded (28) , and these networks are therefore unsuited to the method shown in Fig.1.3(b). Another way to simulate a floating inductor is to use a floating gyrator circuit terminated in a capacitor (29). An example of a simulated floating inductor of a different type is Deboo's circuit (31).

In the above methods the inductors are individually replaced by an active -RC circuit. However, it is also possible to replace the whole inductor subnetwork by an appropriate active -RC network. This approach was proposed by Gorski - Popei who suggested using a multi-terminal P.I.C. network (resistively terminated) to replace the inductor network (32). A similar method, using a multiterminal P.I.I. network, has also been described by Holt and Linggard (33,34).

The inductor simulation method ensures that the capacitors of the active-RC filter corresponding to the capacitors of the original LC filter , will have equally good sensitivities - this is also true for the terminating resistors . However, the components in the active -RC networks used to simulate the original inductors may introduce new sensitivities into the filter that are not present in the original LC filter. Care must therefore be taken that these new sensitivities are acceptably low. In Chapter 2 we will present a survey of the active-RC simulation networks used in the design of active filters. This survey will include the simulated inductance circuits mentioned in this section.

1.3.3 Impedance Scaling Method

Another method of simulating doubly terminated LC ladder filters is the impedance scaling method, proposed originally by Bruton (35,36). This method is based on the fact that the voltage transfer function of a filter, being a nondimensional quantity, is unaffected if the impedances of all the components in the filter are multiplied by the same factor. Consider, for example, the lowpass LC filter shown in Fig.1.4(a). If the impedances in this filter are multiplied by e/p, where e is a positive constant and p is the complex frequency variable, we find that the source and load resistors R_s and R_l become capacitors of value $C_s = 1/eR_s$ and $C_l = 1/eR_l$, the inductors L_i become resistors of value eL_i, and the capacitors C_i become impedances of the form K_i/p^2 where K_i is equal to e/C_i. The new impedances K_i/p^2 are frequently called supercapacitors.

As a result of impedance scaling, the network in Fig.1.4(a) becomes the network in Fig1.4(b) which retains, in principal, the low sensitivity properties of the original LC filter.

The method of impedance scaling by e/p is particularly suited to LC low-pass filters in which all the capacitors are grounded and hence where the remaining sub-network consists solely of inductors. After scaling, the inductive sub-network becomes a resistive network, which is attractive in practice as close tolerance resistors can be used in the design. Also, the impedance scaling method avoids the problem arising in the inductor simulation methods of having to use active -RC circuits to simulate the floating inductors. The grounded capacitors in the LC lowpass filter all become grounded supercapacitors and these can be realised using both single - amplifier and two-amplifier RC networks (35,37,25,27).

Impedance scaling by ep (instead of e/p) is also useful especially in connection with LC networks in which all the inductors are grounded (the remaining sub-network consisting only of capacitors). In this method the capacitors C_i become resistors of value e/C_i, and the grounded inductors L_i are transformed to grounded impedances of the form $M_i p^2$ where $M_i = eL_i$. These new impedances are called superinductors and they can be realised using both single-amplifier and two-amplifier RC networks (35,37,27).

Some details of the F.D.N.R. circuits mentioned in this section will be given later in the survey of simulation networks in chapter 2.

A plausible application of the method of impedance scaling by ep is for LC highpass filters where all the inductors are grounded. The method has the advantage that after impedance scaling the capacitor sub-network becomes a resistive network and close tolerance resistors can be used. However, a drawback of the method is that the terminating resistors of the original LC highpass filter are transformed to inductors and additional active -RC circuits are required to simulate these inductors. This is a disadvantage which does not arise in the impedance scaling by e/p method for LC lowpass filters.

Impedance scaling techniques are also suited to the realisation of active -RC bandpass filters (38,39,40). In one method the original LC bandpass filter is modified so that it consists of a cascade of two sections; one section in which all the capacitors are grounded, and the other section having all its inductors grounded. Appropriate scaling is then applied individually to each section, and the two impedance scaled sections are matched using a suitable type of P.I.C. (38,39).

1.3.4 Resonator Simulation Method

Many LC filters contain series LC resonator circuits. To obtain the active -RC filter one method is to realise these resonator circuits (and their impedance scaled counterparts) by active -RC networks. Some single-amplifier RC resonator circuits have been proposed by Schmidt and Lee (27), and also by Cheng and Lim (41). (their simulation networks will be discussed in more detail in Chapter 2).

1.3.5 Other Approaches

A rather different approach to active filter design has been to represent the relationships between the voltages and currents of the LC filter by a signal flow graph. The variables of the signal flow graph are then regarded as voltages and the relationships between these voltages are realised by suitable active -RC networks. One type of filter which can be considered in this way is the leapfrog feedback filter, proposed originally by Girling and Good (14). It should be mentioned, however, that this filter can also be considered as a multifeedback filter. This method does indeed give rise to active -RC filters that have good sensitivity properties (18). Similar relationships between LC ladder filters and other multifeedback filters have not yet been derived.

Recently other approaches to active-RC filter design have been proposed, namely, the "wave active filter" (42,43,44,45) and the "linear transformation filter" (46, 47) methods. In these methods the voltage and current variables of the original LC filter are transformed to new variables. The active filter is then obtained by realising the relationships between the new variables with suitable active -RC networks, so that the overall transfer function is the same as that of the LC prototype. There is again some evidence that filters having acceptable sensitivity properties can be obtained in this way (43).

1.4 APPROACH USED IN THIS THESIS TO DESIGN ACTIVE-RC FILTERS

The approach to filter design adopted in this thesis is based on the inductor simulation technique described in Section 1.3.2. As mentioned in Section 1.3.2 there are a number of both two-amplifier and single-amplifier RC networks for the simulation of grounded inductors. The particular simulated inductor circuits we will consider, here, are of the type which are obtained by terminating a single-amplifier P.I.I. network in a capacitor, e.g., the Orchard/Willson circuit (26) and the Schmidt/Lee circuit (27). Simulated inductors of this type have the interesting feature that they use the minimum number of amplifiers and capacitors (i.e, 1 amplifier and 1 capacitor) needed for inductor simulation. The Orchard/Willson circuit and Schmidt/Lee circuit are described in detail in Chapter 2 (Chapter 2 also contains descriptions of other S.I. circuits). In Chapter 3 we will present some novel S.I. circuits that are similar to the above circuits in that they also contain only 1 amplifier and 1 capacitor, and can be regarded as single-amplifier P.I.I.s that have been terminated in a capacitor. Henceforward we will refer to simulated inductors of this type as S.A. S.C. S.I.s.

As single-amplifier P.I.I. networks are unsuited to floating inductor simulation (28) we will be concerned only with the active -RC realisation of LC filters in which all the inductors are grounded. This restriction seems at first to be rather severe , however , all highpass filters and a wide range of bandpass filters are still realisable. Examples of these highpass and bandpass filters are shown in Figs. 1.5 (a) to (d), alongwith their typical loss/frequency behaviour. LC lowpass filters require floating inductors , and cannot therefore be simulated using the approach described in this section.

1.5 SPECIFIC AIMS AND OUTLINE OF THESIS

There are two main purposes of this thesis. One is to present some new single-amplifier , single-capacitor , resistor networks for the simulation of a grounded lossless inductor. The other purpose is to present a study of S.I.s of this type (i.e., 1A and 1C) , and also to present a study of active-RC filters that use these S.I. circuits (see section 1.4). In particular we will describe a completely novel approach to compensation for the effects of the finite gainbandwidth products of the amplifiers on the response of active-RC filters that use single-amplifier, single-capacitor , S.I.s. A detailed outline of the thesis follows.

We begin in chapter 2 with a survey of known active-RC simulation networks. This survey includes the S.A. S.C. S.I. circuit due to Orchard and Willson (26) , and the other known circuit of this type due to Schmidt and Lee (27). As general background the survey also covers other S.I. circuits and circuits which realise impedances of the form K/p^2 , Mp^2 , $R + K/p^2$,and $pL + 1/pC$.

The new simulated inductor circuits are described in chapter 3. In common with other S.A. S.C. S.I.s the new circuits rely on precise relationships between their component values in order to achieve the simulation of a lossless inductor. Deviations of the actual component values from the nominal values cause these relationships not to be satisfied exactly and the simulation is not accurate. A model for evaluating the effects of component tolerances on the impedance of the S.I.s is presented. We also present a model for evaluating the effects of the finite gainbandwidth product of the amplifier on the impedance of the S.I.s.

In chapter 4 we present a detailed investigation of one of the new S.I. circuits proposed in chapter 3. We will show how to design this circuit so that the effects of component manufacturing tolerances on the impedance are reduced. We also derive expressions for the inductance $L(\omega)$ and Q-factor $Q(\omega)$ behaviour when the finite gainbandwidth product of the amplifier is taken into consideration. A design procedure for improving the $Q(\omega)$ behaviour will be presented. The $L(\omega)$ and improved $Q(\omega)$ behaviour is then compared with that for two other S.I. circuits , i.e. , Orchard and Willsons' circuit (26) , and Antoniou's two-amplifier S.I. circuit (23). The sensitivities of $L(\omega)$ and $Q(\omega)$ to changes in the component values for the new circuit are also investigated and compared with the sensitivities for the other S.I. circuits.

In chapter 5 we describe a completely novel compensation procedure for overcoming the effects of the finite gainbandwidth of the amplifiers in active-RC filters that contain S.A. S.C. S.I. circuits.In contrast to conventional compensation methods the new procedure does not seek to improve the inductance and Q-factor behaviour of the S.I. circuits , but deliberately designs the simulating networks to have a specific biquadratic impedance function. We then choose an LC filter circuit which can be modified by appropriate transformations so that it produces the required loss/frequency response (apart from an increased basic loss in the highpass filter case) using these biquadratic impedances instead of the original inductors. In this way we can compensate for the effects of the finite gainbandwidth products of the amplifiers - indeed , in the case of highpass filters complete compensation for finite f_T can be obtained over the entire frequency range in which the non-ideal gain of the amplifiers can be adequately described by a single-pole model. The simulated biquadratic impedances required in the new compensation method have been called S.B.I. circuits to distinguish them from S.I. circuits designed using conventional approaches. Design procedures for some S.B.I. circuits will also be presented in chapter 5.

Chapter 6 is concerned with the sensitivity properties of the compensated active-RC filters described in chapter 5. The active filters which use S.B.I.

circuits are designed from original LC filters that have parallel RC terminations instead of purely resistive terminations. The sensitivity properties of LC filters with parallel RC terminations are investigated and compared with those for resistively terminated LC filters. We also investigate the effects of variations in f_T on the impedance of S.B.I. circuits.

Chapter 7 contains the computational and experimental work of the thesis. Various filter examples , highpass and bandpass , have been studied and their computed and measured loss/frequency responses will be given. Functional adjustment procedures for overcoming the effects of component manufacturing tolerances on the response of the filters are presented. We also show how the response of each filter changes when the component values for the filter change.

Finally in chapter 8 we conclude with a summary of the work presented in this thesis and some conclusions are made concerning the practical feasibility of active-RC filters that use S.A. S.C. S.I.s. A recent and very interesting S.A. S.C. S.I. circuit , discovered by the author , is also presented and some suggestions for further work are made. Some of the results of the work presented in this thesis have been published previously by the author (59, 60).

CHAPTER 2

ACTIVE-RC SIMULATION NETWORKS

2.1 INTRODUCTION

In this chapter we make a survey of the active-RC networks that are available for simulating grounded impedances of the form pL , K/p^2 , Mp^2 , $R + K/p^2$, and $pL + 1/pC$. The survey is mainly concerned with simulation networks that have only one amplifier (the theoretical minimum) , however , some two-amplifier circuits will also be described so that we can compare the various single-amplifier circuits with their two-amplifier counterparts.

In general,manufacturing , ageing , and environmental tolerances on the values of the passive components in the circuits give rise to inexact simulation. The passive sensitivity properties of the networks will therefore be discussed in the survey. A possible way of overcoming the problem of manufacturing tolerances is to adjust the values of the resistors in the simulation network (capacitance adjustment is not feasible) until the correct impedance is obtained. The suitability of the networks to adjustment procedures will also be discussed.

Even if we assume the passive component values to be exact , the impedance of the active-RC simulation networks will still be affected by the non-ideal behaviour of the amplifiers. One amplifier imperfection , in particular , is the non-ideal voltage gain μ . Ideally μ should be infinite at all frequencies but in practice it is finite and becomes less as the frequency of operation is increased. Also , the phase difference between the output voltage of the amplifier and the differential input voltage is approximately 90^{o} except at very low frequencies. A simple expression for the gain of the amplifier is:

$$\mu = \frac{1}{\alpha + p/\omega_T}$$

where α = inverse of the D.C. gain

ω_T = finite gainbandwidth product (r/s)

The effects of non-ideal amplifier gain on the impedance of some of the simulation networks will be discussed in the survey.

2.2 CIRCUITS WHICH SIMULATE GROUNDED INDUCTORS

2.2.1 Two-amplifier Circuit

An example of a two-amplifier simulated inductor, due to Antoniou (23), is shown in Fig.2.1. This circuit can be regarded as either a P.I.I. or a p-type P.I.C. network having port 2 suitably terminated , see Figs. 1.3 (a) and (c).

Considering the amplifiers to be ideal,the impedance of the circuit is given by the expression

$$Z_{IND} = pL = \frac{pC_oR_1R_3R_4}{R_2} \qquad (2.1)$$

The expression in (2.1) shows that this S.I. circuit retains its inductance behaviour with arbitrary positive values for its components. Furthermore, a relative change in the value of each component, taken individually, gives rise to the same relative change in either the value of L or 1/L. Since the loss/frequency response of an LC filter can have low sensitivities to the inductance values , we conclude that active-RC filters with equally low sensitivities can be obtained using this S.I. circuit.

To take into consideration the non-ideal behaviour of the amplifiers in the S.I. the general procedure is to represent the circuit's non-ideal impedance as the series combination of a resistance $R(\omega)$ and an inductance $L(\omega)$,i.e.,

$$Z_{IND} = R(\omega) + pL(\omega)$$

The performance of the non-ideal S.I. is then measured in terms of the inductance $L(\omega)$ and the Q-factor $Q(\omega)$ which is defined as

$$Q(\omega) = \frac{\omega L(\omega)}{R(\omega)}$$

Ideally the Q-factor should be infinite at all frequencies and the inductance constant with frequency. However, in practice the non-ideal gain of the amplifiers cause the Q-factor to have finite values and become frequency dependent - $L(\omega)$ also becomes frequency dependent. Bruton has shown how to design the S.I. circuit so that the Q-factor behaviour is improved (49) ; some work on additionally improving $L(\omega)$ has also been described by Haigh and Kunes (50).

Because of manufacturing tolerances on the values of the components in the circuit, the inductance value will not be exactly equal to the specified value and the Q-factor will not have its nominal behaviour. The circuit is particularly suited to resistor adjustments for overcoming both these problems (37) and a wide tolerance capacitor can be used in the design. Furthermore, the adjustment procedure is well suited to microelectonic technology in which the values of the adjusting resistors can only be increased.

The properties of the circuit mentioned above make it particularly attractive for practical filter design. Perhaps the only disadvantage of the circuit is that it uses two amplifiers which is not the minimum required for inductor simulation.

2.2.2 Saraga Circuit

A circuit which simulates a grounded inductor using only one amplifier is shown in Fig.2.2. This circuit is due to Saraga (25) and was derived using his synthesis procedure for active -RC impedances (51). Although the circuit uses only one amplifier, three capacitors are required compared to one in the Antoniou circuit. Furthermore the circuit cannot be regarded as a P.I.I. or P.I.C. which has been suitably terminated.

Assuming the amplifier to be ideal, the impedance of the circuit in Fig.2.2 can be expressed as a biquadratic impedance function in p, the complex frequency variable, as shown in (2.2) (this is somewhat unusual as we would expect the circuit to have a 3rd order impedance function in p as it contains 3 capacitors).

$$Z_{IND} = \frac{A_0 + A_1 p + A_2 p^2}{B_0 + B_1 p + B_2 p^2} \qquad (2.2)$$

where

$$A_0 = R_3R_5 - R_4R_1$$

$$A_1 = R_1R_3(R_5C_2 - R_4C_3) - R_1R_4R_5C_6$$

$$A_2 = -C_6C_3R_1R_4R_5R_3$$

$$B_0 = -R_4$$

$$B_1 = R_3(R_5C_2 - R_4C_3) - R_1R_4C_6$$

$$B_2 = C_6R_1R_3(R_5C_2 - R_4C_3)$$

To obtain lossless inductor simulation with this circuit the conditions

$$A_0 = 0 \quad ; \quad B_2 = 0 \tag{2.3}$$

must first of all be satisfied* so that Z_{IND} can be expressed as

$$Z_{IND} = \frac{pA_1(1 + pA_2/A_1)}{B_0(1 + pB_1/B_0)} \tag{2.4}$$

The correct simulation is then obtained by choosing

$$\frac{A_2}{A_1} = \frac{B_1}{B_0} \; ; \qquad \frac{A_1}{B_0} > 0 \tag{2.5}$$

so that a pole and a zero of the impedance expression in (2.4) cancel and Z_{IND} has the impedance of a <u>positive</u> inductor. One way to satisfy the conditions in (2.3) and (2.5) is to choose

$$\frac{R_4}{R_5} = \frac{C_2}{C_3} \; ; \quad \frac{R_3}{R_1} = \frac{C_6}{C_3} \; ; \quad \text{and } C_6 = C_2 \tag{2.6}$$

The inductance value L is then given by

$$L = R_3R_5C_3 \tag{2.7}$$

The method of obtaining inductor simulation with this circuit is very different to that for the Antoniou

---

* It is worth mentioning that Saraga uses a direct synthesis method (51).

circuit and relies not only on coefficient cancellations, i.e., see (2.3), but also on a pole/zero cancellation in the expression for its impedance. Small errors in the component values give rise to inexact coefficient and pole/zero cancellations and the simulation becomes inexact. Not only will these errors affect the constancy of the inductance value with frequency but the Q factor will also be affected even when the amplifier is assumed to be ideal; we will find later on in the survey that this is also true for other single-amplifier S.I.s. We would expect active filters using Saraga's S.I. circuit to have worse passive sensitivities than for filters using Antoniou's two-amplifier S.I. circuit. This is because tolerances on the component values for Antoniou's circuit affect only the inductance value, and not the Q-factor.

A way of overcoming the problems due to manufacturing errors in the component values is to adjust the values of the resistors in the circuit so that the conditions for lossless inductor simulation are satisfied. The first two conditions in (2.6) and the inductance value condition in (2.7) can be satisfied by resistor adjustment even if wide tolerance capacitors are used. However, the condition $C_6=C_2$ given in (2.6) requires capacitor adjustment and this is not feasible nowadays. Nevertheless, Saraga has shown that the effects of errors in the condition $C_6=C_2$ can be reduced if the ratio $\beta = R_5/R_1 = R_4/R_3$ is made large (25). The effect of amplifier imperfections upon the impedance of the circuit has not yet been investigated.

2.2.3 Sipress circuit

A single-amplifier S.I. circuit that uses two capacitors is shown in Fig. 2.3. The circuit is due to Sipress,and it was derived using his driving point synthesis method which uses a single N.I.C. as the active unit (24). The circuit is similar to Saraga's S.I. circuit in that it cannot be regarded as a P.I.I. or a P.I.C. network having port 2 terminated in the ways shown in Figs.1.3(a) and (c).

Assuming the amplifier to be ideal,the impedance of Sipress' S.I. circuit is given by the expression

$$Z_{IND} = \frac{A_0 + A_1 p + A_2 p^2}{B_0 + B_1 p + B_2 p^2} \tag{2.8}$$

where

$$A_0 = G_4 G_6 R_5 - G_2(1 + G_4 R_3)$$

$$A_1 = C_2(G_6 R_5 - G_2 R_3) + C_1(G_4 G_6 R_1 R_5 - G_2 G_4 R_1 R_3 - G_4 R_3 - G_2 R_1 - 1)$$

$$A_2 = C_1 C_2(G_6 R_1 R_5 - G_2 R_1 R_3 - R_3)$$

$$B_0 = -G_2$$

$$B_1 = C_2(G_4 G_6 R_5 - G_2 G_4 R_3) - C_1(G_2 G_4 R_3 + G_2 G_4 R_1 + G_2)$$

$$B_2 = C_1 C_2(G_4 G_6 R_1 R_5 - G_2 G_4 R_1 R_3 + G_6 R_5 - G_2 R_3 - G_4 R_3)$$

and $G_i = 1/R_i \qquad i = 1, \ldots 6$

Inductor simulation is achieved with this circuit in exactly the same way as for the Saraga circuit. That is, two coefficient cancellations $A_0 = 0$ and $B_2 = 0$ are first of all needed. The condition $A_2/A_1 = B_1/B_0$ is then required so that a pole and a zero of the impedance expression cancel, and finally we require $A_1/B_0 > 0$ so that positive inductor simulation occurs. One set of component values which satisfies these conditions and gives rise to an inductance value of 1.0 H is: $R_1 = R_3 = R_4 = 2\Omega$, $R_5 = R_6 = 1\Omega$, $R_2 = 4\Omega$, $C_1 = 0.125$ F and $C_2 = 0.25$ F.

Because the Sipress and the Saraga S.I. circuits both have 2nd order impedance functions (in p) and achieve inductor simulation in the same way, we would expect the sensitivity properties of the Sipress circuit to be similiar to those for the Saraga circuit. This is interesting because the Saraga circuit uses three capacitors compared to two for the Sipress circuit. A detailed comparison of the sensitivity properties of both circuits is, however, outside the scope of this thesis. Adjustment procedures for overcoming the effects of manufacturing tolerances on the impedance of the Sipress circuit, and an analysis of the effects of amplifier imperfections, have not appeared in the literature.

2.2.4 Orchard/Willson Circuit

An example of a single-amplifier S.I. which uses only one capacitor is shown in Fig.2.4. The circuit is due to Orchard and Willson and was the first circuit of its type to be published (2.6). Although Orchard and Willson do not indicate how the circuit was derived, it is understood from their publication that a sequence of such circuits was found that culminated in the circuit of Fig.2.4. The circuit uses the theoretical minimum number of amplifiers and capacitors, and it can be regarded as a single-amplifier P.I.I. network with port 2 terminated in the capacitor C_0.

Assuming the amplifier to be ideal, the impedance of the circuit can be expressed as a bilinear function in p, i.e.,

$$Z_{IND} = \frac{A_0 + A_1 p}{B_0 + B_1 p} \qquad (2.9)$$

where

$$\begin{aligned}
A_0 &= G_4 G_6 R_1 R_5 - (1 + R_1 G_2)(1 + R_3 G_4) \\
A_1 &= C_0 (G_6 R_1 R_5 - G_2 R_1 R_3 - R_3) \\
B_0 &= G_4 G_6 R_5 - G_2 (1 + R_3 G_4) \\
B_1 &= C_0 (A_0 + 1 - R_3 G_2)
\end{aligned} \qquad (2.10)$$

and $G_i = 1/R_i \quad i = 1, \ldots 6$

The impedance Z_{IND} will be that of an ideal positive inductance if

$$A_0 = 0 \ , \ B_1 = 0 \ , \text{ and } A_1/B_0 > 0 \qquad (2.11)$$

The conditions in (2.11) are satisfied by choosing

$$G_4G_6R_1R_5 = (1 + R_1G_2)(1 + R_3G_4) \qquad (2.12)$$

and $R_2 = R_3$

The inductance value L is then given by the expression

$$L = \frac{R_1R_4C_0(1 + G_2R_1)}{(1 + G_4R_3)}$$

One set of resistance values that satisfies the conditions in (2.11) to give $L = 4C_0$ is : $R_1 = R_2 = R_3 = R_4 = 2\,\Omega$, $R_5 = 4\,\Omega$, and $R_6 = 1\,\Omega$.

The circuit achieves inductor simulation by means of two coefficient cancellations and is unlike both the Saraga and Sipress circuits which additionally require a pole/zero cancellation. Small errors in the resistance values in the circuit give rise to inexact cancellations and both the Q-factor and inductance value are affected. One would therefore expect active-RC filters containing the S.I. circuit to have worse passive component sensitivities than filters using Antoniou's S.I. circuit, however, the sensitivities may be better than those obtained by using the Saraga and Sipress S.I. circuits as fewer cancellations are required to achieve the correct simulation of inductance. This conjecture will have to be left unstudied as a detailed investigation of the sensitivity properties of the various simulation networks is outside the scope of the thesis.

Orchard and Willson have investigated the effects of non-ideal amplifier gain on the impedance of their circuit and they have suggested a design procedure for improving its non-ideal performance (26) (some computed inductance and Q-factor curves showing this performance will be given later on in the thesis). An adjustment procedure for overcoming the effects of component manufacturing tolerances on the impedance has not been proposed.

2.2.5 Schmidt and Lee Circuit

Another example of a single - amplifier, single-capacitor, S.I., which was obtained by Schmidt and Lee using their multipurpose simulation network (27), is shown in Fig.2.5. This circuit uses seven resistors (compared to six for the Orchard/Willson circuit) and can be regarded as a P.I.I. network having port 2 terminated in a capacitor.

Assuming the amplifier to be ideal, the impedance of the circuit in Fig.2.5 can be expressed as

$$Z_{IND} = \frac{A_0 + A_1 p}{B_0 + B_1 p} \qquad (2.13)$$

where

$$A_0 = G_2(G_3G_6 - G_4G_5 - G_1G_4)$$

$$A_1 = C_0(G_2G_3 + G_3G_6 - G_4G_5 - G_1G_4)$$

$$B_0 = G_2G_6(G_1G_3 + G_1G_7 + G_3G_7) - G_2G_4G_5(G_1 + G_7)$$

$$B_1 = C_0 \begin{Bmatrix} G_6(G_1G_3 + G_1G_7 + G_3G_7 + G_2G_3) - \\ G_5(G_1G_4 + G_4G_7 + G_2G_4 + G_2G_7) \end{Bmatrix}$$

and $G_i = 1/R_i$

The circuit achieves inductor simulation in the same way as the Orchard/Willson circuit; that is by means of two coefficient cancellations $A_0 = 0$ and $B_1 = 0$, and by ensuring $A_1/B_0 > 0$ so that a positive inductance is realised. We would therefore expect the sensitivities properties for both these circuits to be similar. Adjustment procedures for overcoming the effects of component manufacturing tolerances on the impedance , and the effects of amplifier imperfections on the impedance of the Schmidt/Lee S.I. circuit, have not yet been investigated.

2.2.6 Imperfect (lossy) Inductor Simulation

Some examples of lossy inductor simulation are shown in Fig. 2.6 (a),(b), and (c). The circuit in Fig. 2.6(a) is due to Ford and Girling (52), the circuit in Fig.2.6(b) is due to Prescott (53), and the circuit in Fig.2.6(c) is due to D. Berndt and S.C.Dutta Roy (54).

Assuming the amplifier to be ideal, the impedance of the circuit in Fig.2.6(a) is

$$Z = \frac{pC_1R_2R_3}{1 + pC_1(R_2 + R_3)} \tag{2.14}$$

which is the impedance of an ideal inductor in parallel with a resistor. The impedance of the circuit in Fig.2.6(b) is given by

$$Z = R_2 + R_3 + pC_1R_2R_3 \tag{2.15}$$

which is the impedance of an ideal inductor in series with a resistor as shown in Fig.2.6(b). The Berndt/Dutta Roy circuit has an impedance

$$Z = \frac{R_2 + pC_0R_1R_2}{1 + pC_0R_2} \tag{2.16}$$

and its equivalent circuit is shown in Fig.2.6(c).

The expressions in (2.14), (2.15) and (2.16) show that the impedances of the circuits do not depend upon coefficient cancellations. However, the circuits are not suitable for incorporation into conventional LC filters where lossless inductors are required. Instead, specially designed filters called "lossy ladder filters", which have worse sensitivity properties than LC ladder filters, have to be used. Nevertheless, Rollett has shown that good performance can still be achieved , and that in some cases the active-RC lossy ladder filters can be significantly less sensitive than cascade filters (55).

2.3 CIRCUITS WHICH SIMULATE GROUNDED F.D.N.Rs

In this section we describe some two-amplifier and single-amplifier networks for the realisation of grounded F.D.N.Rs , i.e. , impedances of the form Mp^2 and K/p^2 . All the single-amplifier circuits make use of coefficient cancellations in their impedance expressions to achieve the correct impedance (one circuit , the Saraga K/p^2 circuit , additionally requires a pole/zero cancellation) . In this respect these circuits are similar to the single-amplifier S.I. circuits described previously.

2.3.1 Two-amplifier F.D.N.R. circuits

Examples of two-amplifier F.D.N.R. circuits for the realisation of K/p^2 and Mp^2 impedances are shown in Figs. 2.7 (a) and (b) alongwith their impedance expressions . These circuits have the same network topology as the two-amplifier S.I. circuit described in section 2.2.1 , and they also have the same good sensitivity properties. Adjustment procedures have been developed for the circuits to overcome the effects of both component manufacturing tolerances and the finite f_T of the amplifiers on their impedances (37). Large tolerance capacitors can be used in the design of the circuits , and they are well suited to microelectronic technology (56).

2.3.2 Saraga Circuit (K/p^2)

A circuit which simulates a K/p^2 type impedance using one amplifier and three capacitors is shown in Fig.2.8. The circuit is due to Saraga (25) and was derived using his synthesis procedure given in (51).

Assuming the amplifier to be ideal, the impedance of the circuit in Fig.2.8 is

$$Z = \frac{A_0 + A_1 p + A_2 p^2}{p(B_1 + B_2 p + B_3 p^2)} \tag{2.17}$$

where

$$A_0 = R_5$$

$$A_1 = R_1R_5C_2 + R_3R_5C_3 - R_1R_4C_3$$

$$A_2 = C_2C_3R_3R_1R_5 - C_3C_6R_1R_4R_5$$

$$B_1 = C_2R_5 - C_3R_4$$

$$B_2 = C_2C_3R_3R_5 + C_6C_2R_1R_5 - C_6C_3R_1R_4$$

$$B_3 = C_2C_3C_6R_1R_3R_5$$

An impedance of the form K/p^2 is achieved by first of all satisfying the conditions $A_2 = 0$ and $B_1 = 0$ so that Z becomes

$$Z = \frac{A_0(1 + pA_1/A_0)}{p^2 B_2(1 + pB_3/B_2)} \tag{2.18}$$

The condition $A_1/A_0 = B_3/B_2$ is then required so that a pole and a zero of the expression in (2.18) cancel, and finally K will be positive if $A_0/B_2 > 0$.

The circuit achieves the correct impedance in the same way as the Saraga and Sipress S.I. circuits achieve lossless inductor simualtion, that is, by means of two coefficient cancellations and one pole/zero cancellation. We would therefore expect the sensitivity properties of the present circuit to be similar to those for the S.I. circuits mentioned. Some detailed work on the sensitivity properties of this circuit, and its performance when the non-ideal behaviour of the amplifier is taken into consideration, has been carried out by Hooshvar (57).

2.3.3 Schmidt/Lee Circuit (K/p^2)

The multipurpose simulation network mentioned in Section 2.2.5 can also be used to obtain a circuit that has an impedance of the form K/p^2. This circuit is shown in Fig.2.9 and it has the interesting feature that it contains only one amplifier and two capacitors (the theoretical minimum).

Assuming the amplifier to be ideal, the impedance of the circuit in Fig. 2.9 is

$$Z = \frac{A_0 + A_1 p}{B_0 + B_1 p + B_2 p^2} \qquad (2.19)$$

where

$$A_0 = G_3(G_2 + G_6) - G_4G_5$$

$$A_1 = C_3(G_2 + G_6) - C_1G_4$$

$$B_0 = G_2G_3G_6 + G_2G_3G_8 + G_3G_6G_8 - G_2G_4G_5 - G_4G_5G_8$$

$$B_1 = C_1(G_3G_6 - G_4G_5 - G_4G_8) + C_3(G_2G_6 + G_2G_8 + G_6G_8)$$

$$B_2 = C_1C_3G_6$$

and $G_i = 1/R_i$.

To obtain the impedance $Z = K/p^2$ the coefficient cancellations $A_1 = 0$, $B_0 = 0$, $B_1 = 0$, are required and for K to be positive we need $A_0/B_2 > 0$. The Schmidt/Lee K/p^2 circuit therefore requires three coefficient cancellations to achieve the correct impedance , and differs from the Saraga circuit which requires two coefficient cancellations and one pole/zero cancellation. Some work on a comparision of the sensitivity properties of both these circuits has been carried out by Hooshvar (57) - it appears that the sensitivities of the F.D.N.R. constant K to the passive component values are similar for both circuits , also , the Q-factor sensitivities ($Q \equiv R_e(Z)/I_m(Z)$) are similar for both circuits.

2.3.4 Schmidt/Lee circuit (Mp^2)

Schmidt and Lee have also used their multipurpose simulation network (27) to realise an ideal superinductor - this circuit is shown in Fig. 2.10. The circuit uses the theoretical minimum number of amplifiers and capacitors , i.e. , 1A and 2 Cs.

Assuming the amplifier to be ideal,the impedance of the circuit can be expressed as:

$$Z = \frac{A_0 + A_1 p + A_2 p^2}{B_0 + B_1 p + B_2 p^2} \tag{2.20}$$

where

$$A_0 = G_1G_3(G_6G_7 - G_4G_5) - G_3G_4(G_5G_7 + G_1G_8 + G_5G_8)$$

$$\begin{aligned} A_1 = {} & C_3(G_3G_6G_8 + G_1G_3G_6 + G_1G_6G_7 + G_3G_6G_7) \\ & -C_3(G_1G_4G_8 + G_4G_5G_8 + G_1G_4G_5 + G_4G_5G_7) \\ & -C_2(G_3G_4G_5 + G_3G_5G_7) \end{aligned}$$

$$A_2 = C_2C_3(G_3G_8 + G_3G_6 - G_4G_5 - G_5G_7)$$

$$B_0 = G_3G_8(G_1G_6G_7 - G_1G_4G_5 - G_4G_5G_7)$$

$$\begin{aligned} B_1 = {} & C_3G_8(G_1G_3G_6 + G_1G_6G_7 + G_3G_6G_7 - G_4G_5G_7 - G_1G_4G_5) \\ & -C_2G_3G_5G_8(G_4 + G_7) \end{aligned}$$

$$B_2 = C_2C_3G_8(G_3G_6 - G_4G_5 - G_5G_7)$$

and $G_i = 1/R_i$

The circuit has the impedance of a positive ideal superinductor , i.e. $Z = Mp^2$, if $A_0 = 0$, $A_1 = 0$, $B_1 = 0$, $B_2 = 0$, and $A_2/B_0 > 0$. One set of component values which satisfy these conditions to give $M = 3C_3^2$ is: $R_1 = R_4 = R_5 = R_7 = 1\,\Omega$, $R_3 = 2\,\Omega$, $R_6 = \frac{1}{4}\,\Omega$, $R_8 = 1\,\Omega$, and $C_2 = 6C_3$.

A sensitivity study for the Schmidt/Lee Mp^2 circuit has not been carried out but we would expect the sensitivity properties to be bad as four coefficient cancellations are required in the impedance expression. Other single-amplifier circuits for the realisation of superinductors have not appeared in the literature.

2.3.5 Imperfect F.D.N.R. simulation

Some active-RC networks that simulate imperfect F.D.N.R.s are shown in Figs. 2.11 (a) and (b) alongwith their equivalent circuits. The networks were derived from the lossy inductor circuits shown in Figs. 2.6 (a) and (b) merely by an RC-CR interchange (this transformation converts a p type impedance into a $1/p^2$ type impedance). The imperfect F.D.N.R.s can be used in filter design in a way similar to that described in section 2.2.6 for lossy inductors.

2.4 SIMULATED RESONATOR CIRCUITS

As mentioned in Chapter 1 , many LC filters have grounded inductors in series with a resonating capacitor. Similarly grounded F.D.N.R. circuits often occur in filters in series with a resonating resistor. Some single-amplifier RC networks simulating these grounded resonators will now be described.

2.4.1 Cheng/Lim circuit ($z = pL + 1/pC$)

A circuit , due to Cheng and Lim (41) , which simulates a series LC shunt branch for use in an LC ladder filter, is shown in Fig. 2.12 . The circuit uses one amplifier and two capacitors which is the theoretical minimum.

Assuming the amplifier to be ideal the impedance of the circuit is

$$Z = \frac{A_0 + A_1 p + A_2 p^2}{B_1 p} \tag{2.21}$$

where

$$A_0 = G_2 G_3 (G_5 + G_7)$$

$$A_1 = C_6 G_3 (G_2 + G_5) + C_4 (G_2 G_3 + G_2 G_7 - G_1 G_5) + C_4 G_2 G_3 R_4 (G_5 + G_7) + C_4 G_2 G_7 R_8 (G_1 + G_3)$$

$$A_2 = C_4 C_6 G_3 R_4 (G_2 + G_5)$$

$$B_1 = C_4 G_2 G_7 (G_1 + G_3) \qquad \text{note : } G_i = 1/R_i$$

The correct simulation of a series LC resonator , whose impedance is $Z = pL + 1/pC$, is achieved by first of all satisfying the condition $A_1 = 0$ so that Z in (2.21) becomes

$$Z = \frac{A_0(1 + p^2A_2/A_0)}{B_1p}$$

The further conditions $B_1/A_0 > 0$ and $A_2/A_0 > 0$ are then required to ensure that the simulated inductance and capacitance values are positive.

The simulated resonator circuit described above is very interesting as it requires only one coefficient cancellation for correct simulation compared to other circuits such as the Orchard/Willson S.I. circuit and the Schmidt/Lee S.I. circuit which require two coefficient cancellations. We would expect this circuit to give rise to active-RC filters with better sensitivity properties than filters which used other single-amplifier simulation networks. However , we would still not expect to obtain sensitivities as good as those for the two-amplifier simulation networks mentioned in previous sections.

Cheng and Lim have proposed an adjustment procedure for their simulated resonator circuit for overcoming the effects of component manufacturing tolerances on the impedance (41). They have also shown how to choose the nominal component values for the circuit so that the effects of the non-ideal gain of the amplifier on the impedance are minimised.

2.4.2 Schmidt and Lee circuit ($Z = R + K/p^2$)

A circuit which realises the impedance of a grounded F.D.N.R. (K/p^2 type) in series with a resonating resistor , is shown in Fig. 2.13. This circuit is due to Schmidt and Lee (27) , and it uses the theoretical minimum number of amplifiers and capacitors.

Assuming the amplifier to be ideal the impedance of the circuit is

$$Z = \frac{A_0 + A_1 p + A_2 p^2}{B_1 p + B_2 p^2} \tag{2.22}$$

where

$$A_0 = G_2 G_3 G_4$$

$$A_1 = C_6 G_3 G_4 + C_4 (G_2 G_3 - G_1 G_4 - G_4 G_5)$$

$$A_2 = C_4 C_6 G_3$$

$$B_1 = C_6 G_3 G_4 (G_1 + G_2) - C_4 G_4 G_5 (G_1 + G_2)$$

$$B_2 = C_4 C_6 G_3 G_4 (G_1 + G_2) \qquad \text{note } G_i = 1/R_i$$

To obtain an impedance $Z = R + K/p^2$ we need two coefficient cancellations $A_1 = 0$ and $B_1 = 0$ so that Z in (2.22) becomes

$$Z = \frac{A_0 + p^2 A_2}{p^2 B_2}$$

The values for R and K are given by the ratios A_2/B_2 and A_0/B_2 respectively - obviously these ratios must be greater than 0 so that R and K are positive.

2.4.3 Cheng/Lim circuit ($R + K/p^2$)

An alternate circuit for the realisation of a series F.D.N.R./resistor resonator is shown in Fig. 2.14. This circuit is due to Cheng and Lim (41) and , like the Schmidt/Lee circuit of section 2.4.2 , it uses the theoretical minimum number of amplifiers and capacitors .

Assuming an ideal amplifier , the impedance of the circuit is

$$Z = \frac{A_0 + A_1 p + A_2 p^2}{B_2 p^2} \tag{2.23}$$

where

$$A_0 = G_2 G_3 G_5$$

$$A_1 = C_4(G_2G_3 - G_1G_5) + C_7G_2G_3$$

$$A_2 = C_4C_7G_2(1 + G_1R_8 + G_3R_8)$$

$$B_2 = C_4C_7G_2(G_1 + G_3) \qquad \text{note : } G_i = 1/R_i$$

The circuit achieves the desired impedance $Z = R + K/p^2$, where R and K are positive , by means of the coefficient cancellation $A_1 = 0$ and the conditions $A_2/B_2 > 0$ and $A_0/B_2 > 0$. As only one coefficient cancellation is required in the impedance expression , we would expect this circuit to have better sensitivity properties than Schmidt and Lees' resonator circuit which requires two coefficient cancellations.

An adjustment procedure for overcoming the effects of component manufacturing tolerances on the impedance of the circuit has been proposed by Cheng and Lim (41). They have also shown how to design the circuit so that the effects of amplifier imperfections on the impedance are reduced.

2.5 SUMMARY AND CONCLUSIONS

The Table in Fig. 2.15 summarises the number of amplifiers , capacitors , coefficient and pole/zero cancellations that are required for the simulation networks to achieve their correct impedances.

As mentioned in Chapter 1,LC filters can be designed to have good sensitivity properties , however , when the simulating networks are included in the filters new sensitivities are introduced by the additional components in the simulating networks. In the case of two-amplifier simulation networks the new passive sensitivities introduced are low as these circuits retain their ideal simulation behaviour for arbitrary positive values for their passive components . Single-amplifier simulation networks , however , require coefficient cancellations (and possibly also pole/zero cancellations) in their impedance expressions , and we would expect the new sensitivities to be larger. Furthermore , we might expect the sensitivity properties of the single-amplifier networks to become worse as the number of cancellations required becomes greater.

Many of the single-amplifier simulation networks do not have adjustment procedures for overcoming the effects of component manufacturing tolerances on their impedances. Indeed , inspection of their impedance expressions shows that in many cases there is no straightforward method of adjusting the circuits. Also , for many of the single-amplifier networks the effects of amplifier imperfections on the impedance have not been investigated.

In some filter applications where the number of amplifiers is at a premium it is thought that the resonator circuits proposed by Cheng and Lim will offer better results than the other single-amplifier networks. This is because these circuits use a minimum number of amplifiers and capacitors , and require only one coefficient cancellation in their impedance expressions. Also , adjustment procedures for these circuits have been proposed. However , the Cheng/Lim circuits are not suitable for LC filters where the shunt arms consist solely of grounded inductors and other simulation networks , such as the Orchard/Willson S.I. circuit and the Schmidt/Lee S.I. circuit, would have to be used.

CHAPTER 3

SOME NOVEL SIMULATED INDUCTOR CIRCUITS

3.1 INTRODUCTION

In this chapter we present some novel S.I. circuits. Each new circuit contains only one amplifier and one capacitor, andcan be regarded as a single-amplifier P.I.I. network having port 2 terminated in a capacitor. In this respect the new circuits are similar to the Orchard/Willson S.I. circuit and the Schmidt/Lee circuit described previously in Sections 2.2.4 and 2.2.5 .

After describing the new S.I. circuits we investigate the effects of passive component tolerances on the impedance of S.A. S.C. S.I.s . Models which show how the impedance is affected will be described , and we will also describe a model which additionally takes into consideration the effects of the non-ideal gain of the amplifier on the impedance of the S.I.s .

3.2 DESCRIPTION OF CIRCUITS

Before describing the new S.I. circuits in detail , it is interesting to mention how many resistors they contain and also to point out a few properties of some of the circuits that the O/W and S/L circuits do not have (note from Sections 2.2.4 and 2.2.5 that the O/W circuit contains six resistors , and the S/L circuit contains seven resistors).

One of the new circuits, referred to as S.I. circuit A ,see Fig.3.1(a), uses seven resistors and it has the interesting feature that its inductance value can be varied by altering the value of a single resistor without affecting the conditions required for lossless inductor simulation. The other new circuits and the O/W and S/L circuits do not possess this property. Furthermore, the inductance value for S.I. circuit A can be varied over a positive and negative range, and the circuit appears to be suited to an adjustment procedure for overcoming manufacturing tolerances on the values of its passive components. Another new circuit, called S.I. circuit B ,see Fig.3.3 , uses only six resistors,which is the same number as for the O/W circuit, and it has the interesting feature that it is a special case of S.I. circuit A. The remaining new S.I. circuits, circuits C,D,E and F, are shown in Figs.3.4 to 3.7; these networks use seven or more resistors and they have no obvious advantages over the O/W and S/L circuits , nor the new S.I. circuits A and B.

As S.I. circuits A and B are considered to be the most important of the new circuits presented in this Chapter, a detailed analysis of the impedance presented by these circuits, for both the ideal and non-ideal amplifier cases, will be presented. Impedance expressions for S.I. circuits C and D, for the ideal amplifier case only, will also be presented, however, the expressions for circuits E and F are not given as these circuits contain a large number of resistors and are unlikely to be useful in practice.

3.2.1 Circuit A

The impedance presented by the circuit in Fig.3.1(a), for both the ideal amplifier and non-ideal amplifier cases, will now be determined.

Firstly, for the purposes of analysis, the amplifier is removed from the circuit in Fig.3.1(a) and the remaining RC network is labelled in the way shown in Fig.3.1(b). By inspection the admittance equations describing the network in Fig. 3.1(b) are

$$\begin{bmatrix} I_1 \\ I_2 \\ I_3 \\ I_4 \\ I_5 \end{bmatrix} = \begin{bmatrix} (G_1+G_7) & 0 & -G_1 & 0 & -G_7 \\ 0 & (PC_0+G_2+G_3) & 0 & -G_3 & -pC_0 \\ -G_1 & 0 & (G_4+G_5+G_1) & -G_4 & 0 \\ 0 & -G_3 & -G_4 & (G_6+G_3+G_4) & -G_6 \\ -G_7 & -pC_0 & 0 & -G_6 & (G_7+pC_0+G_6) \end{bmatrix} \times \begin{bmatrix} V_1 \\ V_2 \\ V_3 \\ V_4 \\ V_5 \end{bmatrix} \quad (3.1)$$

Now, taking the amplifier into consideration, we note from Fig. 3.1(b) that the voltages V_2 , V_3, and V_4 are related by the expression:

$$V_4 = \mu(V_2-V_3) \tag{3.2}$$

where μ is the voltage gain for the amplifier. Substituting this expression for V_4 into eqns. (3.1) gives

$$\begin{array}{c} (a) \\ (b) \\ (c) \\ (d) \\ (e) \end{array} \begin{bmatrix} I_1 \\ I_2 \\ I_3 \\ I_4 \\ I_5 \end{bmatrix} = \begin{bmatrix} (G_1+G_7) & 0 & -G_1 & -G_7 \\ 0 & (pC_0+G_2+G_3-\mu G_3) & \mu G_3 & -pC_0 \\ -G_1 & -\mu G_4 & (G_4+G_5+G_1+\mu G_4) & 0 \\ 0 & (-G_3+\mu(G_6+G_3+G_4)) & (-G_4-\mu G_6+G_3+G_4) & -G_6 \\ -G_7 & -(pC_0+\mu G_6) & \mu G_6 & (G_7+pC_0+G_6) \end{bmatrix} \times \begin{bmatrix} V_1 \\ V_2 \\ V_3 \\ V_5 \end{bmatrix} \tag{3.3}$$

From Figs. 3.1 (a) and (b) we also note

$$I_2 = I_3 = I_5 = 0 \tag{3.4}$$

as no current is taken from nodes 2,3 and 5 (nodes 2 and 3 are connected to the amplifier inputs for which we assume an infinite input impedance). These values for I_2, I_3 and I_5 may be substituted into eqns.(3.3) (b), (c) and (e) to give the following set of equations

$$\begin{bmatrix} 0 \\ G_1 \\ G_1 \end{bmatrix} = \begin{bmatrix} (pC_o+G_2+G_3-\mu G_3) & \mu G_3 & -pC_o \\ -\mu G_4 & (G_4+G_5+G_1+\mu G_4) & 0 \\ -(pC_o+\mu G_6) & \mu G_6 & (G_7+pC_o+G_6) \end{bmatrix} X \begin{bmatrix} V_2 \\ V_3 \\ V_5 \end{bmatrix}$$

(3.5)

The voltages V_3 and V_5 can be expressed in terms of V_1 , the voltage across the Simulated Inductor network , by solving this set of linear equations using Cramer's rule ,i.e. ,

$$V_3 = \frac{D_1}{D_0} V_1 \quad ; \quad V_5 = \frac{D_2}{D_0} V_1 \qquad (3.6)$$

where the expressions for D_0,D_1 and D_2 are

$$D_0 = \begin{Vmatrix} (pC_0+G_2+G_3-\mu G_3) & \mu G_3 & -pC_0 \\ \mu G_4 & (G_4+G_5+G_1+\mu G_4) & 0 \\ -(pC_0+\mu G_6) & \mu G_6 & (G_7+pC_0+G_6) \end{Vmatrix} \qquad (3.7)$$

$$D_1 = \begin{Vmatrix} (pC_0+G_2+G_3-\mu G_3) & 0 & -pC_0 \\ -\mu G_4 & G_1 & 0 \\ -(pC_0+\mu G_6) & G_7 & (G_7+pC_0+G_6) \end{Vmatrix} \tag{3.8}$$

$$D_2 = \begin{Vmatrix} (pC_0+G_2+G_3-\mu G_3) & \mu G_3 & 0 \\ -\mu G_4 & (G_4+G_5+G_1+\mu G_4) & G_1 \\ -(pC_0+\mu G_6) & \mu G_6 & G_7 \end{Vmatrix} \tag{3.9}$$

From eqn.(3.3) (a) we have

$$I_1 = (G_1+G_7)V_1 - (G_1)V_3 - (G_7)V_5 \tag{3.10}$$

Substituting the expressions for V_3 and V_5 given in (3.6) into (3.10) gives:

$$I_1 = (G_1 + G_7) - G_1\frac{D_1}{D_0} - G_7\frac{D_2}{D_0} \quad V_1 \tag{3.11}$$

and from this expression $Z_{IND} = V_1/I_1$ is found to be

$$Z_{IND} = \frac{D_0}{(G_1 + G_7) - G_1D_1 - G_7D_2} \tag{3.12}$$

The expressions for D_0, D_1 and D_2 given in (3.7), (3.8) and (3.9), may now be substituted into (3.12) and with some re-arranging of terms the impedance Z_{IND} can be expressed as:

$$Z_{IND} = \frac{(A_0 + \varepsilon A_2) + p(A_1 + \varepsilon A_3)}{(B_0 + \varepsilon B_2) + p(B_1 + \varepsilon B_3)} \tag{3.13}$$

where

$$\begin{aligned}
A_0 &= (G_6 + G_7)(G_4G_2 - G_3G_5 - G_3G_1) \\
A_1 &= C_0\left\{G_4(G_2 + G_7) - (G_1 + G_5)(G_3 + G_6)\right\} \\
A_2 &= (G_3 + G_2)(G_4 + G_5 + G_1)(G_6 + G_7) \\
A_3 &= C_0(G_4 + G_5 + G_1)(G_2 + G_3 + G_6 + G_7) \\
B_0 &= G_1G_2G_6G_7 + (G_4G_2 - G_3G_5)(G_6G_7 + G_1G_7 + G_1G_6) \\
B_1 &= C_0(G_1 + G_7)(G_2G_4 - G_3G_5 - G_5G_6) \\
B_2 &= (G_2 + G_3)\,(G_4 + G_5)(G_1G_6 + G_1G_7 + G_6G_7) + G_1G_6G_7 \\
B_3 &= C_0\left\{G_1(G_4 + G_5)(G_2 + G_3 + G_6 + G_7) + G_7(G_1 + G_4 + G_5)(G_2 + G_3 + G_6)\right\}
\end{aligned} \tag{3.14}$$

and $\varepsilon = \mu^{-1} = \alpha + p/\omega_T$ where α is the inverse of the D.C. gain, and $\omega_T = 2\pi f_T$ where f_T is the finite gainbandwidth product for the amplifier.

In the ideal amplifier case when the gain is infinite, i.e. $\varepsilon = 0$, the impedance in (3.13) reduces to:

$$Z_{IND} = \frac{A_0 + pA_1}{B_0 + pB_1} \tag{3.15}$$

For lossless inductor simulation the coefficient cancellations

$$A_0 = 0 \quad \text{and} \quad B_1 = 0 \tag{3.16}$$

are required. The inductance value $L = A_1/B_0$ is then given by the expression

$$L = \frac{A_1}{B_0} = \frac{C_0\left\{G_4(G_2 + G_7) - (G_1 + G_5)(G_3 + G_6)\right\}}{(G_4G_2 - G_3G_5)(G_6G_7 + G_1G_7 + G_1G_6) + G_1G_2G_6G_7} \tag{3.17}$$

For arbitrary values for C_0, G_3, G_4, G_5, G_6 and G_7 the conditions $A_0 = 0$ and $B_1 = 0$ may be satisfied by choosing G_1 and G_2 as:

$$\begin{aligned} G_1 &= R_3G_6G_5 \\ G_2 &= G_5R_4(G_3 + G_6) \end{aligned} \tag{3.18}$$

Substituting these expressions for G_1 and G_2 into (3.17) gives

$$L = \frac{C_0(G_4G_7 - G_5G_6 - G_5G_6^2R_3)}{G_5G_6^2(G_7 + G_5G_6R_3 + G_5G_7R_3) + G_7G_6^2G_5^2R_3R_4(G_3 + G_6)} \tag{3.19}$$

This expression shows that S.I. circuit A can be designed to have either a negative or a positive inductance value unlike previously published circuits. For ideal positive inductor simulation we require the inequality

$$G_4G_7 > R_3G_6G_5(G_3+G_6) \tag{3.20}$$

S.I. circuit A is similar to the O/W and S/L circuits in that tolerances on the values of its conductances cause the coefficients A_0 and B_1 to be non-zero, and the circuit no longer simulates a lossless inductor exactly. However, inspection of the expressions for A_0 and B_1 in (3.17) show the following:

(1) The condition $A_0 = 0$ is independent of the values for G_6 and G_7

(2) The condition $B_1 = 0$ is independent of the values for G_1 and G_7

These properties of S.I. circuit A suggest the following straightforward functional adjustment procedure for overcoming the effects of passive component tolerances on the impedance for S.I. circuit A.

(1) Adjust G_1 to give $A_0=0$ and G_6 to give $B_1=0$.

(2) Then adjust G_7 to obtain the desired inductance value L_N.

The last adjustment for L_N does not affect either of the conditions $A_0=0$ and $B_1=0$. Furthermore, the conductance G_7

can be adjusted over a positive range of values to give both a positive and negative range for the inductance value. For example, if we choose $G_1=1\mho$ $G_2=2\mho$, $G_3=1\mho$, $G_4=1\mho$, $G_5=1\mho$, $G_6=1\mho$ and $C_0=1F$, then the variation in inductance value with G_7 is that shown in Fig.3.2. Other known S.I. circuits, both single-amplifier and two-amplifier circuits, do not have this property.

The O/W and S/L circuits, and the remaining S.I. circuits to be described in this Chapter, are all unsuited to a straightforward adjustment procedure of the kind described here for S.I. circuit A. This is so because the value of each resistor in these circuits simultaneously affects the value of the inductance L and at least one of the two coefficient cancellations required for lossless inductor simulation.

3.2.2 Circuit B

S.I. circuit B is shown in Fig.3.3. This circuit is a special case of S.I. circuit A obtained by replacing the conductance G_7 by a short circuit, see Fig.3.1(a). The impedance presented by S.I. circuit B can therefore be obtained simply by letting $G_7 \to \infty$ in the impedance expression for S.I. circuit A and collecting the remaining terms. In this way we obtain for S.I. circuit B

$$Z_{IND} = \frac{(A_0 + \varepsilon A_2) + p(A_1 + \varepsilon A_3)}{(B_0 + \varepsilon B_2) + p(B_1 + \varepsilon B_3)} \tag{3.21}$$

where

$$A_0 = G_4G_2 - G_3G_5 - G_3G_1$$

$$A_1 = C_0G_4$$

$$A_2 = (G_2 + G_3)(G_1 + G_4 + G_5)$$

$$A_3 = C_0(G_1 + G_4 + G_5) \tag{3.22}$$

$$B_0 = (G_1 + G_6)(G_4G_2 - G_3G_5) + G_1G_2G_6$$

$$B_1 = C_0(G_4G_2 - G_3G_5 - G_5G_6)$$

$$B_2 = (G_2 + G_3)\left\{(G_4 + G_5)(G_1 + G_6) + G_1G_6\right\}$$

$$B_3 = C_0\left\{(G_1 + G_2 + G_3 + G_6)(G_4 + G_5) + G_1(G_2 + G_3 + G_6)\right\}$$

and $\varepsilon = \mu^{-1} = \alpha + p/\omega_T$

In the ideal amplifier case when $\mu = \infty$, i.e. $\varepsilon = 0$, the impedance Z_{IND} in (3.21) becomes that of an ideal inductance , i.e. $Z_{IND} = pL$, if

$$A_0 = 0 \qquad \text{and} \qquad B_1 = 0 \tag{3.23}$$

The inductance $L = A_1/B_0$ is given by the expression

$$L = \frac{A_1}{B_0} = \frac{C_0G_4}{(G_1 + G_6)(G_4G_2 - G_3G_5) + G_1G_2G_6} \tag{3.24}$$

For arbitrary values for G_3, G_4, G_5 and G_6 the conditions $A_0 = 0$ and $B_1 = 0$ may be achieved by choosing G_1 and G_2 in the same way as for S.I. circuit A , i.e.,

$$G_1 = G_5 G_6 R_3$$

$$G_2 = G_5 R_4 (G_3 + G_6) \tag{3.25}$$

Substitution of these expressions for G_1 and G_2 into the expression for L in (3.24) gives

$$L = \frac{C_0 G_4}{G_6^2 G_5 (1 + G_5 R_3 + G_5 R_4 + G_5 G_6 R_3 R_4)} \tag{3.26}$$

(note that L is always positive). One set of component values that satisfies the conditions $A_0 = 0$ and $B_1 = 0$ to give $L = 0.25$ H is: $G_1 = 1\mho$, $G_2 = 2\mho$, $G_3 = G_4 = G_5 = 1\mho$, $G_6 = 1\mho$, C_0 1 F .

Two coefficient cancellations are again needed to achieve inductance simulation and we would expect this circuit to have sensitivity properties similar to those for the O/W circuit, the S/L circuit, and the new S.I. circuit A outlined previously in Section 3.2.1 . S.I. circuit B is interesting because it is a special case of S.I. circuit A . Also, S.I. circuit B uses only six resistors which is the same number as for the O/W circuit, and the fewest number of resistors so far found necessary to achieve lossless positive inductance simulation using one amplifier and one capacitor .

3.2.8 Circuit C

The impedance presented by the new S.I. circuit in Fig.3.4(a) will now be determined for the ideal amplifier case only. From Fig. 3.5(b) we find that the admittance equations describing the passive component part of the simulation network are

$$\begin{bmatrix} I_1 \\ I_2 \\ I_3 \\ I_4 \\ I_5 \end{bmatrix} = \begin{bmatrix} (G_1+G_2+pC_0) & -pC_0 & -G_2 & -G_1 & 0 \\ -pC_0 & (pC_0+G_3+G_4) & -G_4 & 0 & 0 \\ -G_2 & -G_4 & (G_2+G_4+G_5) & 0 & -G_5 \\ -G_1 & 0 & 0 & (G_1+G_6+G_7) & -G_6 \\ 0 & 0 & -G_5 & -G_6 & (G_5+G_6) \end{bmatrix} \mathrm{X} \begin{bmatrix} V_1 \\ V_2 \\ V_3 \\ V_4 \\ V_5 \end{bmatrix} \tag{3.27}$$

Now, taking the amplifier into consideration, we note that the voltages V_3 and V_4 are equal , i.e.,

$$V_4 = V_3 \tag{3.28}$$

Making the substitution $V_4 = V_3$ in eqns. (3.27) gives

$$\begin{array}{c} (a) \\ (b) \\ (c) \\ (d) \\ (e) \end{array} \begin{bmatrix} I_1 \\ I_2 \\ I_3 \\ I_4 \\ I_5 \end{bmatrix} = \begin{bmatrix} (G_1+G_2+pC_0) & -pC_0 & -(G_1+G_2) & 0 \\ -pC_0 & (pC_0+G_3+G_4) & -G_4 & 0 \\ -G_2 & -G_4 & (G_2+G_4+G_5) & -G_5 \\ -G_1 & 0 & (G_1+G_6+G_7) & -G_6 \\ 0 & 0 & -(G_5+G_6) & (G_5+G_6) \end{bmatrix} \mathrm{X} \begin{bmatrix} V_1 \\ V_2 \\ V_3 \\ V_5 \end{bmatrix} \tag{3.29}$$

The values of I_2, I_3 and I_4 are zero as no current is taken from nodes 2, 3 and 5 (nodes 3 and 4 are connected to the amplifier inputs). Eqns. (3.29) (b),(c) and (d) can therefore be rewritten as:

$$V_1 \begin{bmatrix} pC_0 \\ G_2 \\ G_1 \end{bmatrix} = \begin{bmatrix} (pC_0+G_3+G_4) & -G_4 & 0 \\ -G_4 & (G_2+G_4+G_5) & -G_5 \\ 0 & (G_1+G_6+G_7) & -G_6 \end{bmatrix} X \begin{bmatrix} V_2 \\ V_3 \\ V_5 \end{bmatrix} \tag{3.30}$$

The voltages V_2 and V_3 can be expressed in terms of V_1 , the voltage across the simulation network, by solving the set of linear equations in (3.30) using Cramer's rule, i.e.,

$$V_2 = \frac{D_1}{D_0} V_1 \quad , \quad V_3 = \frac{D_2}{D_0} V_1 \tag{3.31}$$

where the expressions for D_0,D_1 and D_2 are

$$D_0 = \begin{Vmatrix} (pC_0+G_3+G_4) & -G_4 & 0 \\ -G_4 & (G_2+G_4+G_5) & -G_5 \\ 0 & (G_1+G_6+G_7) & -G_6 \end{Vmatrix} \tag{3.32}$$

$$\begin{aligned} = \; & pC_0(G_1G_5 + G_5G_7 - G_2G_6 - G_4G_6) \\ & + G_5(G_1 + G_7)(G_3 + G_4) - G_6(G_2G_3 + G_2G_4 + G_3G_4) \end{aligned} \tag{3.33}$$

$$D_1 = \begin{Vmatrix} pC_0 & -G_4 & 0 \\ G_2 & (G_2+G_4+G_5) & -G_5 \\ G_1 & (G_1+G_6+G_7) & -G_6 \end{Vmatrix} \tag{3.34}$$

$$= pC_0(G_1G_5 + G_5G_7 - G_2G_6 - G_4G_6) + G_4(G_1G_5 - G_2G_6) \tag{3.35}$$

$$D_2 = \begin{Vmatrix} (pC_0+G_3+G_4) & pC_0 & 0 \\ -G_4 & G_2 & -G_5 \\ 0 & G_1 & -G_6 \end{Vmatrix} \tag{3.36}$$

$$= pC_0(G_1G_5 - G_2G_6 - G_4G_6) + (G_3 + G_4)(G_1G_5 - G_2G_6) \tag{3.37}$$

From equation (3.29) (a) we have

$$I_1 = (G_1 + G_2 + pC_0)V_1 - (pC_0)V_2 - (G_1 + G_2)V_3 \tag{3.38}$$

Substituting the expressions for V_2 and V_3 in (3.31) into (3.38) gives

$$I_1 = (G_1 + G_2 + pC_0) - pC_0 \frac{D_1}{D_0} - (G_1 + G_2) \frac{D_2}{D_0} \quad V_1 \tag{3.39}$$

and from (3.39) the impedance $Z_{IND} = V_1/I_1$ is found to be

$$Z_{IND} = \frac{D_0}{(G_1 + G_2 + pC_0)D_0 - pC_0D_1 - (G_1 + G_2)D_2} \qquad (3.40)$$

The expressions for D_0, D_1 and D_2 given in (3.33), (3.35), and (3.37) may now be substituted into (3.40) and with some re-arranging of terms the impedance Z_{IND} can be expressed as

$$Z_{IND} = \frac{A_0 + pA_1}{B_0 + pB_1} \qquad (3.41)$$

where

$$\begin{aligned}
A_0 &= G_5(G_1 + G_7)(G_3 + G_4) - G_6(G_2G_3 + G_3G_4 + G_2G_4) \\
A_1 &= C_0(G_1G_5 + G_5G_7 - G_2G_6 - G_4G_6) \\
B_0 &= (G_1 + G_2)(G_3G_5G_7 + G_4G_5G_7 - G_3G_4G_6) \\
B_1 &= C_0\left\{G_5G_7(G_1 + G_2 + G_3 + G_4) + G_1G_3G_5 - G_3G_6(G_2 + G_4)\right\}
\end{aligned} \qquad (3.42)$$

Once again two coefficient cancellations are required to achieve lossless inductance simulation. One set of conductance values which satisfy these conditions to give the inductance value $L = C_0/27$ is $G_1=G_2=G_4=G_5=G_6=G_7=1℧$, $G_3=6℧$, and $G_4=3℧$.

3.2.4 Circuit D

The impedance presented by the S.I. circuit shown in Fig. 3.5(a), for the ideal amplifier case, was obtained in the following way.

The admittance equations describing the RC network are first of all determined by inspection of Fig.3.5(b), i.e.,

$$
\begin{bmatrix} I_1 \\ I_2 \\ I_3 \\ I_4 \\ I_5 \end{bmatrix}
=
\begin{bmatrix}
(G_1+G_2) & -G_1 & 0 & -G_2 & 0 \\
-G_1 & (G_1+G_3+pC_0) & -pC_0 & 0 & -G_3 \\
0 & -pC_0 & (G_6+G_7+pC_0) & 0 & -G_6 \\
-G_2 & 0 & 0 & (G_2+G_4+G_5) & -G_4 \\
0 & -G_3 & -G_6 & -G_4 & (G_3+G_4+G_6)
\end{bmatrix}
\times
\begin{bmatrix} V_1 \\ V_2 \\ V_3 \\ V_4 \\ V_5 \end{bmatrix}
\tag{3.43}
$$

Now, taking the amplifier into consideration, we note from Fig. 3.5(a) that the voltages V_4 and V_2 are equal, i.e.,

$$V_4 = V_2 \tag{3.44}$$

Making this substitution for V_4 in equations (3.43) gives

$$
\begin{array}{c}
(a) \\ (b) \\ (c) \\ (d) \\ (e)
\end{array}
\begin{bmatrix} I_1 \\ I_2 \\ I_3 \\ I_4 \\ I_5 \end{bmatrix}
=
\begin{bmatrix}
(G_1+G_2) & -(G_1+G_2) & 0 & 0 \\
-G_1 & (G_1+G_3+pC_0) & -pC_0 & -G_3 \\
0 & -pC_0 & (G_6+G_7+pC_0) & -G_6 \\
-G_2 & (G_2+G_4+G_5) & 0 & -G_4 \\
0 & -(G_3+G_4) & -G_6 & (G_3+G_4+G_6)
\end{bmatrix}
\times
\begin{bmatrix} V_1 \\ V_2 \\ V_3 \\ V_5 \end{bmatrix}
\tag{3.45}
$$

The currents I_2, I_3 and I_4 are equal to zero and eqns.(3.45) (b),(c) and (d) can therefore be rewritten as:

$$V_1 \begin{bmatrix} G_1 \\ 0 \\ G_2 \end{bmatrix} = \begin{bmatrix} (G_1+G_3+pC_0) & -pC_0 & -G_3 \\ -pC_0 & (G_6+G_7+pC_0) & -G_6 \\ (G_2+G_4+G_5) & 0 & -G_4 \end{bmatrix} \times \begin{bmatrix} V_2 \\ V_3 \\ V_5 \end{bmatrix} \tag{3.46}$$

The voltage V_2 can be expressed in terms of V_1 by solving the set of linear equations given in (3.46) using Cramer's rule, i.e.,

$$V_2 = \frac{D_1}{D_0} V_1 \tag{3.47}$$

where the expressions for D_0, and D_1 are

$$D = \left\| \begin{matrix} (G_1+G_3+pC_0) & -pC_0 & -G_3 \\ -pC_0 & (G_6+G_7+pC_0) & -G_6 \\ (G_2+G_4+G_5) & 0 & -G_4 \end{matrix} \right\| \tag{3.48}$$

$$\begin{aligned} = \; & (G_6 + G_7)(G_2G_3 + G_3G_5 - G_1G_4) \quad + \\ & pC_0\left\{(G_3 + G_6)(G_2 + G_5) - G_4(G_1 + G_7)\right\} \end{aligned} \tag{3.49}$$

$$D_1 = \left\| \begin{matrix} G_1 & -pC_0 & -G_3 \\ 0 & (G_6+G_7+pC_0) & -G_6 \\ G_2 & 0 & -G_4 \end{matrix} \right\| \tag{3.50}$$

$$= (G_6 + G_7)(G_2G_3 - G_1G_4) + pC_0(G_2G_3 + G_2G_6 - G_1G_4) \tag{3.51}$$

From equation (3.45)(a) we have:

$$I_1 = (G_1 + G_2)V_1 - (G_1 + G_2)V_2 \tag{3.52}$$

and substituting the expression for V_2 in (3.47) gives

$$I_1 = (G_1 + G_2)(1 - D_1/D_0)\ V_1$$

The impedance $Z_{IND} = V_1/I_1$ is therefore given by

$$Z_{IND} = \frac{D_0}{(G_1 + G_2)(D_0 - D_1)} \tag{3.53}$$

The expressions for D_0 and D_1 given in (3.49) and (3.51) may now be substituted into (3.53) and with some re-arranging of terms we obtain

$$Z_{IND} = \frac{A_0 + pA_1}{B_0 + pB_1} \tag{3.54}$$

where

$$\begin{aligned}
A_0 &= (G_6 + G_7)(G_2G_3 + G_3G_5 - G_1G_4) \\
A_1 &= C_0\{(G_3 + G_6)(G_2 + G_5) - G_4(G_1 + G_7)\} \\
B_0 &= G_3G_5(G_1 + G_2)(G_6 + G_7) \\
B_1 &= C_0(G_1 + G_2)(G_3G_5 + G_5G_6 - G_4G_7)
\end{aligned} \tag{3.55}$$

The circuit achieves lossless inductor simulation in the same way as the previously mentioned circuits, i.e., by means of the conditions $A_0=0$, $B_1=0$, and $A_1/B_0>0$. One set of component values which satisfy these conditions to give an inductance value $L=C_0/15$ is: $G_1 = G_6 = 2\mho$, $G_7 = 3\mho$, $G_2 = G_3 = G_4 = G_5 = 1\mho$.

3.2.5 Circuits E and F

Two more S.A. S.C. S.I. circuits were discovered by the author, but these circuits contain a large number of resistors and have no obvious advantages over the other S.I.s mentioned in this Chapter. The two circuits are shown in Figs.3.6 and 3.7 alongwith sets of resistance values which gives rise to lossless positive inductor simulation. These resistance values were found by matrix manipulation without fully deriving explicit impedance expressions, but the simulation of a lossless inductor was verified by computer analysis of the circuits.

3.3 EFFECTS OF PASSIVE COMPONENT TOLERANCES

In this Section we investigate the effects of passive component tolerances on the impedance of the single-amplifier, single-capacitor, S.I.s discussed in this thesis.

Assuming the amplifiers to be ideal, the S.I. circuits all have impedance expressions of the form

$$Z_{IND} = \frac{A_0 + pA_1}{B_0 + pB_1} \tag{3.56}$$

and the expressions for A_0, A_1, B_0, and B_1 for each circuit have been given previously. To obtain lossless positive inductor simulation it is necessary to choose nominal values for the passive components in each circuit so that the nominal values for the coefficients in (3.56), which we shall call A_{ON}, A_{1N}, B_{ON}, and B_{1N}, satisfy the following conditions.

$$A_{ON} = 0 \quad , B_{1N} = 0 \ , A_{1N}/B_{ON} > 0 \tag{3.57}$$

Equation (3.56) then becomes $Z_{IND} = pL_N$ where the nominal inductance value L_N is equal to A_{1N}/B_{ON}. Tolerances on the passive component values for each circuit, however, cause the actual values for the coefficients in (3.56) not to be equal to their nominal values, i.e.,

$$
\begin{aligned}
A_0 &= A_{0N} + \Delta A_0 = \Delta A_0 \\
A_1 &= A_{1N} + \Delta A_1 \\
B_0 &= B_{0N} + \Delta B_0 \\
B_1 &= B_{1N} + \Delta B_1 = \Delta B_1
\end{aligned}
\qquad (3.58)
$$

and the simulation is no longer that of a lossless inductor. The actual impedance presented by the non-ideal S.I. circuits is easily found by substituting the expressions in (3.58) into (3.56) , i.e., we obtain

$$
Z_{IND} = \frac{\Delta A_0 + p(A_{1N} + \Delta A_1)}{B_{0N} + \Delta B_0 + p\Delta B_1} \qquad (3.59)
$$

(note that A_{0N} and B_{1N} are zero and do not appear in (3.59)). Two different models which both describe this impedance function will now be presented.

3.3.1 MODEL 1

One way of describing the impedance in (3.59) is by the well known model in Fig. 3.8 (a). For $p = j\omega$, we consider the impedance Z_{IND} in (3.59) as the series combination of a frequency dependent resistance $R(\omega)$ and an inductor whose inductance value $L(\omega)$ is also frequency dependent, i.e.,

$$
Z_{IND} = R(\omega) + j\,L(\omega) \qquad (3.60)
$$

The frequency behaviour of Z_{IND} is then described by $L(\omega)$

and the Q-factor $Q(\omega)$ which is defined as

$$Q(\omega) = L(\omega)/R(\omega) \tag{3.61}$$

For an ideal lossless inductor $L(\omega)$ is constant with frequency and $Q(\omega)$ is infinite at all frequencies. However, for the S.I.s under study, whose coefficients have the small errors shown in (3.58) , we find that $L(\omega)$ is frequency dependent and $Q(\omega)$ has finite values which are also frequency dependent. Expressions for $L(\omega)$ and $Q(\omega)$ may be obtained from eqns. (3.59), (3.60), and (3.61), i.e.,

$$L(\omega) = \frac{A_{1N}B_{ON} + B_{ON}\Delta A_1 + A_{1N}\Delta B_O + \Delta A_1\Delta B_O - \Delta A_O\Delta B_1}{B_{ON}^2 + 2B_{ON}\Delta B_O + \Delta B_O^2 + \omega^2\Delta B_1^2} \tag{3.62}$$

$$Q(\omega) = \frac{\omega(A_{1N}B_{ON} + B_{ON}\Delta A_1 + A_{1N}\Delta B_O + \Delta A_1\Delta B_O - \Delta A_O\Delta B_1)}{\Delta A_O B_{ON} + \omega^2\Delta B_1 A_{1N} + \Delta A_O\Delta B_O + \omega^2\Delta B_1\Delta A_1} \tag{3.63}$$

Simpler expressions for $L(\omega)$ and $Q(\omega)$, than those in (3.62) and (3.63) , are obtained if we neglect second order effects, i.e., $L(\omega)$ becomes

$$L(\omega) \approx \frac{A_{1N}B_{ON} + B_{ON}\Delta A_1 + A_{1N}\Delta B_O}{B_{ON}^2 + 2B_{ON}\Delta B_O}$$

$$= L_N(1 + \Delta A_1/A_{1N} - \Delta B_O/B_{ON}) \tag{3.64}$$

where L_N is the nominal inductance value A_{1N}/B_{0N}. The expression in (3.64) does not contain any terms due to ΔA_0 and ΔB_1 asthese errors have only a second order effect on $L(\omega)$. The simplified expression for $Q(\omega)$ is

$$Q(\omega) \approx \frac{\omega A_{1N} B_{0N}}{\Delta A_0 B_{0N} + \omega^2 \Delta B_1 A_{1N}}$$

$$= \frac{\omega L_N}{\dfrac{\Delta A_0}{B_{0N}} + \omega^2 L_N^2 \dfrac{\Delta B_1}{A_{1N}}} \qquad (3.65)$$

This expression shows that the errors ΔA_0 and ΔB_1 have a 1st order effect on $Q(\omega)$. We also note that the errors ΔA_0 and ΔB_1 are mainly due to tolerances on the conductances in the S.I. circuits and not the capacitor tolerance. This is because A_0 is independent of the capacitance value C_0, and because B_1 is independent of C_0 when B_1 has its nominal value $B_{1N} = 0$. For example, for S.I. circuit B (see Section 3.2.2) A_0 is given by the expression

$$A_0 = G_4 G_2 - G_3 G_5 - G_3 G_1$$

and B_1 is given by

$$B_1 = C_0 (G_4 G_2 - G_3 G_5 - G_5 G_6)$$

The expression for B_1 shows that the tolerance on C_0 can only have a second order effect on the value for B_1 when the tolerances on G_2, G_3, G_4, G_5 and G_6 are taken into consideration.

The frequency behaviour for $|Q(\omega)|$,as determined from (3.65) , is shown in Fig. 3.8 (c). We find that two types of behaviour are possible depending upon the signs for ΔA_0 and ΔB_1 . For both the maximum value for $|Q(\omega)|$ occurs at the frequency

$$\omega_M = \sqrt{\left|\frac{\Delta A_0}{L_N \Delta B_1}\right|} \tag{3.66}$$

When ΔA_0 and ΔB_1 have opposite signs the value for $|Q(\omega)|$ is infinite at $\omega = \omega_M$, and when they have the same sign the maximum value for $|Q(\omega)|$ is

$$|Q(\omega)|_{max} = \frac{1}{2}\sqrt{\frac{A_{1N}B_{ON}}{\Delta A_0 \Delta B_1}} \tag{3.67}$$

Unfortunately , in practice , the values for the conductances in the S.I. circuits are not known accurately, and the exact values for ΔA_0 and ΔB_1 will therefore be unknown. Hence it is not possible to predict the values for $|Q(\omega)|_{max}$ and ω_M that one would obtain. However , for the given tolerances on the conductances for the S.I.s we can determine the worst possible values for ΔA_0 and ΔB_1 and hence determine the worst case behaviour for $|Q(\omega)|$. Consider , for example, S.I. circuit B for the case where the amplifier is ideal and the passive components in the circuit have values within 1% of the following nominal values: $G_1 = 1\mho$, $G_2 = 2\mho$, $G_3 = G_4 = G_5 = G_6 = 1\mho$, $C_0 = 1$ F. From (3.22) we find that for this design the values for A_{1N} and B_{ON} are

$$A_{1N} = 1 \quad ; \quad B_{ON} = 4 \tag{3.68}$$

and the worst case values for ΔA_0 and ΔB_1 are

$$\Delta A_0 = \Delta B_1 \approx 8/100 \tag{3.69}$$

The worst case (w.c.) behaviour for $|Q(\omega)|$ can now be determined by substituting these values into eqns. (3.66) and (3.67). In this case we obtain

$$|Q(\omega)|_{\max(w.c.)} = 12.5$$

and this occurs at

$$\omega_{M(w.c.)} = 2.0 \text{ r/s}$$

An accurate plot of the worst case behaviour for $|Q(\omega)|$, calculated from equation (3.65), is shown in Fig. 3.8 (d). To conclude we can say that in practice the actual $|Q(\omega)|$ values, due to the 1% conductance tolerances, must lie somewhere on the shaded area shown in this diagram.

3.3.2 MODEL 2

Rather than describing the non-ideal impedance of the S.I.s (see (3.59)) as the series combination of a frequency dependent resistance and an inductor whose inductance value is also frequency dependent, an alternative model is that shown in Fig. 3.9. For the circuit in Fig. 3.9 we have

$$Z = \frac{R_X R_Y + pLR_Y}{R_X + R_Y + pL} \tag{3.70}$$

This expression is of the same form as the expression in (3.59) for the non-ideal impedance of the S.I.s, i.e., a bilinear expression in p. Expressions for the resistances R_X and R_Y and the inductance L for the model in Fig. 3.9 are obtained by equating the impedance expression in (3.70) to the non-ideal impedance in (3.59). Before doing this, however, it is convenient to re-express eqns. (3.70) and (3.59) in the following way.

$$Z = \frac{\dfrac{R_X R_Y}{R_X + R_Y} + \dfrac{pLR_Y}{R_X + R_Y}}{1 + \dfrac{pL}{R_X + R_Y}} \tag{3.71}$$

$$Z_{IND} = \frac{\dfrac{\Delta A_0}{B_{ON} + \Delta B_0} + \dfrac{p(A_{1N} + \Delta A_1)}{B_{ON} + \Delta B_0}}{1 + \dfrac{p\Delta B_1}{B_{ON} + \Delta B_0}} \tag{3.72}$$

Now we note that the impedance expressions in (3.71) and (3.72) are equal for the following relationships

$$\frac{R_X R_Y}{R_X + R_Y} = \frac{\Delta A_0}{B_{ON} + \Delta B_0}$$

$$\frac{L R_Y}{R_X + R_Y} = \frac{A_{1N} + \Delta A_1}{B_{ON} + \Delta B_0} \qquad (3.73)$$

$$\frac{L}{R_X + R_Y} = \frac{\Delta B_1}{B_{ON} + \Delta B_0}$$

From these relationships we obtain the following expressions for R_X, R_Y, and L

$$R_Y = \frac{A_{1N} + \Delta A_1}{\Delta B_1}$$

$$R_X = \frac{\Delta A_0 (A_{1N} + \Delta A_1)^2}{(A_{1N} + \Delta A_1)(B_{ON} + \Delta B_0) - \Delta A_0 \Delta B_1} \qquad (3.74)$$

$$L = \frac{(A_{1N} + \Delta A_1)^2}{(A_{1N} + \Delta A_1)(B_{ON} + \Delta B_0) - \Delta A_0 \Delta B_1}$$

These equations show that when the impedance of the non-ideal S.I.s is represented by the the circuit in Fig. 3.9 , the component values R_X, R_Y, and L for the model are all frequency <u>independent</u> . In this respect the alternative model differs from MODEL 1 which has frequency dependent component values. When the effects of 2^{nd} order changes are neglected from the expressions in (3.74) we obtain

$$
\begin{aligned}
R_Y &\approx A_{1N}/\Delta B_1 \\
R_X &\approx \Delta A_0/B_{ON} \qquad (3.75)\\
L &\approx L_N(1 + \Delta A_1/A_{1N} - \Delta B_0/B_{ON})
\end{aligned}
$$

where $L_N = A_{1N}/B_{ON}$. Note that the inductance expression in (3.75) is the same as that for MODEL 1 when 2^{nd} order changes are ignored, see (3.64) .

In the ideal case , when the conductances in the S.I.s have their nominal values so that ΔA_0 and ΔB_1 are zero , R_Y will be infinite and R_X will be zero as expected (see (3.74)). However, in the practical case, when the conductances have tolerances causing ΔA_0 and ΔB_1 to be non-zero , R_Y becomes finite and R_X becomes non-zero. Futhermore, the values for ΔA_0 and ΔB_1 will not be known accurately and it is not possible to predict the values for R_Y and R_X that are obtained. However, for given tolerances on the conductances we can calculate the maximum possible values for $|\Delta A_0|$ and $|\Delta B_1|$ and hence find the worst case values for $|R_Y|$ and $|R_X|$ using eqns. (3.75). Consider, for example, S.I. circuit B for the case where the passive components in the circuit have values within 1% of the following nominal values: $G_1 = 1\,\mho$, $G_2 = 2\,\mho$, $G_3 = G_4 = G_5 = G_6 = 1\,\mho$, and $C_0 = 1$ F. The values for A_{1N} and B_{ON} for this choice of component values have been calculated previously and are shown in (3.68) . The worst case values for $|\Delta A_0|$ and $|\Delta B_1|$ have also been calculated previously and are shown in (3.69). Making use of the values in (3.68) and (3.69) in equation (3.75) we obtain

$$|R_Y|_{(w.c)} \approx 12.5 \ \Omega$$

$$|R_X|_{(w.c)} \approx 0.02 \ \Omega$$

3.4 EFFECTS OF NON-IDEAL AMPLIFIER GAIN (A GENERAL DISCUSSION)

Even if the passive components in the S.I. circuits have zero tolerances the impedance of the circuits will still be that of a lossy inductance due to amplifier imperfections. These imperfections include the non-infinite input resistances for the amplifier, the non-zero output resistance, the non-zero input capacitances, and the non-ideal voltage gain μ for the amplifier which, to a 1^{st} order approximation is given by $\mu = (\alpha + p/\omega_T)^{-1}$. Taking into consideration the non-ideal gain μ, and ignoring other amplifier imperfections, we find that the impedance presented by the non-ideal S.I. circuits has the general form of a biquadratic in p, i.e.,

$$Z_{IND} = \frac{a_0 + a_1 p + a_2 p^2}{b_0 + b_1 p + b_2 p^2} \tag{3.76}$$

This form of impedance is not only confirmed by the impedance expressions in (3.13) and (3.21) for S.I. circuits A and B, but it is to be expected as each S.I. circuit has two frequency dependent parameters, namely the impedance of the capacitor C_0, and secondly the gain μ of the non-ideal amplifier. To investigate the quality of inductance simulation due to the non-ideal gain, we can use the same approaches as used in Section 3.3 for investigating the effects of passive component tolerances on the impedance of the S.I.s.

One of these approaches is to model the non-ideal impedance of the S.I. by the series combination of a frequency dependent resistance and an inductance whose inductance value is also frequency dependent. For $p = j\omega$, the impedance expression in (3.76) can be used with eqns. (3.60) and (3.61) to determine expressions for the inductance and Q-factor behaviour. This approach has been used by Orchard and Willson for their S.I. circuit and detailed results of their investigations may be found in (26). The same approach will also be adopted by the author for S.I. circuit B and the results of this work will be presented in Chapter 4.

The other approach used in Section 3.3 was to model the impedance of the non-ideal S.I. by the circuit in Fig. 3.9. The impedance of the circuit in Fig. 3.9 was given previously in (3.70), but it is convenient here to make the substitution $p = j\omega$ in (3.70) and re-express the impedance as

$$Z = \frac{\dfrac{R_X R_Y}{R_X + R_Y} + \dfrac{j\omega L R_Y}{R_X + R_Y}}{1 + \dfrac{j\omega L}{R_X + R_Y}} \qquad (3.77)$$

Similarly, for $p = j\omega$, it is convenient to re-express the impedance in (3.76) for the non-ideal S.I. circuit as

$$Z_{IND} = \frac{\dfrac{a_0 - \omega^2 a_2}{b_0 - \omega^2 b_2} + \dfrac{j\omega a_1}{b_0 - \omega^2 b_2}}{1 + \dfrac{j\omega b_1}{b_0 - \omega^2 b_2}} \tag{3.78}$$

For the circuit in Fig. 3.9 to model the non-ideal impedance of the S.I. it is now obvious from eqns. (3.77) and (3.78) that the following relationships must hold

$$\begin{aligned} \frac{R_X R_Y}{R_X + R_Y} &= \frac{a_0 - \omega^2 a_2}{b_0 - \omega^2 b_2} \\ \frac{L R_Y}{R_X + R_Y} &= \frac{a_1}{b_0 - \omega^2 b_2} \\ \frac{L}{R_X + R_Y} &= \frac{b_1}{b_0 - \omega^2 b_2} \end{aligned} \tag{3.79}$$

From these relationships we now obtain the following expressions for R_X, R_Y, and L

$$\begin{aligned} R_Y &= a_1/b_1 \\ R_X(\omega) &= \frac{a_1(a_0 - \omega^2 a_2)}{(a_1 b_0 - b_1 a_0) - \omega^2(b_2 a_1 - b_1 a_2)} \\ L(\omega) &= \frac{a_1^2}{(a_1 b_0 - b_1 a_0) - \omega^2(b_2 a_1 - b_1 a_2)} \end{aligned} \tag{3.80}$$

When the non-ideal amplifier gain is taken into consideration we therefore find that for the model of Fig. 3.9 the resistance R_Y remains frequency independent, and the values for R_X and L both become frequency dependent. The frequency dependent inductance , however, may be replaced by the parallel combination of a frequency independent inductance L' and a frequency independent capacitance C' if

$$L' = \frac{a_1^2}{a_1 b_0 - b_1 a_0}$$

$$C' = \frac{(a_1 b_0 - b_1 a_0)(b_2 a_1 - b_1 a_2)}{a_1^2} \tag{3.81}$$

This gives rise to the new model in Fig. 3.10 for which the only frequency dependent component is the resistance $R_X(\omega)$.

With the help of the model in Fig. 3.10 the author was able to develope a novel compensation procedure for overcoming the effects of the non-ideal amplifier gain on the loss/frequency response of active filters containing S.A. S.C. S.I.s - this compensation procedure will be described later in Chapter 5.

3.5 SUMMARY AND CONCLUSIONS

In this chapter we presented some new circuits which simulate the impedance of a lossless positive grounded inductor using only one amplifier, one capacitor, and a number of resistors. As an alternative to the O/W and S/L circuits , one of the new circuits, circuit A, has the interesting feature that its inductance value can be varied over a positive and negative range by means of a single resistor, without affecting the conditions required for lossless inductor simulation. Futhermore , this new circuit is well suited to a straightforward functional adjustment procedure for overcoming the effects of passive component tolerances on the impedance. Another new circuit, circuit B, uses only six resistors , which is the same number as for the O/W circuit , and it has the feature that it is a special case of S.I. circuit A.

All the new S.I. circuits rely on two coefficient cancellations in their impedance expressions to obtain the correct simulation. Tolerances on the resistance values for the circuits cause these cancellations to be inexact and the simulation is no longer that of a lossless inductor. The impedance for the S.I. circuits under these conditions has been discussed in Section 3.3. The effects of the non-ideal voltage gain of the amplifier on the impedance of the S.I. circuits were briefly discussed in Section 3.4.

CHAPTER 4

A STUDY OF SIMULATED INDUCTOR CIRCUIT B

4.1 INTRODUCTION

In this chapter we carry out a study of one of the new S.I. circuits presented in Chapter 3, namely , S.I. circuit B.

In Section 4.2 we consider the amplifier in S.I. circuit B to be ideal and investigate the effects of passive component tolerances on the impedance. We then show how to choose the nominal component values for the circuit so that the effects of resistance tolerances on the impedance are reduced.

In Section 4.3 we consider the passive components in the S.I. circuit to have exactly their nominal values, i.e. zero tolerances, and investigate the effects of the non-ideal voltage gain of the amplifier on the impedance. Expressions for the $L(\omega)$ and $Q(\omega)$ behaviour are derived, and we show how to design the S.I. circuit so that the $Q(\omega)$ behaviour is improved.

In Section 4.4 we make a sensitivity study for S.I. circuit B. We take into consideration the non-ideal voltage gain of the amplifier and show how the $L(\omega)$ and $Q(\omega)$ behaviour change when the passive component values change from the nominal values.

In Section 4.5 we compare S.I. circuit B with two other S.I. circuits, namely , the Orchard/Willson circuit (see Section 2.3.1) and Antoniou's two-amplifier circuit (see Section 2.3.2). This comparison includes the $L(\omega)$ and $Q(\omega)$ behaviour for the circuits due to the non-ideal voltage gains for their amplifiers, and the sensitivities of the $L(\omega)$ and $Q(\omega)$ behaviour to the component values for the circuits.

A summary of the work presented in this chapter is given in Section 4.6.

4.2 EFFECTS OF PASSIVE COMPONENT TOLERANCES

In this section we consider the amplifier in S.I. circuit B to be ideal and investigate the effects of passive component tolerances on the impedance for the circuit.

4.2.1 TYPICAL EFFECTS OF PASSIVE COMPONENT TOLERANCES

In the ideal amplifier case S.I. circuit B has an impedance

$$Z = \frac{A_0 + pA_1}{B_0 + pB_1} \tag{4.1}$$

where

$$\begin{aligned} A_0 &= G_4G_2 - G_3G_5 - G_3G_1 \\ A_1 &= C_0G_4 \\ B_0 &= (G_1 + G_6)(G_4G_2 - G_3G_5) + G_1G_2G_6 \\ B_1 &= C_0(G_4G_2 - G_3G_5 - G_5G_6) \end{aligned} \tag{4.2}$$

Let us now choose the following nominal values for the passive components in the S.I. circuit:

	R_{1N}	R_{2N}	R_{3N}	R_{4N}	R_{5N}	R_{6N}	C_{0N}	
VALUE	10	5	10	10	10	10	4	(4.3)
UNITS	KΩ	KΩ	KΩ	KΩ	KΩ	KΩ	nF	

Note that the subscript N has been used in (4.3) to denote nominal capacitance and resistance values. The nominal conductance values G_{iN} may be calculated from the relationship $G_{iN} = 1/R_{iN}$ and then used in (4.2), along with the value for C_{ON}, to obtain the following nominal coefficient values:

	A_{ON}	A_{1N}	B_{ON}	B_{1N}
VALUE	0	4.10^{-13}	4.10^{-12}	0

(4.4)

From (4.1) we now find that the impedance is that of a lossless inductance having the nominal value $L_N = A_{1N}/B_{ON}$ = 100 mH.

Tolerances on the capacitance and resistance values for the S.I. circuit B will cause the coefficients in (4.1) not to have the nominal values in (4.4), and the impedance will no longer be that of a lossless inductance of value L_N. Various models which show the typical effects of the component tolerances were described in Section 3.3. One model, shown in Fig. 3.8(a), likens the non-ideal impedance to that of a frequency dependent resistance in series with a frequency dependent inductance. An alternative model is shown in Fig. 3.9, and this model has no frequency dependent component values. We will now adopt the model in Fig. 3.9 and give values for its components when each passive component in S.I. circuit B has, in turn, a 1% tolerance from its nominal value in (4.3). Note that for the model in Fig. 3.9 R_Y should be ideally infinite, R_X should be zero, and L equal to L_N.

From (4.2) we accurately calculate the values for A_0, A_1, B_0, and B_1 due to each component tolerance, and hence determine the errors ΔA_0, ΔA_1, ΔB_0, and ΔB_1 from the nominal coefficient values in (4.4). Then the values R_X, R_Y, and L for the model in Fig. 3.9 are calculated from eqns. (3.74). In this way we obtain the values shown in the Table in Fig. 4.1 (for convenience we show % changes in L due to each component tolerance instead of the actual inductance value). The largest value for $|R_X|$ is $50\,\Omega$ and this occurs for a 1% change in any one of the resistances R_2, R_3, and R_4 for the S.I. circuit. The smallest value for $|R_Y|$ is 0.5 $M\Omega$ and this occurs for 1% changes in R_2, R_4, and R_5. The % changes in the inductance value L_0 due to the 1% component tolerances lie in the region 1.5%. Note also, that the 1% changes in C_0 affect only the inductance value.

So far we have considered only the effects of individual tolerances, however, in practice the actual values for R_X, R_Y, and L are due to a combination of component tolerances. Although we do not know accurately each component value for S.I. circuit B, and hence the accurate values for R_X, R_Y, and L, we can still calculate the worst possible values for $|R_X|$, $|R_Y|$, and L due to the tolerances. The worst possible values for $|R_X|$ and $|R_Y|$ occur when the values for $|\Delta A_0|$ and $|\Delta B_1|$ are the largest possible, see equation (3.75). From the expressions for A_0 and B_1 in (4.2) we see that this is the case when the conductances G_2 and G_4 have a $\pm$ 1% change and the conductances G_1, G_3, G_5, and G_6 have a $\mp$ 1% change. The worst case (w.c) values calculated using (3.75) are then

$$
\begin{aligned}
|R_X|_{w.c} &\approx 200\ \Omega \\
|R_Y|_{w.c} &\approx 125\ k\Omega
\end{aligned}
\qquad (4.5)
$$

The changes shown in Fig. 4.1 suggest that the largest change in L occurs when R_1, R_2,R_6 and C_0 have a $\pm$ 1% change, and R_3 and R_5 have a $\mp$ 1% change. For this case we obtain the values for A_0 and B_1 using (4.2), and then from (3.75) we find that the largest error in L is approx. $\pm$ 5.0 %.

The model in Fig. 3.8 may also be used to describe the non-ideal impedance for S.I. circuit B due to 1% component tolerances. From (3.65) we see that the $|Q(\omega)|$ behaviour is worst when the values for ΔA_0 and ΔB_1 are as large as possible. Once again, this occurs when the conductances G_1, G_3, G_5, and G_6 have a $\mp$ 1% change, and G_2 and G_4 have $\pm$ 1% changes. Calculating ΔA_0 and ΔB_1 from (4.2) , and then making use of (3.65) , we obtain the worst case $|Q(\omega)|$ behaviour shown in Fig. 4.2. This behaviour shows that at 7.96 kHz the value for $|Q(\omega)|$ cannot be less than 12.5

4.2.2 REDUCING THE EFFECTS OF COMPONENT TOLERANCES

For the model in Fig. 3.9 R_X should ideally be zero, R_Y should be infinite, and L should be equal to the specified inductance value L_N. However , due to tolerances on the passive components for S.I. circuit B , the value for R_X will be non-zero, R_Y will be finite, and L will not be exactly equal to L_N. In this section we show how to choose the nominal component values for S.I. circuit B so that the worst possible values for $|R_X|$ and $|R_Y|$ due to component tolerances are minimised and maximised accordingly.

Previously in Section 3.3 we derived expressions for R_X and R_Y due to the coefficient errors A_0, A_1, B_0, and B_1 for the impedance expression in (4.1). The exact expressions for R_X and R_Y are given in (3.74), and approximations,which ignore second order effects, are given in (3.75). For convenience the approximate expressions are again repeated here, i.e.,

$$\begin{aligned} R_X &\approx \Delta A_0/B_{ON} \\ R_Y &\approx A_{1N}/\Delta B_1 \end{aligned} \tag{4.6}$$

Assuming R_X and R_Y to be given by the above approximations, the worst possible values for $|R_X|$ and $|R_Y|$ occur when the values for ΔA_0 and ΔB_1 are the largest possible.

The expressions for A_0 and B_1 in (4.2) show that this is the case when the conductances G_4 and G_2 differ by the fractional changes $\pm x$ from their nominal values, and the conductances G_1, G_3, G_5 and G_6 differ by $\mp x$ fractional changes. Note from (4.2) that a small fractional change x for the value for C_0 does not affect the value for ΔA_0, and it has only a second order effect on the value for ΔB_1.

Let us now denote the nominal conductance values as G_{iN} so that the actual conductance values G_i due to fractional changes $\pm x$, are given by

$$G_i = (1 \pm x) G_{iN} \tag{4.7}$$

Substituting the conductance values in (4.7), with the appropriate signs for x mentioned above, into the expression for A_0 in (4.2) gives

$$A_0 = G_{4N}(1 \pm x)G_{2N}(1 \pm x) - G_{3N}(1 \mp x)\, G_{5N}(1 \mp x) + G_{1N}(1 \mp x) \tag{4.8}$$

and for small values for x we can ignore terms in x^2 to give

$$A_0 = G_{4N}G_{2N} - G_{3N}(G_{5N} + G_{1N}) \pm 2x(G_{4N}G_{2N} + G_{3N}G_{5N} + G_{3N}G_{1N}) \tag{4.9}$$

We now note from (4.2) that the nominal value for A_0 is given by the expression

$$A_{0N} = G_{4N}G_{2N} - G_{3N}(G_{5N} + G_{1N}) = 0 \tag{4.10}$$

and we also note that the coefficient error ΔA_0 is given by the expression

$$\Delta A_0 = A_0 - A_{0N} \qquad (4.11)$$

Making use of eqns. (4.11), (4.10) and (4.9) gives the following expression for the largest possible value for $|\Delta A_0|$

$$|\Delta A_0|_{max} = 2x(G_{4N}G_{2N} + G_{3N}G_{5N} + G_{3N}G_{1N}) \qquad (4.12)$$

In a similar way we can show that the largest possible value for ΔB_1, due to the fractional changes $\pm$ x for the conductance values, is given by the expression

$$|\Delta B_1|_{max} = 2xC_{0N}(G_{4N}G_{2N} + G_{3N}G_{5N} + G_{3N}G_{6N}) \qquad (4.13)$$

Note that C_{0N} is the nominal value for C_0.

Expressions for the nominal values for A_1 and B_0 may be obtained from (4.2), i.e. we obtain

$$A_{1N} = C_{0N}G_{4N}$$

$$(4.14)$$

$$B_{0N} = (G_{1N} + G_{6N})(G_{4N}G_{2N} - G_{3N}G_{5N}) + G_{1N}G_{2N}G_{6N}$$

Now, substituting the expressions in (4.14), (4.13) and

(4.12) into (4.6) we obtain the following expressions for the worst case (w.c) values for $|R_X|$ and $|R_Y|$ due to the fractional changes $\pm$ x for the conductance values

$$|R_X|_{w.c} = \frac{2x(G_{4N}G_{2N} + G_{3N}G_{5N} + G_{3N}G_{1N})}{(G_{1N} + G_{6N})(G_{4N}G_{2N} - G_{3N}G_{5N}) + G_{1N}G_{2N}G_{6N}} \qquad (4.15)$$

$$|R_Y|_{w.c} = \frac{G_{4N}}{2x(G_{4N}G_{2N} + G_{3N}G_{5N} + G_{5N}G_{6N})} \qquad (4.16)$$

In Section 3.2.2 we showed that the nominal values G_{3N}, G_{4N}, G_{5N} and G_{6N} for S.I. circuit B could be chosen arbitrarily and the conditions $A_{0N} = 0$ and $B_{1N} = 0$ satisfied by choosing

$$\begin{aligned} G_{1N} &= G_{6N}G_{5N}/G_{3N} \\ G_{2N} &= G_{5N}(G_{3N} + G_{6N})/G_{4N} \end{aligned} \qquad (4.17)$$

Also, the specified inductance value L_N can always be obtained by choosing the nominal value for C_0 as

$$C_{0N} = \frac{L_N G_{6N}^2 G_{5N}(G_{3N}G_{4N} + G_{4N}G_{5N} + G_{3N}G_{5N} + G_{5N}G_{6N})}{G_{3N}G_{4N}^2} \qquad (4.18)$$

We will now show how to choose the values for G_{3N}, G_{4N}, G_{5N} and G_{6N} so that $|R_X|_{w.c}$ in (4.15) is as small as possible for any given values for x, and so that $|R_Y|_{w.c}$ in (4.16) is as large as possible.

Substituting the expressions for G_{1N} and G_{2N} in (4.17) into eqns. (4.15) and (4.16) gives

$$|R_X|_{w.c} = \frac{4xG_{3N}G_{4N}(G_{3N} + G_{6N})}{G_{6N}^2(G_{4N}G_{5N} + G_{3N}G_{4N} + G_{3N}G_{5N} + G_{5N}G_{6N})} \quad (4.19)$$

$$|R_Y|_{w.c} = \frac{G_{4N}}{4xG_{5N}(G_{3N} + G_{6N})} \quad (4.20)$$

Inspection of these expressions suggested that one way to achieve our objective is to choose large values for G_{4N} and G_{6N}, and to choose small values for G_{3N} and G_{5N}. For example let us choose $G_{4N} = G_{6N} = G_L$ and $G_{3N} = G_{5N} = G_S$. Substituting these values in (4.19) and (4.20) gives

$$|R_X|_{w.c} = \frac{4x(G_S + G_L)}{G_L(3G_L + G_S)} \quad (4.21)$$

$$|R_Y|_{w.c} = \frac{G_L}{4xG_S(G_S + G_L)} \quad (4.22)$$

These expressions show clearly that for large values for G_L

and small values for G_S, $|R_X|_{w.c}$ becomes small and $|R_Y|_{w.c}$ becomes large, i.e. from (4.21) and (4.22) we obtain

$$|R_X|_{w.c} \approx 4x/3G_L$$

$$|R_Y|_{w.c} \approx 1/4xG_S$$

The values for G_{1N}, G_{2N} and C_{0N} that are required when G_{3N}, G_{4N}, G_{5N} and G_{6N} are chosen in the way described previously, may be obtained from eqns. (4.17) and (4.18). The entire set of component values which achieves our objective is therefore

$$\begin{aligned} G_{1N} &= G_L \\ G_{2N} &= G_S(1 + G_S/G_L) \\ G_{3N} &= G_S \\ G_{4N} &= G_L \\ G_{5N} &= G_S \\ G_{6N} &= G_L \\ C_{0N} &= L_N G_S G_L(3 + G_S/G_L) \end{aligned} \qquad (4.23)$$

where G_L is large and G_S is small.

To show the advantages to be gained by designing S.I. circuit B in the way shown in (4.23) let us choose $L_N = 100$ mH, $G_L = 10^{-3}$ and $G_S = 10^{-5}$. Making use of (4.23) and the relationship $R_{iN} = 1/G_{iN}$, we obtain the following nominal component values for S.I. circuit B

	R_{1N}	R_{2N}	R_{3N}	R_{4N}	R_{5N}	R_{6N}	C_{ON}
VALUE	1	99.01	100	1	100	1	332.2
UNITS	KΩ	KΩ	KΩ	KΩ	KΩ	KΩ	pF

(4.24)

We now investigate how the impedance for S.I. circuit B changes, when each passive component value changes by $\pm$ 1.0 % (i.e., $x = 0.01$) from the nominal value in (4.24). Making use of eqns. (4.2) and (3.74) we calculate the values for R_X, R_Y and the % change in L for the model in Fig. 3.9. In this way we obtain the values shown in Fig. 4.3. We find that the values for R_X and R_Y are much closer to their ideal values, i.e. $R_X = 0$ and $R_Y = \infty$, than the values shown in Fig. 4.1 for the design example of Section 4.2.1, also, the % changes in L for the new design still lie in approximately the same range of values as for our previous example. The worst case values for $|R_X|$ and $|R_Y|$ due to combined tolerances were found to be

$$|R_X|_{w.c} = 13.33\ \Omega$$

$$|R_Y|_{w.c} = 2.50\ \mathrm{M}\Omega \qquad (4.25)$$

These values were calculated in the same way as the values in (4.5) for our previous design example, see Section 4.2.1. Note that the values in (4.25) are a significant improvement on those in (4.5). The worst case $|Q(\omega)|$ behaviour for the new design was also calculated in the way described in Section 4.2.1 for the previous design, and is shown in Fig. 4.4. At the frequency 8.0 kHz we find that $|Q(\omega)|$ cannot be less than 200 despite the 1.0 % component tolerances for S.I. circuit B.

4.3 EFFECT OF NON-IDEAL AMPLIFIER GAIN

In Section 3.2.2 we showed that the impedance for S.I. circuit B , when the non-ideal voltage gain μ of the amplifier is taken into consideration, is given by the expression

$$Z_{IND} = \frac{(A_0 + \varepsilon A_2) + p(A_1 + \varepsilon A_3)}{(B_0 + \varepsilon B_2) + p(B_1 + \varepsilon B_3)} \tag{4.26}$$

where

$$\begin{aligned}
A_0 &= G_4G_2 - G_3G_5 - G_3G_1 \\
A_1 &= C_0G_4 \\
A_2 &= (G_2 + G_3)(G_1 + G_4 + G_5) \\
A_3 &= C_0(G_1 + G_4 + G_5) \\
B_0 &= (G_1 + G_6)(G_4G_2 - G_3G_5) + G_1G_2G_6 \\
B_1 &= C_0(G_4G_2 - G_3G_5 - G_5G_6) \\
B_2 &= (G_2 + G_3)\left\{(G_4 + G_5)(G_1 + G_6) + G_1G_6\right\} \\
B_3 &= C_0\left\{(G_1 + G_2 + G_3 + G_6)(G_4 + G_5) + G_1(G_2 + G_3 + G_6)\right\}
\end{aligned} \tag{4.27}$$

and $\varepsilon = \mu^{-1} = \alpha + p/\omega_T$

In the following section we investigate the typical effects of the non-ideal voltage gain on the $L(\omega)$ and $Q(\omega)$ behaviour for S.I. circuit B. Then, in later sections, we will make use of eqns. (4.26) and (4.27) to derive expressions for this $L(\omega)$ and $Q(\omega)$ behaviour, and we will also describe a method of choosing the nominal passive component values for S.I. circuit B so that the $Q(\omega)$ behaviour due to the non-ideal gain is improved. As we are interested here only in the effects of the non-ideal voltage gain of the amplifier, we shall assume that the passive components in the S.I. circuit have exactly their nominal values, so that A_0 and B_1 in (4.26) are exactly zero as required for lossless inductor simulation in the ideal amplifier case.

4.3.1 TYPICAL EFFECTS OF NON-IDEAL AMPLIFIER GAIN

For the passive components in S.I. circuit B we chose the nominal values shown in Table (a) of Fig. 4.5, and for the non-ideal amplifier gain μ we chose $\alpha = 10^{-5}$ and $f_T = 10^6$ Hz (see (4.27)). The $Q(\omega)$ and $L(\omega)$ behaviour for this design were then evaluated at a number of frequencies using a computer analysis program. $L(\omega)$ is shown as curve 1 in Fig. 4.6 (a), and $Q(\omega)$ is shown as curve 1 in Fig. 4.6 (b). Ideally the inductance value should be 100 mH , however, we find that this is only approximately the case at low frequencies, and at higher frequencies the inductance value becomes larger. The largest value for $Q(\omega)$ is approximately 2000 and this occurs at about 300 Hz.

4.3.2 EXPRESSIONS FOR L(ω)

4.3.2.1 EXACT EXPRESSION FOR L(ω)

To derive an expression for L(ω) it is convenient to first of all express Z_{IND} in (4.26) in the form shown below where the substitution $p = j\omega$ has been made

$$Z_{IND} = \frac{(\alpha A_2 - \omega^2 A_3/\omega_T) + j\omega(A_1 + \alpha A_3 + A_2/\omega_T)}{(B_0 + \alpha B_2 - \omega^2 B_3/\omega_T) + j\omega(\alpha B_3 + B_2/\omega_T)} \qquad (4.28)$$

As the passive components for S.I. circuit B are assumed to have exactly their nominal values, we have not included the coefficients A_0 and B_1 in (4.28) as these are nominally zero. Strictly speaking, the subscript N should be used for the coefficients in (4.28) to denote nominal values, however, the subscripts have been omitted to avoid complexity in the mathematical expressions which follow. When Z_{IND} in (4.28) is rewritten in the form

$$Z_{IND} = R(\omega) + j\omega L(\omega) \qquad (4.29)$$

we obtain the following expression for L(ω)

$$L(\omega) = \frac{(B_0 + \alpha B_2 - \omega^2 B_3/\omega_T)(A_1 + \alpha A_3 + A_2/\omega_T) - (\alpha A_2 - \omega^2 A_3/\omega_T)(\alpha B_3 + B_2/\omega_T)}{(B_0 + \alpha B_2 - \omega^2 B_3/\omega_T)^2 + \omega^2(\alpha B_3 + B_2/\omega_T)^2}$$

(4.30)

When the expression in (4.30) is expanded, we find that the terms in α/ω_T appearing in the numerator have the coefficient

$$E = B_2A_2 + \omega^2B_3A_3 - B_2A_2 - \omega^2B_3A_3$$

which is exactly zero. Similarly, when the α/ω_T terms in the denominator of (4.30) are collected together we find that these also cancel. Our expression for $L(\omega)$ therefore reduces to

$$L(\omega) = \frac{A_1B_0 + \alpha(B_2A_1 + B_0A_3) + (A_2B_0 - \omega^2B_3A_1)/\omega_T + (\alpha^2 + \omega^2/\omega_T)(B_2A_3 - A_2B_3)}{B_0^2 + 2\alpha B_0B_2 - 2\omega^2B_0B_3/\omega_T + (\alpha^2 + \omega^2/\omega_T)(B_2^2 + \omega^2B_3^2)} \tag{4.31}$$

4.3.2.2 APPROXIMATION FOR $L(\omega)$

An approximation for the $L(\omega)$ behaviour in (4.31) can be obtained in the following way. For both the numerator and denominator in (4.31) we ignore the 2^{nd} order terms in α and $1/\omega_T$ but retain all the remaining terms. In this way we obtain

$$L(\omega) = \frac{A_1B_0 + \alpha(B_2A_1 + B_0A_3) + (A_2B_0 - \omega^2B_3A_1)/\omega_T}{B_0^2 + 2\alpha B_0B_2 - 2\omega^2B_0B_3/\omega_T} \tag{4.32}$$

To show that this expression approximates the actual inductance behaviour, we evaluated (4.32) at a number of frequencies . Choosing the values in Table (a) of Fig. 4.5 for the passive components in S.I. circuit B, and $\alpha = 10^{-5}$

and $f_T = 10^6$ Hz for the non-ideal amplifier gain, we calculate the values for the coefficients in (4.27), and then from (4.32) we obtain the approximated $L(\omega)$ behaviour shown as curve 2 in Fig. 4.6 (a). We find that the expression in (4.32) is, indeed, a very good approximation to the actual inductance behaviour which is shown as curve 1 in Fig. 4.6 (a).

4.3.3 EXPRESSIONS FOR $Q(\omega)$

4.3.3.1 EXACT EXPRESSION FOR $Q(\omega)$

The impedance expression in (4.28) may be re-written in the form $Z_{IND} = R(\omega) + j\omega L(\omega)$ and then , making use of the definition for $Q(\omega)$, i.e.,

$$Q(\omega) = \omega L(\omega)/R(\omega) \tag{4.33}$$

we obtain

$$Q(\omega) = \frac{\omega\left\{(B_0 + \alpha B_2 - \omega^2 B_3/\omega_T)(A_1 + \alpha A_3 + A_2/\omega_T) - (\alpha A_2 - \omega^2 A_3/\omega_T)(\alpha B_3 + B_2/\omega_T)\right\}}{(B_0 + \alpha B_2 - \omega^2 B_3/\omega_T)(\alpha A_2 - \omega^2 A_3/\omega_T) + \omega^2(A_1 + \alpha A_3 + A_2/\omega_T)(\alpha B_3 + B_2/\omega_T)} \tag{4.34}$$

When the numerator and denominator of the expression in (4.34) are expanded we find, once again, that the terms in α/ω_T cancel. Equation (4.34) therefore becomes

$$Q(\omega) = \frac{\omega\left\{A_1 B_0 + \alpha(A_1 B_2 + B_0 A_3) + (B_0 A_2 - \omega^2 A_1 B_3)/\omega_T + (\alpha^2 + \omega^2/\omega_T^2)(B_2 A_3 - A_2 B_3)\right\}}{\alpha(B_0 A_2 + \omega^2 A_1 B_3) + \omega^2(A_1 B_2 - B_0 A_3)/\omega_T + (\alpha^2 + \omega^2/\omega_T^2)(A_2 B_2 + \omega^2 A_3 B_3)} \tag{4.35}$$

For the passive component values in Table (a) of Fig. 4.5 , and $\alpha = 10^{-5}$ and $f_T = 10^6$ Hz, we calculated the values for the the coefficients in (4.27), and then (4.35) was evaluated at a number of frequencies. The $Q(\omega)$ behaviour obtained in this way was found to be identical to the $Q(\omega)$ behaviour obtained using a computer analysis program, i.e. see curve 1 in Fig. 4.6 (b).

4.3.3.2 APPROXIMATION FOR $Q(\omega)$

An approximation for the Q-factor expression in (4.35) can be obtained in the following way. For the numerator in (4.35) we retain the term that is independent of α and $1/\omega_T$, and ignore the 1st and 2nd order terms in α and $1/\omega_T$ - for the denominator we retain the 1st order terms in α and $1/\omega_T$ and ignore the 2nd order terms. In this way we obtain

$$Q(\omega) = \frac{\omega A_1 B_0}{\alpha(B_0 A_2 + \omega^2 A_1 B_3) + \omega^2 (A_1 B_2 - B_0 A_3)/\omega_T} \tag{4.36}$$

For a specified frequency range this expression can always be made valid by choosing sufficiently small values for α and $1/\omega_T$ - at higher frequencies the approximation breaks down as shown by the exact expression for $Q(\omega)$ in (4.35).

It is interesting to determine the $Q(\omega)$ values that are obtained from the approximation in (4.36) when the passive components in the S.I. circuit have the nominal values shown in Table (a) of Fig. 4.5, and $\alpha = 10^{-5}$ and $f_T = 10^6$ Hz. Calculating the coefficient values from (4.27), and then using the expression in (4.36), we obtain the approximated $Q(\omega)$ behaviour shown as curve 2 in Fig. 4.6 (b). The agreement with the actual $Q(\omega)$ behaviour, curve 1 in Fig. 4.6 (b), is quite close over the frequency range 0.0 Hz to about 2.0 kHz when the discrepancy is approximately 10 % of the actual $Q(\omega)$ value.

4.3.4 DESIGN FOR IMPROVING $Q(\omega)$

Inspection of the approximation in (4.36) suggested that the actual $Q(\omega)$ behaviour might be improved by designing the S.I. circuit B so that the term in ω^2/ω_T in (4.36) was zero. We will, of course, still have to design the S.I. circuit so that it has the nominal inductance value L_N, and so that the coefficients A_0 and B_1 are both zero as required for lossless inductor simulation in the ideal amplifier case. The coefficient for the ω^2/ω_T term in (4.36) , which we shall now call T , can be made to be zero in the following way.

From (4.36) we note that T is given by the expression

$$T = A_1B_2 - B_0A_3 \tag{4.37}$$

and substituting for A_1, B_2, B_0 and A_3 from (4.27) we obtain

$$T = C_0 \left\{ \begin{array}{l} G_4(G_2 + G_3)\left[(G_4 + G_5)(G_1 + G_6) + G_1G_6\right] \quad - \\ (G_1 + G_4 + G_5)\left[(G_1 + G_6)(G_4G_2 - G_3G_5) + G_1G_2G_6\right] \end{array} \right\} \tag{4.38}$$

In Section 3.2.2 we showed that for arbitrary values for G_3, G_4, G_5 and G_6 , the coefficients A_0 and B_1 could be made zero by choosing G_1 and G_2 as

$$\begin{aligned} G_1 &= G_5G_6/G_3 \\ G_2 &= G_5(G_3 + G_6)/G_4 \end{aligned} \tag{4.39}$$

We also showed that the desired inductance value L_N could be obtained by choosing C_0 as

$$C_0 = \frac{L_N G_6^2 (G_3 G_4 G_5 + G_3^2 G_4 + G_3 G_5^2 + G_5^2 G_6)}{G_3 G_4^2} \tag{4.40}$$

When the expressions for G_1 and G_2 in (4.39) are substituted into (4.38) we obtain

$$T = \frac{C_0 (G_3 G_4 + G_3 G_5 + G_5 G_6)\left\{G_6^2 G_5^2 + G_6 G_5^2 (G_3 + G_4) - G_3 G_4 (G_4 + G_5)(G_3 + G_5)\right\}}{G_3^2} \tag{4.41}$$

This expression shows that for any arbitrary positive values for G_3, G_4 and G_5, T can be made to be zero by choosing G_6 to have the positive value that is obtained as a solution of the following quadratic in G_6.

$$G_6^2 G_5^2 + G_6 G_5^2 (G_3 + G_4) - G_3 G_4 (G_4 + G_5)(G_3 + G_5) = 0 \tag{4.42}$$

Note that the solution of this equation always leads to one positive value for G_6. Hence, our proposed design procedure is to choose arbitrary positive values for G_3, G_4 and G_5, then solve the quadratic in G_6 in (4.42) to make T = 0, and finally the conditions $A_0 = 0$, $B_1 = 0$, and $L = L_N$ are achieved by choosing G_1, G_2 and C_0 in the way shown in (4.39) and (4.40). We should remember , however, that when C_0 is chosen in the way shown in (4.40) the actual $L(\omega)$ values will only be approximately equal to L_N because of the non-ideal voltage gain for the amplifier.

To show the improvement in $Q(\omega)$ when the above approach is used , we designed S.I. circuit B in the following way. First of all the component values G_3, G_4 and G_5 were chosen as in Table (a) of Fig. 4.5, i.e., the same as for the design example studied in Section 4.3.1. The conductances G_6, G_1 and G_2 were then calculated using eqns. (4.42) and (4.39), and C_0 was determined from (4.40) using the same value for L_N as in our previous design example,i.e., $L_N = 100$ mH. In this way we obtained the set of nominal passive component values shown in Table (b) of Fig. 4.5. Once again we chose $\alpha = 10^{-5}$ and $f_T = 10^6$ Hz for the non-ideal amplifier gain, see (4.27), and then we determined the $L(\omega)$ and $Q(\omega)$ behaviour using a circuit analysis program. The inductance behaviour for the new design is shown in Fig. 4.7 (a), and we find that it is very similar to the behaviour for the design example of Section 4.3.1, i.e., see curve 1 in Fig. 4.6 (a). The new $Q(\omega)$ behaviour is shown as curve 1 in Fig. 4.7 (b), and we find that this is a significant improvement on the previous behaviour shown as curve 1 in Fig. 4.6 (b).

When the ω^2/ω_T term in (4.36) is zero our approximation for $Q(\omega)$ reduces to

$$Q(\omega) = \frac{\omega A_1 B_0}{\alpha(B_0 A_2 + \omega^2 A_1 B_3)} \qquad (4.43)$$

It is of interest to compare the approximate $Q(\omega)$ values obtained from this expression with the actual $Q(\omega)$ values. By numerical evaluation of (4.43) we obtain curve 2 in Fig. 4.7 (b). Comparing this curve with curve 1 in Fig.4.7(b) we find that the approximation is still valid at low frequencies but at high frequencies it breaks down.

4.3.5 DESIGN FOR OBTAINING $Q(\omega)_{max}$ AT A SPECIFIED FREQUENCY

In this section we discuss how to choose the nominal passive component values for S.I. circuit B so that the Q-factor has its maximun value $Q(\omega)_{max}$ at a specified operating frequency f_{op}.

4.3.5.1 INITIAL ASSUMPTIONS

Let us assume that in the frequency range of interest the inductance behaviour $L(\omega)$ can be approximated by the expression in (3.24) for the ideal amplifier case, i.e.,

$$L(\omega) = L = \frac{C_0 G_4}{(G_1 + G_6)(G_4 G_2 - G_3 G_5) + G_1 G_2 G_6} \tag{4.44}$$

Let us also assume that the design procedure of Section 4.3.4 has been carried out, and that the $Q(\omega)$ behaviour can be approximated by the expression in (4.43), i.e.,

$$Q(\omega) = \frac{\omega A_1 B_0}{\alpha(B_0 A_2 + \omega^2 A_1 B_3)} \tag{4.45}$$

The largest value for the Q-factor expression in (4.45) is

$$Q(\omega)_{max} = \frac{1}{2\alpha} \sqrt{\frac{A_1 B_0}{A_2 B_3}} \tag{4.46}$$

and this occurs at the frequency ω_{max} given by

$$\omega_{max} = \sqrt{\frac{B_0 A_2}{A_1 B_3}} \qquad (4.47)$$

When the expressions for A_1, A_2, B_0 and B_3 in (4.27) are substituted into (4.46) and (4.47) we obtain

$$Q(\omega)_{max} = \frac{1}{2\alpha} \cdot \frac{G_4\left\{(G_2 + G_3)(G_4G_2 - G_3G_5) + G_1G_2G_6\right\}}{(G_2 + G_3)(G_1 + G_4 + G_5)\left\{\begin{array}{l}(G_4 + G_5)(G_1 + G_2 + G_3 + G_6) \\ + \; G_1(G_2 + G_3 + G_6)\end{array}\right\}} \qquad (4.48)$$

$$\omega_{max} = \frac{1}{C_0} \cdot \frac{(G_2 + G_3)(G_1 + G_4 + G_5)\left\{(G_1 + G_6)(G_4G_2 - G_3G_5) + G_1G_2G_6\right\}}{G_4\left\{(G_4 + G_5)(G_1 + G_2 + G_3 + G_6) + G_1(G_2 + G_3 + G_6)\right\}} \qquad (4.49)$$

4.3.5.2 OUTLINE OF DESIGN PROCEDURE

First of all we introduce a reference conductance G_0 so that we obtain the normalised conductance values

$$K_i = G_i/G_0 \qquad (4.50)$$

where $i = 1$ to 6. Rewriting (4.39) in normalised form we find that the coefficients A_0 and B_1 will be zero if we choose

$$K_1 = K_5K_6/K_3$$
$$K_2 = K_5(K_3 + K_6)/K_4 \qquad (4.51)$$

Also, condition (4.42) for improving $Q(\omega)$ becomes a quadratic in K_6, i.e.,

$$K_6^2K_5^2 + K_6K_5^2(K_3 + K_4) - K_3K_4(K_4 + K_5)(K_3 + K_5) = 0 \tag{4.52}$$

and eqns. (4.44) and (4.49) for L and ω_{max} become

$$L = M_1C_0/G_0^2 \tag{4.53}$$

$$\omega_{max} = \frac{G_0}{C_0}\sqrt{M_2} \tag{4.54}$$

where

$$M_1 = \frac{K_4}{(K_1 + K_6)(K_4K_2 - K_3K_5) + K_1K_2K_6} \tag{4.55}$$

$$M_2 = \frac{(K_2 + K_3)(K_1 + K_4 + K_5)\left\{(K_1 + K_6)(K_4K_2 - K_3K_5) + K_1K_2K_6\right\}}{K_4\left\{(K_4 + K_5)(K_1 + K_2 + K_3 + K_6) + K_1(K_2 + K_3 + K_6)\right\}} \tag{4.56}$$

Note that the values for M_1 and M_2 in (4.55) and (4.56) depend only on the normalised conductance values and not on the values for G_0 and C_0. The conditions in (4.51) and (4.52) also depend only on the K_i values and not on G_0 nor C_0.

The following procedure can now be used to design the S.I. circuit B so that ω_{max}, the frequency at which $Q(\omega)_{max}$ occurs, is equal to the desired frequency ω_{op}. We start by assuming that the values for K_3, K_4 and K_5 are given (the best choice for these values will be discussed later in Section 4.3.6.2). For these values we solve the quadratic in (4.52) to obtain the value for K_6. Then the values for K_1 and K_2 are found from (4.51), and this enables us to evaluate M_1 and M_2 using eqns. (4.55) and (4.56). From eqns. (4.53) and (4.54) we now find that the values for G_0 and C_0 which give rise to $L = L_N$ and $\omega_{max} = \omega_{op}$ are

$$G_0 = \frac{M_1 M_2}{\omega_{op} L_N} \tag{4.57}$$

$$C_0 = \frac{M_1 M_2^2}{\omega_{op}^2 L_N} \tag{4.58}$$

Having found G_0 we can obtain the actual conductance values G_i using (4.50).

4.3.6 SOME DESIGN EXAMPLES

To demonstrate the design procedure of Section 4.3.5 let us consider the following example. We shall specify that the S.I. circuit is to have an inductance value L_N = 100 mH, and that $Q(\omega)_{max}$ is to occur for f_{op} = 1.0 kHz. For the non-ideal amplifier gain we will choose $\alpha = 10^{-5}$ and $f_T = 10^6$ Hz, as in the design examples of Sections 4.3.1 and 4.3.4.

4.3.6.1 INITIAL DESIGN

Previously, in Section 4.3.5.2, we mentioned that the values for K_3, K_4, and K_5 could be chosen arbitrarily in the design procedure for obtaining $Q(\omega)_{max}$ at a specified frequency. The best choice for these values will be discussed later in Section 4.3.6.1 but, as an initial design example, let us choose here $K_3 = K_4 = K_5 = 1$. For these values we obtain from (4.52) $K_6 = 1.23607$, and then from (4.51) we obtain $K_1 = 1.23607$ and $K_2 = 2.23607$. Using the values for K_1 to K_6 in eqns. (4.55) and (4.56) gives $M_1 = 0.154508$ and $M_2 = 2.000000$, and then from eqns. (4.57) and (4.58) we obtain $G_0 = 4.91816\ 10^{-4}$ ℧, and $C_0 = 1.56550\ 10^{-7}$ F. Finally, the actual conductance values G_i are obtained from (4.50), and making use of the relationship $R_i = 1/G_i$ we we obtain the set of nominal passive component values shown in the Table in Fig. 4.8.

The $L(\omega)$ and $Q(\omega)$ behaviour for the above design were determined by a computer circuit analysis program and are shown in Figs. 4.9 (a) and (b). We find that the actual $Q(\omega)$ behaviour reaches its largest value at approximately 800 Hz instead of the specified frequency of 1.0 kHz. This error arises because we used the approximations for $L(\omega)$ and $Q(\omega)$ in (4.44) and (4.45) in the design of the S.I. circuit. A design based on more accurate approximation for $L(\omega)$ and $Q(\omega)$ has not been attempted.

4.3.6.2 IMPROVING $L(\omega)$ AND $Q(\omega)$ BY INTRODUCING A LARGER RESISTANCE SPREAD

For the design example of Section 4.3.6.1 we specified $L_N = 100$ mH, $f_{op} = 1.0$ kHz, and we chose K_3, K_4 and K_5 to be equal to unity. By retaining $K_3 = K_5 = 1$ and choosing $K_4 = m$, where m is large compared to one, we found that the overall behaviour for both $L(\omega)$ and $Q(\omega)$ were improved. Computed $L(\omega)$ and $Q(\omega)$ curves for m = 1, 5, 10 and 100 are shown in Figs. 4.10 and 4.11. The component values for S.I. circuit B corresponding to these values for m are shown in the Tables in Fig. 4.12.

The curves in Figs. 4.10 and 4.11 show clearly that there is some advantage in choosing a reasonably large value for m. However, we should note that as m is made large the resistance spread for the S.I. circuit is increased (see Fig. 4.12) and in some cases this may be undesirable. Note also that for values of m larger than 10,the $L(\omega)$ and $Q(\omega)$ behaviour are not much more improved.

4.3.6.3 DESIGNS FOR DIFFERENT OPERATING FREQUENCIES

For the design example of Section 4.3.6.1 we specified L_N = 100 mH and f_{op} = 1.0 kHz, and the design procedure of Section 4.3.5 was carried out using $K_3 = K_4 = K_5 = 1.0$. For the example of Section 4.3.6.2 the design specification was the same but different values for K_4 were used. In this Section we will keep L_N = 100 mH , choose $K_3 = K_5 = 1$ and $K_4 = 10$, and investigate the design procedure of Section 4.3.5 for three different operating frequencies, i.e., f_{op} = 100 H_z, 1.0 kHz and 10.0 kHz.

The component values which are obtained when S.I. circuit B is designed in the way mentioned above, are shown in the Tables in Fig. 4.13. Once again, the $L(\omega)$ and $Q(\omega)$ behaviour for the designs were determined using a computer circuit analysis program. The curves in Fig. 4.14 show the $Q(\omega)$ behaviour plotted against a normalised frequency f/f_{op}. The curve for f_{op} = 100 Hz shows that $Q(\omega)$ reaches its largest value exactly at the specified operating frequency. This suggests that the design procedure of Section 4.3.5 is successful for low operating frequencies. For higher operating frequencies, i.e. f_{op} = 1.0 kHz, the design procedure still works reasonably well and the Q-factor reaches its peak at a frequency close to the specified operating frequency. However , for high values for f_{op}, i.e. f_{op} = 10 kHz, we find that the design procedure of Section 4.3.5 is unsatisfactory.

It is interesting to show the variation of inductance by two different representations. Fig. 4.15 shows the $L(\omega)$ behaviour for each design example plotted against f/f_{op}, and Fig. 4.16 shows the $L(\omega)$ behaviour plotted against frequency f. The curves in Fig. 4.15 show that the actual inductance value is closer to the specified value for designs based on a low operating frequency. However, when S.I. circuit B is designed using a high value for f_{op} we find that the inductance value remains more constant over a greater range of frequency as shown by the curves in Fig. 4.16.

4.4 COMBINED EFFECTS OF NON-IDEAL AMPLIFIER GAIN AND COMPONENT TOLERANCES

In this Section we investigate how the $L(\omega)$ and $Q(\omega)$ behaviour, due to the non-ideal amplifier gain, are affected when the passive component values for S.I. circuit B change from their nominal values. We will also investigate how the $L(\omega)$ and $Q(\omega)$ behaviour change when the f_T value for the amplifier changes from its nominal value. As an example for study we will choose the values in Fig. 4.8 for the passive components in the S.I. circuit, with $\alpha = 10^{-5}$ and $f_T = 10^6$ Hz for the non-ideal amplifier gain. These values are for the design example studied in Section 4.3.6.1 where we specified L_N = 100 mH and f_{op} = 1.0 kHz, and chose $K_3 = K_4 = K_5 = 1$; the nominal $L(\omega)$ and $Q(\omega)$ behaviour for this design are shown in Figs. 4.9 (a) and (b).

We now investigated the effects of ± 1.0 % changes in the passive component values on the $L(\omega)$ behaviour. Using a computer circuit analysis program , we found that, at the operating frequency f_{op} = 1.0 kHz, the ± 1.0 % passive component changes produce the % changes in $L(\omega)$ shown in the Table in Fig. 4.17. The changes in $L(\omega)$ are all reasonably small, i.e., the magnitude for the largest % change in $L(\omega)$ is only 1.4. We also investigated the effects of ± 10.0 % changes in f_T, but we found that the % changes in $L(\omega)$ for $f = f_{op}$ were extremely small.

Rather than determining the % changes in $Q(\omega)$

produced by the component tolerances, for $f = f_{op}$, it is more interesting to show the actual changes produced in the overall $Q(\omega)$ behaviour. When the resistance values R_1 to R_5 are altered by $\pm$ 0.001% and $\pm$ 1.0 %, and R_6 is altered by $\pm$ 0.01 % and $\pm$ 1.0 %, we obtain the changes in $Q(\omega)$ shown in Figs. 4.18 (a) to (f). The effects of $\pm$ 10.0 % changes in C_0 and f_T are shown in Figs. 4.18 (g) and (h). We find that the 1.0 % changes in the resistance values cause large changes in $Q(\omega)$ whereas the 10.0 % changes in C_0 and f_T have only a small effect on the $Q(\omega)$ values. This is because the resistance changes cause the coefficients A_0 and B_1 in (4.26) not to be nominally zero, whereas the changes in C_0 and f_T do not affect the values for A_0 and B_1 , see (4.27)(note that the general $Q(\omega)$ behaviour due to the coefficient errors ΔA_0 and ΔB_1 has been previously investigated in Section 3.3).

For the small changes in the resistance values, i.e. 0.001 %, we find from Figs. 4.18 (a) to (f) that the changes in $Q(\omega)$ are very much smaller as expected. Nevertheless, these small resistance changes can still give rise to significant changes in the frequency at which the maximum value for $Q(\omega)$ occurs. This shows that the design procedure in Section 4.3.5, for obtaining $Q(\omega)_{max}$ at a specified frequency, depends on extremely close matching of the resistance values in the circuit(Orchard and Willson have pointed out (26) that this is also true for their S.I. circuit). In view of this, the design procedure of Section 4.3.5 is very unlikely to be of use in practice.

Although small variations in the values for the resistors in S.I. circuit B can give rise to large changes in $Q(\omega)$, the changes they produce in the loss/frequency response of active filters containing these S.I. circuits may be very much smaller. Later on in the thesis , i.e. in Chapter 7, we will show that this is indeed the case, and that one can obtain active-RC filters which are suitable for practical realisation.

4.5 COMPARISION WITH OTHER SIMULATED INDUCTOR CIRCUITS

In this Section we compare S.I. circuit B with two other S.I. circuits, namely, the Orchard/Willson circuit of Section 2.2.1, and Antoniou's two-amplifier circuit described in Section 2.2.2. We will compare the $L(\omega)$ and $Q(\omega)$ behaviour for these circuits due to the non-ideal voltage gain for their amplifiers, and we will also compare the sensitivities of the $L(\omega)$ and $Q(\omega)$ values to the passive component values and the f_T values for the circuits.

4.5.1 $L(\omega)$ AND $Q(\omega)$ BEHAVIOUR

All three S.I. circuits mentioned above were designed to meet the same specification, i.e. L_N = 100 mH and f_{op} = 1.0 kHz. For the non-ideal voltage gain for the amplifiers in the circuits we chose $\alpha = 10^{-5}$ and $f_T = 10^6$ Hz. The Orchard/Willson circuit was designed in the way suggested by the originators in (26) and the Antoniou circuit was designed in the way suggested by Bruton in (49). The component values that arise from these design procedures are given in Tables (a) and (b) of Fig. 4.19. In the design procedure for the O/W circuit the spread in the resistance values was restricted to 100 : 1. S.I. circuit B has already been designed to meet the above specification for a similar resistance spread, see Section 4.3.6.2, and for comparision purposes its component values are shown again in Table (c) of Fig. 4.19.

The $L(\omega)$ and $Q(\omega)$ behaviour for all three S.I.s were obtained by computational circuit analysis and are shown in Figs. 4.20 and 4.21. We find that S.I. circuit B has slightly higher $Q(\omega)$ values than the Orchard/Willson circuit, and slightly worse values than those for Antoniou's circuit. Also, the $L(\omega)$ behaviour S.I. circuit B is practically identical to the behaviour for Antoniou's circuit, and more constant with frequency than the $L(\omega)$ behaviour for Orchard and Willsons' circuit(recently Haigh and Kunes have pointed out that the inductance behaviour for Antoniou's circuit can be made more constant with frequency by introducing a larger resistance spread into its design (50)).

4.5.2 L(ω) AND Q(ω) SENSITIVITIES

The changes in $L(\omega)$ and $Q(\omega)$ for S.I. circuit B due to changes in its component values, have already been investigated in Section 4.4. For the design example studied in that section we found that for $f = f_{op} = 1.0$ kHz, and for 1.0 % changes in the passive component values, we obtain the % changes in $L(\omega)$ shown in the Table in Fig. 4.17. The magnitude for the largest % change in $L(\omega)$ is only 1.4. The effects of changes in the passive component values on the $Q(\omega)$ behaviour are shown in Figs. 4.18 (a) to (g), and the effects on $Q(\omega)$ of changes in the f_T value are shown in Fig. 4.18 (h). We pointed out in Section 4.4 that the large changes in $Q(\omega)$ produced by the 1.0 % resistance changes, arise because of the errors ΔA_0 and ΔB_1 in the impedance expression for S.I. circuit B, see (4.26) and (4.27).

The impedance for Antoniou's S.I. circuit, for the ideal amplifier case , is given by

$$Z = pL = \frac{pC_0R_1R_2R_3}{R_4} \tag{4.59}$$

This expression shows that 1.0 % changes in the passive component values give rise to either $\pm$ 1.0 % or $\mp$ 1.0 % changes in the inductance value L. When the non-ideal voltage gains for the amplifiers in Antoniou's circuit are taken into consideration, we would expect similar % changes for $L(\omega)$. The % changes in $L(\omega)$ for Antoniou's circuit should therefore be similar to those in Fig. 4.17 for S.I. circuit B. However, unlike S.I. circuit B, the Antoniou circuit does not make use of coefficient cancellations in its impedance expression, and we would expect the effects of component tolerances on its $Q(\omega)$ behaviour to be very much smaller than the effects shown in Figs. 4.18 (a) to (h). To show this we chose the values in Table (b) of Fig. 4.19 for the passive components in Antoniou's circuit, and we investigated the effects of $\pm$ 1.0 % changes in these values on the nominal $Q(\omega)$ behaviour. The nominal $Q(\omega)$ behaviour is shown in Fig. 4.21 and this is for amplifiers having $\alpha = 10^{-5}$ and $f_T = 10^6$ Hz. Using a computer circuit analysis program we found that the changes in R_1 do not affect $Q(\omega)$. The changes in R_2 and R_3 produce the curves in Figs. 4.22 (a) and (b), and for the changes in R_4 and C_0, $Q(\omega)$ is affected so little that the $Q(\omega)$ changes are not shown. The largest changes produced in $Q(\omega)$ are for R_2 and R_3 and, as expected, they are very much smaller than the changes shown in Figs. 4.18 (a) to (f) for S.I. circuit B.

The effects of component tolerances on the $L(\omega)$ and $Q(\omega)$ behaviour for the Orchard/Willson S.I. circuit have not been determined, however, we would expect these effects to be similar to those for S.I. circuit B as both circuits achieve inductor simulation in the same way, i.e., by means of the conditions $A_0 = 0$ and $B_1 = 0$ in their impedance expressions.

4.6 SUMMARY

In Section 4.2 we considered the amplifier in S.I. circuit B to be ideal, we chose an experimental design for the circuit, and then we investigated the effects of passive component tolerances on the impedance. After this investigation we showed how to choose the nominal passive component values for S.I. circuit B so that the effects of tolerances on the impedance were reduced.

In Section 4.3 we considered the passive component tolerances for S.I. circuit B to be zero, and we investigated the effects of the non-ideal voltage gain for the amplifier on the impedance. A design procedure for improving the overall $Q(\omega)$ behaviour was described, and we also showed how to design S.I. circuit B so that $Q(\omega)$ had its largest value at a specified operating frequency f_{op}. This later design procedure, however, depends on extremely close matching of the resistance values for the S.I. circuit, and it is unlikely to be useful in practice.

In Section 4.4 we again took the non-ideal voltage gain for the amplifier into consideration, and we investigated how the $L(\omega)$ and $Q(\omega)$ behaviour change when the passive component values change from their nominal values. We also investigated the effects of f_T variations on $L(\omega)$ and $Q(\omega)$. The large changes in $Q(\omega)$ due to the resistance changes, arise because of errors for the values of the coefficients A_0 and B_1 in the impedance expression for S.I. circuit B, see (4.26) (note that A_0 and B_1 are both nominally zero).

In Section 4.5 we compared S.I. circuit B with Antoniou's two-amplifier S.I. circuit and Orchard and Willsons' single-amplifier S.I. circuit. We showed that all three S.I.s have similar $L(\omega)$ and $Q(\omega)$ behaviour due to the non-ideal voltage gain for their amplifiers. We also showed that the effects of component value changes on the $L(\omega)$ behaviour are similar, however, Antoniou's two-amplifier circuit has much better $Q(\omega)$ sensitivities to its resistance values and this is why it is preferred to the other circuits, in scme applications.

CHAPTER 5

FILTER DESIGN USING SIMULATED BIQUADRATIC IMPEDANCES

5.1 INTRODUCTION

In Chapter 3 we described some single-amplifier, single-capacitor, networks for simulating the impedance of a lossless inductor. The simulation, however, is exact only if the amplifiers in the simulation networks are considered ideal. When the non-ideal voltage gain for the amplifiers is taken into consideration, the impedance for the simulating networks becomes a biquadratic expression in p , and only approximates the impedance of an ideal inductance over a limited frequency range. In this chapter we take into consideration the non-ideal amplifier gain, and deliberately re-design the simulation networks of Chapter 3 to have a specific biquadratic impedance. We then show how various types of LC filters, with their terminating resistors, may be modified so as to produce the required loss/frequency response using these biquadratic impedances instead of the originally required inductors.

The specific biquadratic impedance function chosen for the simulating networks is discussed in Section 5.2, and the way of modifying LC filters to include the biquadratic impedances is described in Section 5.3. In Section 5.4 we show how to design some simulating networks so that they have the required specific biquadratic impedance. As these simulating networks now have, ideally, a specific biquadratic impedance, and are no longer required to simulate an ideal inductor, we shall henceforward refer to these networks as 'S.B.I.' circuits where S.B.I. is an abbreviation for simulated biquadratic impedance.

An advantage of the approach mentioned above is that the non-ideal voltage gain for the amplifiers in the simulating networks, is taken into consideration in the design of the active filter. For bandpass filters using the S.B.I. circuits, the passband loss/frequency response is correct at the frequencies of maximum power transfer for the original LC filter. The response at other frequencies may be incorrect but a high degree of compensation for the non-ideal voltage gain of the amplifiers can still be obtained. For highpass filters complete compensation for the non-ideal voltage gain can be obtained over the entire frequency range in which the gain of the amplifier can be adequately described by a single-pole model. Even in the case of two-amplifier S.I.s this has not been achieved, as these circuits are usually designed to offer compensation for the non-ideal amplifier gain only in the neighourhood of a particular frequency (49).

5.2 THE S.B.I. CIRCUIT

When the amplifier is considered ideal the single-amplifier, single-capacitor, simulation networks discussed in this thesis have an impedance of the general form

$$Z = \frac{A_0 + pA_1}{B_0 + pB_1} \tag{5.1}$$

and the design criteria

$$A_0 = 0 \ , \ B_1 = 0 \ , \ A_1/B_0 > 0 \qquad (B_0 \neq 0) \tag{5.2}$$

are needed to give lossless positive inductor simulation. When the non-ideal voltage gain for the amplifier is taken into consideration, the impedance for the simulation networks becomes

$$Z = \frac{a_0 + a_1 p + a_2 p^2}{b_0 + b_1 p + b_2 p^2} \tag{5.3}$$

as pointed out in Section 3.4. The design criteria in (5.2) are only applicable for the <u>ideal</u> amplifier case, and a different approach will be used for the non-ideal amplifier case.

For reasons which will become apparent our design criteria for the non-ideal amplifier case will be

$$a_0 = 0 \ , \ b_1 = 0 \ , \ a_1/b_0 > 0, \ a_2/b_0 > 0 \ , \ b_2/b_0 > 0 \tag{5.4}$$

where b_0 is non-zero. When these conditions are satisfied the impedance Z in (5.3) becomes

$$Z = \frac{a_1 p(1 + pa_2/a_1)}{b_0(1 + p^2 b_2/b_0)} \tag{5.5}$$

and this expression can be rewritten as

$$Z = \frac{pL(1 + p\tau)}{1 + p^2 LC} \tag{5.6}$$

where

$$L = a_1/b_0 \;,\; C = b_2/a_1 \;,\; \tau = a_2/a_1 \tag{5.7}$$

Note from (5.4) and (5.7) that the values for L, C and τ are positive. Rather than regarding the simulation networks with the impedance in (5.6) as non-ideal S.I.s, we now regard them as ideal specific biquadratic impedances called 'S.B.I.s'. Equation (5.6) shows that the impedance of the S.B.I.s is the same as that for a parallel LC resonator whose impedance is scaled, i.e. multiplied, by a factor $(1 + p\tau)$.

In addition to the criteria in (5.4) it will be necessary, in general, to design the S.B.I.s in a filter so that they each have a different specified value for L. It is also important that the time constant τ, which has the dimension of an RC product, has the same value for all S.B.I.s in a filter irrespective of the different L values. For any initial design for the S.B.I. circuit, other designs having different L values but the same value for τ can be obtained by scaling the impedances of the resistors and capacitor in the S.B.I. circuit by the same constant. Impedance scaling does not affect the value for τ because it has the dimension RC, but it does affect the value for C in (5.6). When an S.B.I. circuit is designed to have a specified value for L, i.e. $L = L_N$, we shall write Z_N for the impedance in (5.6) and we shall write the values for C and τ in (5.6) as C_N and τ_N.

5.3 FILTER DESIGN USING S.B.I. CIRCUITS

5.3.1 GENERAL APPROACH

The form for the impedance Z in (5.6) suggests, if initially we ignore the scaling term $(1 + p\tau)$, that we may be able to use the S.B.I.s in filters which incorporate grounded parallel LC circuits. Such circuits occur naturally in bandpass filters, see Figs. 1.5 (c) and (d), but this is not the case with highpass filters, see Figs. 1.5 (a) and (b), nor lowpass filters. Since we are concerned here with both highpass and bandpass filter design a circuit modification for the highpass filters will have to be made so that parallel LC circuits can be introduced. This modification will be described in Section 5.3.2.1.

To take into consideration the impedance scaling term $(1 + p\tau)$ in (5.6) we shall impedance scale the LC filter, with its terminating impedances, by the same factor $(1 + p\tau)$. This does not affect the voltage transfer ratio for the filter , and the parallel LC resonators are transformed to have an impedance of the same form as in (5.6). These new impedances can be realised using S.B.I. circuits to obtain the active filter. Impedance scaling by $(1 + p\tau)$ also modifies the other impedances in the filter - these transformations are shown in Fig. 5.1.

5.3.2 HIGHPASS FILTER DESIGN

In this section we describe how to design Cauer and Polynomial type highpass filters using S.B.I. circuits (note that Cauer and Polynomial type highpass filters have the typical loss/frequency characteristics shown in Figs. 1.5 (a) and (b)). Before outlining these design procedures, however, it is necessary to describe a network transformation for LC filters that was proposed by Nightingale and Rollett (58).

5.3.2.1 PRELIMINARY NETWORK TRANSFORMATION

Consider the LC lowpass filter shown in Fig. 5.2 (a). To obtain an active-RC version of this filter we shall use Bruton's method of impedance scaling the components in the LC filter by k/p , to give the circuit in Fig. 5.2 (b). The F.D.N.R.s in the scaled filter, which arise from impedance scaling the capacitors in the original LC network, may be realised by the two-amplifier circuit of Fig. 2.7 (a). Unfortunately, the amplifiers in this simulating network give rise to a practical problem which we shall now outline.

The input connections to operational amplifiers require a D.C. bias and must therefore be connected by a resistive path to a point of fixed potential chosen so that the quiescent output voltage of the amplifier is not biased too far towards one or other of the power-supply voltages. When the two-amplifier F.D.N.R. of Fig. 2.7 (a) is incorporated into the filter circuit in Fig. 5.2 (b), we find that some of the amplifier inputs do not have a D.C. bias.

A general technique for overcoming the above problem (proposed originally by D.G. Haigh (37)) is to modify the F.D.N.R. lowpass filter in the way shown in Fig. 5.2 (c). The two resistors R_a and R_b in Fig. 5.2 (c) now connect the previously mentioned amplifier inputs to suitable points of fixed potential and provide the required D.C. bias. Unfortunately, the inclusion of these bias resistances in the filter may additionally cause the voltage transfer response for the filter to become distorted. The distortion can be reduced by reducing the filter impedances relative to the D.C. bias resistances which are determined by the D.C. properties of the amplifiers, however, the capacitances are then increased, and the size and cost of the filter are also increased. A way of avoiding the distortion completely has been proposed by Nightingale and Rollett (58), and will now be briefly described.

When the modified F.D.N.R. filter in Fig. 5.2 (c) is converted back to its equivalent LC filter we obtain the circuit in Fig. 5.2 (d). The D.C. path resistors of Fig. 5.2 (c) are now equivalent to the inductors L_a and L_b placed across the terminating resistors of the original LC filter. For a chosen ratio L_a/R_s for the lowpass filter in Fig. 5.2 (d) (when normalised to have a passband edge frequency equal to 1.0 r/s) Nightingale and Rollett described a design procedure (58) so that the loss/frequency response could be made substantially the same as that for the original LC filter in Fig. 5.2 (a). They found that the response for the filter in Fig. 5.2 (d) could be made exactly equal to that for the filter in Fig. 5.2 (a) except for an additional constant loss term. They also found that their design procedure is applicable to lowpass filters that have finite zeros in the transfer function.

In the following sections we will make use of the Nightingale/Rollett design procedure mentioned above to obtain active-RC highpass filters that use S.B.I. circuits. Some comments on the sensitivity properties of the Nightingale/Rollett filters will be made later in the thesis in Chapter 6.

5.3.2.2 <u>CAUER TYPE FILTERS</u>

The first step is to obtain an LC highpass filter circuit in which the inductors appear only as parts of grounded parallel LC resonators. For Cauer type highpass filters this may be achieved in the following way.

Consider, for example, the resistively terminated 5^{th} order highpass filter shown in Fig. 5.3 (a). The corresponding lowpass filter is shown in Fig. 5.3 (b). For this filter we can use Nightingale and Rolletts' design method to obtain the equivalent lowpass filter with parallel RL terminations shown in Fig. 5.3 (c). Now, by lowpass to highpass filter transformation, we obtain the highpass filter circuit in Fig. 5.3 (d) which contains parallel RC terminations. We shall refer to this filter as a Nightingale/Rollett type highpass filter. The loss/frequency characteristic for the filter in Fig. 5.3 (d) will be identical to that in Fig 5.3 (a) except for an additional constant loss term that arises in the Nightingale /Rollett design procedure. Also, for a normalised passband edge frequency of 1.0 r/s, many designs are possible depending upon the value one chooses for the product R_SC_S. This is because there is some freedom of choice for the ratio L_S/R_S in the design of the Nightingale/Rollett lowpass filter in Fig 5.3 (c). From the circuit in Fig. 5.3 (d) we obtain the filter circuit of Fig. 5.3 (h), which is our goal, by means of the following transformations.

First of all the Norton transformation shown in Fig. 5.4 (a) is applied to the capacitors C_5 and C_L in Fig. 5.3 (d) to give the filter circuit in Fig. 5.3 (e) (note that this transformation does not affect the voltage transfer function for the filter in Fig. 5.3 (d)). This was done so that a capacitor C_X appears across the tuned circuit L_2C_4 , and so that some capacitance remains in parallel with the load resistor R_L. The ideal transformer arising from this transformation can be eliminated using the transformation of Fig. 5.4 (b) to obtain the circuit in Fig. 5.3 (f). This step involves impedance scaling the components to the right of the transformer in Fig. 5.3 (e) by the factor ϕ^2 , where ϕ is the transformer turns ratio. This procedure will alter the basic loss for the filter, where the loss is defined as $20\log_{10} \frac{V_{OUT}}{V_{IN}}$, but the shape for the loss/frequency characteristic remains unchanged. To the circuit in Fig. 5.3 (f) we again apply the Norton transformation of Fig. 5.4 (a) to the capacitor C_3 taken with part of C_X and again eliminate the resulting transformer in the way shown in Fig. 5.4 (b). When this is done we obtain the circuit in Fig. 5.3 (g) where a parallel capacitor has been provided to each series tuned circuit. The circuit in Fig. 5.3 (g) can now be transformed into the circuit of Fig. 5.3 (h) using the equivalence shown in Fig. 5.5. In this way we have achieved our first aim of obtaining an LC highpass filter in which the inductors exist only as parts of grounded parallel LC resonator circuits.

The next step is to design two S.B.I. circuits so that the parameter L in their impedance expression, see (5.6), has the inductance values L_A and L_B shown in Fig. 5.3 (h). Associated with these two designs there will be two values C_A and C_B for the parameter C in (5.6) (different C values for different L values), but the values for τ in (5.6) will be the same if we follow the design procedure outlined in Section 5.3. We now proceed by re-drawing the filter circuit of Fig. 5.3 (h) in the way shown in Fig. 5.3 (i) so that the capacitors C_S, C_L''', C_6 and C_7 (see Fig. 5.3 (h)) are split in such a way that the capacitors C_S', C_L'''', C_6' and C_7' (see Fig. 5.3 (i)) have the values $C_S' = \tau/R_S$, $C_L'''' = \tau/R_L''$, $C_6' = C_6 - C_A$ and $C_7' = C_7 - C_B$. The filter in Fig. 5.3 (i) can now be impedance scaled by $(1 + p\tau)$ making use of the transformations given in Fig. 5.1. This results in the filter of Fig. 5.3 (j), in which the impedances Z_A and Z_B are realised by the S.B.I. circuits. Note that for the practical realisation of the final active-RC filter it is of course necessary that the capacitance values C_S'', C_L'''', C_6' and C_7' in Fig. 5.3 (i) are all positive.

It is of interest to compare the active filter of Fig. 5.3 (j) with that which is obtained when S.I.s are used to replace directly the inductors in the LC filter of Fig. 5.3 (a). We find that four additional capacitors, i.e., C_S'', C_6', C_7' and C_L'''', are required for the new design procedure. A plausible approach, not yet tested, for reducing the number of additional capacitors will now be discussed.

There are some degrees of freedom in the design procedure outlined here, namely, our choice for the product R_SC_S in the filter of Fig. 5.3 (d), and secondly the amount of load capacitance C_L in Fig. 5.3 (d) that we distribute across the inductors in the filter of Fig. 5.3 (h). It may be possible to use these degrees of freedom to design the LC filter of Fig. 5.3 (h) so that, after the design of the S.B.I.s , the additional capacitances C_6', C_7' and C_L'''' in Fig. 5.3 (i) are exactly zero. This implies that the values for C_6 and C_7 in Fig. 5.3 (h) would have to be equal , respectively, to the values C_A and C_B associated with the S.B.I. circuits, and that C_L''' was exactly equal to τ/R_L''. In this case impedance scaling by $(1 + p\tau)$ would give rise to the active-RC filter of Fig. 5.3 (k). For this filter there is only one additional capacitor, namely, C_S''.

The design procedure outlined here for a 5^{th} order filter can be applied in the same way to filters of higher order.

5.3.2.3 POLYNOMIAL TYPE FILTERS

Polynomial type highpass filters can be designed in the same way as the Cauer type filters except that the transformation shown in Fig. 5.5 is not required.

Consider, for example, the resistively terminated 5^{th} order polynomial type filter shown in Fig. 5.6 (a). Fig. 5.6 (b) shows the equivalent Nightingale/Rollett type highpass filter. Continuing in the same way as in Section 5.3.2.2, the filter of Fig. 5.6 (b) is now transformed to the filter of Fig. 5.6 (c). This filter is then re-drawn in the way shown in Fig. 5.6 (d) and, finally, impedance scaled by $(1 + p\tau)$ to obtain the filter in Fig. 5.6 (e) where Z_A and Z_B represent the S.B.I. circuits.

As in the case for Cauer type filters there are some degrees of freedom in the design procedure outlined here. Once again, it may be possible to use these degrees of freedom to eliminate some of the capacitors in the active-RC filter of Fig. 5.6 (e), to obtain the filter of Fig. 5.6 (f). This filter uses only one more capacitor than the equivalent active-RC filter obtained by replacing the inductors in the filter of Fig. 5.6 (a) by S.I. circuits.

5.3.3 BANDPASS FILTER DESIGN

5.3.3.1 POLYNOMIAL TYPE FILTERS

Bandpass filters that contain grounded parallel LC circuits and no floating inductors, are also suited to the new design procedure. Consider, for example, the equally resistively terminated 6^{th} order polynomial type filter shown in Fig. 5.7 (a), designed so that its loss/frequency response in the passband contains points of maximum power transfer. The S.B.I. circuits can be designed so that the parameter L for their impedance expression in (5.6) has the inductance values L_A, L_B and L_C shown in Fig. 5.7 (a). Along with these L values the S.B.I.s will have the parameter values C_A, C_B and C_C, and a common value for τ. We now proceed by re-drawing the filter of Fig. 5.7 (a) in the way shown in Fig. 5.7 (b), and for this circuit we choose $C_1' = C_1 - C_A$, $C_3' = C_3 - C_B$, $C_5' = C_5 - C_C - C_X$, and $C_X = \tau/R_L$ (note that positive values for C_1', C_3' and C_5' are required for realisability). The filter circuit of Fig. 5.7 (b) can now be impedance scaled by $(1 + p\tau)$, making use of the transformations shown in Fig. 5.1, to give the filter circuit of Fig. 5.7 (c) in which the impedances Z_A, Z_B and Z_C represent the S.B.I. circuits. However, impedance scaling by $(1 + p\tau)$ transforms the source resistor in Fig. 5.7 (b) into the series inductor/resistor combination shown in Fig. 5.7 (c), and it becomes necessary to delete the undesirable inductor in some way. In the highpass filter design procedure this difficulty does not arise because the scaling transformation can be applied to a parallel RC circuit, and this results in a pure resistor.

To eliminate the inductor in Fig. 5.7 (c) we consider now the frequencies f_{oi} for which maximum power transfer occurs in the filter of Fig. 5.7 (a). At these frequencies the impedance to the right of the line XX' in Fig. 5.7 (a) will be purely resistive and have a value $R = R_S$. For the impedance scaled filter of Fig. 5.7 (c), the impedance to the right of XX' will be $R_S(1 + p\tau)$ at $f = f_{oi}$, as shown in Fig. 5.8 (a). Also, at the frequencies f_{oi}, the voltage gain for the circuit in Fig. 5.8 (a) is given by $V_X/V_{IN} = \frac{1}{2}$. This is also the gain for the circuit in Fig. 5.8 (b) at $f = f_{oi}$, because of the well known equivalence shown in Fig. 5.8 (c). We can apply the equivalence between the circuits in Figs. 5.8 (a) and (b) to the filter of Fig. 5.7 (c), to obtain the new filter circuit shown in Fig. 5.7 (d)(note that the two series RC circuits on either side of XX' in Fig. 5.7 (d) can be combined into a single series RC circuit because their RC products are the same). The voltage transfer function for the filter in Fig. 5.7 (d) will be identical to that for the circuit in Fig. 5.7 (a) at the frequencies f_{oi}, and at zero frequency. At frequencies other than f_{oi} and zero frequency, we would expect the response to be different to an extent which depends on the value for τ used in the impedance scaling procedure.

Some computed and experimental work on bandpass filters of the type discussed here will be presented later in Chapter 7. The results indicate that although the design procedure here is not exact, extremely good results can still be obtained. Note, also, that the design procedure described here does not require additional capacitors as is the case for highpass filters.

5.3.3.2 FILTERS WITH FINITE ZEROS

LC bandpass filters having finite transmission zeros, and no floating inductors, can also be modified to obtain active filters that use S.B.I. circuits.

Consider, for example, the channel filter shown in Fig. 5.9 (a) which has been investigated by Valihora, Lim, and Bruton (21). Making use of the transformation shown in Fig. 5.5, the circuit in Fig. 5.9 (a) is re-drawn as shown in Fig. 5.9 (b) so that each inductor is associated with a parallel capacitor. Once again the S.B.I.s are now designed, as outlined in Section 5.2, to have the parameter values L_A to L_F shown in Fig. 5.9 (b). Proceeding in the same way as before, we re-draw the circuit of Fig. 5.9 (b) in the way shown in Fig. 5.9 (c), and then impedance scale by $(1 + p\tau)$. When this is done we obtain the filter circuit of Fig. 5.9 (d) where Z_A to Z_F represent the S.B.I. circuits. The small inductance L' arising in the circuit of Fig. 5.9 (d) can be eliminated in the same way as in Section 5.3.3.1, i.e. by making use of the transformation of Fig. 5.8, to obtain the final active-RC filter shown in Fig. 5.9 (e). The two series RC circuits on either side of XX' in Fig. 5.8 (e) can be combined so that the design procedure does not require the use of additional capacitors.

5.3.3.3 RE-INTERPRETATION OF DESIGN PROCEDURE FOR BANDPASS FILTERS

The design procedure for bandpass filters may be re-interpreted in the following way.

Let us represent the original LC bandpass filters of Figs. 5.7 (a) and 5.9 (a) by the more general circuit diagram of Fig. 5.10 (ignoring temporarily the capacitors C). For the frequencies f_{oi} of maximum power transfer, the impedance to the right of the line XX' in Fig. 5.10 will be purely resistive of value R_S, and the voltage V_X will be equal to $V_{IN}/2$. If two capacitors of equal value are inserted into the filter, as shown in Fig. 5.10, the voltage V_X will be unchanged at the frequencies f_{oi}; and hence the voltage gain for the filter, V_{OUT}/V_{IN} , will be unchanged at the frequencies f_{oi}. The gain for other frequencies will of course differ from the gain before the insertion of the capacitors, but for suitably small values for C it may be possible to meet the required filter specification using the modified filter circuit.

For these modified LC bandpass filters, with their parallel RC source impedance, we can choose $C = \tau/R_S$ and follow our usual design procedure for filters containing S.B.I. circuits, see Section 5.3.1. In the present case, however, impedance scaling by $(1 + p\tau)$ transforms the modified source impedance to a pure resistor, and this avoids the unwanted inductor that arose in the design procedures of

Sections 5.3.3.1 and 5.3.3.2. In these Sections impedance scaling by $(1 + p\tau)$ was applied to a source impedance consisting of a pure resistor - this resulted in a series RL combination, and the unwanted inductor was eliminated using the transformation shown in Fig. 5.8. The active-RC bandpass filters that are obtained using the new approach, however, are identical to the active-RC filters obtained previously, and we shall therefore regard the design approach here as a re-interpretation of the methods of Sections 5.3.3.1 and 5.3.3.2.

5.4 DESIGN OF SOME S.B.I. CIRCUITS

Previously, in Sections 3.2.1 and 3.2.2 we showed that for the ideal amplifier case, the networks in Figs. 3.2 (a) and 3.4 may be designed to simulate the impedance of a lossless positive inductor. When the non-ideal voltage gain for the amplifiers is taken into consideration, the networks become non-ideal S.I.s. In this section we show how to design the networks in Figs. 3.2 (a) and 3.4 so that, after taking into consideration the non-ideal voltage gain for the amplifiers, they become ideal S.B.I. circuits.

5.4.1 PROCEDURE FOR S.B.I. CIRCUIT B

Before describing how the simulating network in Fig. 3.3 can become an ideal S.B.I. circuit, it is convenient to first of all consider the gain for the amplifier ideal, i.e. infinite, and review the design procedure for obtaining an ideal S.I..

5.4.1.1 REVIEW OF IDEAL AMPLIFIER CASE

When the gain for the amplifier is assumed to be ideal, the simulating network in Fig. 3.3 has an impedance

$$Z = \frac{A_0 + pA_1}{B_0 + pB_1} \tag{5.8}$$

and the coefficients A_0 to B_1 are given by the expressions

$$A_0 = G_4G_2 - G_3G_5 - G_3G_1$$

$$A_1 = C_0G_4$$

$$B_0 = (G_1 + G_6)(G_4G_2 - G_3G_5) + G_1G_2G_6 \tag{5.9}$$

$$B_1 = C_0(G_4G_2 - G_3G_5 - G_5G_6)$$

The circuit therefore has the impedance of a lossless inductor of value $L = A_1/B_0$ provided the conditions $A_0 = 0$ and $B_1 = 0$ are satisfied. From (5.9) these conditions are

$$G_4G_2 - G_3G_5 - G_3G_1 = 0$$

$$C_0(G_4G_2 - G_3G_5 - G_5G_6) = 0 \tag{5.10}$$

and the inductance value L is

$$L = \frac{C_0G_4}{(G_1 + G_6)(G_4G_2 - G_3G_5) + G_1G_2G_6} \tag{5.11}$$

In Section 3.2.2 we satisfied the conditions in (5.10) by choosing arbitrary values for G_3, G_4, G_5 and G_6, and then specifying G_1 and G_2 as

$$G_1 = R_3G_6G_5$$

$$G_2 = G_5R_4(G_3 + G_6) \tag{5.12}$$

In this section, however, it is more convenient to satisfy the conditions in (5.10) by choosing arbitrary values for G_1, G_2, G_4 and G_5, and specifying G_3 and G_6 as

$$G_3 = \frac{G_4 G_2}{G_1 + G_5}$$
$$G_6 = \frac{G_1 G_2 G_4}{G_5(G_1 + G_5)} \qquad (5.13)$$

Substitution of these expressions into (5.11) gives

$$L = \frac{C_0 G_5 (G_5 + G_1)^2}{G_1^2 G_2 (G_1 G_5 + G_5^2 + G_1 G_2 + G_2 G_4 + G_2 G_5)} \qquad (5.14)$$

and the desired inductance value, $L = L_N$, can be obtained by specifying C_0 as

$$C_0 = \frac{L_N G_1^2 G_2 (G_1 G_5 + G_5^2 + G_1 G_2 + G_2 G_4 + G_2 G_5)}{G_5 (G_5 + G_1)^2} \qquad (5.15)$$

Note from eqns. (5.13) and (5.15) that, for arbitrary positive values for G_1, G_2, G_4, G_5 and L_N, the values for G_3, G_6 and C_0 are always positive.

5.4.1.2 NON-IDEAL AMPLIFIER CASE

The impedance for the simulating network in Fig. 3.3, for the non-ideal amplifier case, was given previously in eqns. (3.21) and (3.22). When the impedance expression in (3.21) is re-written in the form

$$Z = \frac{a_o + a_1 p + a_2 p^2}{b_o + b_1 p + b_2 p^2} \tag{5.16}$$

we find that the coefficients a_o to b_2 are given by

$$a_o = G_2G_4 - G_1G_3 - G_3G_5 + \alpha(G_2 + G_3)(G_1 + G_4 + G_5)$$

$$a_1 = C_0G_4 + \alpha C_0(G_1 + G_4 + G_5) + (G_2 + G_3)(G_1 + G_4 + G_5)/\omega_T$$

$$a_2 = C_0(G_1 + G_4 + G_5)/\omega_T \tag{5.17}$$

$$b_o = (G_1 + G_6)(G_4G_2 - G_3G_5) + G_1G_2G_6 + \alpha(G_2 + G_3)\left\{(G_4 + G_5)(G_1 + G_6) + G_1G_6\right\}$$

$$b_1 = C_0(G_4G_2 - G_3G_5 - G_5G_6) + (G_2 + G_3)\left\{(G_4 + G_5)(G_1 + G_6) + G_1G_6\right\}/\omega_T + \alpha C_0\left\{(G_1 + G_4 + G_5)(G_2 + G_3 + G_6) + G_1(G_4 + G_5)\right\}$$

$$b_2 = C_0\left\{(G_1 + G_4 + G_5)(G_2 + G_3 + G_6) + G_1(G_4 + G_5)\right\}/\omega_T$$

The design criteria $a_o = 0$ and $b_1 = 0$ in (5.4) are therefore given by

$$G_2G_4 - G_1G_3 - G_3G_5 + \alpha(G_2 + G_3)(G_1 + G_4 + G_5) = 0 \qquad (5.18)$$

$$C_0\left\{\begin{array}{l} G_4G_2 - G_3G_5 - G_5G_6 + (G_2 + G_3)\left[(G_4 + G_5)(G_1 + G_6) + G_1G_6\right]/\omega_T C_0 \\ +\alpha\left[(G_1 + G_4 + G_5)(G_2 + G_3 + G_6) + G_1(G_4 + G_5)\right] \end{array}\right\} = 0$$

(5.19)

and when these conditions are satisfied the simulating network becomes an ideal S.B.I. circuit having the impedance

$$Z = \frac{pL(1 + p\tau)}{1 + p^2LC} \qquad (5.20)$$

where

$$L = \frac{C_0\left\{G_4 + \alpha(G_1 + G_4 + G_5) + (G_2 + G_3)(G_1 + G_4 + G_5)/\omega_T C_0\right\}}{(G_1 + G_6)(G_4G_2 - G_3G_5) + G_1G_2G_6 + \alpha(G_2 + G_3)\left\{(G_4 + G_5)(G_1 + G_6) + G_1G_6\right\}}$$

(5.21)

$$C = \frac{(G_1 + G_4 + G_5)(G_2 + G_3 + G_6) + G_1(G_4 + G_5)}{\omega_T\left\{G_4 + \alpha(G_1 + G_4 + G_5) + (G_2 + G_3)(G_1 + G_4 + G_5)/\omega_T C_0\right\}}$$

(5.22)

$$\tau = \frac{(G_1 + G_4 + G_5)}{\omega_T\left\{G_4 + \alpha(G_1 + G_4 + G_5) + (G_2 + G_3)(G_1 + G_4 + G_5)/\omega_T C_0\right\}}$$

(5.23)

In addition to the conditions $a_o = 0$ and $b_1 = 0$ in (5.18) and (5.19), it will be necessary to design the S.B.I. circuit so that the parameter L in (5.20) is equal to the desired value L_N. For given values for the amplifier parameters, α and ω_T, these objectives may be achieved in the following way

Inspection of the expression for a_o in (5.17) shows that a_o is dependent on the values for G_1, G_2, G_3, G_4 and G_5, but independent of the values for G_6 and C_0. Similarly, from (5.17) and (5.21), we find that b_1 and L are functions of all the passive component values for the simulating network, i.e., G_1, G_2, G_3, G_4, G_5, G_6 and C_0. To achieve the conditions $a_o = 0$, $b_1 = 0$, and $L = L_N$, one approach is to first of all satisfy $a_o = 0$ by choosing a suitable value for G_3, and then we find the appropriate values for G_6 and C_0 which satisfy the conditions $b_1 = 0$ and $L = L_N$. The choice of values for G_6 and C_0 do not affect the value for a_o since a_o is independent of these components. This approach will now be outlined in detail.

For given values for the amplifier parameters α and ω_T, for a specified value L_N, and for arbitrary conductance values G_1, G_2, G_4 and G_5, let us first of all satisfy the condition $a_o = 0$ in (5.18) by choosing G_3 as

$$G_3 = \frac{G_4G_2 + \alpha(G_1 + G_4 + G_5)}{G_1 + G_5 - \alpha(G_1 + G_4 + G_5)} \tag{5.24}$$

To satisfy the condition $b_1 = 0$ in (5.19) we begin by rewriting (5.19) in the form

$$K_1 + K_2G_6 + K_3C_0 + K_4G_6C_0 = 0 \tag{5.25}$$

where

$$K_1 = G_1(G_2 + G_3)(G_4 + G_5)/\omega_T$$

$$K_2 = (G_2 + G_3)(G_4 + G_5 + G_1)/\omega_T \tag{5.26}$$

$$K_3 = G_4G_2 - G_3G_5 + \alpha\left\{(G_1 + G_4 + G_5)(G_2 + G_3) + G_1(G_4 + G_5)\right\}$$

$$K_4 = \alpha(G_1 + G_4 + G_5) - G_5$$

From the expression for L in (5.21), with $L = L_N$, we also note the relationship

$$C_0 = \frac{K_5 + K_6G_6}{K_7} \tag{5.27}$$

where

$$K_5 = L_NG_1\left\{G_4G_2 - G_3G_5 + \alpha(G_2 + G_3)(G_4 + G_5)\right\} - (G_2 + G_3)(G_1 + G_4 + G_5)/\omega_T$$

$$K_6 = L_N\left\{G_4G_2 + G_1G_2 - G_3G_5\right\} + \alpha(G_2 + G_3)(G_1 + G_4 + G_5)$$

$$K_7 = G_4 + \alpha(G_1 + G_4 + G_5) \tag{5.28}$$

Now, substituting the expression for C_0 in (5.27) into (5.25), we find that the condition for $b_1 = 0$ can be re-expressed as a quadratic in G_6 that is independent of C_0, i.e., we obtain

$$X_1G_6^2 + X_2G_6 + X_3 = 0 \tag{5.29}$$

where

$$\begin{aligned} X_1 &= K_4K_6 \\ X_2 &= K_2K_7 + K_3K_6 + K_4K_5 \\ X_3 &= K_1K_7 + K_3K_5 \end{aligned} \tag{5.30}$$

For the given values α, ω_T, L_N, G_1, G_2, G_4 and G_5, and the value for G_3 obtained from (5.24), we can calculate the values for K_1 to K_7 in (5.26) and (5.28), and hence we can determine the values for X_1 to X_3 in (5.30). To satisfy the conditions $b_1 = 0$ and $L = L_N$ we now solve the quadratic in (5.29) to obtain the required value for G_6, and then from (5.27) we obtain the value for C_0. This solution, of course, will be significant only if the value for G_6 is positive real, and also provided the value for C_0 is positive. We will now discuss whether or not this is the case.

Let us start our discussion by comparing the design conditions required in the ideal amplifier case of Section 5.4.1.1, with those for the non-ideal amplifier case studied here. We find that the expressions for $A_0 = 0$ and $B_1 = 0$ in (5.10) are similar to those for $a_0 = 0$ and $b_1 = 0$ in (5.18) and (5.19). Also, the inductance expression in (5.11) is similar to the expression in (5.21) for the parameter L . Indeed, the expressions for the non-ideal amplifier case differ only in that they contain additional terms due to the amplifier parameters α and ω_T. Continuing our comparision, we find that in both the ideal and non-ideal amplifier cases the design approach is to obtain values for G_3, G_6, and C_0 that satisfy the relevant design conditions. In the ideal amplifier case of Section 5.4.1.1 we found that for arbitrary positive values for G_1, G_2, G_4 and G_5, the values for G_3, G_6 and C_0 are always positive. However, in the non-ideal amplifier case this is not necessarily the case as negative signs, due to α and $1/\omega_T$ terms, appear in the expressions which determine G_3, G_6 and C_0, e.g., see (5.24). Nevertheless, for sufficiently small values for α and $1/\omega_T$, the values for G_3, G_6 and C_0 in the non-ideal amplifier case should be close to those for the ideal amplifier case. We can therefore conclude that for the non-ideal amplifier case, there should be a wide range of values for G_1, G_2, G_4 and G_5 which give rise to positive real values for G_3, G_6 and C_0.

5.4.2 PROCEDURE FOR S.B.I. CIRCUIT A

Before describing how the simulating network in Fig. 3.1 (a) can become an ideal S.B.I. circuit, it is again convenient to consider the voltage gain for the amplifier to be ideal, and review the design procedure for obtaining an ideal S.I..

5.4.2.1 REVIEW OF IDEAL AMPLIFIER CASE

When the voltage gain for the amplifier is assumed to be ideal, the simulating network in Fig. 3.1 (a) has an impedance

$$Z = \frac{A_0 + pA_1}{B_0 + pB_1} \tag{5.31}$$

where

$$\begin{aligned}
A_0 &= (G_6 + G_7)(G_4G_2 - G_3G_5 - G_1G_3) \\
A_1 &= C_0\left\{G_4(G_2 + G_7) - (G_1 + G_5)(G_3 + G_6)\right\} \\
B_0 &= G_1G_2G_6G_7 + (G_4G_2 - G_3G_5)(G_6G_7 + G_1G_7 + G_1G_6) \\
B_1 &= C_0(G_1 + G_7)(G_2G_4 - G_3G_5 - G_5G_6)
\end{aligned} \tag{5.32}$$

The circuit therefore has the impedance of a lossless inductance of value $L = A_1/B_0$ provided the conditions $A_0 = 0$ and $B_1 = 0$ are satisfied. From (5.32) these conditions are

$$(G_6 + G_7)(G_4G_2 - G_3G_5 - G_1G_3) = 0$$

$$C_0(G_1 + G_7)(G_4G_2 - G_3G_5 - G_5G_6) = 0 \tag{5.33}$$

and the inductance value L is

$$L = \frac{C_0\left\{ G_4(G_2 + G_7) - (G_1 + G_5)(G_3 + G_6)\right\}}{(G_4G_2 - G_3G_5)(G_6G_7 + G_1G_7 + G_1G_6) + G_1G_2G_6G_7} \tag{5.34}$$

To satisfy the conditions in (5.33) let us choose arbitrary positive values for G_1, G_2, G_4, G_5 and G_7, and specify G_3 and G_6 as

$$G_3 = \frac{G_4G_2}{G_1 + G_5} \tag{5.35}$$

$$G_6 = \frac{G_1G_2G_4}{G_5(G_1 + G_5)} \tag{5.36}$$

Substitution of these expressions into (5.34) gives

$$L = \frac{C_0(G_5G_7 - G_1G_2)(G_1 + G_5)^2}{G_1^2G_2\left\{G_7(G_1 + G_5)(G_2 + G_5) + G_4G_2(G_1 + G_7)\right\}} \tag{5.37}$$

and the desired inductance value, $L = L_N$, can be obtained by specifying C_0 as

$$C_0 = \frac{L_NG_1^2G_2\left\{G_7(G_1 + G_5)(G_2 + G_5) + G_4G_2(G_1 + G_7)\right\}}{(G_5G_7 - G_1G_2)(G_1 + G_5)^2} \tag{5.38}$$

Equation (5.38) shows that for C_0 to be positive the following inequality must hold.

$$G_5 G_7 > G_1 G_2 \qquad (5.39)$$

The values for G_1, G_2, G_5 and G_7 should therefore be chosen so that the above condition is satisfied.

5.4.2.2 NON-IDEAL AMPLIFIER CASE

The impedance for the simulating network in Fig. 3.1 (a), for the non-ideal amplifier case, was shown previously in eqns. (3.13) and (3.14). When the impedance expression in (3.13) is rewritten in the form

$$Z = \frac{a_o + a_1 p + a_2 p^2}{b_o + b_1 p + b_2 p^2} \tag{5.40}$$

we find that the coefficients a_o to b_2 are given by

$$a_o = (G_6 + G_7)\left\{G_2G_4 - G_1G_3 - G_3G_5 + \alpha(G_2 + G_3)(G_1 + G_4 + G_5)\right\}$$

$$a_1 = C_0 \left\{\begin{array}{l} G_4(G_2 + G_7) - (G_1 + G_5)(G_3 + G_6) \quad + \\ \alpha(G_1 + G_4 + G_5)(G_2 + G_3 + G_6 + G_7) + \\ (G_2 + G_3)(G_6 + G_7)(G_1 + G_4 + G_5)/\omega_T C_0 \end{array}\right\}$$

$$a_2 = C_0(G_1 + G_4 + G_5)(G_2 + G_3 + G_6 + G_7)/\omega_T \tag{5.41}$$

$$\begin{aligned} b_o = {} & (G_4G_2 - G_3G_5)(G_6G_7 + G_1G_7 + G_1G_6) + G_1G_2G_6G_7 \; + \\ & \alpha(G_2 + G_3)\left\{(G_4 + G_5)(G_1G_6 + G_1G_7 + G_6G_7) + G_1G_6G_7\right\} \end{aligned}$$

$$b_1 = C_0\left\{\begin{array}{l} (G_1 + G_7)(G_2G_4 - G_3G_5 - G_5G_6) \quad + \\ \alpha\left[G_1(G_4 + G_5)(G_2 + G_3 + G_6 + G_7) + G_7(G_1 + G_4 + G_5)(G_2 + G_3 + G_6)\right] \\ + \; (G_2 + G_3)\left[(G_4 + G_5)(G_1G_6 + G_1G_7 + G_6G_7) + G_1G_6G_7\right] / \omega_T C_0 \end{array}\right\}$$

$$b_2 = C_0\left\{G_1(G_4 + G_5)(G_2 + G_3 + G_6 + G_7) + G_7(G_1 + G_4 + G_5)(G_2 + G_3 + G_6)\right\}/\omega_T$$

The design criteria $a_o = 0$ and $b_1 = 0$ in (5.4) are therefore given by

$$(G_6 + G_7)\left\{G_2G_4 - G_1G_3 - G_3G_5 + \alpha(G_2 + G_3)(G_1 + G_4 + G_5)\right\} = 0 \tag{5.42}$$

$$C_0 \left\{\begin{array}{c} (G_1 + G_7)(G_2G_4 - G_3G_5 - G_5G_6) + \\ \alpha\left[G_1(G_4 + G_5)(G_2 + G_3 + G_6 + G_7) + G_7(G_1 + G_4 + G_5)(G_2 + G_3 + G_6)\right] \\ + (G_2 + G_3)\left[(G_4 + G_5)(G_1G_6 + G_1G_7 + G_6G_7) + G_1G_6G_7\right] /\omega_T C_0 \end{array}\right\} = 0 \tag{5.43}$$

and when these conditions are satisfied the simulating network becomes an S.B.I. circuit with the impedance

$$Z = \frac{pL(1 + p\tau)}{1 + p^2LC} \tag{5.44}$$

where

$$L = \frac{C_0\left\{\begin{array}{l} G_4(G_2 + G_7) - (G_1 + G_5)(G_3 + G_6) + \\ \alpha(G_1 + G_4 + G_5)(G_2 + G_3 + G_6 + G_7) + \\ (G_2 + G_3)(G_6 + G_7)(G_1 + G_4 + G_5)/\omega_T C_0 \end{array}\right\}}{\begin{array}{l}(G_4G_2 - G_3G_5)(G_6G_7 + G_1G_7 + G_1G_6) + G_1G_2G_6G_7 + \\ \alpha(G_2 + G_3)\left[(G_4 + G_5)(G_1G_6 + G_1G_7 + G_6G_7) + G_1G_6G_7\right]\end{array}} \tag{5.45}$$

$$C = \frac{G_1(G_4 + G_5)(G_2 + G_3 + G_6 + G_7) + G_7(G_1 + G_4 + G_5)(G_2 + G_3 + G_6)}{\omega_T \left\{ \begin{array}{l} G_4(G_2 + G_7) - (G_1 + G_5)(G_3 + G_6) \quad + \\ \alpha(G_1 + G_4 + G_5)(G_2 + G_3 + G_6 + G_7) + \\ (G_2 + G_3)(G_6 + G_7)(G_1 + G_4 + G_5)/\omega_T C_0 \end{array} \right\}} \tag{5.46}$$

$$\tau = \frac{(G_1 + G_4 + G_5)(G_2 + G_3 + G_6 + G_7)}{\omega_T \left\{ \begin{array}{l} G_4(G_2 + G_7) - (G_1 + G_5)(G_3 + G_6) \quad + \\ \alpha(G_1 + G_4 + G_5)(G_2 + G_3 + G_6 + G_7) + \\ (G_2 + G_3)(G_6 + G_7)(G_1 + G_4 + G_5)/\omega_T C_0 \end{array} \right\}} \tag{5.47}$$

We now have to determine a way of choosing the passive component values for the simulating network so that the conditions in (5.42) and (5.43) are satisfied, and so that L in (5.45) is equal to the desired value L_N. To achieve this we used the following procedure, which is similar to that for S.B.I. circuit B.

For given values for α, ω_T and L_N, and for chosen values for G_1, G_2, G_4, G_5 and G_7, we first of all satisfied the condition $a_o = 0$ in (5.42) by choosing G_3 as

$$G_3 = \frac{G_4 G_2 + \alpha(G_1 + G_4 + G_5)}{G_1 + G_5 - \alpha(G_1 + G_4 + G_5)} \tag{5.48}$$

The condition $a_o = 0$ in (5.42) is independent of the values for G_6 and C_O, so we therefore chose these component values to satisfy the remaining two conditions $b_1 = 0$ and $L = L_N$. This was achieved in the following way.

First of all we rewrite the expression for $b_1 = 0$ in (5.43) in the form

$$K_1 + K_2 G_6 + K_3 C_O + K_4 G_6 C_O = 0 \tag{5.49}$$

where

$$\begin{aligned}
K_1 &= G_1 G_7 (G_2 + G_3)(G_4 + G_5)/\omega_T \\
K_2 &= (G_2 + G_3)\left[G_1 G_7 + (G_4 + G_5)(G_1 + G_7)\right]/\omega_T \\
K_3 &= (G_1 + G_7)(G_2 G_4 - G_3 G_5) + \\
&\quad \alpha\left\{G_1(G_4 + G_5)(G_2 + G_3 + G_7) + G_7(G_2 + G_3)(G_1 + G_4 + G_5)\right\} \\
K_4 &= \alpha\left\{G_1(G_4 + G_5) + G_7(G_1 + G_4 + G_5)\right\} - G_5(G_1 + G_7)
\end{aligned} \tag{5.50}$$

From the expression for L in (5.45), with $L = L_N$, we also obtain the relationship

$$C_O = \frac{K_5 + K_6 G_6}{K_7 + K_8 G_6} \tag{5.51}$$

where

$$\begin{aligned}
K_5 = {} & L_N G_1 G_7 \left\{ G_2 G_4 - G_3 G_5 + \alpha(G_2 + G_3)(G_4 + G_5)\right\} \\
& - G_7(G_2 + G_3)(G_1 + G_4 + G_5)/\omega_T
\end{aligned}$$

$$K_6 = L_N\left\{(G_1 + G_7)(G_4G_2 - G_3G_5) + G_1G_2G_7\right\} - (G_2 + G_3)(G_1 + G_4 + G_5)/\omega_T$$
$$+ \alpha L_N(G_2 + G_3)\left\{(G_1 + G_7)(G_4 + G_5) + G_1G_7\right\}$$

$$K_7 = G_4(G_2 + G_7) - G_3(G_1 + G_5) + \alpha(G_2 + G_3 + G_7)(G_1 + G_4 + G_5)$$

$$K_8 = \alpha(G_1 + G_4 + G_5) - (G_1 + G_5) \tag{5.52}$$

Now, by substituting the expression for C_0 in (5.51) into (5.49), we re-express the condition $b_1 = 0$ as a quadratic in G_6 that is independent of C_0, i.e., we obtain

$$X_1G_6^2 + X_2G_6 + X_3 = 0 \tag{5.53}$$

where

$$X_1 = K_2K_8 + K_4K_6$$

$$X_2 = K_1K_8 + K_2K_7 + K_3K_6 + K_4K_5 \tag{5.54}$$

$$X_3 = K_1K_7 + K_3K_5$$

For the values for G_1, G_2, G_4, G_5, G_7, L_N, α and ω_T, and the value for G_3 obtained from (5.48), we can calculate the values for K_1 to K_8 using eqns. (5.50) and (5.52), and hence obtain the values for X_1 to X_3 in (5.54). The value for G_6 can then be obtained by solving the quadratic in (5.53), and the value for C_0 is obtained from (5.51). As before, this solution will be significant only if the value for G_6 is positive real, and provided C_0 is also positive. For sufficiently small values for α and $1/\omega_T$, the range of values for G_1, G_2, G_4, G_5 and G_7, for which G_6 and C_0 are positive, should be similar to that for the ideal amplifier case of Section 5.4.2.1. In that section we showed that a positive real solution is obtained provided the inequality shown below is satisfied.

$$G_5G_7 > G_1G_2 \tag{5.55}$$

We would expect this condition to be also necessary for the non-ideal amplifier case studied here.

5.5 CONCLUSIONS

We have pointed out that single-amplifier, single-capacitor, S.I. circuits can have the impedance of a lossless inductance only if the amplifiers in the circuits are considered ideal. When the non-ideal voltage gain for the amplifiers is taken into consideration, the impedance for the simulating networks becomes a biquadratic expression in p, and only approximates the impedance of an ideal inductance over a limited frequency range. A biquadratic expression in p arises because each simulating network contains a capacitor with a 1^{st} order impedance function, an amplifier whose voltage gain is assumed to have a 1^{st} order roll off, and no other elements with frequency dependent characteristics. In this chapter we took into consideration the non-ideal voltage gain for the amplifier, and deliberately re-designed the simulating networks to have a biquadratic impedance of the form

$$Z = \frac{pL(1 + p\tau)}{1 + p^2 LC}$$

Circuits having this type of impedance were referred to as S.B.I.s where "S.B.I." is an abbreviation for Simulated Biquadratic Impedance. We showed how various types of LC highpass and bandpass filters, with their terminating resistors, may be modified so as to produce the required loss/frequency response using the S.B.I. circuits instead of the originally required inductors.

An advantage of the approach described here is that the non-ideal voltage gain for the amplifiers in the simulating networks, is taken into consideration in the design of the active filter. For bandpass filters using the S.B.I. circuits, the passband loss/frequency response is correct at the frequencies of maximum power transfer for the original LC filter. The response at other frequencies can be incorrect but a high degree of compensation for the non-ideal voltage gain of the amplifiers may still be achieved. We will show that this is so later in the thesis in Chapter 7. For highpass filters complete compensation for the non-ideal voltage gain can be obtained over the entire frequency range in which the gain of the amplifier can be adequately described by a single-pole model. Even in the case of two-amplifier S.I.s this has not been achieved, as these circuits are usually designed to offer compensation for the non-ideal voltage gain only in the neighbourhood of a particular frequency.

A disadvantage of the new filter design method, when compared with the method of directly replacing the inductors in an LC filter with S.I. circuits, is that additional capacitors are required for the highpass filter case. However, as mentioned earlier, it may be possible to reduce the number of additional capacitors to only one regardless of the order of the filter. A sensitivity investigation for the new types of filters described here will be carried out in later chapters.

CHAPTER 6

SOME SENSITIVITY FEATURES FOR ACTIVE-RC FILTERS THAT USE SIMULATED BIQUADRATIC IMPEDANCES

6.1 INTRODUCTION

In Section 5.3.2 we showed that active-RC highpass filters,which use S.B.I. circuits, are derived from LC filters that have parallel RC terminations. In Section 5.3.3 we used an original LC filter with purely resistive terminations in the design procedure for active-RC bandpass filters using S.B.I.s. However, this later design procedure involves an approximation, and in Section 5.3.3.3 we showed that the active bandpass filters can, instead, be more precisely considered as being derived from LC filters that are modified to have parallel RC terminations. Thus both the highpass and bandpass filters may be regarded as being derived from LC filters having parallel RC terminations. In this chapter we will investigate the sensitivity properties for LC filters of this type, and compare the properties to those for LC filters that have purely resistive terminations.

Another purpose of this chapter is to investigate the effects of f_T variations on the impedance for S.B.I. circuits. In particular we will be concerned with deriving expressions for the 1^{st} order normalised differential sensitivities of the real and imaginary parts of the impedance to $1/\omega_T$. Later in the thesis, in Chapter 7, we will describe how to choose the nominal passive component values for S.B.I. circuit B so that the sensitivity of the imaginary part of the impedance to variations in f_T, is minimised. We will show that this strategy also reduces the effects of f_T variations on the loss/frequency response of active filters that contain the S.B.I. circuits B.

6.2 SOME SENSITIVITY FEATURES FOR LC FILTERS

6.2.1 LC FILTERS WITH RESISTIVE TERMINATIONS

The good sensitivity properties of resistively terminated LC filters were first stated by Orchard (1), when he pointed out that the 1^{st} order differential sensitivities of the loss to the reactive components, are zero at frequencies f_{oi} in the passband _if_, at these frequencies, maximun possible transfer of power takes place from the source to load termination.

To investigate Orchard's point let us consider the resistively terminated LC filter shown in Fig. 6.1. Maximum real power will be dissipated to the right hand side (R.H.S.) of the line XX' in Fig. 6.1 whenever the circuit to the right of XX' has the same impedance as the source resistance R_S. The voltage V_X, shown in Fig. 6.1, will then be equal to $V_{IN}/2$, and the maximum power dissipated in the circuit to the R.H.S. of XX' will be $|V_{IN}|^2/4R_S$. This power must be dissipated in the load resistor R_L as this is the only resistive component to the right of XX'. For any output voltage, V_{OUT}, the power dissipated in R_L will be given by $|V_{OUT}|^2/ R_L$. The voltage gain for the filter, for which maximum power generation occurs, can now be determined by equating the maximum power which can be dissipated to the R.H.S. of XX' to the actual power dissipated in R_L, i.e., we obtain

$$\frac{|V_{IN}|^2}{4R_S} = \frac{|V_{OUT}|^2}{R_L} \tag{6.1}$$

and rearrangeing this expression gives

$$\frac{|V_{OUT}|}{|V_{IN}|} = \frac{1}{2}\cdot\sqrt{\frac{R_L}{R_S}} \tag{6.2}$$

It is possible to design resistively terminated LC filters so that, at a number of frequencies f_{oi} in the passband, the actual voltage gain for the filter is equal to the gain shown in (6.2) for which R_L dissipates its maximum power. For such filters we can now argue that, at the frequencies f_{oi}, positive or negative variations in the values of the reactive components in the LC filter can only cause R_L to dissipate less power. Hence the voltage gain for the filter can only decrease, and we can conclude that at the frequencies f_{oi} the 1st order differential sensitivities for the reactive components must be zero.

To illustrate the good sensitivity properties that resistively terminated LC filters can have, let us consider the particular filter circuit shown in Fig. 6.2. The component values for this circuit are also shown in Fig. 6.2, and the nominal loss/frequency response is shown in Figs. 6.3 (a) and (b). The component values in Fig. 6.2 show that R_L is equal to R_S, and from (6.2) we deduce that the voltage gain for the filter must be 0.5 for maximum possible transfer of power to occur. From the nominal loss/frequency behaviour shown in Fig. 6.3 (a) we find that the actual response for the filter does, indeed, contain frequency points where this is the case. To investigate the sensitivity properties for the filter, we took the approach of showing how the loss/frequency response changes when the component values are altered from their nominal values - these curves are shown in Figs. 6.4 (a) to (i). We find that for changes in the capacitor and inductor values, the loss/frequency response cannot rise above the line 6.021 dB which corresponds to a voltage gain of 0.5. Some of the curves for the reactive components also show that the loss for the filter increases a little at the frequencies for maximum possible transfer of power. We can explain this by pointing out that in our discussion we have been concerned only with 1^{st} order differential sensitivities, and the effects of 5.0 and 10.0 % changes in the component values cannot fully be taken into consideration using only these sensitivities.

6.2.2 LC FILTERS WITH PARALLEL RC TERMINATIONS

To investigate the sensitivity properties for LC filters with parallel RC terminations we will again take the approach of studying a particular circuit, and showing how its loss/frequency response is affected by changes in the values of its components. Before this investigation, however, it is interesting to determine the conditions for these filters, for which the transfer of power from the source to load termination is the maximum possible.

Consider the LC filter with parallel RC terminations shown in Fig. 6.5. For this filter maximum real power will be dissipated to the R.H.S. of the line XX' in Fig. 6.5 whenever the impedance to the right of XX' is equal to the complex conjugate of the source impedance. We can prove this in the following way.

Consider the diagram shown in Fig. 6.6 - this shows a voltage V_{IN}, with a source impedance of the general form $Z_S = a_1 + jb_1$, connected to an impedance of the form $Z_X = a_2 + jb_2$. Since both Z_S and Z_X are passive for the filter in Fig. 6.5, both a_1 and a_2 will be positive, but b_1 and b_2 can have different signs. We now determine the values for a_2 and b_2 which cause maximum power to be dissipated to the R.H.S. of the line XX' in Fig. 6.6. From Fig. 6.6 we find that the current I_{IN} is given by

$$I_{IN} = \frac{V_{IN}}{a_1 + a_2 + j(b_1 + b_2)} \tag{6.3}$$

and from this expression we obtain

$$|I_{IN}|^2 = \frac{|V_{IN}|^2}{(a_1 + a_2)^2 + (b_1 + b_2)^2} \qquad (6.4)$$

The power dissipated to the right of XX', P_{XX}', is therefore given by

$$P_{XX}' = a_2 |I_{IN}|^2 = \frac{a_2 |V_{IN}|^2}{(a_1 + a_2)^2 + (b_1 + b_2)^2} \qquad (6.5)$$

and for this expression to be a maximum it is necessary to choose $b_2 = -b_1$, and $a_2 = a_1$, i.e., we must choose Z_X to be the complex conjugate of Z_S. Note, from (6.5), that for this case the maximum value for P_{XX}' is

$$P_{XX}'(\max) = \frac{|V_{IN}|^2}{4a_1} \qquad (6.6)$$

For the LC filter in Fig. 6.5 the source impedance is given by

$$Z_S = R_S/(1 + pR_SC_S) \qquad (6.7)$$

and this can be written in the form $Z_S = a_1 + jb_1$ where

$$\begin{aligned} a_1 &= R_S/(1 + \omega^2 R_S^2 C_S^2) \\ b_1 &= -\omega C_S R_S^2/(1 + \omega^2 R_S^2 C_S^2) \end{aligned} \qquad (6.8)$$

Making use of the above expression for a_1 in (6.6), we find that the maximum possible power which can be dissipated to the R.H.S. of XX' in Fig. 6.5 is given by

$$P_{XX'}(\max) = \frac{|V_{IN}|^2(1 + \omega^2 R_S^2 C_S^2)}{4R_S} \qquad (6.9)$$

The power dissipated to the right of XX' can only be due to the load resistor R_L, and is given by the expression

$$P_L = \frac{|V_{OUT}|^2}{R_L} \qquad (6.10)$$

Now, by equating $P_{XX'}(\max)$ in (6.9) to P_L in (6.10), we can find the magnitude of the voltage gain V_{OUT}/V_{IN} for which the power dissipated by R_L is a maximum, i.e.,

$$\frac{|V_{OUT}|^2}{R_L} = \frac{|V_{IN}|^2(1 + \omega^2 R_S^2 C_S^2)}{4R_S} \qquad (6.11)$$

and, by rearrangement, we obtain

$$\left|\frac{V_{OUT}}{V_{IN}}\right| = \frac{R_L(1 + \omega^2 R_S^2 C_S^2)}{4R_S} \qquad (6.12)$$

Note that this expression is frequency dependent unlike the expression in (6.2) for the resistively terminated LC filter case.

An example of an LC filter with parallel RC terminations is shown in Fig. 6.7 (thanks are due to C. Nightingale, Post Office Research Centre, for designing this filter). The component values for the filter are also shown in Fig. 6.7, and the nominal loss/frequency behaviour is shown in Figs. 6.8 (a) and (b). By substituting the values for R_S, R_L and C_S into equation (6.12), we can determine the voltage gain required for maximum possible transfer of power to take place in the filter - this behaviour is shown in Fig. 6.8 (a) alongwith the passband loss/frequency response for the filter. We find that the passband response does not contain frequency points for which maximum transfer of power occurs. Computed curves showing how the loss for the filter is affected by changes in the component values, are shown in Figs. 6.9 (a) to (k). For the capacitor and inductor changes we find that the altered loss/frequency response can rise above its nominal behaviour, unlike the changes shown previously in Figs. 6.4 (c) to (i) for the resistively terminated LC filter case. Comparing the curves in Fig. 6.4 with those in Fig. 6.9, we find that, on the whole, the sensitivities for the LC filter studied here are worse than those for the resistively terminated filter studied in Section 6.2.1.

Some comments on the sensitivity properties of LC lowpass filters with parallel RL terminations have been made by Nightingale and Rollett (58). They suggest that the component sensitivities for these filters are improved as we choose a smaller ratio for the normalised inductance and resistance values for the source impedance. By 'normalised source inductance and source resistance values' we mean the values that arise when the filters have been normalised to have a passband edge frequency of 1.0 r/s. Since LC highpass filters with parallel RC terminations are obtained from LC lowpass filters with parallel RL terminations, merely by lowpass to highpass transformation , we would expect the component sensitivities for the highpass filters to be improved as we chose a smaller product for the normalised capacitance and resistance values for the source impedance. Further investigation of this point,however, has not been undertaken.

6.3 EFFECTS OF F_T VARIATIONS ON THE IMPEDANCE FOR S.B.I. CIRCUITS

6.3.1 GENERAL EFFECTS

In Section 3.4 we pointed out that the single-amplifier, single-capacitor, simulation networks discussed in this thesis have an impedance of the form

$$Z = \frac{a_0 + pa_1 + p^2a_2}{b_0 + pb_1 + p^2b_2} \tag{6.13}$$

when the non-ideal voltage gain for the amplifier is taken into consideration. In Section 5.3 we suggested designing the simulating networks so that the coefficients a_0 and b_1 in (6.13) are zero, and we then showed that the impedance Z becomes

$$Z = \frac{pL(1 + p\tau)}{1 + p^2LC} \tag{6.14}$$

where

$$L = a_1/b_0 \quad , \quad C = b_2/a_1 \quad , \quad \tau = a_2/a_1 \tag{6.15}$$

We referred to networks having this type of impedance as ideal S.B.I. circuits. In this section we express the impedance for the S.B.I. circuits in the form

$$Z = R_E(\omega) + jI_M(\omega) \tag{6.16}$$

and then we derive expressions for the normalised sensitivities

$S^{R_E(\omega)}_{1/\omega_T}$ and $S^{I_M(\omega)}_{1/\omega_T}$. These sensitivities are defined as

$$S^{R_E(\omega)}_{1/\omega_T} = \frac{dR_E(\omega)}{d(1/\omega_T)} \cdot \frac{1/\omega_T}{R_E(\omega)} \tag{6.17}$$

$$S^{I_M(\omega)}_{1/\omega_T} = \frac{dI_M(\omega)}{d(1/\omega_T)} \cdot \frac{1/\omega_T}{I_M(\omega)} \tag{6.18}$$

First of all we rewrite equation (6.13) in the following form

$$Z = \frac{M + pL(1 + p\tau)}{1 + pN + p^2LC} \tag{6.19}$$

where the expressions for L, C, and τ are the same as those in (6.15), and M and N are given by

$$M = a_0/b_0 \quad , \quad N = b_1/b_0 \tag{6.20}$$

To obtain an S.B.I. circuit we now need to choose M = 0 and N = 0 in (6.19). When the impedance expression in (6.19) is written in the form shown in (6.16) we obtain

$$R_E(\omega) = \frac{(M - \omega^2L\tau)(1 - \omega^2LC) + \omega^2NL}{(1 - \omega^2LC)^2 + \omega^2N^2} \tag{6.21}$$

$$I_M(\omega) = \frac{\omega L(1 - \omega^2LC) - \omega N(M - \omega^2L\tau)}{(1 - \omega^2LC)^2 + \omega^2N^2} \tag{6.22}$$

Note that the substitution $p = j\omega$ has been made in (6.19) to enable the impedance to be expressed in the form shown in (6.16). When the nominal values M = 0, N = 0, $L = L_N$, $C = C_N$ and $\tau = \tau_N$, are substituted into (6.21) and (6.22) we find that the S.B.I.s have, ideally, an impedance with a real and imaginary part given by

$$R_E^*(\omega) = \frac{-\omega^2 L_N \tau_N}{1 - \omega^2 L_N C_N} \tag{6.23}$$

$$I_M^*(\omega) = \frac{\omega L_N}{1 - \omega^2 L_N C_N} \tag{6.24}$$

In general variations in the f_T value for the amplifier in the S.B.I. circuits will alter the values for M, N, L, C and τ from their nominal values. Because of these changes, the real and imaginary parts of the impedance for the S.B.I.s will not have the nominal values shown in (6.23) and (6.24). For sufficiently small changes in M N, L, C and τ from the nominal values, the changes in $R_E(\omega)$ and $I_M(\omega)$ will, in general, be given by

$$\Delta I_M(\omega) = \frac{\partial I_M(\omega)}{\partial L}\Delta L + \frac{\partial I_M(\omega)}{\partial C}\Delta C + \frac{\partial I_M(\omega)}{\partial \tau}\Delta \tau + \frac{\partial I_M(\omega)}{\partial M}\Delta M + \frac{\partial I_M(\omega)}{\partial N}\Delta N \tag{6.25}$$

$$\Delta R_E(\omega) = \frac{\partial R_E(\omega)}{\partial L}\Delta L + \frac{\partial R_E(\omega)}{\partial C}\Delta C + \frac{\partial R_E(\omega)}{\partial \tau}\Delta \tau + \frac{\partial R_E(\omega)}{\partial M}\Delta M + \frac{\partial R_E(\omega)}{\partial N}\Delta N \tag{6.26}$$

Expressions for the partial derivatives shown in (6.25) and (6.26) may be found from equations (6.21) and (6.22). For the nominal values $M = 0$, $N = 0$, $L = L_N$, $C = C_N$ and $\tau = \tau_N$ we obtain

$$\frac{\partial I_M(\omega)}{\partial L} = \frac{\omega}{(1 - \omega^2 L_N C_N)^2} \qquad \frac{\partial R_E(\omega)}{\partial L} = \frac{-\ \omega^2 \tau_N}{(1 - \omega^2 L_N C_N)^2}$$

$$\frac{\partial I_M(\omega)}{\partial C} = \frac{\omega^3 L_N^2}{(1 - \omega^2 L_N C_N)^2} \qquad \frac{\partial R_E(\omega)}{\partial C} = \frac{-\ \omega^4 L_N^2 \tau_N^2}{(1 - \omega^2 L_N C_N)^2}$$

$$\frac{\partial I_M(\omega)}{\partial \tau} = 0 \qquad \frac{\partial R_E(\omega)}{\partial \tau} = \frac{-\ \omega^2 L_N}{1 - \omega^2 L_N C_N}$$

$$\frac{\partial I_M(\omega)}{\partial M} = 0 \qquad \frac{\partial R_E(\omega)}{\partial M} = \frac{1}{1 - \omega^2 L_N C_N}$$

$$\frac{\partial I_M(\omega)}{\partial N} = \frac{\omega^3 L_N \tau_N}{(1 - \omega^2 L_N C_N)^2} \qquad \frac{\partial R_E(\omega)}{\partial N} = \frac{\omega^2 L_N}{(1 - \omega^2 L_N C_N)^2}$$

(6.27)

When the expressions in (6.27) are substituted into (6.25) and (6.26) we obtain

$$\Delta I_M(\omega) = \frac{\omega(\Delta L + \omega^2 L_N^2 \Delta C + \omega^2 \tau_N L_N \Delta N)}{(1 - \omega^2 L_N C_N)^2} \tag{6.28}$$

$$\Delta R_E(\omega) = \frac{\left\{\begin{array}{l} \omega^2 L_N \Delta N - \omega^2 \tau_N \Delta L - \omega^4 L_N^2 \tau_N \Delta C + \\ (1 - \omega^2 L_N C_N)\Delta M - \omega^2 L_N (1 - \omega^2 L_N C_N)\Delta \tau \end{array}\right\}}{(1 - \omega^2 L_N C_N)^2} \tag{6.29}$$

These expressions show how the small changes ΔL, ΔC, $\Delta\tau$, ΔM and ΔN affect the impedance for the S.B.I.s. We now continue investigating the case where the small changes in L, C, τ, M and N are caused by variations in f_T. Since f_T is very large, however, we will follow the general procedure of considering the effects of small changes in $1/\omega_T$, where $\omega_T = 2\pi f_T$.

For sufficiently small changes in $1/\omega_T$, the changes in L, C, τ, M and N are given by the general expressions

$$\Delta L = \frac{\partial L}{\partial(1/\omega_T)}\Delta(1/\omega_T) \qquad \Delta C = \frac{\partial C}{\partial(1/\omega_T)}\Delta(1/\omega_T)$$

$$\Delta\tau = \frac{\partial \tau}{\partial(1/\omega_T)}\Delta(1/\omega_T) \qquad \Delta M = \frac{\partial M}{\partial(1/\omega_T)}\Delta(1/\omega_T)$$

$$\Delta N = \frac{\partial N}{\partial(1/\omega_T)}\Delta(1/\omega_T) \tag{6.30}$$

Substituting these expressions into (6.28) gives

$$\Delta I_M(\omega) = \frac{\Delta(1/\omega_T)\left\{\omega\dfrac{\partial L}{\partial(1/\omega_T)} + \omega^3 L_N^2\dfrac{\partial C}{\partial(1/\omega_T)} + \omega^3 L_N \tau_N \dfrac{\partial N}{\partial(1/\omega_T)}\right\}}{(1 - \omega^2 L_N C_N)^2} \tag{6.31}$$

and the differential sensitivity $\dfrac{dI_M(\omega)}{d(1/\omega_T)}$ is found by letting $\Delta(1/\omega_T) \rightarrow 0$ in (6.31), i.e.,

$$\frac{dI_M(\omega)}{d(1/\omega_T)} = \frac{\omega\dfrac{\partial L}{\partial(1/\omega_T)} + \omega^3 L_N^2\dfrac{\partial C}{\partial(1/\omega_T)} + \omega^3 L_N \tau_N \dfrac{\partial N}{\partial(1/\omega_T)}}{(1 - \omega^2 L_N C_N)^2} \tag{6.32}$$

The normalised differential sensitivity can now be found from eqns. (6.18), (6.24) and (6.32), i.e., we obtain

$$S^{I_M(\omega)}_{(1/\omega_T)} = \frac{\dfrac{\partial L}{\partial(1/\omega_T)} + \omega^2 L_N^2\dfrac{\partial C}{\partial(1/\omega_T)} + \omega^2 L_N \tau_N \dfrac{\partial N}{\partial(1/\omega_T)}}{\omega_T L_N(1 - \omega^2 L_N C_N)^2} \tag{6.33}$$

Before deriving an expression for $S^{R_E(\omega)}_{(1/\omega_T)}$, we note that $\partial M/\partial(1/\omega_T)$ is zero for the following reason

Equation (6.19) shows that the parameter M represents the D.C. resistance for the simulating networks. The value for the D.C. resistance, i.e. M, depends on the values for the passive components in the simulating networks, and also on the gain of the amplifier at D.C.. In general the gain G is given by $G = 1/(\alpha + j\omega/\omega_T)$, and at D.C. this expression is equal to $1/\alpha$. The parameter M is therefore independent of ω_T, and hence of $1/\omega_T$, and we can conclude that $\partial M/\partial(1/\omega_T) = 0$. Note that we are considering here only the effects of ω_T variations on the impedance of the S.B.I.s and <u>not</u> the effects of variations in α.

Substituting the expressions in (6.30) into (6.29), and putting $\partial M/\partial(1/\omega_T) = 0$, gives

$$\Delta R_E(\omega) = \frac{-\Delta(1/\omega_T)\left\{\omega^2\tau_N \dfrac{\partial L}{\partial(1/\omega_T)} + \omega^4 L_N^2 \tau_N \dfrac{\partial C}{\partial(1/\omega_T)} + \omega^2 L_N(1 - \omega^2 L_N C_N)\dfrac{\partial \tau}{\partial(1/\omega_T)} - \omega^2 L_N \dfrac{\partial N}{\partial(1/\omega_T)}\right\}}{(1 - \omega^2 L_N C_N)^2} \tag{6.34}$$

From this expression we obtain

$$\frac{dR_E(\omega)}{d(1/\omega_T)} = \frac{-1}{(1 - \omega^2 L_N C_N)^2}\left\{\omega^2\tau_N \frac{\partial L}{(1/\omega_T)} + \omega^4 L_N^2 \tau_N \frac{\partial C}{(1/\omega_T)} + \omega^2 L_N(1 - \omega^2 L_N C_N)\frac{\partial \tau}{(1/\omega_T)} - \omega^2 L_N \frac{\partial N}{\partial(1/\omega_T)}\right\} \tag{6.35}$$

and the normalised sensitivity, obtained from eqns. (6.17), (6.23) and (6.35), is given by

$$S_{1/\omega_T}^{R_E(\omega)} = \frac{1}{\omega_T L_N \tau_N (1 - \omega^2 L_N C_N)} \left\{ \tau_N \frac{\partial L}{\partial(1/\omega_T)} + \omega^2 L_N^2 \tau_N \frac{\partial C}{\partial(1/\omega_T)} + L_N(1 - \omega^2 L_N C_N) \frac{\partial \tau}{\partial(1/\omega_T)} - L_N \frac{\partial N}{\partial(1/\omega_T)} \right\} \tag{6.36}$$

6.3.2 EFFECTS OF F_T VARIATIONS ON THE IMPEDANCE FOR S.B.I. CIRCUIT B

To evaluate the normalised sensitivities $S^{I_M(\omega)}_{(1/\omega_T)}$ and $S^{R_E(\omega)}_{(1/\omega_T)}$ for S.B.I. circuit B, it will not only be necessary to know the nominal values L_N, C_N and τ_N appearing in (6.33) and (6.36), but also the values for the partial derivatives $\partial L/\partial(1/\omega_T)$, $\partial C/\partial(1/\omega_T)$, $\partial\tau/\partial(1/\omega_T)$ and $\partial N/\partial(1/\omega_T)$. For any set of nominal component values for S.B.I. circuit B we can use eqns. (5.21), (5.22) and (5.23) to calculate L_N, C_N and τ_N. We can also use these equations to determine expressions for the partial derivatives $\partial L/\partial(1/\omega_T)$, $\partial C/\partial(1/\omega_T)$ and $\partial\tau/\partial(1/\omega_T)$, i.e., differentiating eqns. (5.21), (5.22) and (5.23) with respect to $1/\omega_T$ we obtain

$$\frac{\partial L}{\partial(1/\omega_T)} = \frac{(G_2 + G_3)(G_1 + G_4 + G_5)}{(G_1 + G_6)(G_4G_2 - G_3G_5) + G_1G_2G_6 + \alpha(G_2 + G_3)\left\{(G_4 + G_5)(G_1 + G_6) + G_1G_6\right\}} \tag{6.37}$$

$$\frac{\partial C}{\partial(1/\omega_T)} = \frac{\left[G_4 + \alpha(G_1 + G_4 + G_5)\right]\left[(G_2 + G_3 + G_6)(G_1 + G_4 + G_5) + G_1(G_4 + G_5)\right]}{\left\{G_4 + \alpha(G_1 + G_4 + G_5) + (G_2 + G_3)(G_1 + G_4 + G_5)/\omega_T C_0\right\}^2} \tag{6.38}$$

$$\frac{\partial \tau}{\partial(1/\omega_T)} = \frac{(G_1 + G_4 + G_5)\left\{G_4 + \alpha(G_1 + G_4 + G_5)\right\}}{\left\{G_4 + \alpha(G_1 + G_4 + G_5) + (G_2 + G_3)(G_1 + G_4 + G_5)/\omega_T C_0\right\}^2} \tag{6.39}$$

To determine the expression for $\partial N/\partial(1/\omega_T)$, it is first of all necessary to determine the expression for N in (6.19). Making use of eqns. (6.20) and (5.17) we find that, for S.B.I. circuit B, N is given by

$$N = \frac{C_0\left\{\begin{aligned}&G_4G_2 - G_5(G_3 + G_6) + (G_2 + G_3)\left[(G_4 + G_5)(G_1 + G_6) + G_1G_6\right]/\omega_T C_0\\ &+ \alpha\left[(G_2 + G_3 + G_6)(G_1 + G_4 + G_5) + G_1(G_4 + G_5)\right]\end{aligned}\right\}}{(G_1 + G_6)(G_4G_2 - G_3G_5) + G_1G_2G_6 + \alpha(G_2+G_3)\left[(G_4+G_5)(G_1+ G_6) + G_1G_6\right]} \tag{6.40}$$

and differentiating this expression w.r.t. $1/\omega_T$ gives

$$\frac{\partial N}{\partial(1/\omega_T)} = \frac{(G_2 + G_3)\left\{(G_4 + G_5)(G_1 + G_6) + G_1G_6\right\}}{(G_1 + G_6)(G_4G_2 - G_3G_5) + G_1G_2G_6 + \alpha(G_2+G_3)\left\{(G_4+G_5)(G_1+G_6) + G_1G_6\right\}} \tag{6.41}$$

The expression for M in (6.19), for S.B.I. circuit B, may also be found from eqns. (6.20) and (5.17), i.e. , we obtain

$$M = \frac{G_4G_2 - G_3(G_1 + G_5) + \alpha(G_2 + G_3)(G_1 + G_4 + G_5)}{(G_1 + G_6)(G_4G_2 - G_3G_5) + G_1G_2G_6 + \alpha(G_2+G_3)\left\{(G_4+G_5)(G_1+G_6) + G_1G_6\right\}} \tag{6.42}$$

Note that this expression does not contain any ω_T terms as mentioned previously in Section 6.3.1.

For any choice of nominal component values for S.B.I. circuit B, we can use eqns. (6.37), (6.38), (6.39) and (6.41) to evaluate $\partial L/\partial(1/\omega_T)$, $\partial C/\partial(1/\omega_T)$, $\partial \tau/\partial(1/\omega_T)$ and $\partial N/\partial(1/\omega_T)$. We can then use these values, and the values for L_N, C_N and τ_N, in (6.33) and (6.36) to determine the normalised sensitivities $S^{I_M(\omega)}_{(1/\omega_T)}$ and $S^{R_E(\omega)}_{(1/\omega_T)}$. In Chapter 7 we will show how to choose the nominal passive component values for S.B.I. circuit B so that, in addition to the usual design requirements $M = 0$, $N = 0$ and $L = L_N$, the value for $S^{I_M(\omega)}_{(1/\omega_T)}$ is minimised at a chosen frequency. We will then use this design procedure to obtain active-RC filters whoose loss/frequency responses have low sensitivities to f_T variations.

6.4 CONCLUSIONS

This chapter has been concerned with the sensitivity properties for active filters that use S.B.I. circuits. We pointed out that both highpass and bandpass filters that use S.B.I.s , can be considered as being derived from LC filters having paralell RC terminations. We briefly investigated the sensitivity properties for filters of this type, and showed that they can be significantly more sensitive than LC filters having purely resistive terminations.

We also investigated the effects of f_T variations on the real and imaginary parts of the impedance for the S.B.I. circuits. General expressions for the 1st order normalised differential sensitivities $S^{I_M(\omega)}_{(1/\omega_T)}$ and $S^{R_E(\omega)}_{(1/\omega_T)}$ were derived, and we showed, in particular, how to calculate these sensitivities for the S.B.I. circuit B. In Chapter 7 we choose the nominal passive component values for the S.B.I. circuit B so that the sensitivity $S^{I_M(\omega)}_{(1/\omega_T)}$ is minimised, and we then show that this strategy helps to reduce the effects of f_T variations on the loss/frequency response of active filters that contain S.B.I. circuits B.

CHAPTER 7

EXPERIMENTAL INVESTIGATIONS

7.1 HIGHPASS FILTER USING S.B.I. CIRCUIT B

In this section we describe an active-RC highpass filter which uses S.B.I. circuit B, and whose loss/frequency response is the same as that for a 5^{th} order Cauer type LC filter having the nominal behaviour: stopband attenuation $\leqslant 30$ dB, loss variation in passband $\leqslant 0.1$ dB above 2.0 kHz.

7.1.1 DESIGN OF THE ACTIVE FILTER

As mentioned in Section 5.3.2.2, the first step in designing the active highpass filter is to choose an LC lowpass filter, with parallel RL terminations, whose loss/frequency response has the corresponding lowpass behaviour: stopband attenuation $\leqslant 30$ dB, loss variation in passband $\leqslant 0.1$ dB below 2.0 kHz. An appropriate lowpass filter having the above behaviour, except that the passband edge frequency ω_c is 1.0 r/s, is shown in Fig. 7.1 (a), and its component values are given in Table (a) of Fig. 7.2 (thanks are due to C. Nightingale, British Post Office Research Centre, for designing this filter). A new set of component values which cause the response to have the required lowpass behaviour, i.e. $f_c = 2.0$ kHz, can be obtained by denormalisation. That is, we multiply the capacitor values in Table (a) of Fig. 7.2 by $1/2\pi f_c R$, the inductor values by $R/2\pi f_c$, and the source and load resistors by R, where R can be chosen arbitrarily. The component values that are obtained for the case $R = 2.0\ K\Omega$ are shown in Table (b) of Fig. 7.2.

From the lowpass filter in Fig. 7.1 (a) we obtain, by lowpass to highpass transformation, the LC highpass filter with parallel RC terminations shown in Fig. 7.1 (b). This transformation involves replacing the inductors L_i in the lowpass filter by capacitors of value $1/\omega_c^2 L_i$, and replacing the capacitors C_i in the lowpass filter by inductors of value $1/\omega_c^2 C_i$ - the component values that are obtained for the highpass filter are shown in Table (c) of Fig. 7.2. We now transform the filter in Fig. 7.1 (b) in the way described in Section 5.3.2.2, to obtain the LC highpass filter in Fig. 7.1 (c), for which the inductors L_A and L_B appear as parts of grounded parallel LC resonators - the component values for this circuit are shown in Table (d) of Fig. 7.2.

The next step in the design procedure is to choose two sets of nominal component values for S.B.I. circuit B so that the conditions $a_0 = 0$ and $b_1 = 0$ in (5.4) are satisfied, and so that L in (5.6) is equal to the inductance values L_A and L_B for the LC filter in Fig. 7.1 (c). To satisfy these conditions we used the design procedure for S.B.I. circuit B described previously in Section 5.4.1.2. As mentioned in Section 5.4.1.2, there are many ways of choosing the nominal component values for S.B.I. circuit B so that the conditions $a_0 = 0$ and $b_1 = 0$ are achieved, and so that L has a specified nominal value. The component values used here, which are for an amplifier having $\alpha = 10^{-5}$ and $f_T = 10^6$ Hz, are shown in Tables (a) and (b) of Fig 7.3. Note that we obtained the component values in Table (b) of Fig 7.3, which are for the case $L = L_B$, by multiplying the resistance values for the case $L = L_A$ by the constant L_A/L_B, and by multiplying the capacitance value for $L = L_A$ by the constant L_B/L_A. As mentioned in Section 5.3, this ensures that the values of associated with the designs for $L = L_A$ and $L = L_B$, see (5.6), are the same. This value of τ, and the values C_A and C_B associated with the two designs for the S.B.I. circuit, see (5.6), are shown in the Tables of component values in Fig 7.3.

To complete the design of the active high pass filter, the LC filter in Fig 7.1 (c) was modified in the way described in Section 5.3.2.2, see also Fig 5.7 (e), and then impedance scaled by $(1 + p\tau)$ to give the active RC filter shown in Fig 7.4 (a) - the full set of component values for this filter is given in Fig 7.4 (b).

7.1.2 EXPERIMENTAL ADJUSTMENT PROCEDURE FOR HIGHPASS FILTER

The active filter of Fig 7.4 (a) was constructed using resistors and capacitors having values within $\pm$ 1% of the specified values shown in Fig 7.4 (b), however, some of the resistors with very small values, ie, R_{C2} and R_{C5}, were not included in the realisation. These tolerances and omissions cause the loss/frequency response for the experimental filter to deviate from the nominal response; also, the f_t values for the amplifiers will not be precisely equal to their nominal values, and this again causes the response to be non-ideal.

Ideally the S.B.I. circuits B in the active filter have the impedance:

$$Z = \frac{pL_N(1 + p\tau_N)}{1 + p^2 L_N C_N} \qquad (7.1)$$

where L_N, τ_N, and C_N represent the nominal values shown in Tables (a) and (b) of Fig 7.3. However, due to passive component tolerances and f_T tolerances, the S.B.I.s will instead have impedances of the form

$$Z = \frac{M + pL(1 + p\tau)}{1 + pN + p^2 LC} \qquad (7.2)$$

Thus, for the S.B.I.s to have their ideal impedances, it would be necessary to adjust the resistances for each circuit so that the following five conditions were obtained: $M = 0$, $N = 0$, $L = L_N$, $C = C_N$ and $\tau = \tau_N$. It is impossible in practice, however, to make resistance adjustments for S.B.I circuit B so that all these conditions are achieved simultaneously. Also, if such adjustments were possible, we would still not be overcoming the effects on the highpass filter response, of tolerances on the remaining components in the filter. Instead, as a compromise, we adopted the following adjustment strategy which we have found to be satisfactory:

The adjustment strategy adopted here is to try to achieve both the following conditions:

(i) Each S.B.I. circuit has zero D.C. resistance (from (7.2) the D.C. resistance is given by M which is ideally zero).

(ii) The shunt arms in the highpass filter have their ideal impedance of zero , at their appropriate nominal transmission zero frequency.

These conditions were achieved in practice by iteratively adjusting the three resistors R3, R6, and R5 in each S.B.I. circuit using the experimental procedure described below:

First of all we adjust the conductance G_3 in eachS.B.I. circuit so that the condition M = O was achieved. From (6.42) we have:

$$M = \frac{G_4G_2 - G_3(G_1 + G_5) + \alpha(G_2 + G_3)(G_1 + G_4 + G_5)}{(G_1 + G_6)(G_4G_2 - G_3G_5) + G_1G_2G_6 + \alpha(G_2+G_3)\left\{(G_4+G_5)(G_1+G_6) + G_1G_6\right\}} \tag{7.3}$$

and from (7.2 we note that M represents the D.C. resistance for the S.B.I. circuit. We can therefore make M equal to zero in practice, by connecting a resistance meter across the S.B.I. circuit and adjusting G_3 until the resistance is zero.

The next part of the adjustment procedure is to iteratively adjust the resistors R6 and R5 for each S.B.I. circuit, so that the shunt arms of the active highpass filter not only have their nominal transmission zero frequencies, but so that the impedance at these frequencies is zero. Each shunt arm is di connected from the filter, connected to a series resistor, and driven at the appropriate transmission zero frequency, as shown in Fig 7.5. The resistors R6 and R5 are then adjusted iteratively so that the voltage V_{OUT} shown in Fig 7.5 is as close as possible to zero. The shunt arms are then reconnected to the filter. Note that we are taking into consideration the tolerances on the components C2, C6, C4, C7, RC2, RC6, RC4 and RC7 in Fig 7.4 (a), as well as the tolerances for the components in the S.B.I. circuits at the appropriate transmission zero frequency.

Adjusting R6 does not affect the value of M, for M = 0, as shown in (7.3). However, the adjustments made to R5 will affect the M value and hence change the D.C.resistance from zero Ω s. For the adjustment procedure to be successful, it is necessary that the adjustments of R5 introduce only small changes in the D.C. resistance values for the S.B.I.s. Examination of (7.3) has shown that this will be the case if the S.B.I.s can be designed using large values for R2, R3 and R5 and small values for R1, R4 and R6. Hence, the spread in the resistance values for the S.B.I.s show in Fig 7.4 (b). A detailed investigation of the adjustment procedure has not been undertaken, however, it is probably the case that the variations in R6 affect the values of both the imaginary and real parts of the impedance presented by the S.B.I. circuit, whereas the same percentage variations in R5 affect the real part (and hence the Q of the S.B.I. circuit) and have a much smaller affect on the imaginary part.

Investigation of adjustment procedures for filters using other types of S.B.I. circuit, rather than type B, would be desirable but has not been undertaken owing to lack of time. Nevertherless, the general strategy described above seems to be satisfactory as will be demonstrated by the measured filter performance given in the next section.

7.1.3 COMPUTED AND MEASURED RESULTS

The loss/frequency response for the active-RC highpass filter was determined using a computer analysis program, and is shown in Fig. 7.6. We find that this behaviour precisely suits our desired specification, namely: stopband attenuation $\leqslant 30$ dB, and loss variation in passband $\leqslant 0.1$ dB above 2.0 kHz.

For the practical filter we adjusted the S.B.I. circuits in the way described in Section 7.1.2, and then we measured the loss/frequency response to obtain the behaviour shown in Fig. 7.7. The measured response agrees fairly closely with the computed response in Fig. 7.6 and shows that the adjustment procedure for overcoming the passive component and f_T tolerances is satisfactory, at least for the filter example studied here. The passband loss for the practical filter, measured at 10.0 kHz, was 7.9 dB $\pm$ 0.1 dB measuring error, and is in close agreement with the computed value 7.86 dB.

7.1.4 SENSITIVITY INVESTIGATION

To investigate the passive component sensitivities for the highpass filter, we took the approach of showing how the loss/frequency response changes, when the passive component values are altered from their nominal values - these curves are shown in Figs. 7.8 (a) to (b). For comparision purposes, we decided to show how the response of a low sensitivity LC filter is affected by changes in its component values. The LC filter is shown in Fig.7.9 alongwith its nominal passive component values, and the changes in the loss/frequency behaviour for this filter are shown in Figs. 7.10 (a) and (b).

The curves in Figs. 7.8 (a) to (b), for the capacitance changes for the active highpass filter, show that the loss can become less than the basic loss, i.e., 7.8 dB. This behaviour was also observed in Section 6.2.2, where we investigated the effects of passive component changes on the loss/frequency response for an LC filter with parallel RC terminations. Note, from the curves in Figs. 7.10 (a) and (b), that, for the resistively terminated LC filter in Fig. 7.9, the capacitance and inductance changes cannot cause the loss to become less than the basic passband loss of 6.021 dB (see Section 6.2.1).

The computed curves for the resistors in the S.B.I. circuits in the active filter, show that the altered loss/frequency response is not much worse than that for the capacitors in the S.B.I.s. This is interesting as the changes in the resistance values affect the conditions $M = 0$ and $N = 0$ required in the impedance expression for the S.B.I.s (see (6.19), whereas the changes in the capacitance values for the S.B.I.s do not alter M from zero (see (6.42), and they have only a 2nd order effect, due to f_T, on the value for N (see (6.40).

The effects of small tolerances on the components C_L, R_{CL}, R_{CS}, R_{C1} to R_{C6}, on the highpass filter's response, are very small and have not been shown. Note also, from Fig. 7.8 (b), that the changes for the capacitors C_S, C_6 and C_7 are very small in the region of the passband edge frequency but become larger at higher frequencies. The computed effects of $\pm$ 20.0 % simultaneous changes in the f_T values of both amplifiers in the active filter are shown in Fig. 7.11 - once again, we find that the loss/frequency response for the highpass filter is not much affected near the passband edge frequency, but the effect at higher frequencies becomes more significant.

On the whole the altered loss/frequency responses for the capacitors in the active highpass filter are worse than those for the LC highpass filter in Fig. 7.9. It may be possible to improve the sensitivities for the capacitors in the active filter by redesigning the LC filter circuit in Fig. 7.1 (c), from which the active filter was obtained, so that its sensitivities were closer to those for the LC filter in Fig. 7.9. This may be achieved by choosing a smaller time constant $R_S C_S$ for the filter in Fig. 7.1 (b), however, this possibility has not been investigated further.

7.2 RESONATOR CIRCUIT USING S.B.I. CIRCUIT B

In this section we discuss the active RC realisation for the LC network shown in Fig 7.12 (a) using S.B.I. circuit B. This nwtwork consists of a parallel LC resonator connected to a source resistance R_S, but, for convenience, we refer here to the entire circuit in Fig 7.12 (a) as a resonator circuit. In Section 7.2.1 we show how to obtain the active-RC realisation for the LC resonator circuit, then we choose a typical design for the active resonator, and investigate the effects of f_T variations on its loss/frequency response. A design procedure for reducing the effects of f_T variations is presented in Section 7.2.2.

7.2.1 DESIGN FOR THE ACTIVE RESONATOR CIRCUIT

We now describe how the passive resonator in Fig 7.12 (a) can be realised using S.B.I. circuit B, which has an impedance of the form

$$Z = \frac{pL(1 + p\tau)}{1 + p^2LC} \qquad (7.4)$$

First of all the S.B.I. circuit B is designed so that the parameter L in (7.4) has the inductance value L_R for the passive resonator . The parameters C and τ in (7.4) will then have the nominal values C_R and τ_R. The circuit in Fig. 7.12 (a) is now modified in the way shown in Fig. 7.12 (b), and this circuit is then impedance scaled by $(1 + p\tau)$ to obtain the circuit in Fig. 7.12 (c), where Z_R represents the impedance in (7.13) for the case $L = L_R$, $C = C_R$ and $\tau = \tau_R$. Impedance scaling the source resistor R_S in Fig. 7.12 (b) by $(1 + p\tau)$ gives rise to the small inductance L' shown in Fig. 7.12 (c). In the case of the equally resistively terminated bandpass filters discussed in Section 5.3.3 it was possible to eliminate this unwanted inductor using the transformation shown in Fig. 5.8, however,this is not possible here as the circuit in Fig. 7.12 (c) is singly terminated. Instead we shall ignore the small inductance to obtain the active-RC resonator circuit shown in Fig. 7.12 (d).

We will now describe, in detail, the design of the active resonator in Fig. 7.12 (d) for the case where the original passive resonator has a resonance frequency $f_R = 1.0$ kHz, and a Q of 10. The parameters f_R and Q refer to the transfer function for the passive resonator in Fig. 7.12 (a) which is of the form

$$T(p) = \frac{pL_R}{R_S + pL_R + p^2 L_R C_N R_S} \qquad (7.5)$$

This expression can be rewritten as

$$T(p) = \frac{D(p/\omega_R)}{1 + D(p/\omega_R) + (p/\omega_R)^2} \qquad (7.6)$$

where

$$\omega_R = \frac{1}{\sqrt{L_R C_N}} \quad , \quad D = \frac{1}{R_S}\sqrt{\frac{L_R}{C_N}} \qquad (7.7)$$

The resonance frequency f_R is given by $\omega_R/2\pi$, and Q is defined as the inverse of D, i.e., $Q = D^{-1}$. Making use of the inverse relationships $\omega_R = 2\pi f_R$ and $D = Q^{-1}$ in (7.7), and then solving for L_R and C_N, we obtain

$$L_R = \frac{R_S}{2\pi f_R Q} \qquad C_N = \frac{Q}{2\pi f_R R_S} \qquad (7.8)$$

These expressions show how to choose the values L_R and C_N for the passive resonator in Fig. 7.12 (a), so that it has the required resonance frequency and Q value - note, from (7.8), that the value R_S for the passive resonator can be chosen arbitrarily. Choosing $R_S = 10.0\ k\Omega$, with $f_R = 1.0$ kHz and $Q = 10$, we obtain: $L_R = 159.15$ mH, and $C_N = 159.15$ nF.

The S.B.I. circuit B is now designed in the way proposed in Section 5.4.1.2, so that the parameter L in (7.4) is equal to the inductance value L_R determined above. As mentioned in Section 5.4.1.2 there are some degrees of freedom in our choice of values for the components G_1, G_2, G_4 and G_5 in the S.B.I. circuit B. For the present example we chose: $G_1 = G_2 = G_4 = G_5 = 10^{-4}\mho$, and for the non-ideal amplifier gain we chose $\alpha = 10^{-5}$ and $f_T = 10^6$ Hz. Using these values in the design procedure of Section 5.4.1.2 we obtain: $G_3 = 50.002\ \mu\mho$, $G_6 = 54.294\ \mu\mho$ and $C_0 = 2.0203$ nF. The values C_R and τ_R associated with the impedance for the S.B.I. circuit, see (7.4), are: $C_R = 120$ pF and $\tau_R = 4.61107 \cdot 10^{-7}$, and the values for C_X and R_X in the active resonator of Fig. 7.12 (d) are: $C_X = 159.03$ nF and $R_X = 2.8995\ \Omega$. The complete set of component values for the active resonator circuit is shown in Table (a) of Fig. 7.13.

It is interesting to compare the component values in Table (a) of Fig. 7.13 with those that are obtained if we consider the voltage gain of the amplifier in the active resonator to be ideal, i.e., $\alpha = 0$ and $f_T = \infty$. A design procedure for S.I. circuit B, for the ideal amplifier case, has been presented in Section 5.4.1.1. Using this design procedure with the same values for G_1, G_2, G_4 and G_5 as chosen for the non-ideal amplifier case, i.e., $G_1 = G_2 = G_4 = G_5 = 10^{-4}\ \mho$, we obtain the component values shown in Table (b) of Fig. 7.13 for the active resonator circuit. Comparison of Tables (a) and (b) in Fig. 7.13 show how the non-ideal voltage gain affects the design.

The computed loss/frequency response for the active resonator circuit is shown as curve (a) in Fig. 7.14, and the response for the original LC resonator of Fig. 7.12 (a) is shown as curve (b) in Fig. 7.14. We find that both these loss/frequency responses are very similar, except for very high frequencies. In a practical application, however, the small discrepancy at high frequencies would be insignificant. Fig. 7.15 shows the changes in the passband loss/frequency response for the active resonator, when the value for $1/f_T$ is altered by $\pm$ 50.0 % - note that the frequency of resonance changes by approx. $\pm$ 1.0 %.

7.2.2 REDUCING THE EFFECTS OF F_T VARIATIONS

In this section we discuss how to design the active resonator of Fig. 7.12 (d) so that the effects of f_T variations on the loss/frequency response are reduced. To achieve our objective we investigate the approach of minimising the sensitivity $S^{I_M(\omega_R)}_{(1/\omega_T)}$ for the S.B.I. circuit B in the active resonator. The measure referred to is the normalised differential sensitivity of the imaginary part of the S.B.I's impedance to $1/\omega_T$, calculated at the nominal resonance frequency ω_R for the resonator. To minimise $S^{I_M(\omega_R)}_{(1/\omega_T)}$ we can use the following approach.

In Section 5.4.1.2 we showed how to choose the nominal passive component values for S.B.I. circuit B, so that we achieve the conditions $a_0 = 0$ and $b_1 = 0$ for (5.16), and so that the parameter L in the S.B.I's impedance expression, see (7.4), is equal to a specified value L_N. We also pointed out that in this design procedure, the values for G_1, G_2, G_4 and G_5 could be chosen arbitrarily. We now describe how to choose the values for these conductances so that the sensitivity $S^{I_M(\omega_R)}_{(1/\omega_T)}$ is minimised.

For given values for the the amplifier parameters α and f_T, and for a specified value L_N, we first of all choose an initial set of values for the conductances G_1, G_2, G_4 and G_5 in the S.B.I. circuit B. Once these values are chosen, the values for G_3, G_6 and

C_0 are determined in the way described in Section 5.4.1.2., and the sensitivity $S^{I_M(\omega_R)}_{(1/\omega_T)}$ is determined in the way described in Section 6.3.2.. A computer minimisation routine is now used to find a new set of values for G_1, G_2, G_4 and G_5 so that the value for $S^{I_M(\omega_R)}_{(1/\omega_T)}$ becomes smaller, and this procedure is repeated until a minimum for $S^{I_M(\omega_R)}_{(1/\omega_T)}$ is found.

We made use of the above approach to redesign the S.B.I. circuit B in the active resonator of Fig. 7.12 (d). In the computer minimisation routine we used a starting value of $10^{-4}\mho$ for G_1, G_2, G_4 and G_5, and during the minimisation the values for these conductances were constrained to lie between the limits $G_{min} = 10^{-5}\mho$ and $G_{max} = 10^{-3}\mho$. The minimum value achieved for $S^{I_M(\omega_R)}_{(1/\omega_T)}$ was 0.00408,* and the passive component values corresponding to this minimum were: $G_1 = 0.59529$ m$\mho$, $G_2 = 10.0$ $\mu\mho$, $G_4 = 0.60305$ m$\mho$, $G_5 = 10.0$ $\mu\mho$, $G_3 = 9.96343$ $\mu\mho$, $G_6 = 0.717602$ m$\mho$ and $C_0 = 3.1761$ nF. The nominal values for the parameters L, C and τ in the impedance expression for the S.B.I. circuit, see (7.13), were $L_R = 0.15915$, $C_R = 330 \cdot 10^{-12}$ and $\tau_R = 3.18267 \cdot 10^{-7}$, and we obtained $C_X = 158.824$ nF and $R_X = 2.0039\,\Omega$ for the active resonator in Fig. 7.12 (d). For comparison purposes the new component values for the active resonator are shown in Table (c) of Fig. 7.13 alongside our initial set of values in Table (a), and the values for the ideal amplifier case shown in Table (b).

* The starting value was 0.08

Fig. 7.16 shows the computed loss/frequency response for the optimised resonator circuit, and the computed effects of ± 50.0 % changes in $1/f_T$ on the passband response are shown in Fig. 7.17. We find that the loss/frequency behaviour for the optimised active resonator is very similar to that for the original LC resonator, i.e., see curve (b) in Fig. 7.14. Also, the 50.0 % changes in $1/f_T$ alter the frequency of resonance by only approx. ± 0.1 %. This change is about a tenth of the change shown in Fig. 7.15 for the non-optimised design discussed in Section 7.2.1 (note that the horizontal scales in Figs. 7.15 and 7.17 are different).

7.3 BANDPASS FILTER USING S.B.I. CIRCUIT B

In this section we have chosen the LC bandpass filter in Fig. 7.18 as a basis for study. We discuss how to realise this filter using S.B.I. circuit B, but in particular we will be concerned with designing the active realisation so that the effects of f_T variations on its loss/frequency response are minimised. The LC bandpass filter is 6^{th} order, having five transmission zeros at zero frequency and one zero at infinite frequency, and its nominal loss/frequency behaviour is shown in Fig. 7.19. Note that the passband frequency range for the LC filter is from 9.75 kHz to 10.25 kHz, and the loss variation in the passband is 0.5 dB. This is considered a challenging design. For a lumped element LC filter an inductor Q of approx 200 would be required.

7.3.1 DESIGN OF THE ACTIVE FILTER

To obtain the active filter we followed the general design procedure described in Section 5.3.3.1, and to minimise the effects of f_T variations on the loss/frequency response for the active filter we used the same approach as for the active resonator circuit of Section 7.2.2. That is, we chose the nominal passive component values for the S.B.I.s in the active filter so that the sensitivity $S^{I_M(\omega)}_{(1/\omega_T)}$ for each S.B.I. circuit was minimised at a chosen frequency. The minimisations of $S^{I_M(\omega)}_{(1/\omega_T)}$ were carried out at the nominal resonance frequencies for the grounded parallel LC resonators in the passive filter of Fig. 7.18, and in the computer minimisation routine the values G_1, G_2, G_4 and G_5 for the S.B.I. circuit B were confined to the limits $G_{min} = 10^{-5}\mho$ and $G_{max} = 10^{-3}\mho$. For the amplifiers in the S.B.I. circuits we chose $\alpha = 10^{-5}$ and $f_T = 3.5$ MHz. The nominal passive component values that are obtained for the S.B.I. circuits, are shown in Fig. 7.20. The values for the parameters L, C and τ associated with each S.B.I's impedance, see (7.13), are also shown in Fig. 7.20. Note that the L values in Fig. 7.20 are identical, as all three inductors in the LC filter of Fig. 7.18 have the same inductance value.

In the general design procedure of Section 5.3.3.1 it is necessary to have the same τ value for all S.B.I.s in a filter. For our bandpass filter, however, we find that the S.B.I. circuits have different values for τ. This is because each S.B.I. had its sensitivity $S^{I_M(\omega)}_{(1/\omega_T)}$ minimised at a different frequency, namely, the frequency of resonance for the appropriate LC resonator in the passive bandpass filter of Fig. 7.18. Nevertheless, the τ values for the S.B.I. circuits are very similar, as the LC resonators in Fig. 7.18 have similar resonance frequencies, and we decided to use an average value of $\tau = 9.09 \,.\, 10^{-8}$ in the remaining design steps of Section 5.3.3.1. The active bandpass filter that is obtained is shown in Fig. 7.21, and the full set of component values for this filter are shown in Fig. 7.22.

7.3.2 EXPERIMENTAL PROCEDURE

The active filter of Fig. 7.21 was constructed using resistors and capacitors having values within about 1.0 % of the nominal values in Fig. 7.22. The amplifiers used had a nominal finite gainbandwidth product of 3.5 MHz with a tolerance of approx. ± 10.0 %. To reduce the effects of the passive component and f_T tolerances we carried out the following adjustment procedure, which is similar to that for the active highpass filter example of Section 7.1.

First of all we adjusted the conductance G_3 in each S.B.I. circuit until the D.C. resistance for the S.B.I. was zero - this is equivalent to obtaining $M = 0$ for the general impedance expression in (7.2). Then, the remaining part of the adjustment procedure was to adjust the conductances G_6 and G_5 in each S.B.I., so that the resonators in the shunt arms of the bandpass filter had the ideal impedances of infinity at their nominal resonance frequencies. From the point of view of adjustment, however, it is impractical to measure a very large impedance, so instead the resonators were rearranged to form the corresponding <u>series</u> resonator circuits shown in Fig. 7.23. We then used each series resonator in the measuring setup of Fig. 7.24 and iteratively adjusted G_6 and G_5 in the S.B.I. circuit until the loss $|V_{OUT}/V_{IN}|$ shown in Fig. 7.24 was as large as possible at the nominal resonance frequency. This is equivalent to obtaining a small impedance for the series resonator, or a large impedance for the parallel resonator at resonance. After adjusting the series resonators we reformed the parallel resonator circuits and connected them to the bandpass filter.

7.3.3 COMPUTED AND MEASURED RESULTS

The computed loss/frequency response for the active bandpass filter is shown in Figs 7.25 (a) and (b). We find that the active filter has a passband response which is almost identical to that shown in Fig 7.19 (a) for the original LC bandpass filter. The stopband response for the active filter is also very similar to that for the LC filter, see Fig 7.19 (b), except for very high frequencies when they begin to differ. In a practical application however, this small discrepancy would be insignificant.

The computed effects of $\pm$ 20.0 % variations in the f_T values for all three amplifiers in the active filter are shown in Fig 7.26 (a). The shift in the centre frequency is only about $\pm$ 10.0 Hz, ie $\pm$ 0.1% of the nominal centre, and the loss in the passband is affected very little.

The measured loss/frequency response for the active bandpass filter is shown in Figs 7.27 (a) and (b). These curves are very similar to the computed curves in Figs 7.25 (a) and (b).

The dynamic range for the experimental filter was also investigated. We found that the loss/frequency response for the filter deteriorated for passband output levels greater than approx 1.0 r.m.s. Some measured noise levels for the filter are shown in Figs 7.28 (a) and (b). These results are for measurement bandwidths of 100 and 1000 Hz respectively, and the curves are shown on a graph were 0.0 dB on the vertical scale represents the maximum passband output level of 1.0V r.m.s.

7.3.4 SENSITIVITY INVESTIGATION

To investigate the passive component sensitivities for the active bandpass filter, we took the approach of showing how the loss/frequency response changes, when the passive component values are altered from their nominal values - these curves are shown in Figs. 7.29 (a) to (c). For comparison purposes similar curves for the original LC bandpass filter are shown in Fig. 7.30.

The loss/frequency changes for the capacitors in the active filter, see Fig. 7.29 (a), are practically identical to those in Fig. 7.30 for the corresponding capacitors and inductors in the original LC bandpass filter. Also, the loss/frequency changes for R_S and R_L in the active filter are very similar to those for the LC filter case. In these respects the active filter retains the low sensitivity features for the original passive filter.

For the resistors in the S.B.I. circuits at the terminating ends of the active filter, we find that the changes produced in the active filter's loss/frequency response are about the same as those for the capacitors in these S.B.I. circuits, see Figs. 7.29 (b) and (c). However , for the S.B.I. circuit in the middle of the active filter, we find that the resistance changes affect the filter's response significantly more than the capacitance change for the S.B.I., see Figs. 7.29 (b) and (a). The sensitivities of the loss to the resistors R_{C1} ,

R_{C2}, R_{C3}, R_{C4} and R_{C5}, are all very small as shown by the curves in Fig. 7.29 (c). The effects of f_T variations on the loss/frequency response for the active filter, have already been investigated in Section 7.3.3.

CHAPTER 8

SUMMARY AND CONCLUSIONS

8.1 REVIEW OF THESIS

In Chapter 1 we outlined various approaches to the design of active-RC filters. Of these approaches the one we decided to explore in this thesis was the 'inductance simulation method', where the inductors in an LC filter are replaced by simulated inductor circuits. In particular we have been concerned with LC filters where all the inductors are grounded, and where these inductors are replaced by single-amplifier S.I. networks. The approach of using simulated inductances has the advantage that the active filter can retain some of the good sensitivity features for the original LC filter. For instance, the source and load resistors in the active filter, and the capacitors in the active filter which correspond to the capacitors in the LC filter, can all have the same low sensitivities as for the LC filter. The advantage of using single-amplifier S.I.s is that the number of amplifiers for the active filter is a minimum, however, a possible disadvantage is that the components in the S.I. networks may introduce new unacceptably large sensitivities for the active filter.

In Chapter 2 we reviewed all the single-amplifier S.I. networks that have appeared in the literature, and, for interest, we also reviewed the single-amplifier networks for simulating impedances of the form Mp^2, K/p^2, $pL + 1/pC$, and $R + K/p^2$. A useful way of classifying these networks was to indicate how many capacitors they contained, and also how many coefficient and pole/zero cancellations that are required in their impedance expressions. This information was shown in Fig. 2.15, and we found that the S.I. circuit due to Orchard and Willson (26), and the circuit due to Schmidt and Lee (27), both had only one capacitor and needed the fewest number of conditions required for inductance simulation, i.e., two coefficient cancellations each for their impedance expressions. As these S.I.s contain only one capacitor, they can be regarded as single-amplifier immittance inverter circuits having port 2 terminated by a capacitor. Henceforward, we were concerned with single-amplifier S.I.s of this type, as the title of the thesis indicates.

As alternatives to the O/W and S/L circuits, some new single-amplifier, single-capacitor, S.I. circuits were proposed in Chapter 3 - these networks can also be regarded as single-amplifier immittance inverters having port 2 terminated by a capacitor. One of the new circuits, called S.I. circuit A, has the interesting feature that its inductance value can be changed by altering the value of a single resistor, without affecting the conditions required for lossless inductance simulation; the other new circuits, and the O/W and S/L circuits, do not possess this property. Furthermore, the inductance value can be varied over a positive and negative range, and the circuit appears suited to a straightforward adjustment procedure for reducing the effects of passive component tolerances on its impedance. Another new circuit, called S.I. circuit B, uses only six resistors, and it has the interesting feature that it is a special case of S.I. circuit A.

Also, in Chapter 3, we investigated the general effects of passive component tolerances on the impedance for the single-amplifier, single-capacitor, S.I.s. One way to describe these effects is by the model in Fig. 3.9, which shows a resistance R_X in series with the parallel combination of an inductance L and a resistance R_Y. The interesting feature for this model is that the passive component tolerances give rise to frequency <u>independent</u> values for R_X, R_Y and L. We also briefly investigated the general effects due to the non-ideal voltage gain for the amplifier, and pointed out that the impedance for the S.I.s becomes a biquadratic in p. This is because each simulating network contains a capacitor with a 1^{st} order impedance function, an amplifier whose voltage gain is assumed to have a 1^{st} roll off, and no other elements with frequency dependent characteristics.

In Chapter 4 we made a study of the new S.I.

circuit B. We showed how to choose the nominal passive component values for this circuit, so that the effects of component tolerances on its impedance were reduced. To do this we made use of the model in Fig. 3.9 - note that, for this model, R_X is ideally zero, R_Y is ideally infinite, and L should be equal to the specified inductance value L_N. We derived expressions for the worst case values for $|R_X|$ and $|R_Y|$, due to fractional changes x_i for the conductances in the S.I. circuit B, and we then showed how to minimise and maximise these expressions accordingly, while still obtaining only small changes in L for the conductance changes. This approach is very interesting as it can be used for other single-amplifier, single-capacitor, S.I. networks.

Also, in Chapter 4, we investigated how the impedance for S.I. circuit B is affected by the non-ideal voltage gain for the amplifier. Expressions for the $L(\omega)$ and $Q(\omega)$ behaviour due to the non-ideal gain were derived, and we showed the behaviour for a typical design for S.I. circuit B. We then showed how to choose the nominal passive component values for the S.I. circuit, so that the $Q(\omega)$ values were larger, and so that $Q(\omega)$ had its maximum value at a specified frequency. However, a sensitivity study showed that the $Q(\omega)$ behaviour is very sensitive to changes in the resistance values for S.I. circuit B, and we decided that the approach of obtaining $Q(\omega)_{max}$ at a specified frequency is unlikely to be useful in practice. Although small changes in the resistances produce large changes in the $Q(\omega)$ behaviour, we pointed out that they may, nevertheless, produce much smaller changes in the loss/frequency response for an active filter containing the S.I. circuits B. In Chapter 4 we also compared the S.I. circuit B with two other S.I. circuits, namely, the O/W circuit of Section 2.2.4, and Antoniou's two-amplifier circuit of Section 2.2.1. We found that these circuits had similar $L(\omega)$ and $Q(\omega)$ behaviour due to the non-ideal voltage gain for their amplifiers, however, the two-amplifier S.I. circuit has much better $Q(\omega)$ sensitivities to its resistance values, and this is one reason why it is preferred to the other circuits, in some applications.

In Chapter 5 we described an interesting method for overcoming the effects of the non-ideal amplifier gain on the loss/frequency response of active filters that contain single-amplifier, single-capacitor, S.I.s. We pointed out that single-amplifier, single-capacitor, S.I.s can have the impedance of a lossless inductance only if the amplifiers in the circuits are considered ideal. When the non-ideal voltage gain for the amplifiers is taken into consideration, the impedance for the simulating networks becomes a biquadratic expression in p, and only approximates the impedance of an ideal inductance over a limited frequency range. Taking the non-ideal amplifier gain into consideration, we deliberately redesigned the simulating networks to have a biquadratic impedance of the form

$$Z = \frac{pL(1 + p\tau)}{1 + p^2LC}$$

and we referred to circuits having this type of impedance as ideal "S.B.I.s", where S.B.I. is an abbreviation for Simulated Biquadratic Impedance. We then showed how various types of LC highpass and bandpass filters, with their terminating resistors, can be modified so as to produce the required loss/frequency response using the S.B.I. circuits instead of the originally required inductors.

An advantage of the approach described in Chapter 5 is that the non-ideal voltage gain for the amplifiers is taken into consideration in the design of the active filter. For bandpass filters using the S.B.I. circuits, the passband loss/frequency response is correct at the frequencies of maximum power transfer for the original LC filter. The response at other frequencies can be incorrect but a high degree of compensation for the non-ideal voltage gain of the amplifiers may still be achieved. For highpass filters complete compensation for the non-ideal voltage gain can be obtained over the entire frequency range in which the gain of the amplifier can be adequately described by a single-pole model. Even in the case of two-amplifier S.I.s this has not been achieved, as these circuits are usually designed to offer compensation for the non-ideal voltage gain only in the neighbourhood of a particular frequency. A disadvantage of the new filter design method, when compared with the method of directly replacing the inductors in an LC filter by S.I. circuits, is that additional capacitors are required for the highpass filter case. However, as mentioned in Chapter 5, it may be possible to reduce the number of additional capacitors to only one regardless of the order of the filter.

In Chapter 6 we described some sensitivity features for active filters that use S.B.I. circuits. We pointed out that both highpass and bandpass filters that use S.B.I.s can be considered as being derived from LC filters having parallel RC terminations. We briefly investigated the sensitivity properties for filters of this type, and showed that they can be significantly more sensitive than LC filters having purely resistive terminations. However, we suggested that their sensitivities might approach those for purely resistively terminated LC filters, as the time constant R_sC_s for the source impedance is chosen to be smaller. In Chapter 6 we also investigated the effects of f_T variations on the real and imaginary parts of the impedance for the S.B.I. circuits. General expressions for the 1^{st} order normalised differential sensitivities $S^{I_M(\omega)}_{(1/\omega_T)}$ and $S^{R_E(\omega)}_{(1/\omega_T)}$ were derived, and we showed, in particular, how to calculate these sensitivities for the S.B.I. circuit B.

In Chapter 7 we described some active-RC filters that used S.B.I. circuits. One filter example we described was a 5^{th} order Cauer type highpass filter that contained the S.B.I. circuits B described in Section 5.4.1. The resistance values for the S.B.I. circuits B were chosen so that we could carry out an adjustment procedure, for overcoming the effects of component tolerances on the loss/frequency response for the practical filter. The computed loss/frequency behaviour precisely met the original specification, and the measured response was very similar to the computed response. We also carried out a sensitivity study for the active filter, and found that the passive component sensitivities were significantly larger than those for a low sensitivity LC filter. However, the sensitivities may still be acceptably low for some applications, and it may also be possible to redesign the active highpass filter to have better sensitivities.

Also, in Chapter 7, we were concerned with minimising the effects of f_T variations on the loss/frequency response for active filters that use S.B.I. circuits. As an example for study we investigated how to reduce these effects on the loss/frequency response for an active-RC resonator circuit that contained the S.B.I. circuit B. We pointed out that in the design procedure for the S.B.I. circuit B, see Section 5.4.1, the values for the conductances G_1, G_2, G_4 and G_5 could be chosen arbitrarily. To achieve our objective we chose these conductance values so that the sensitivity $S_{(1/\omega_T)}^{I_M(\omega)}$, for the S.B.I's impedance, was minimised at the nominal resonance frequency for the active resonator. The effects of f_T variations on the resonator's loss were then so small that we regarded this approach as successful.

Another filter example described in Chapter 7, was a 6^{th} order bandpass filter again using the S.B.I. circuits B. To reduce the effects of f_T variations on the filter's loss, we designed the S.B.I. circuits so that their sensitivities $S_{(1/\omega_T)}^{I_M(\omega)}$ were minimised at the nominal resonance frequencies for the parallel LC resonators in the original LC filter. We also described an adjustment procedure for the practical filter, for reducing the effects of component tolerances on the measured loss/frequency behaviour. The computed loss/frequency response for the active filter was almost identical to that for the original LC bandpass filter, and the response for the practical filter was also very similar. We carried out a sensitivity study for the active filter and showed that the loss has, indeed, a low sensitivity to f_T. The sensitivities of the active filter's loss to its capacitance values, were practically identical to the capacitance and inductance sensitivities for the original LC bandpass filter. Also, we obtained low sensitivities for the resistors in the S.B.I. circuits at the terminating ends of the active filter. The resistance sensitivities, for the remaining S.B.I. circuit, were larger but may well be acceptable for some filter applications.

8.2 RECENT DEVELOPMENTS

An exciting recent development has been the discovery of a new single-amplifier, single-capacitor, S.I. circuit, that requires only one coefficient cancellation in its impedance expression. The new S.I. circuit is derived from the Cheng/Lim network of Section 2.4.1, which simulates the impedance of a grounded series LC resonator. For this reason we briefly describe Cheng and Lim's circuit once again here.

The Cheng/Lim simulation network is shown in Fig. 8.1 and, assuming an ideal amplifier, it has an impedance

$$Z = \frac{A_0 + A_1 p + A_2 p^2}{B_1 p} \qquad (8.1)$$

where

$$\begin{aligned}
A_0 &= G_2 G_3 (G_5 + G_7) \\
A_1 &= C_6 G_3 (G_2 + G_5) + C_4 (G_2 G_3 + G_2 G_7 - G_1 G_5) \\
&\quad + C_4 G_2 G_3 R_4 (G_5 + G_7) + C_4 G_2 G_7 R_8 (G_1 + G_3) \qquad (8.2) \\
A_2 &= C_4 C_6 G_3 R_4 (G_2 + G_5) \\
B_1 &= C_4 G_2 G_7 (G_1 + G_3)
\end{aligned}$$

note : $G_i = 1/R_i$

To obtain an impedance $Z = pL_R + 1/pC_R$ the coefficient cancellation $A_1 = 0$ is needed so that (8.1) becomes

$$Z = \frac{A_0 + A_2 p^2}{B_1 p} \tag{8.3}$$

We then have $L_R = A_2/B_1$ and $C_R = B_1/A_0$ - note that the conditions $A_2/B_1 > 0$ and $B_1/A_0 > 0$ are needed for L_R and C_R to be positive.

By merely shortcircuiting the capacitor C_4 in Cheng and Lims' simulation network we obtain the new S.I. circuit shown in Fig. 8.2. The impedance for the new circuit can be found by letting $C_4 \to \infty$ in (8.1), i.e., we obtain

$$Z = \frac{A_0 + A_1 p}{B_0} \tag{8.4}$$

where

$$\begin{aligned} A_0 &= G_2G_3 + G_2G_7 - G_1G_5 + G_2G_3R_4(G_5 + G_7) \\ &\quad + G_2G_7R_8(G_1 + G_3) \\ A_1 &= C_6R_4G_3(G_2 + G_5) \\ B_0 &= G_2G_7(G_1 + G_3) \end{aligned} \tag{8.5}$$

For lossless inductance simulation the condition $A_0 = 0$

must hold. From the expression for A_0 in (8.5) we find that this condition can be satisfied by choosing G_1 as

$$G_1 = \frac{G_2(G_3 + G_7 + R_4G_3G_5 + R_4G_3G_7 + R_8G_3G_7)}{G_5 - R_8G_2G_7} \tag{8.6}$$

Note that the inequality $G_5 > R_8G_2G_7$ must hold for (8.6) if the value for G_1 is to be positive. A very simple way to satify this inequality is to choose $R_8 = 0$, i.e., we replace the resistor R_8 in Fig. 8.2 by a short-circuit. The inductance value for the new S.I. circuit is given by the relationship $L = A_1/B_0$. Making use of the expressions for A_1 and B_0 in (8.5) we obtain

$$L = \frac{C_6R_4G_3(G_2 + G_5)}{G_2G_7(G_1 + G_3)} \tag{8.7}$$

When the expression for G_1 in (8.6) is substituted into (8.7) we obtain

$$L = \frac{C_6R_4G_3(G_2 + G_5)(G_5 - R_8G_2G_7)}{G_2G_7\left\{ G_3(G_5 - R_8G_2G_7) + G_2G_3 + G_2G_7 + R_4G_2G_3G_5 + R_4G_2G_3G_7 \right\}} \tag{8.8}$$

Once again, if the inequality $G_5 > R_8G_2G_7$ holds, then the inductance value L will be positive. One set of component values which satisfy the condition $A_0 = 0$ to give $L = 100$ mH is : $R_1 = 2.5$ kΩ , $R_2 = R_3 = R_4 = R_5 = R_7 = 10.0$ kΩ , $R_8 = 0$, and $C_6 = 2.5$ nF.

The expression in (8.7) shows that the inductance value L is independent of the value for R_8. To overcome the effects of passive component tolerances on the impedance for the new S.I. circuit, we might therefore adjust anyone of the conductances G_1 to G_7 to ensure that L is equal to the desired inductance value L_N, and then adjust R_8 so that the coefficient A_0 in (8.5) was zero. This last adjustment will not affect the inductance value.

The new S.I. circuit is very interesting as it requires only one coefficient cancellation in its impedance expression. Previous single-amplifier S.I. circuits have required at least two coefficient cancellations, as shown by the Table in Fig. 2.15. When the Table in Fig. 2.15 is updated to include the new S.I. circuit, we obtain the new Table shown in Fig. 8.3. Further additions to this Table have not been investigated owing to lack of time.

8.3 SUGGESTIONS FOR FURTHER WORK

(a) Active filters that use S.I. circuits A

In theory the S.I. circuit A, described in Section 3.2.1, has the advantage over other single-amplifier S.I.s, that it is suited to a functional adjustment procedure for overcoming the effects of passive component tolerances on its impedance. It would be worthwhile investigating this adjustment procedure in practice, and also investigating how we could make use of the adjustment procedure to reduce the effects of passive component tolerances on the loss/frequency response for active filters that contained the S.I. circuits A.

(b) Reducing the effects of component tolerances on the impedance for S.I. circuit A

In Section 4.2.2 we showed how to choose the nominal passive component values for S.I. circuit B so that the effects of passive component tolerances on the impedance were reduced. It would also be worthwhile investigating how to reduce the effects of passive component tolerances on the impedance for S.I. circuit A. Even though the S.I. circuit A is suited to a functional adjustment procedure for overcoming the effects of component tolerances, the above objective is still worthwhile as it reduces the effects of post adjustment variations on the impedance for S.I. circuit A. Such post adjustment variations might be due to ageing of the components, or to environmental changes such as temperature fluctuations.

(c) Sensitivity investigations for active filters that contain the S.I. circuits B

It would be interesting to investigate the sensitivity features for an active filter that contained the S.I. circuits B, and where these S.I.s are designed in the way described in Section 4.2.2, so that the effects of of passive component tolerances on their impedances are reduced. In particular, it would be interesting to determine whether the sensitivities of the filter's loss to the passive components in the S.I. circuits B were reduced as a result of designing the S.I.s in the way described above. If so, we might use the same approach to reduce the sensitivities for active filters containing the S.I. circuits A.

(d) Active filters using the S.I. circuit described in Section 8.2

Assuming an ideal amplifier, the new S.I. circuit described in Section 8.2 needs only one coefficient cancellation for its impedance expression and, in theory, the effects of passive component tolerances on its impedance can be overcome by adjusting the values for just two resistors in the circuit. Further useful work might be to investigate the effects of the non-ideal voltage gain of the amplifier on the impedance, to investigate practical adjustment procedures for the circuit, and to explore the use of the circuit in active-RC filter design.

(e) Reducing the passive component sensitivities for active filters that contain the S.B.I. circuits B

In the design procedure for S.B.I. circuit B, described in Section 5.4.1, we pointed out that the values for the conductances G_1, G_2, G_4 and G_5 could be chosen arbitrarily. In Sections 7.2.2 and 7.3.1 we used these degrees of freedom to minimise the effects of f_T variations on the loss/frequency response for active filters that contained the S.B.I. circuits B. It would be interesting to explore how the degrees of freedom might, instead, be used to minimise the passive component sensitivities for the active filters.

(f) Active filters using the S.B.I. circuits A

We might investigate how to minimise the passive component sensitivities for active filters that used the S.B.I. circuit A described previously in Section 5.4.2, and we might also explore how to adjust the resistances for these S.B.I. circuits so as to reduce the effects of passive component tolerances on the loss/frequency response for the active filters. It may also be worthwhile investigating how to minimise the effects of f_T variations on the loss/frequency response for the active filters.

REFERENCES

(1) H J ORCHARD, 'Inductorless filters', Electronics letters, vol 2, No 6, pp 224-225, June 1966.

(2) K C SMITH and A SEDRA, 'The current conveyor: A new circuit building block', Proc IEEE, 1968, 56, pp 1368-1369

(3) A SEDRA and K C SMITH, 'A second generation current conveyor and its applications', IEEE Trans., 1970, CT-17, pp 132-133.

(4) J G LINVILL, 'RC-active filters', Proc IRE, vol 42, pp 555-564, March 1954

(5) T YANAGISAWA, 'RC active networks using current inversion type negative impedance converters', IRE Trans CT-4, pp 140-144, Sept 1975

(6) S K MITRA, 'Active-RC filters employing a single operational amplifier as the active element', Proc Hawaii International Conference on System Sciences, Honolulu, Hawaii, Jan 1968

(7) A G J HOLT and F W STEPHENSON, 'The effects of error in the element values and the converter characteristic on the responses of active-RC filters', The Radio and Electronic Engineer, vol 26, 1963 pp 449-457

(8) G S MOSCHYTZ, 'Linear integrated circuits - design', Bell Telephone Series, Van Nostrand Reinhold Co, 1975

(9) R P SALLEN and E L KEY, 'A practical method of designing RC-active filters', IRE Trans. Circuit Theory, vol CT-2 pp 78-85, March 1955.

(10) R JEFFERS and D HAIGH, 'Active-RC lowpass filters for F.D.M. and R.C.M. systems, Proc, IEE, vol 120 pp 945-953, Sept 1973.

(11) A G J HOLT and M R LEE, 'Sensitivity comparison of active-cascade and inductance simulation schemes', Proc IEE, vol 119, pp 277-282, March 1972.

(12) N FLIEGE, 'A new class of 2nd order RC-active filters with two operational amplifiers', NTZ, vol 26, no 6, pp 279-282, 1973.

(13) Not referred to.

(14) F E GIRLING and E F GOOD, 'The leapfrog feedback filter' RRE memorandum, Sept 1955.

(15) D J PERRY, 'Multifarious multifeedback filters', IEE Colloquium on Electronic filters, May 1976

(16) R L Adams, 'On reduced sensitivity active filters', in Proc. 14 March Midwest Symp. Circuit Theory, May 1971, pp 14-3-1-14-3-8.

(17) K R LAKER and M S GHAUSI, ' comparison of active multiple-loop feedback techniques for realising high order bandpass filters', IEEE CAS-21, no 6, pp 774-783, Nov 1974.

(18) R W TURPIN and W SARAGA, 'Sensitivity comparison of three types of active-RC circuits', Proc IEEE ISCAS, 1976, (Munich)

(19) M SILVA, Phd thesis, Imperial College, London 1976

(20) H J ORCHARD and D F SHEAHAN, 'Inductorless bandpass filters', IEEE Jour Solid State Circuits, vol SC-5 pp 108-118, June 1970.

(21) J VALIHORA, J T LIM and L T BRUTON, 'The feasibility of active filtering in Frequency Division Multiplex Systems', proc IEEE Int Symp Circuits and Systems pp 121-125, San Fransisco, 1974.

(22) R H S RIORDAN, 'Simulated inductors using differential amplifiers', Electronics Letters, vol 3, pp 50-51 Feb 1967.

(23) A ANTONIOU, 'Realisation of gyrators using operational amplifiers', and their use in RC-active-network synthesis, Proc IEE, 1969, 116 (11), pp 1838-1850.

(24) J M SIPRESS, 'Synthesis of active-RC networks' IRE Trans, 1961, CT-18, pp 260-269

(25) W SARAGA, 'A contribution to the design of low sensitivity active RC networks' proceeding of the IEEE International Symposium on Circuits and Systems, San Fransisco, 1974, pp 191-195.

(26) H J ORCHARD and A N WILLSON (jun), 'New active gyrator circuit', Electronics letters, 1974, 10, (13) pp 261-262.

(27) C E SCHMIDT and M S LEE, 'Multipurpose simulation network with a single amplifier', Electronics Letters, 1975, 11, (1), pp 9-10.

(28) M M SILVA, 'On the realisation of One-nullor gyrators', Proc IEEE Int Symp Circuits and Systems, pp 273-276, Boston, April 1975.

(29) M M SILVA and W SARAGA, 'On the classification of active-RC circuits simulating floating inductors', Proc 3rd Int Symp on Network Theory, pp 489-496, Split, Yugoslavia, Sept 1975.

(30) A G HOLT and J TAYLOR, 'Method of replacing ungrounded inductors by grounded gyrators , Electronics letters, vol 1, p105, June 1965.

(31) G J DEBOO, 'Application of a gyrator-type circuit to realise ungrounded inductors', IEEE Trans Circuit Theory, vol CT-14, pp 101-102, March 1967

(32) J GORSKI-POPIEL, 'RC-active synthesis using positive immittance converters', Electronics Letters, Vol 3, pp 381-382, Aug 1967

(33) A G HOLD and R LINGGARD, 'The multiterminal gyrator', Proc IEEE, vol 56, pp 1354-1355, Aug 1976.

(34) A G J HOLT and R L LINGGARD, 'Multipurpose gyrator', Proc. IEE, vol 117, pp 1591-1598, Aug 1970

(35) L T BRUTON, Phd thesis, University of Newcastle-upon-Tyne, 1971

(36) L T BRUTON, 'network transfer functions using the concept of frequency-dependent negative resistance', IEEE Trans. Circuit Theory, vol CT-16, pp 406-408, Aug 1969

(37) D G HAIGH, Phd, thesis, Imperial College, University of London, 1976

(38) K PANZER, 'Active bandpass filters with impedance converters and a minimum number of capacitors',(in German), NTZ, 27, 1974, H10.

(39) D G HAIGH and W SARAGA, 'Practical LC filter simulation techniques for the design of active-RC bandpass filters', Proc 1st European Conf Circ Theory and Design, pp 336-341 London, July 1974

(40) R H CHENG and J T LIM, 'Single-amplifier immittance network' USA Patent No 4, 001735, Jan 4th 1977

(41) R H CHENG and J T LIM, 'Single opamp networks for shunt arms in ladder filters', Proceeding of the IEEE International Symposium on Circuits and Systems Phoenix, Arizona, 1977, pp 313-316

(42) H WUPPER and K MEERKOTTER, 'New active filter synthesis based on scattering parameters', IEEE Trans, CAS-22, pp 594-602, 1975.

(43) H WUPPER, 'Scattering parameter active filters with reduced number of active elements', IEEE Trans, CAS-23, pp 318-322, 1976

(44) S H WUPPER and K MEERKOTER, 'New active filter synthesis based on scattering parameters', IEEE Trans, CAS-22, pp 594-602, 1975.

(45) G HARITANTIS, AG CONSTANTINIDES and T DELIYANNIS, 'Wave active filters', Proc IEE, vol 123, pp 676-682, 1976.

(46) A G CONSTANTINIDES and H G DIMOPOULOS,' Active RC filters derivable from LC ladder filters via linear transformation', Electronic Circuits and Systems (London), vol 1, no 1, pp 17-21, Sept. 1976.

(47) A M ALI, Pro 16th Annual Alletton Conf on Communication Control and Computing, Monticello, Illinois, USA, Oct 1978.

(48) Not Referred to.

(49) L T BRUTON, 'Non-ideal performance of two-amplifier PICs', IEEE Trans., CT-17, no 4, pp 541-549, 1970.

(50) D HAIGH, M KUNES, 'A contribution to the optimum design of active-RC filters using Positive Impedance Converter 1979, IEEE ISCAS, pp 203-206

(51) W SARAGA, 'A contribution to active RC network synthesi in Recent Developments in Network Theory (ed S R Deards Pergamon Press, 1963

(52) R L FORD and F E GIRLING, 'Active filters and oscillators using simulated inductance', Electronics letters, 2, pp 52, 1966.

(53) A J PRESCOTT, 'Loss compensated active gyrator using differential input operational amplifiers', Electronics Letters, vol 2, no 7, pp 283-284, July 1966.

(54) D BERNDT and S C DUTTA ROY', Inductance simulation using a single unity gain amplifier', IEEE J Solid State Circuits, vol SC-4, no 3, pp 161-162, June 1969.

(55) J M ROLLETT, 'Economical RC active lossy ladder filters', Electronics Letters, vol 9, no 3, Feb 1973.

(57) H HOOSHVAR, 'Investigation of a single-amplifier 3-capacitor circuit useable for realisation of supercapacitors', MSc thesis, Imperial College (London) 1977.

(58) C NIGHTINGALE and J M ROLLETT, 'Exact synthesis of active lowpass frequency-dependent negative-resistance filters' Electronics Letters, 10, (3), pp 34-35, 1974.

(59) W T RAMSEY, 'Active RC highpass filters using single-amplifier impedance inverters for inductor simulation' IEE colloquium on electronic filters, May 1977.

(60) W T RAMSEY 'Highpass and Bandpass filters using a new single-amplifier simulated inductor', Electronic Circuits and Systems, May 1978, vol 2, No 3.

$$T(p) = \frac{V_2(p)}{I_1(p)}$$

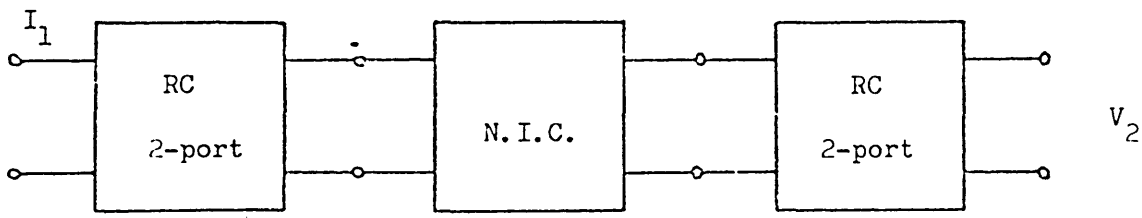

Fig. 1.1 Linvill's method for active-RC filter design

$$T(p) = \frac{V_2(p)}{V_1(p)}$$

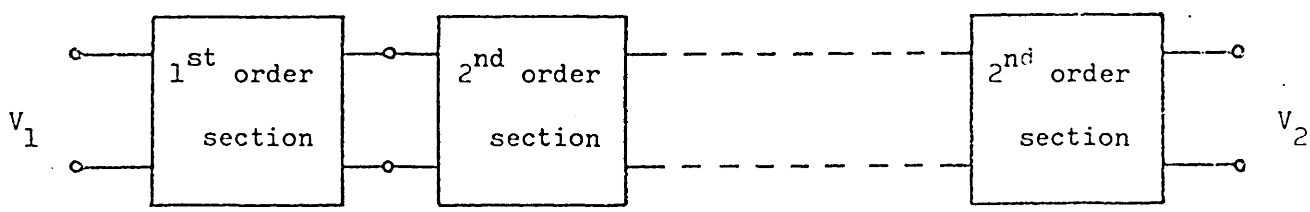

Fig. 1.2 "Cascade method" for active-RC filter design

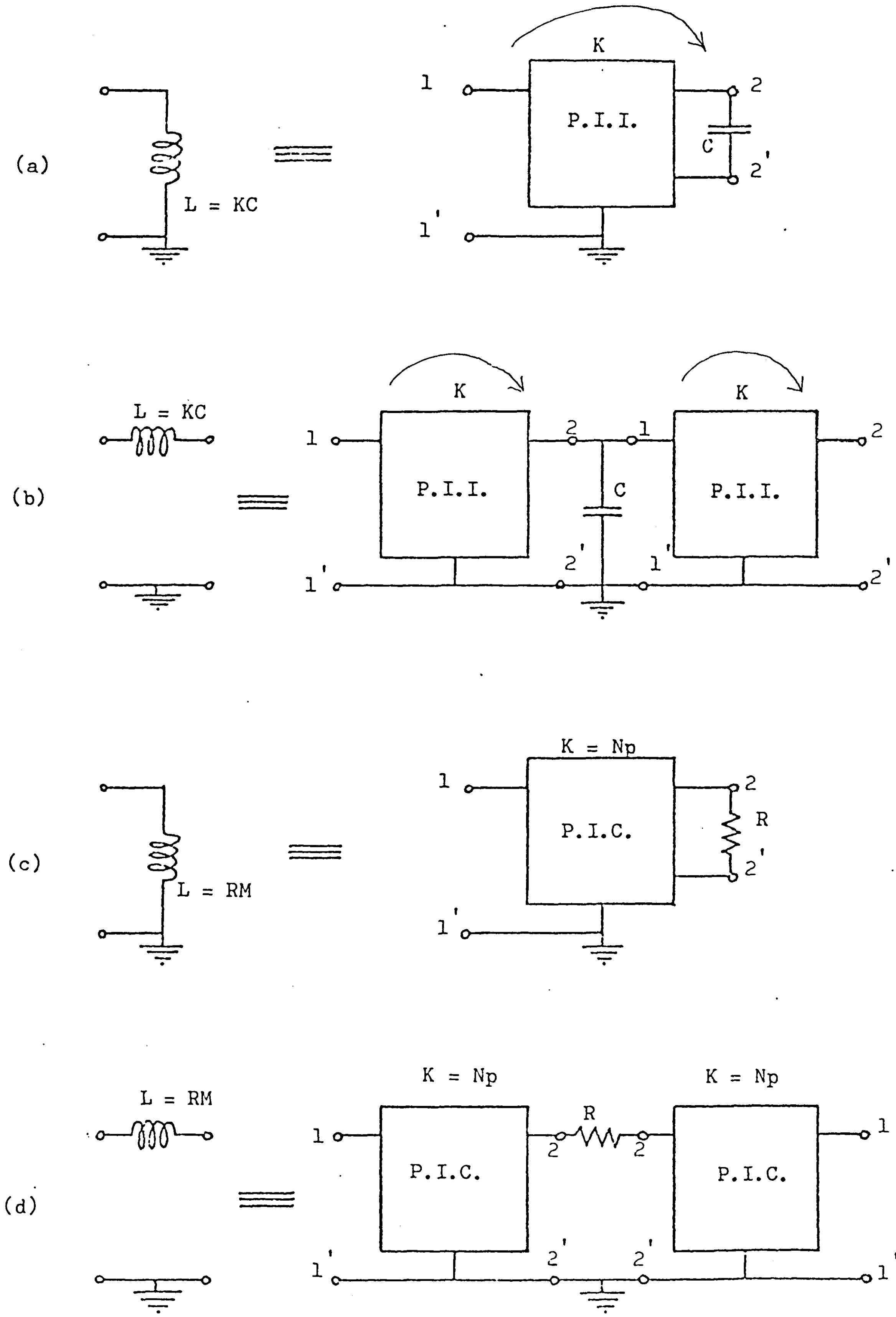

Fig. 1.3 Some methods for the simulation of inductors

$$T(p) = \frac{V_2(p)}{V_1(p)}$$

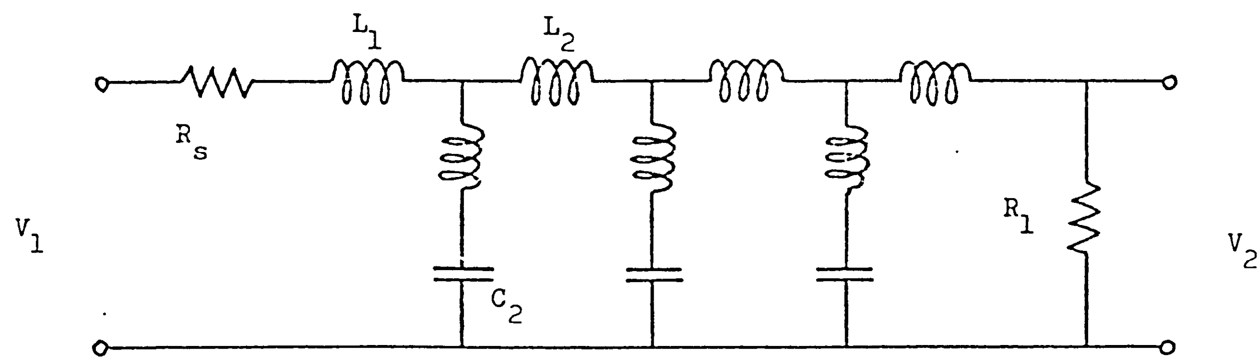

Fig. 1.4(a) LC lowpass filter

$$T'(p) = \frac{V_2'(p)}{V_1'(p)} = T(p)$$

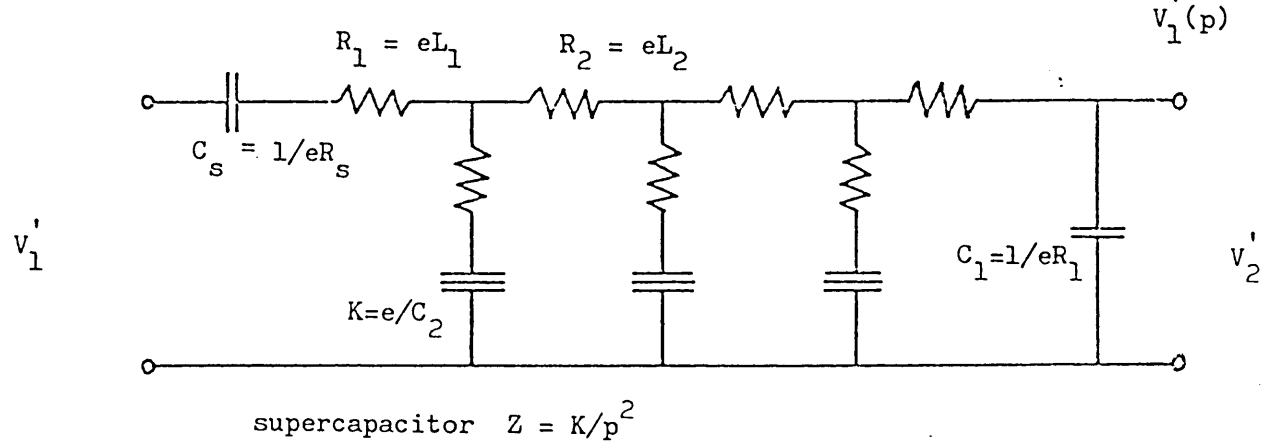

Fig. 1.4(b) Lowpass filter after impedance scaling by e/p (T(p) unchanged)

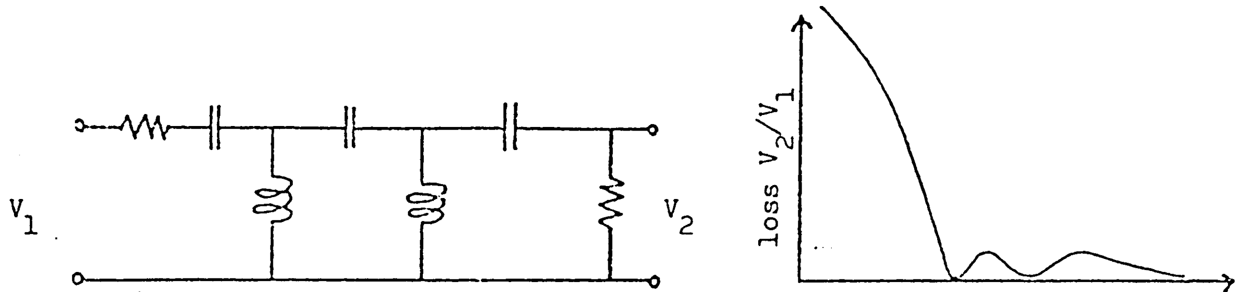

(a) Polynomial type highpass filter

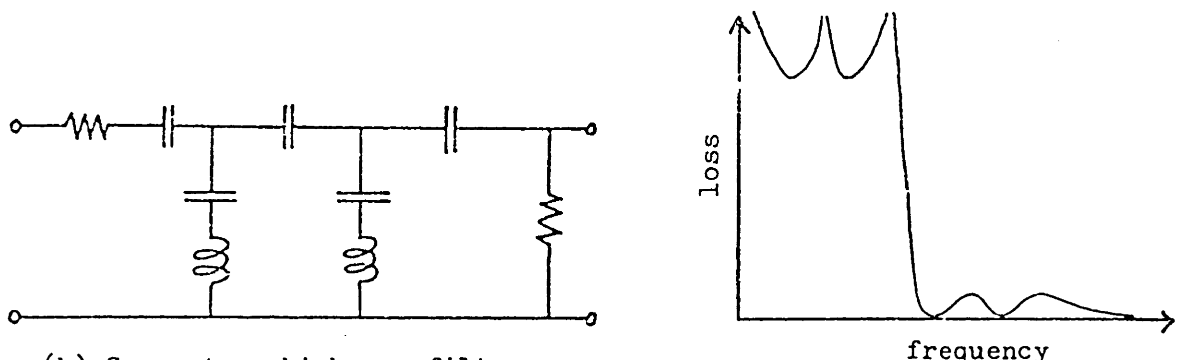

(b) Cauer type highpass filter

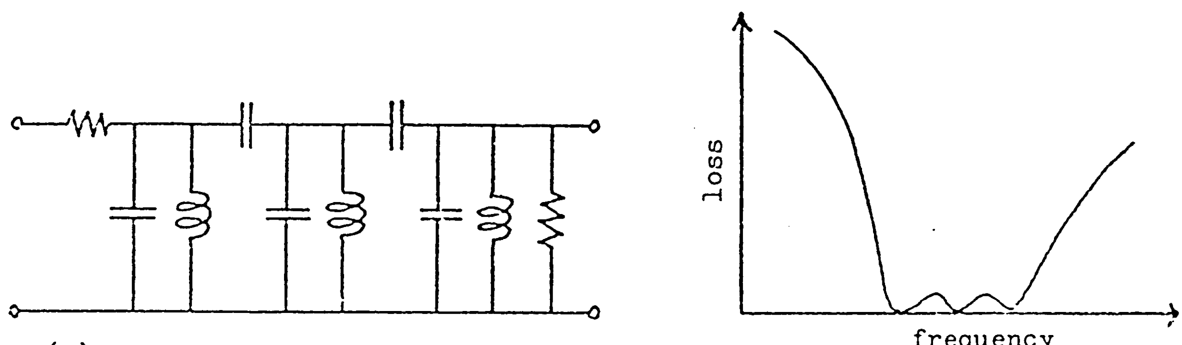

(c) Polynomial type bandpass filter

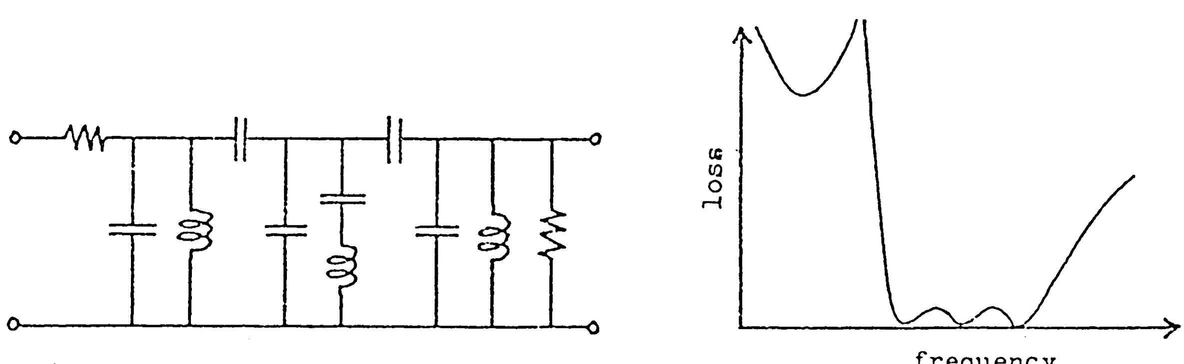

(d) Bandpass filter with 1 transmission zero at a finite frequency

Fig. 1.5 LC filter types where all Ls are grounded

$$Z = \frac{pC_0R_1R_3R_4}{R_2}$$

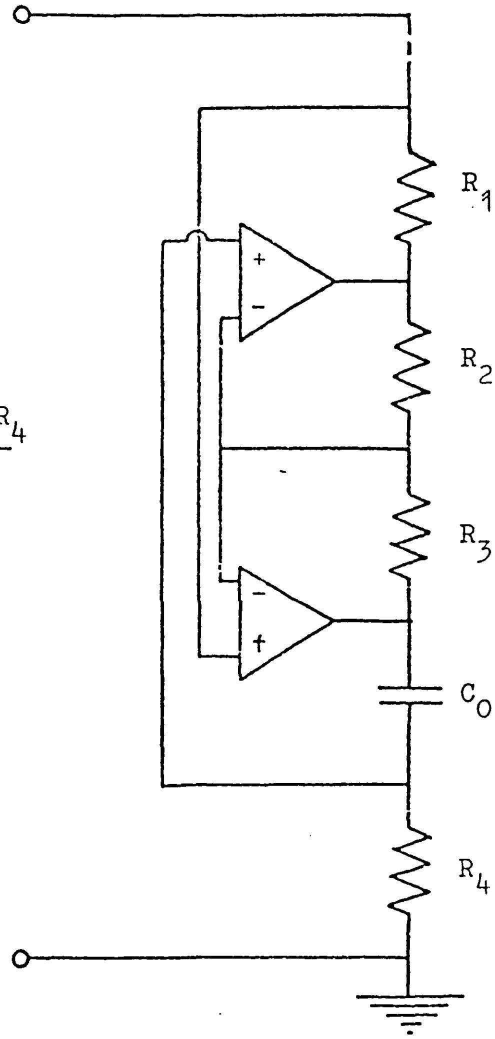

Fig. 2.1 Two-amplifier circuit ($Z = pL$)

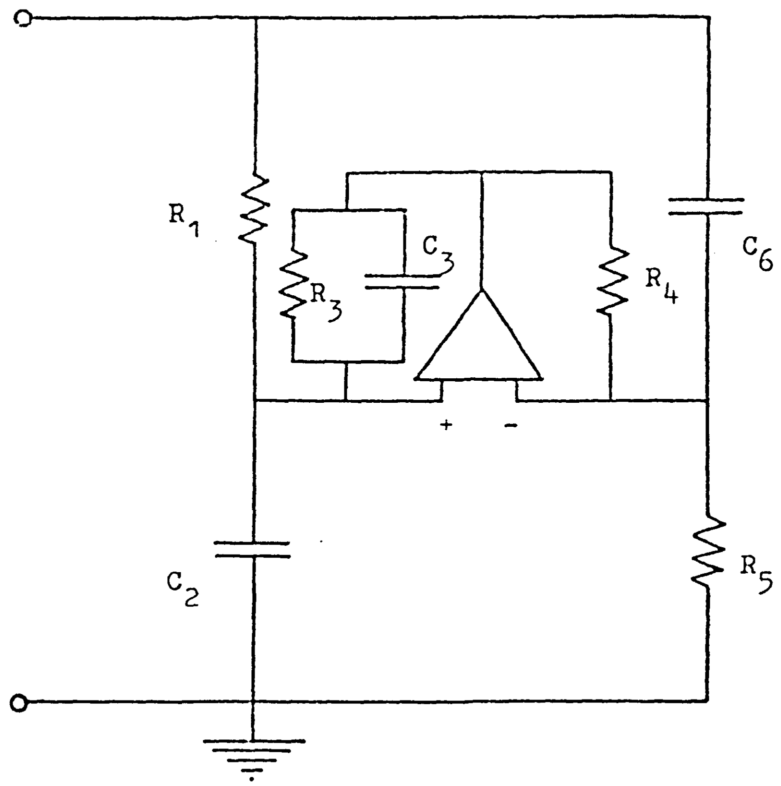

Fig. 2.2 Saraga circuit (Z = pL)

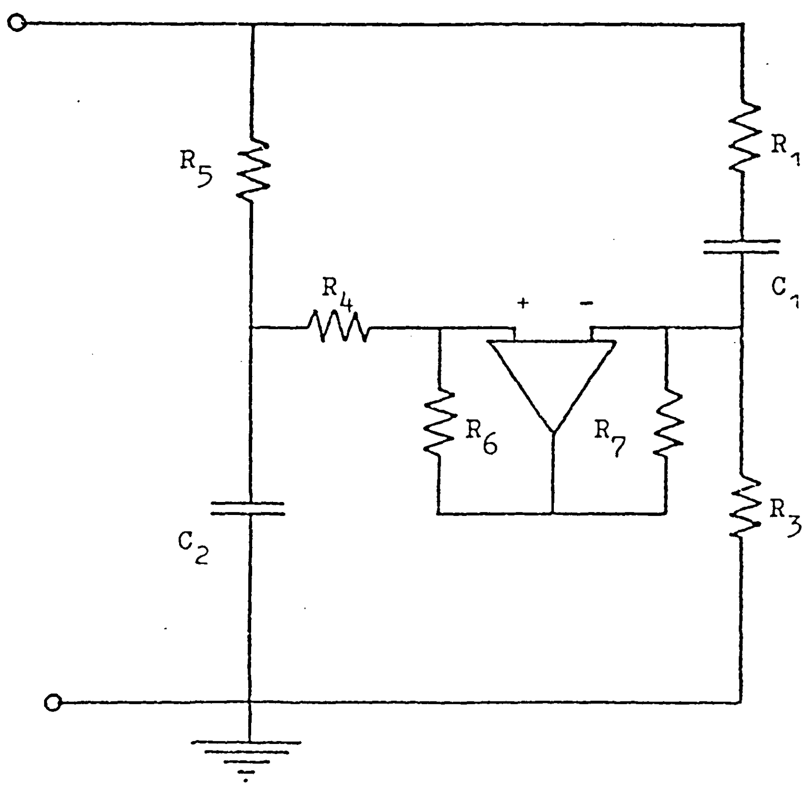

Fig. 2.3 Sipress circuit (Z = pL)

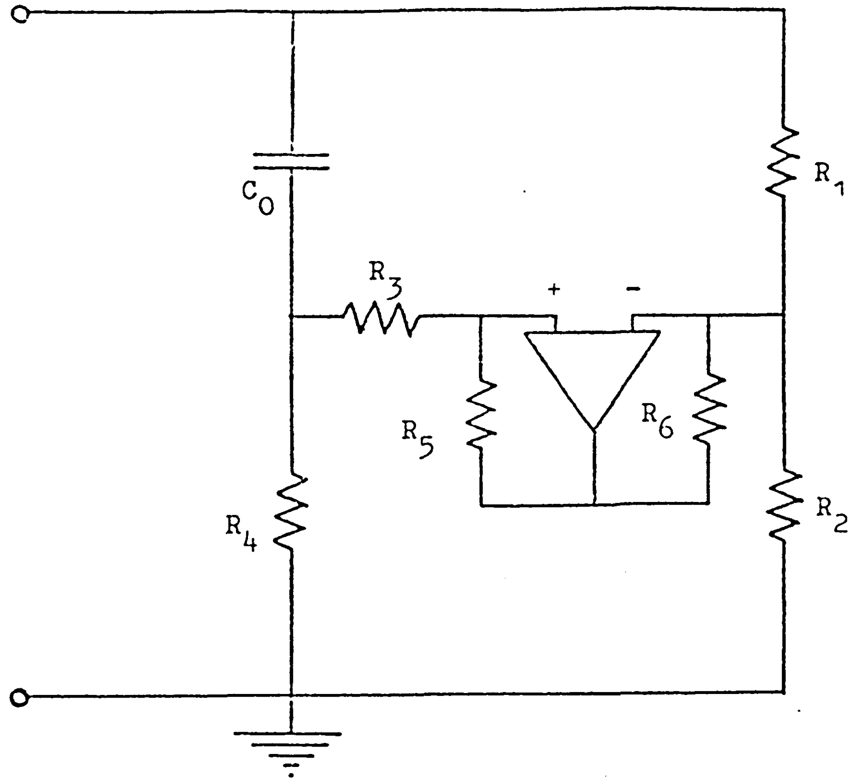

Fig. 2.4 Orchard/Willson circuit ($Z = pL$)

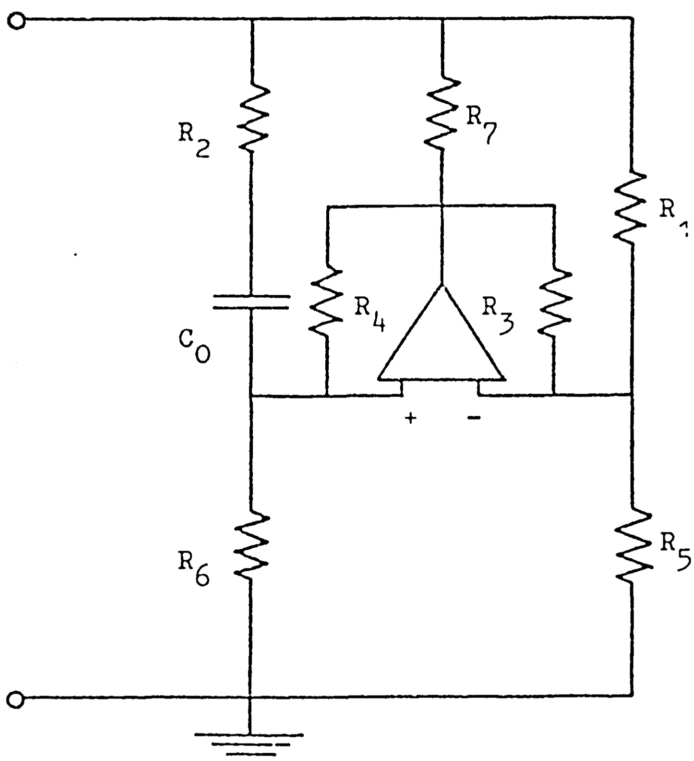

Fig. 2.5 Schmidt/Lee circuit ($Z = pL$)

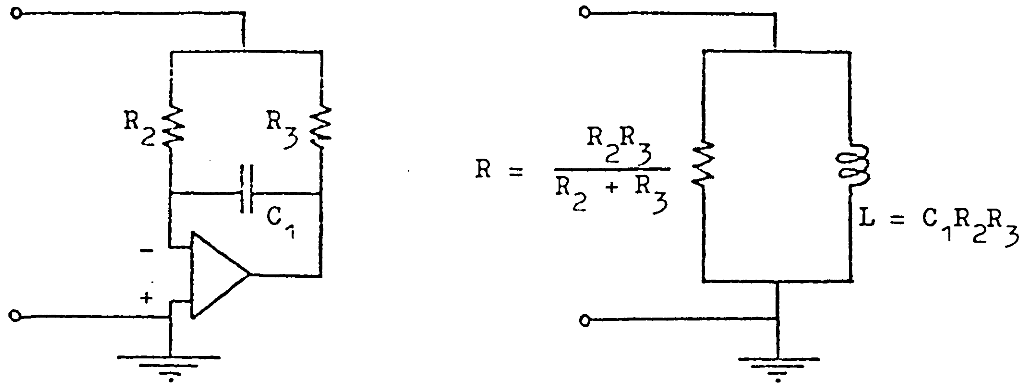

(a) Ford and Girling circuit

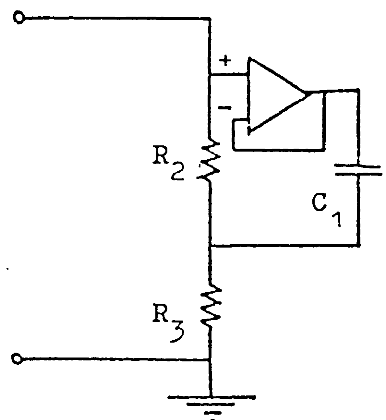

(b) Prescott circuit

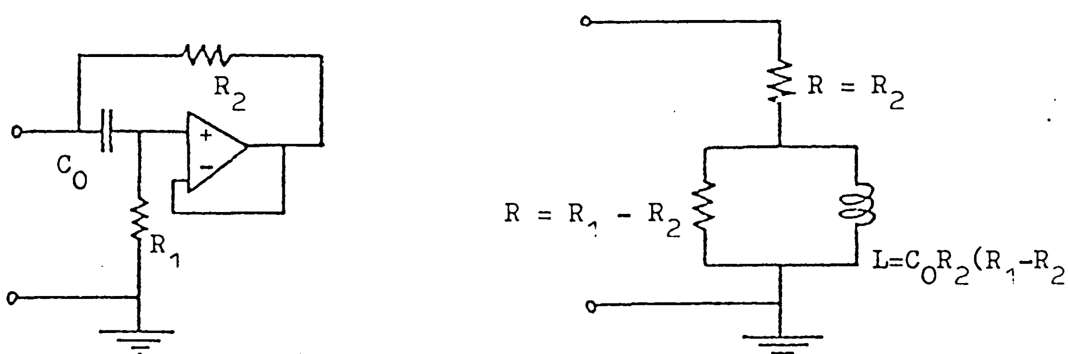

(c) Berndt and Dutta Roy circuit

Fig. 2.6 Some "lossy" simulated inductor circuits

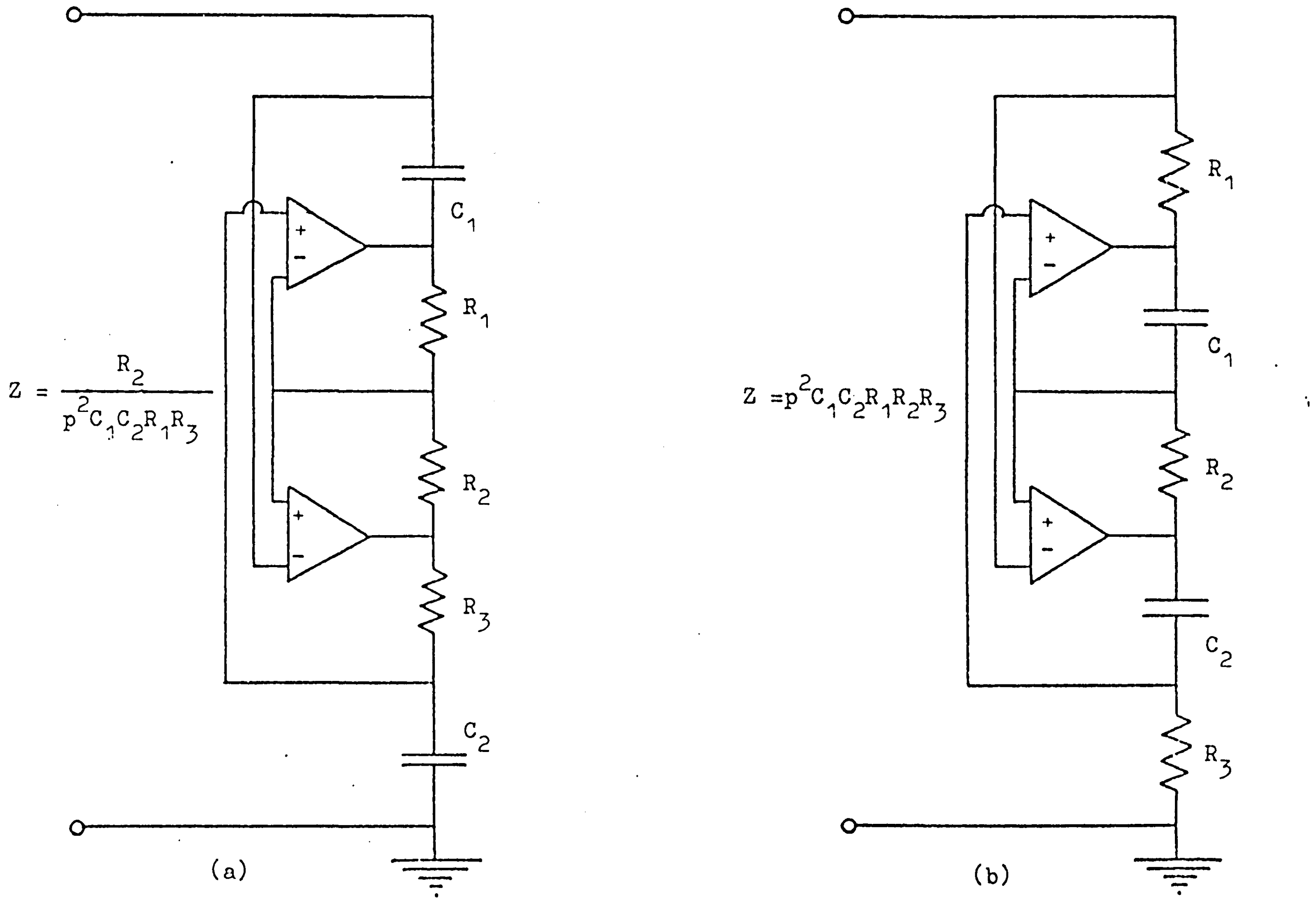

Fig. 2.7 Two-amplifier F.D.N.R. circuits

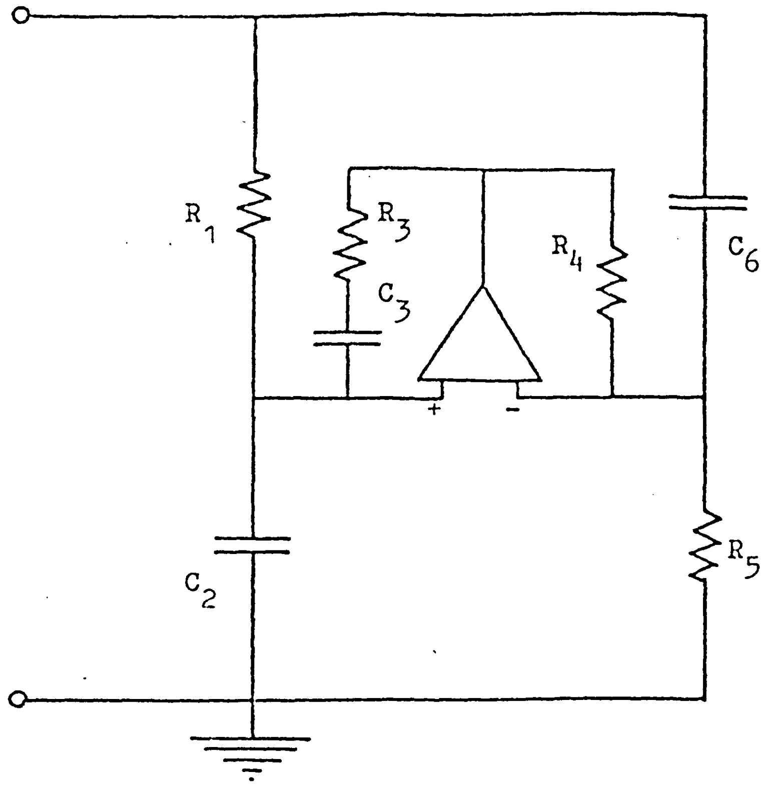

Fig. 2.8 Saraga circuit ($Z = K/p^2$)

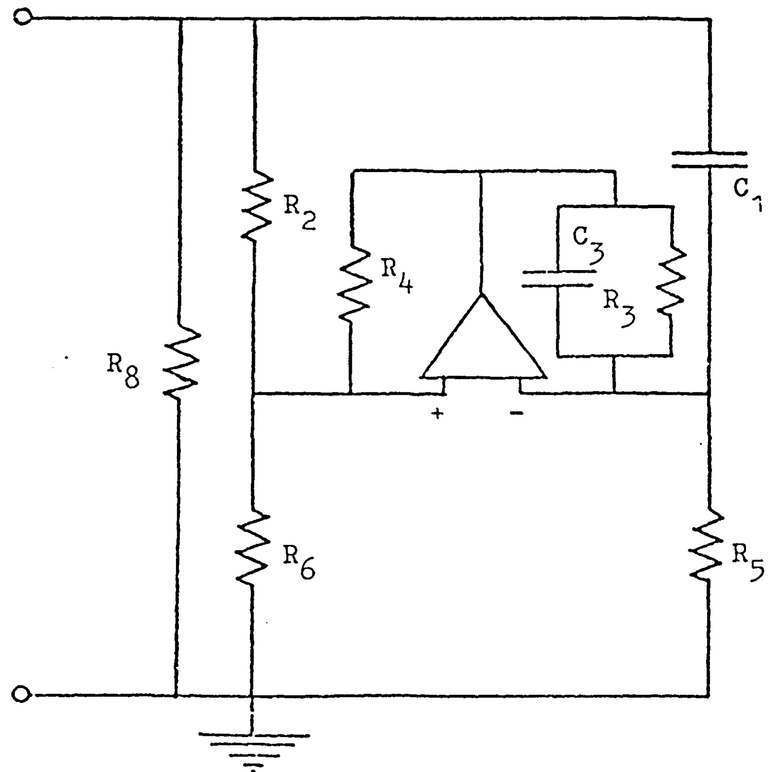

Fig. 2.9 Schmidt/Lee circuit ($Z = K/p^2$)

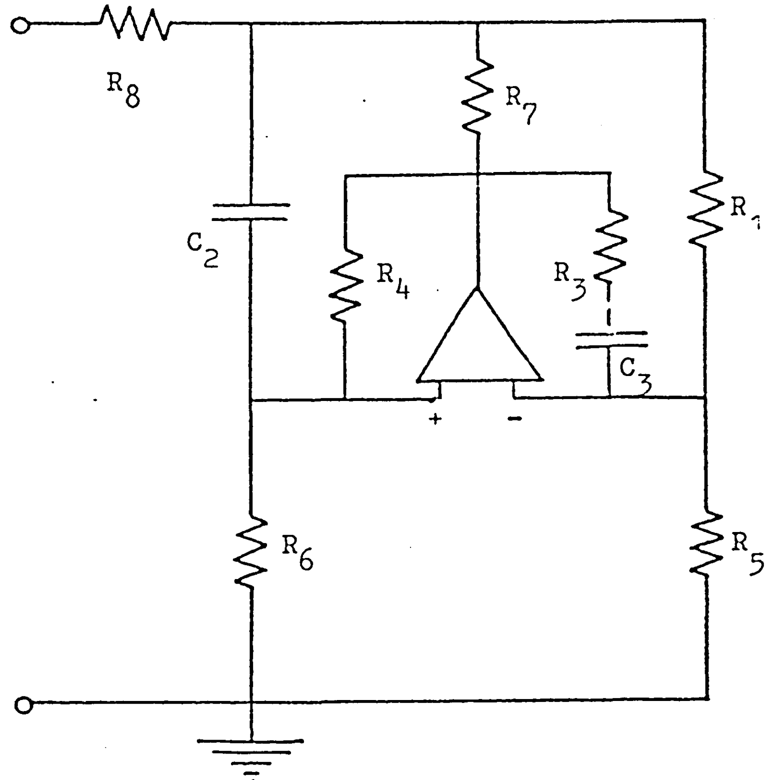

Fig. 2.10 Schmidt/Lee circuit ($Z = Mp^2$)

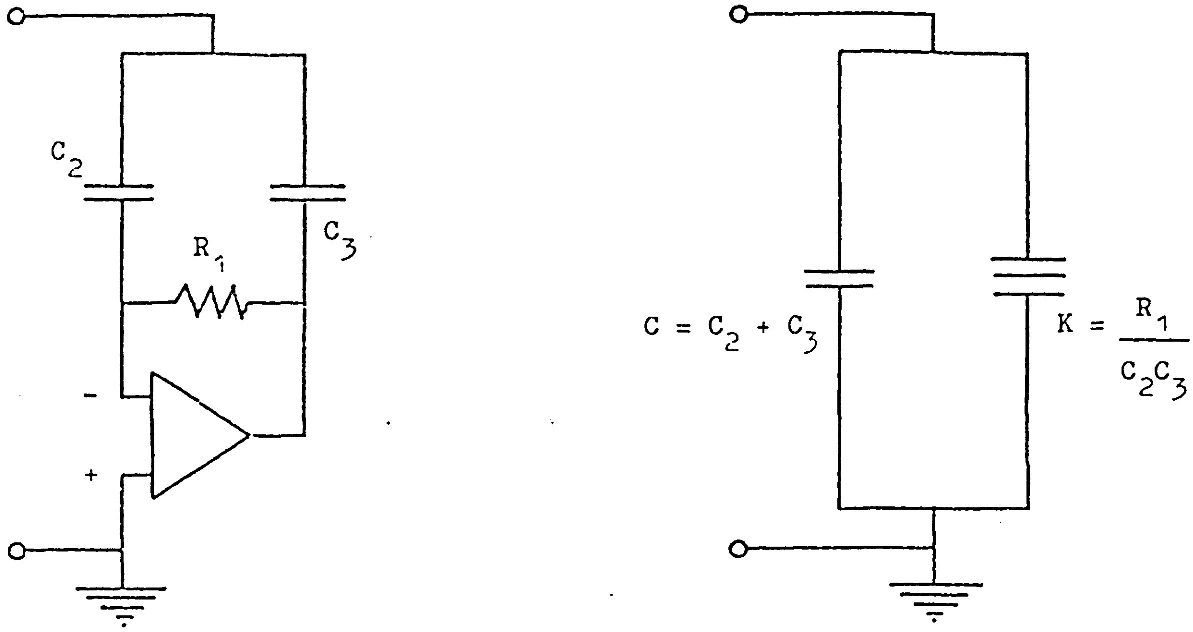

(a) $$Z = \frac{K}{p(\ p + CK\ )}$$

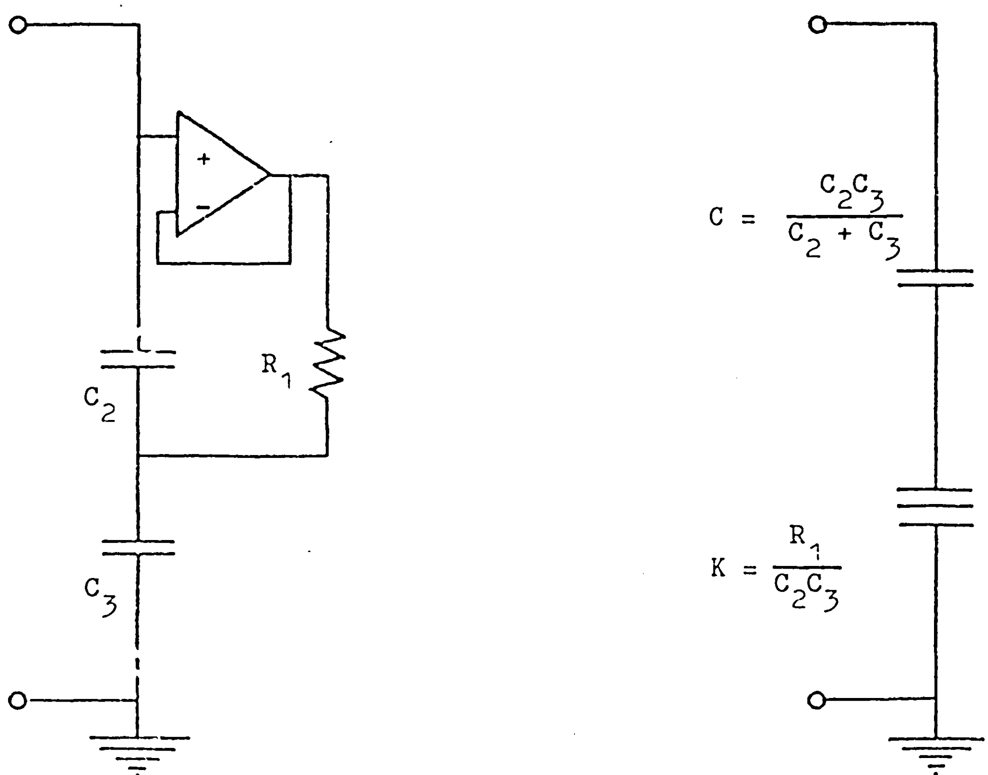

(b) $$Z = K/p^2 + 1/pC$$

Fig. 2.11 Some imperfect F.D.N.R. circuits

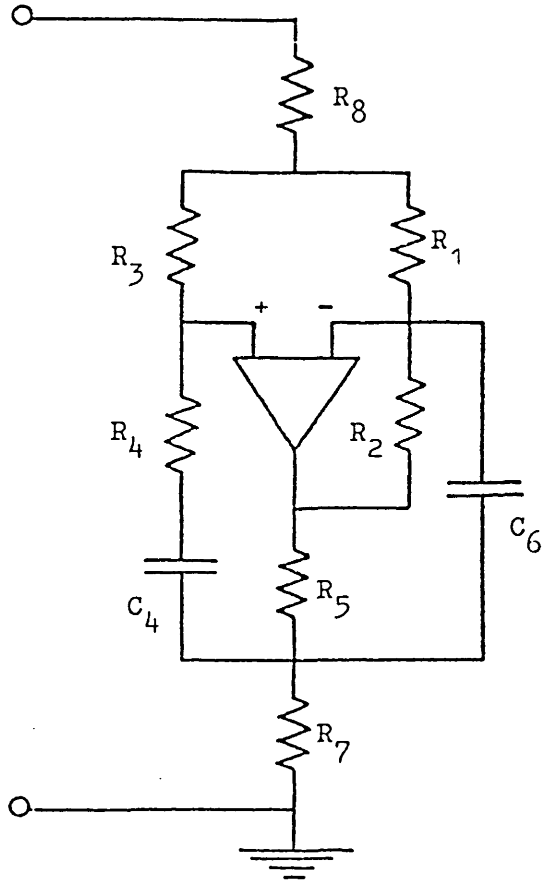

Fig. 2.12 Cheng/Lim circuit ($z = pL + 1/pC$)

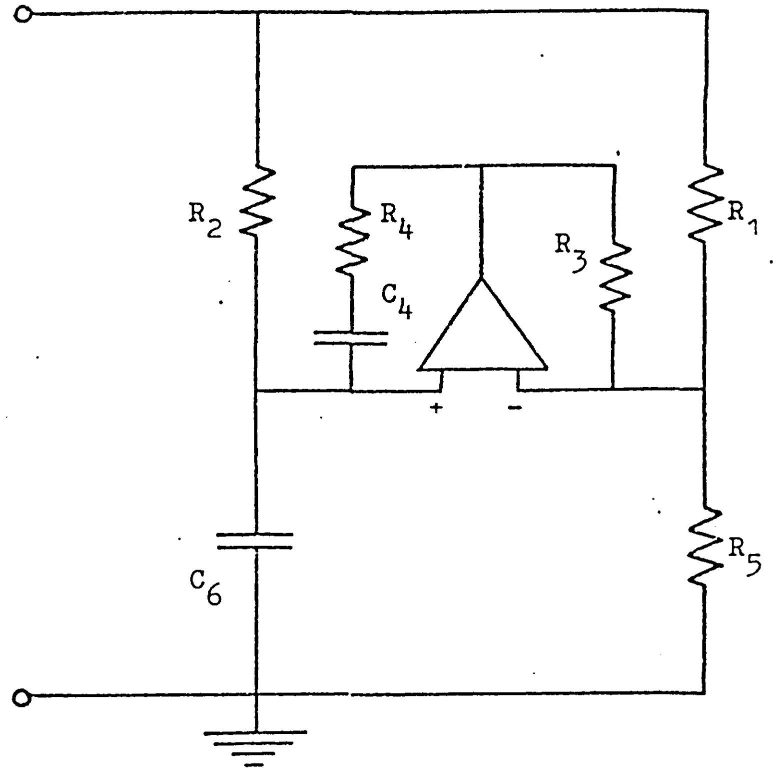

Fig. 2.13 Schmidt/Lee circuit ($Z = R + K/p^2$)

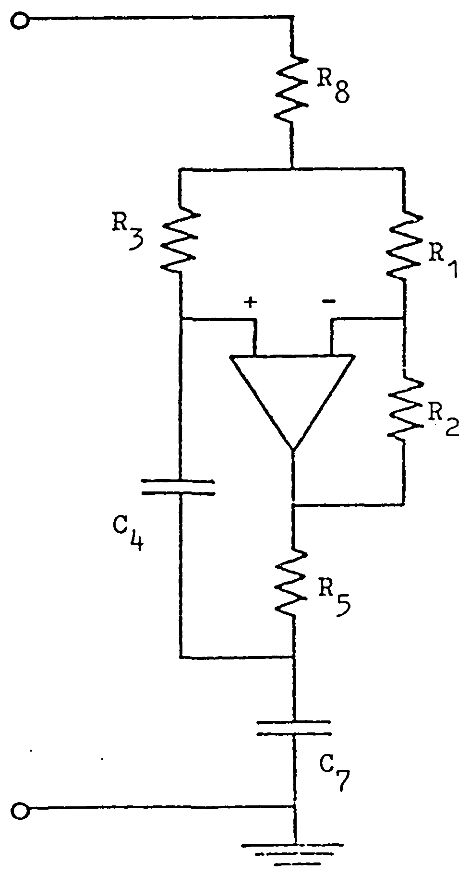

Fig. 2.14 Cheng/Lim circuit ($Z = R + K/p^2$)

circuit	no. of amps.	no. of capacitors	coeff. cancells.	pole/zero cancells.
Saraga (pL)	1	3	2	1
Sipress (pL)	1	2	2	1
Orchard/Willson (pL)	1	1	2	0
Schmidt/Lee (pL)	1	1	2	0
Cheng/Lim (pL+1/pC)	1	2	1	0
Two-amp. circuit (pL)	2	1	0	0

Schmidt/Lee (Mp^2)	1	2	4	0
Schmidt/Lee (K/p^2)	1	2	3	0
Saraga (K/p^2)	1	3	2	1
Schmidt/Lee ($R+K/p^2$)	1	2	2	0
Cheng/Lim ($R+K/p^2$)	1	2	1	0
Two-amp. circuit $\frac{K}{p^2}$, Mp^2	2	2	0	0

Fig. 2.15 Number of amplifiers, capacitors, coefficient and pole/zero cancellations required by the simulation networks.

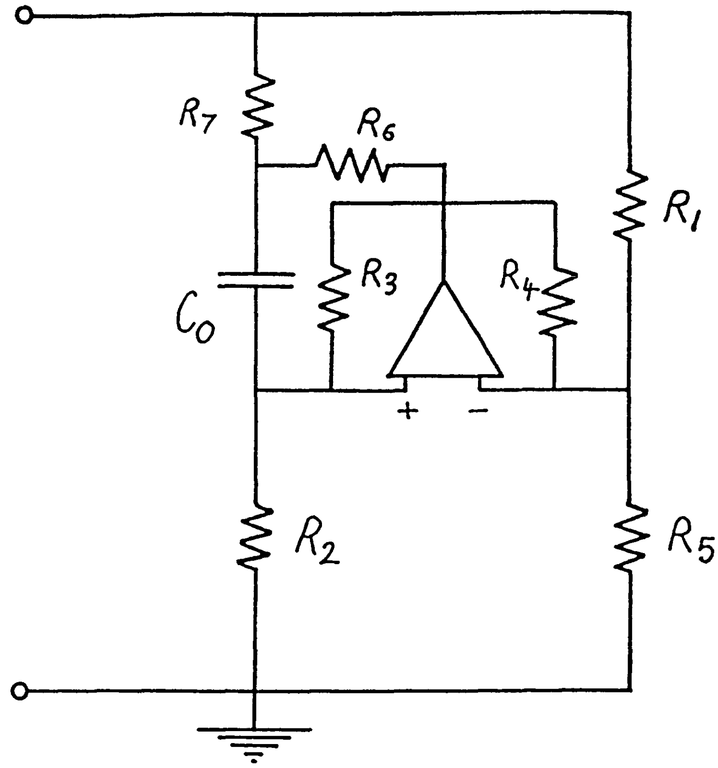

Fig. 3.1 (a) S.I. circuit A

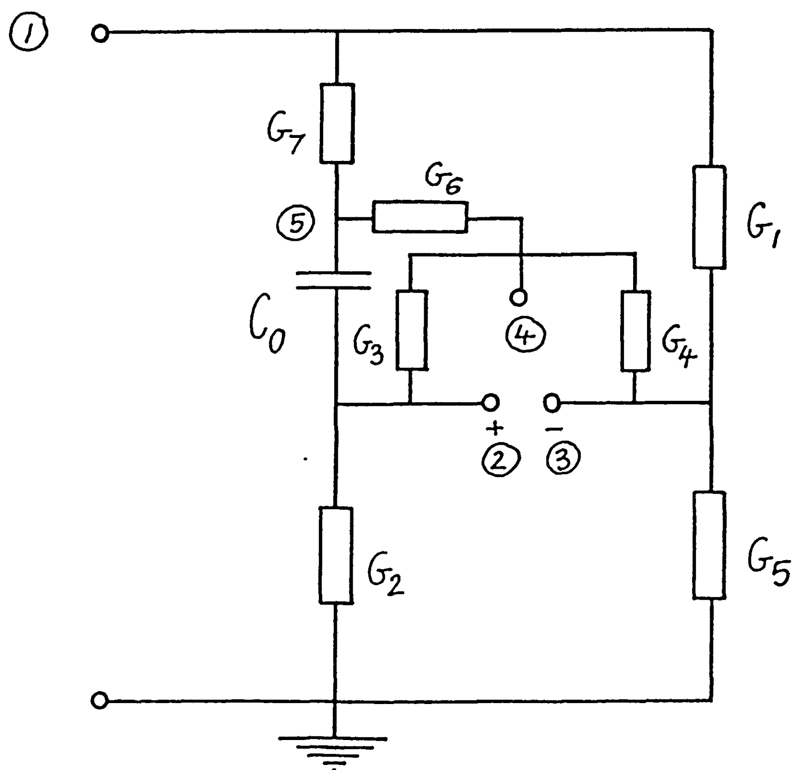

Fig. 3.1 (b) RC network for S.I. circuit A

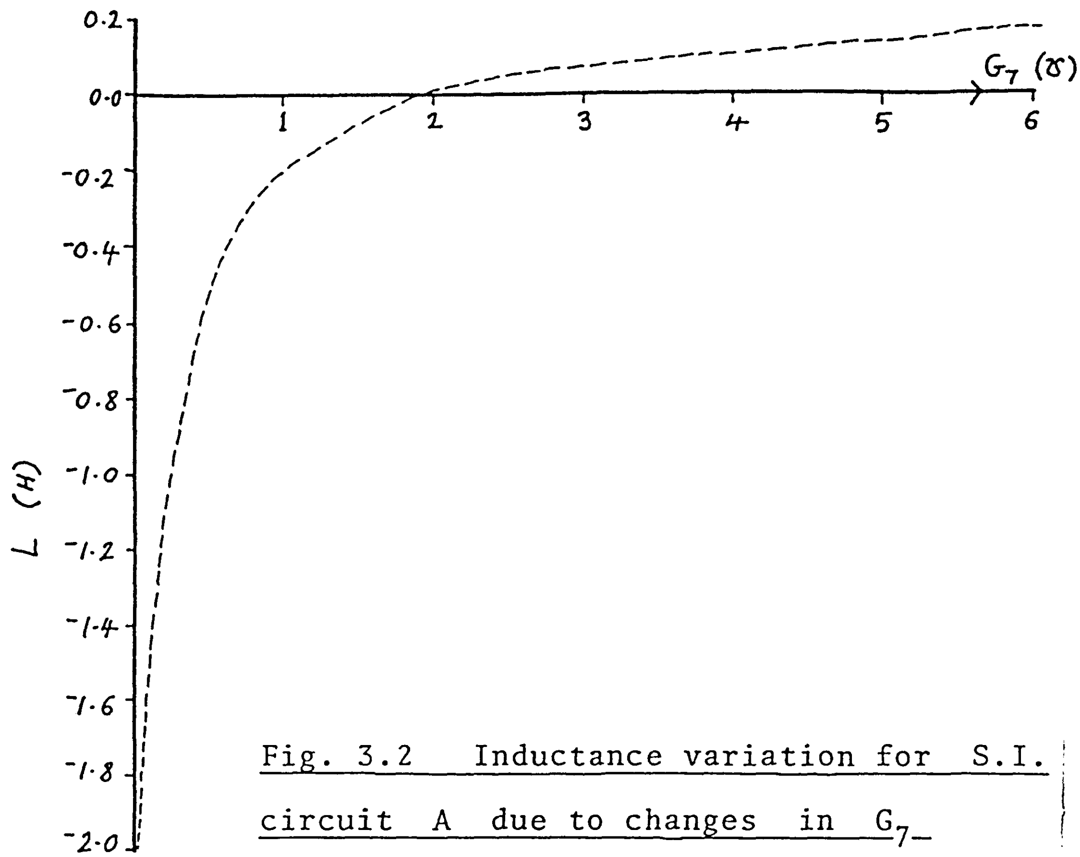

Fig. 3.2 Inductance variation for S.I. circuit A due to changes in G_7

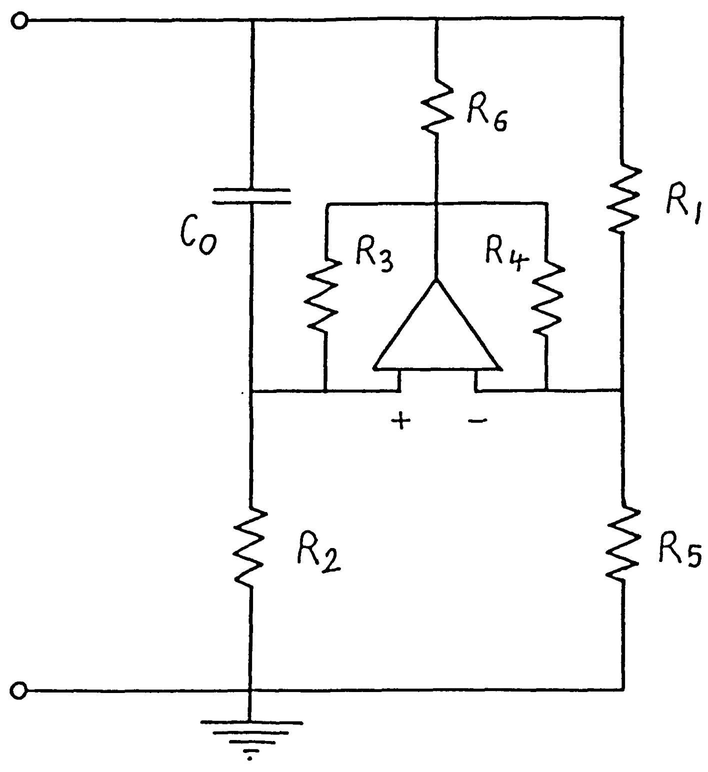

Fig. 3.3 S.I. circuit B

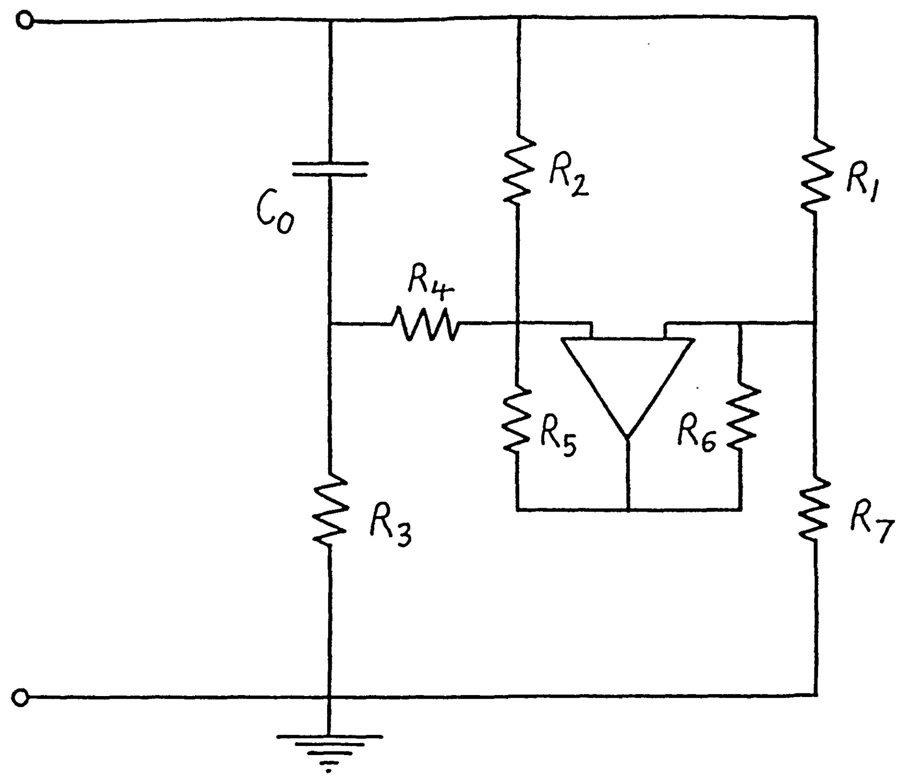

Fig. 3.4 (a) S.I. circuit C

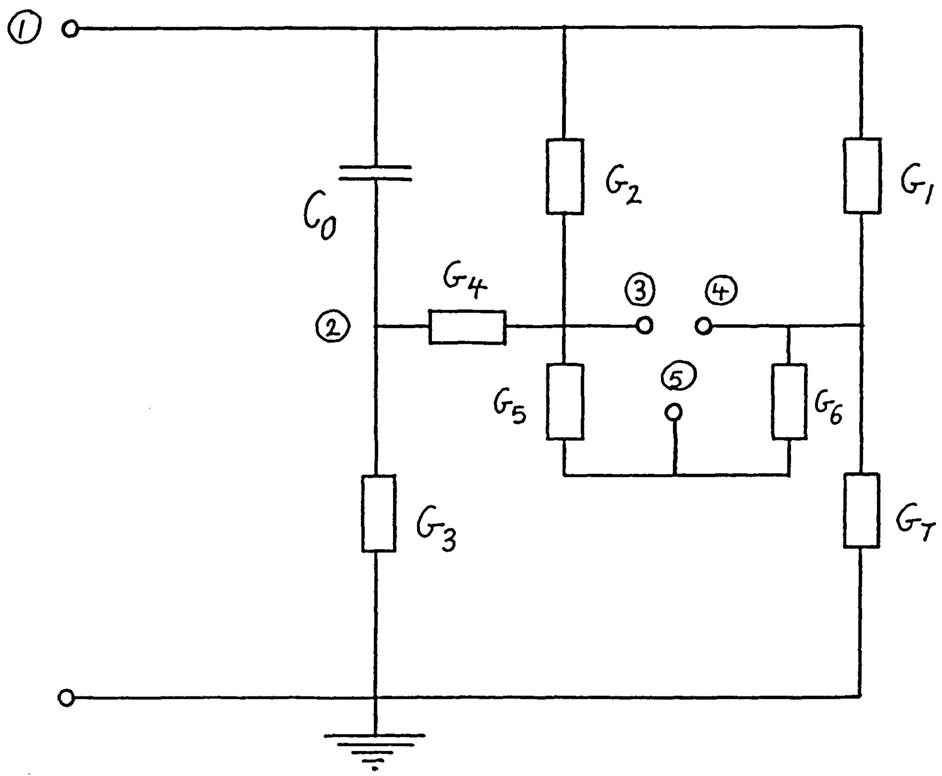

Fig. 3.4 (b) RC network for S.I. circuit C

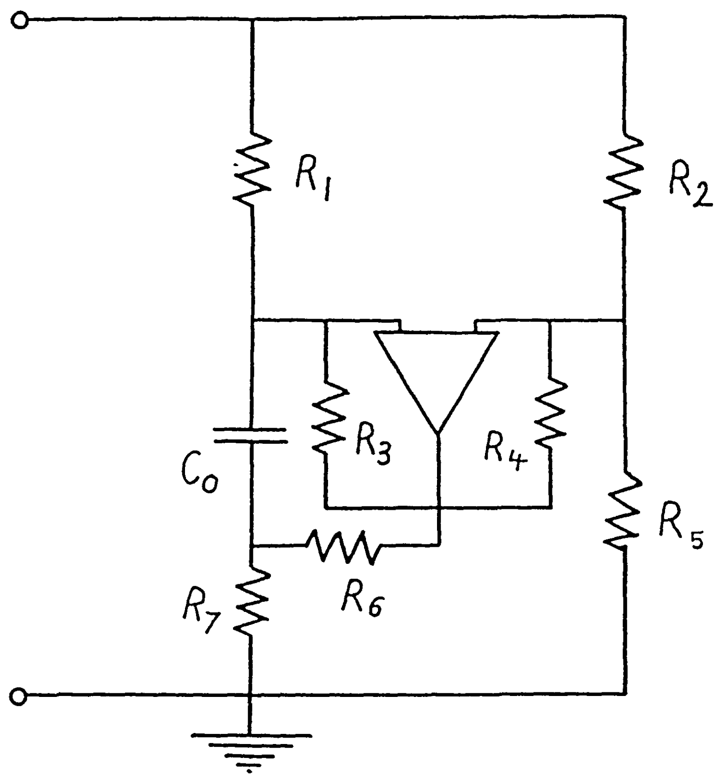

Fig. 3.5 (a) S.I. circuit D

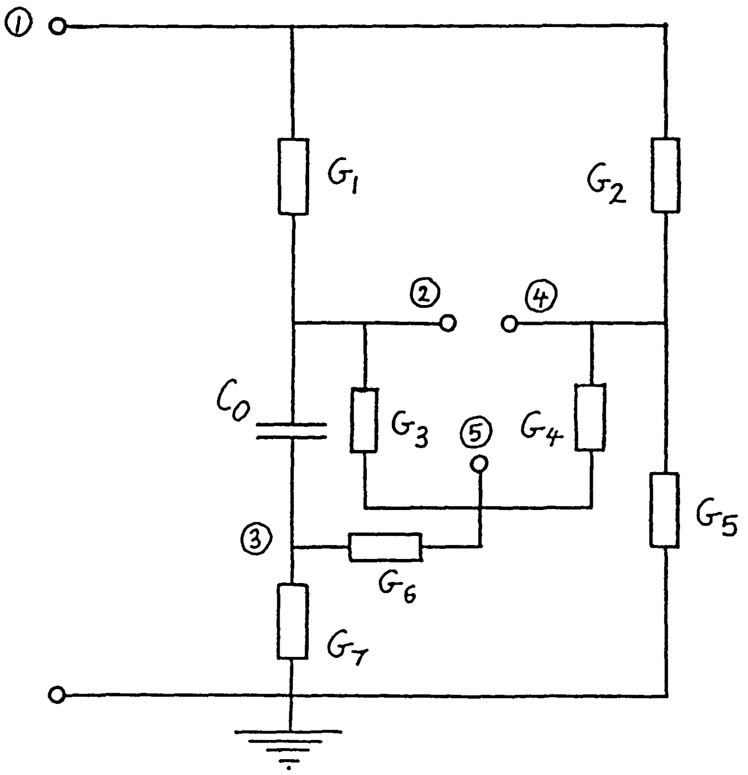

Fig. 3.5 (b) RC network for S.I. circuit D

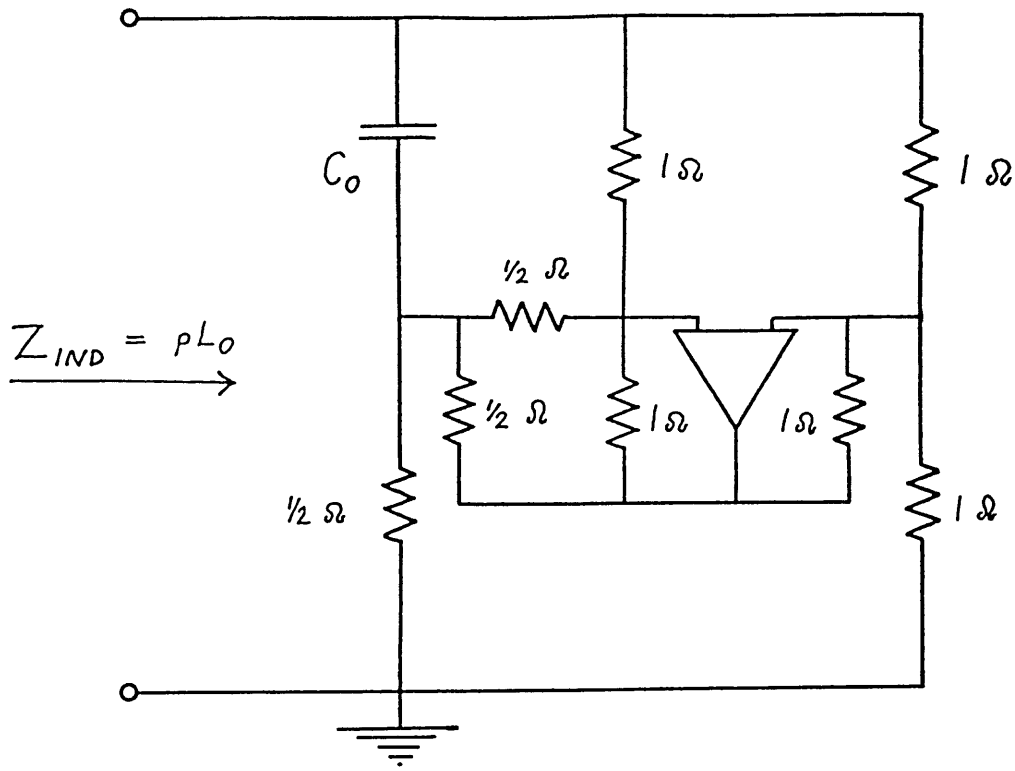

Fig. 3.6 S.I. circuit E

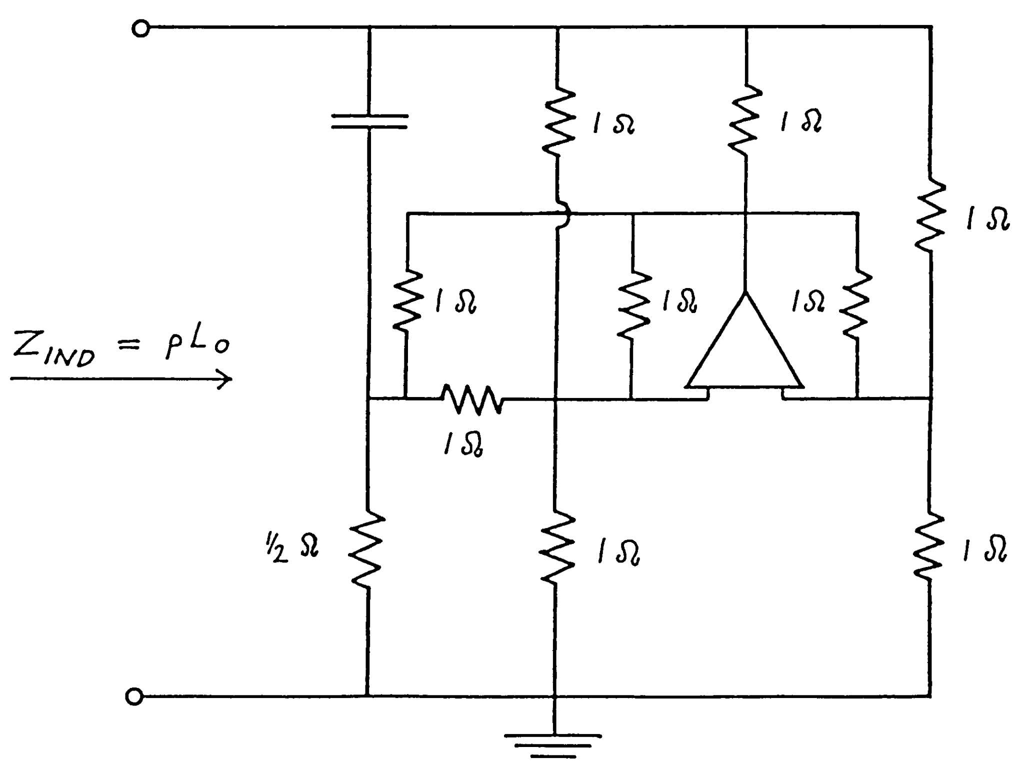

Fig. 3.7 S.I. circuit F

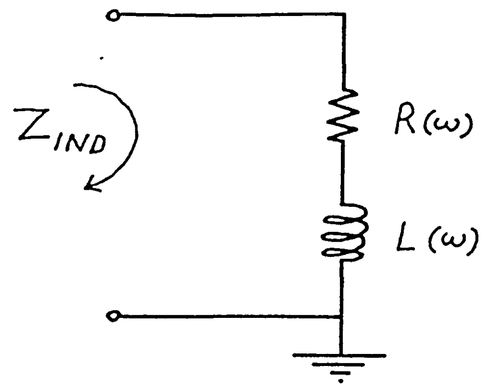

Fig. 3.8 (a) Model for showing the effects of passive component tolerances

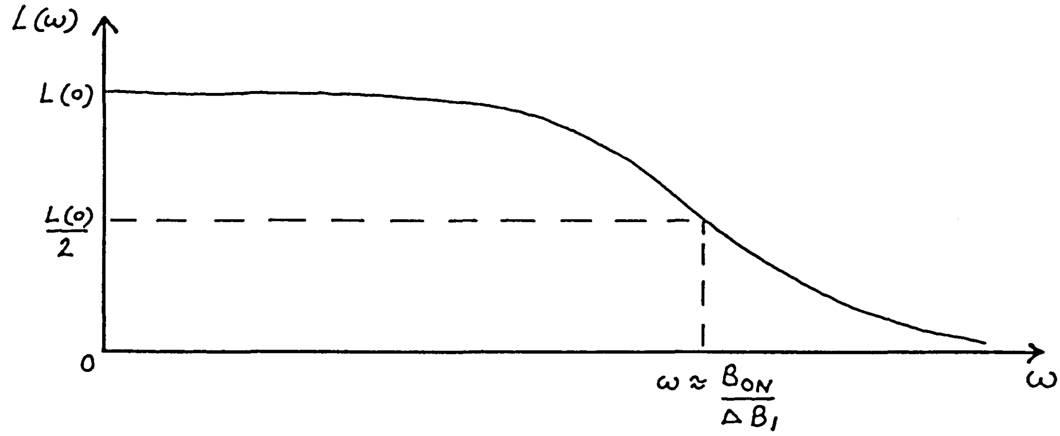

Fig. 3.8 (b) Typical L(ω) behaviour

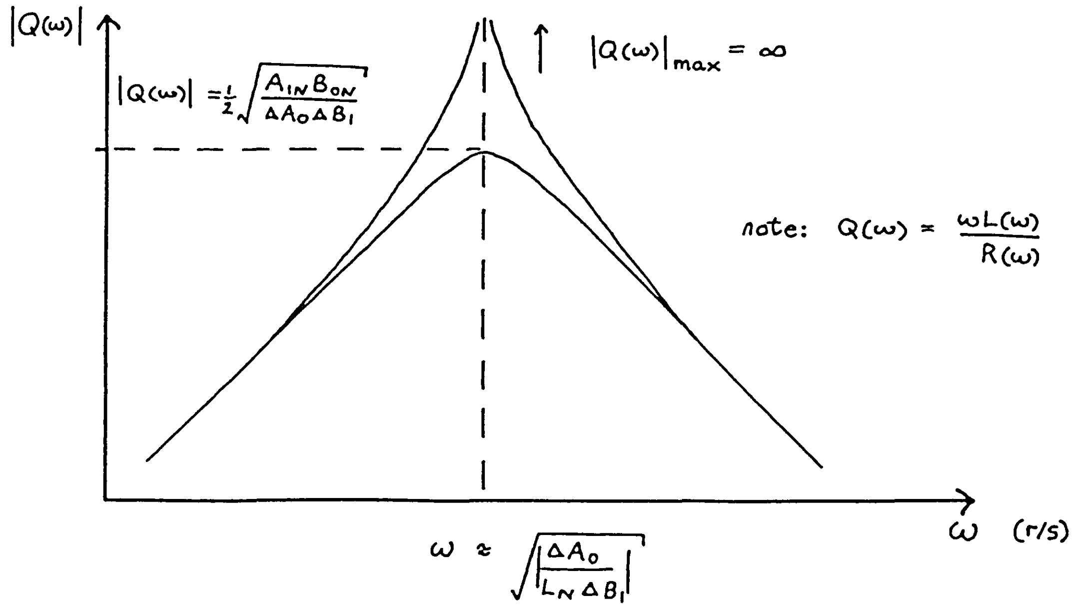

Fig. 3.8 (c) Typical Q(ω) behaviour

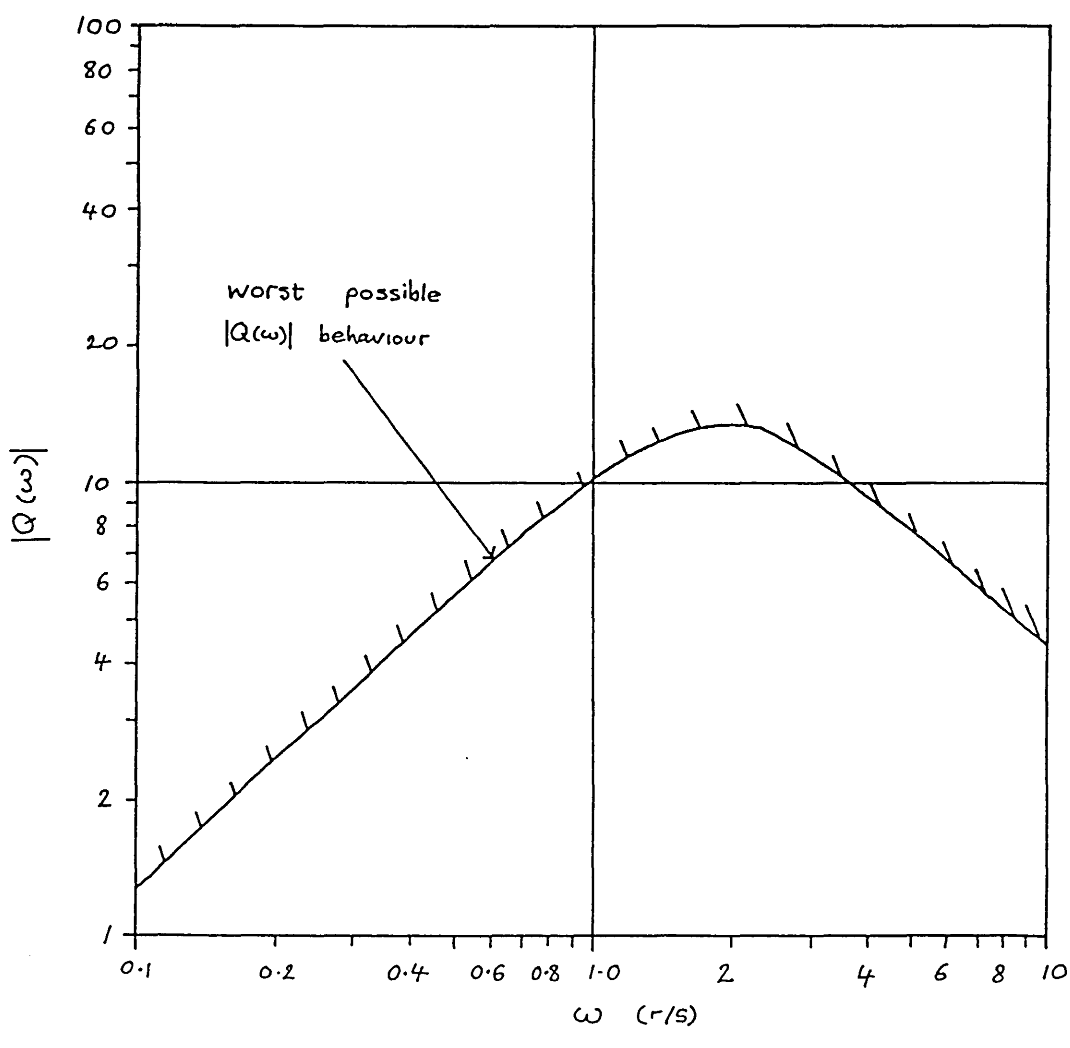

Fig. 3.8 (d) Worst possible $|Q(\omega)|$ behaviour due to 1.0 % conductance tolerances

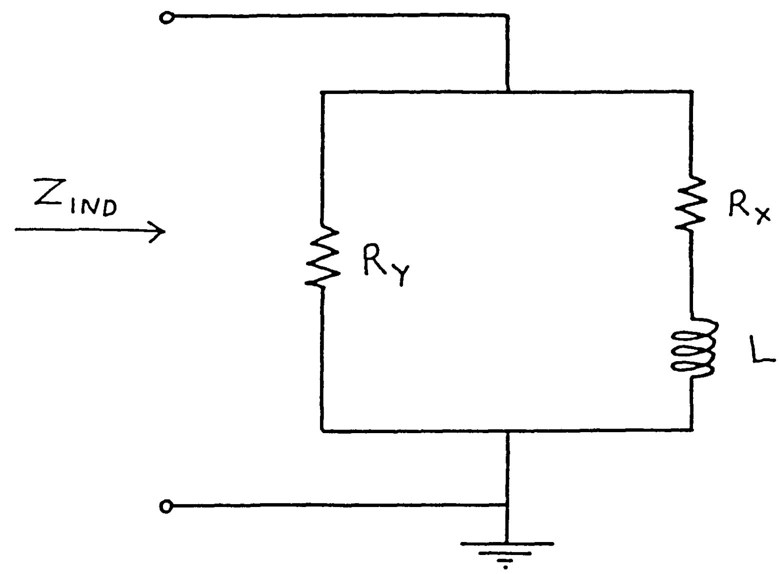

Fig. 3.9 Alternative model for showing the effects of passive component tolerances

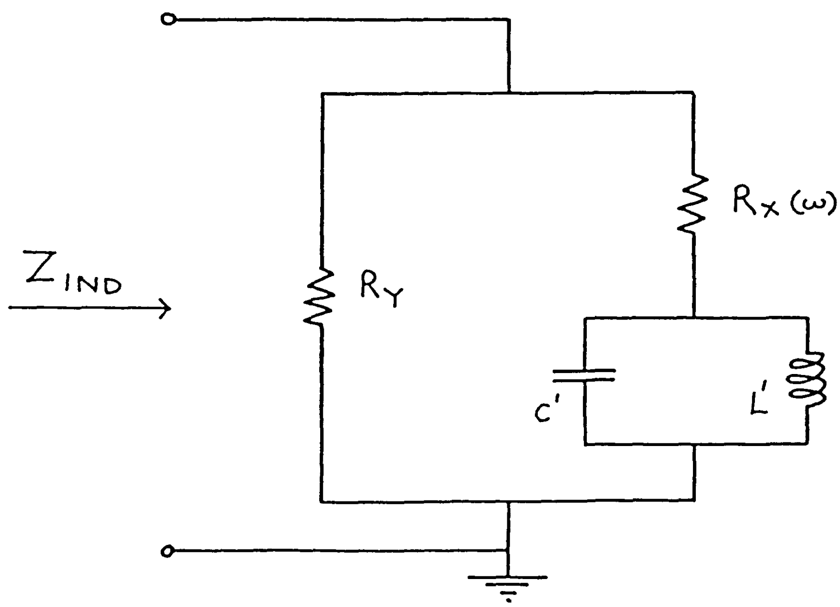

Fig. 3.10 Model for showing the effects of the non-ideal amplifier gain

component	value	change	R_X (Ω)	R_Y ($M\Omega$)	% L
R_{1N}	10 kΩ	$\pm$ 1 %	$\pm$ 25	∞	$\pm$ 0.75
R_{2N}	5 kΩ	"	$\mp$ 50	$\mp$ 0.5	$\pm$ 1.5
R_{3N}	10 kΩ	"	$\pm$ 50	$\pm$ 1.0	$\mp$ 0.5
R_{4N}	10 kΩ	"	$\mp$ 50	$\mp$ 0.5	0
R_{5N}	10 kΩ	"	$\pm$ 25	$\pm$ 0.5	$\mp$ 0.5
R_{6N}	10 kΩ	"	0	$\pm$ 1.0	$\pm$ 0.75
C_{ON}	4 nF	"	0	∞	$\pm$ 1.0

Fig. 4.1 Typical effects of component tolerances

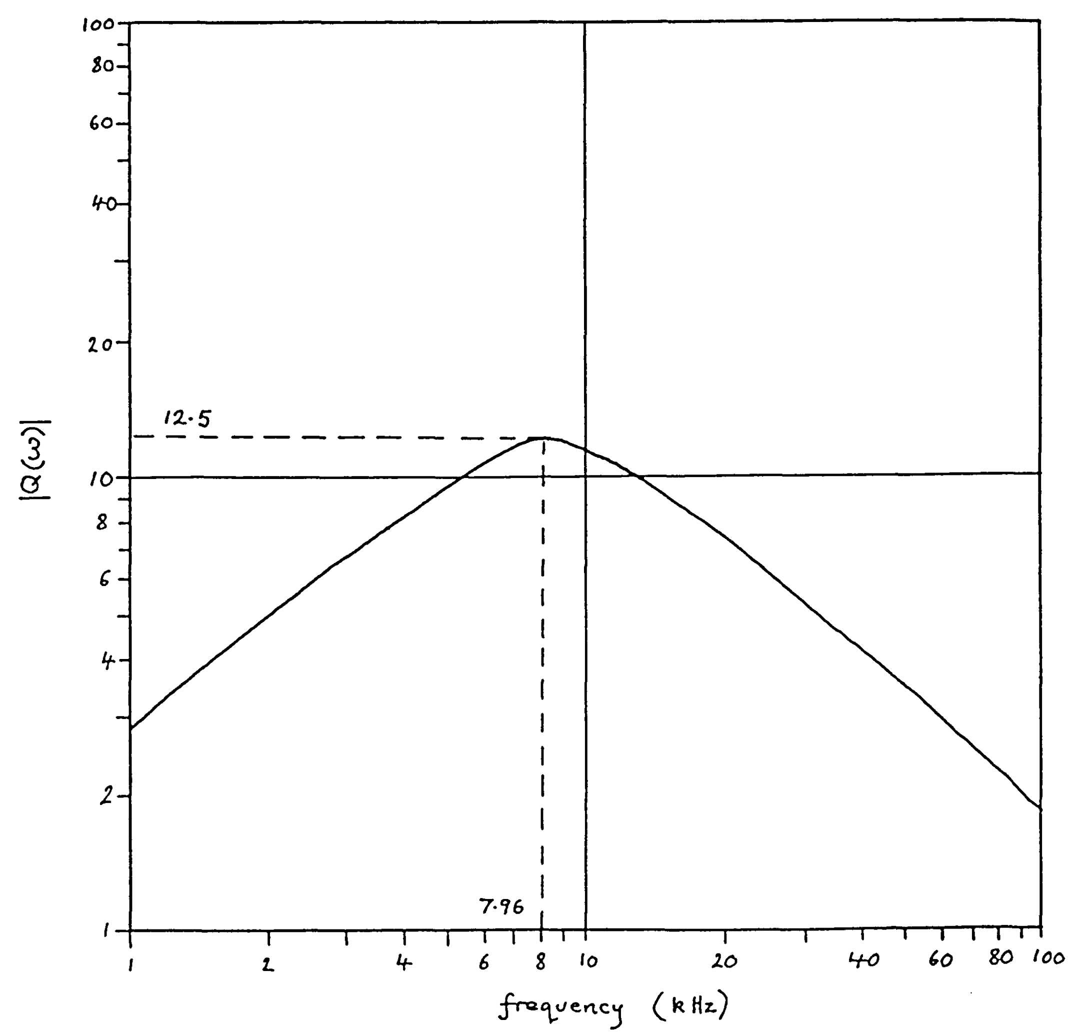

Fig. 4.2 Worst possible $|Q(\omega)|$ behaviour due to 1 % passive component tolerances

component	value	change	R_X (Ω)	R_Y ($M\Omega$)	% L
R_{1N}	1 kΩ	$\pm$ 1 %	$\pm$ 3.32	∞	$\pm$0.67
R_{2N}	99.01 kΩ	"	$\mp$ 3.36	$\mp$ 9.9	$\pm$1.01
R_{3N}	100 kΩ	"	$\pm$ 3.36	$\pm$ 1000	$\mp$.0066
R_{4N}	1 kΩ	"	$\mp$ 3.36	$\mp$ 10	$\mp$0.33
R_{5N}	100 kΩ	"	$\pm$0.033	$\pm$ 9.9	$\mp$.0066
R_{6N}	1 kΩ	"	0	$\pm$ 10	$\pm$0.67
C_{0N}	332.2 pF	"	0	∞	$\pm$ 1.0

Fig. 4.3 Effects of component tolerances for improved design

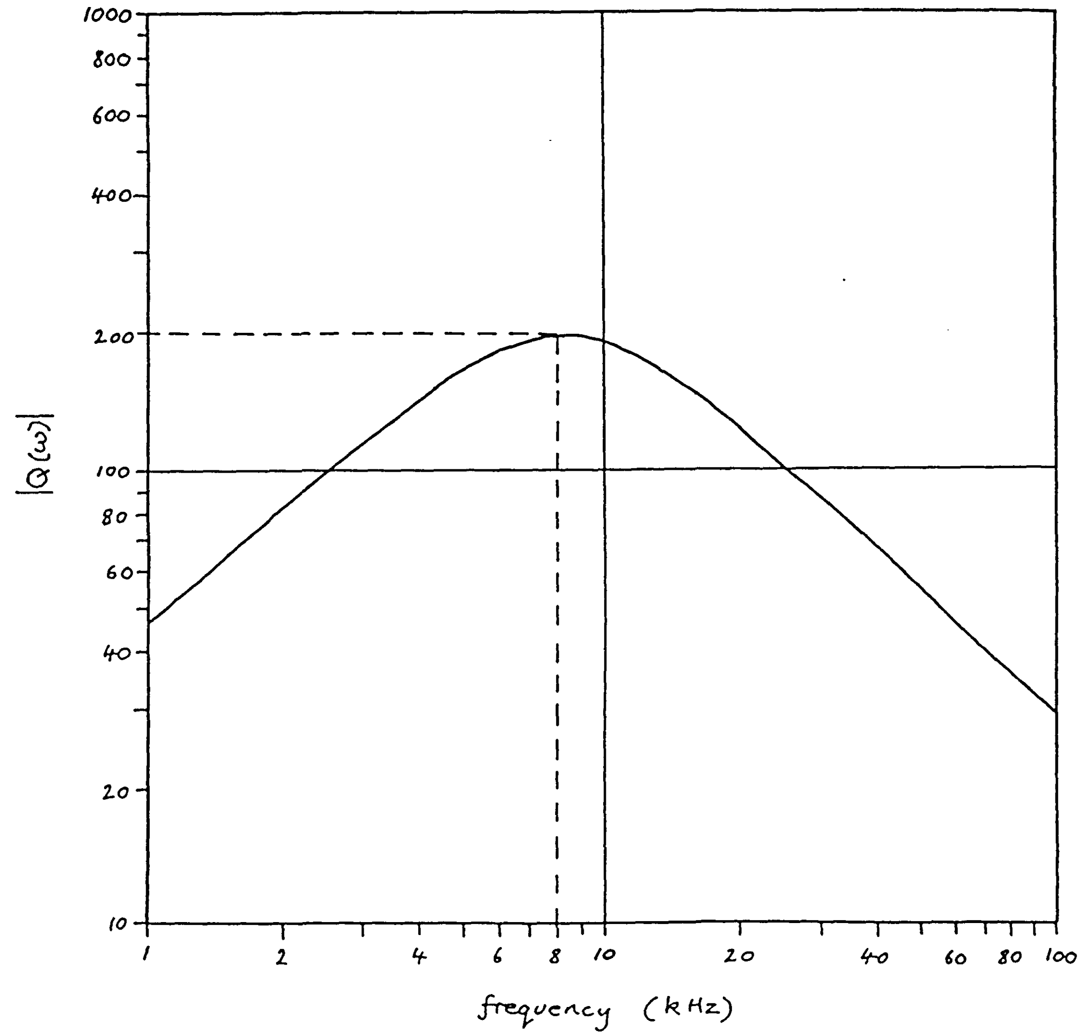

Fig. 4.4 Worst possible $|Q(\omega)|$ behaviour for improved design (due to 1 % passive component tolerances)

COMPONENT	VALUE
R_1	1·61804 kΩ
R_2	0·89443 "
R_3	2·0 "
R_4	2·0 "
R_5	2·0 "
R_6	1·61804 "
C_0	161·803 nF

Table (b) - values for improving the $|Q(\omega)|$ behaviour due to finite f_T

COMPONENT	VALUE
R_1	2·0 kΩ
R_2	1·0 "
R_3	2·0 "
R_4	2·0 "
R_5	2·0 "
R_6	2·0 "
C_0	100 nF

Table (a) - initial choice for the passive component values

Fig. 4.5 Passive component values for S.I. circuit B

(b)

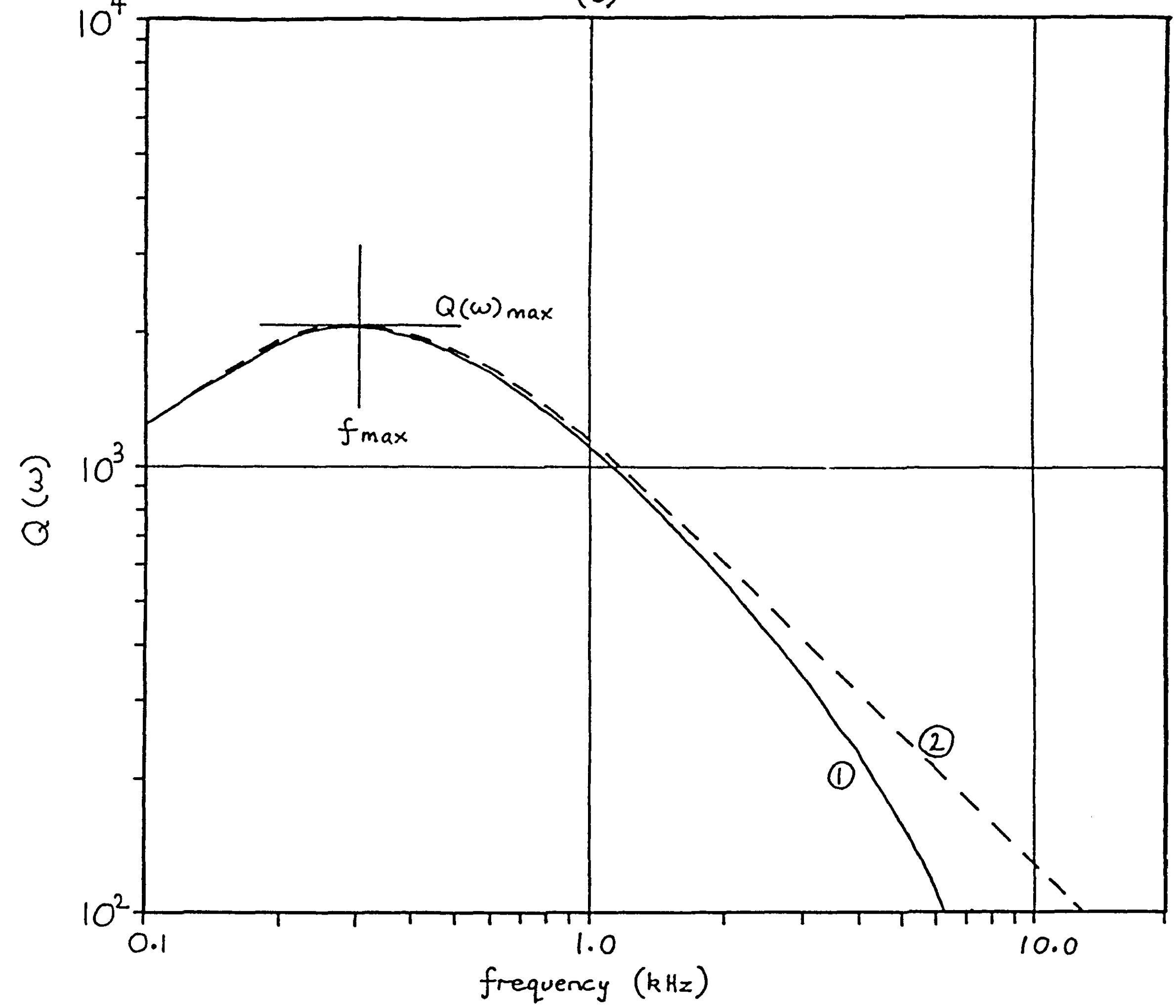

(a)

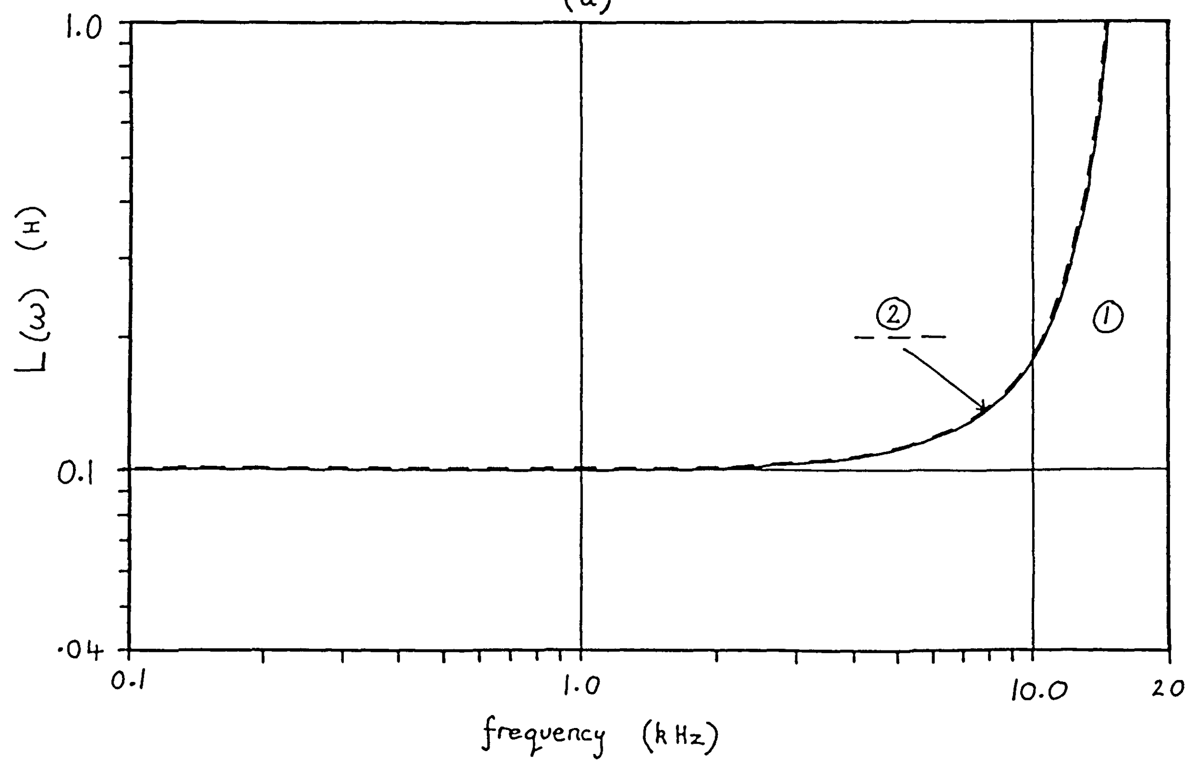

Fig. 4.6 L(ω) and Q(ω) behaviour for initial design

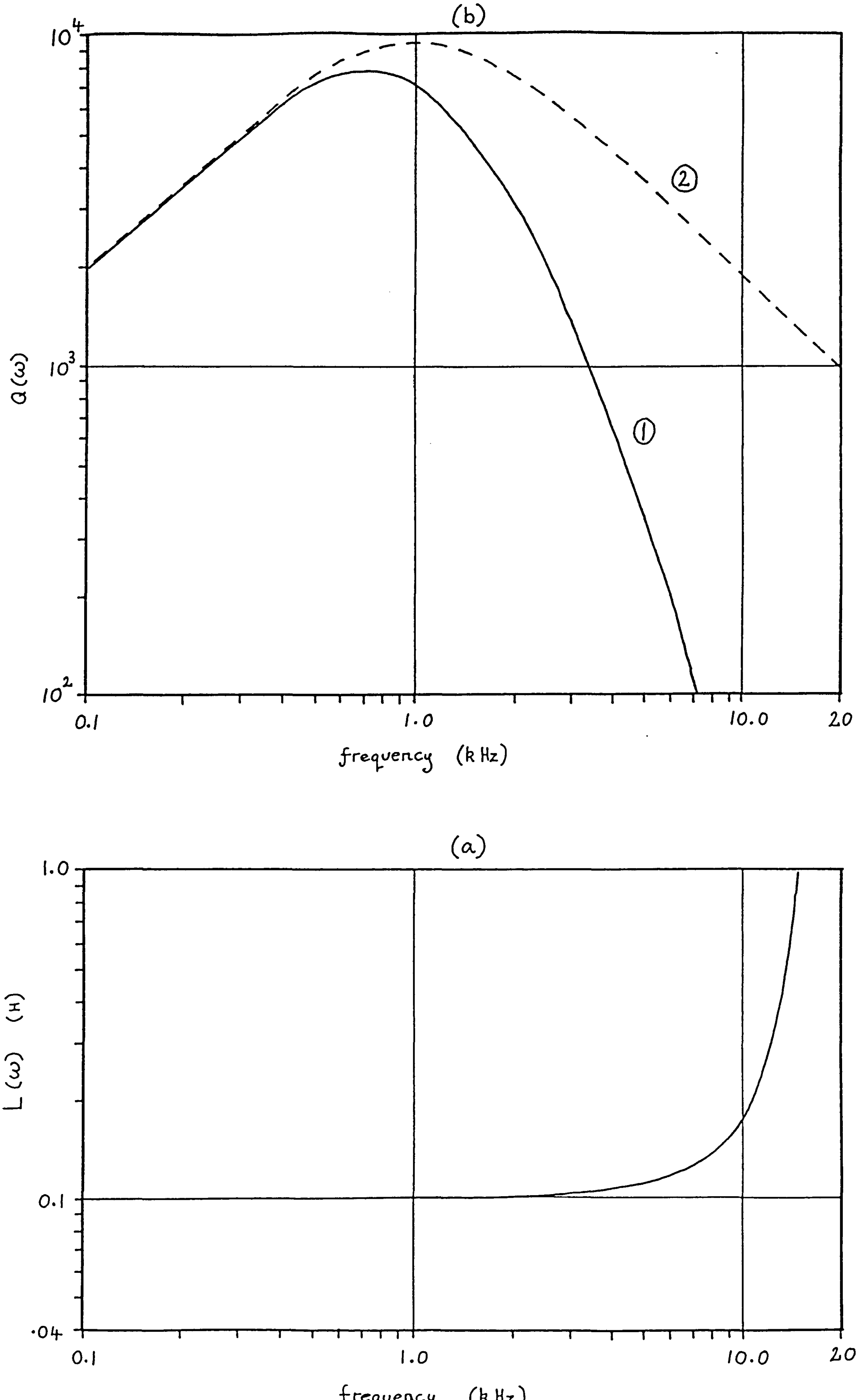

Fig. 4.7 $L(\omega)$ and $Q(\omega)$ behaviour for improved design

component	value
R_1	1.64496 kΩ
R_2	0.909311 "
R_3	2.03328 "
R_4	2.03328 "
R_5	2.03328 "
R_6	1.64496 "
C_0	156.55 nF

Fig. 4.8 Passive component values for obtaining $Q(\omega)_{max}$ at 1.0 kHz

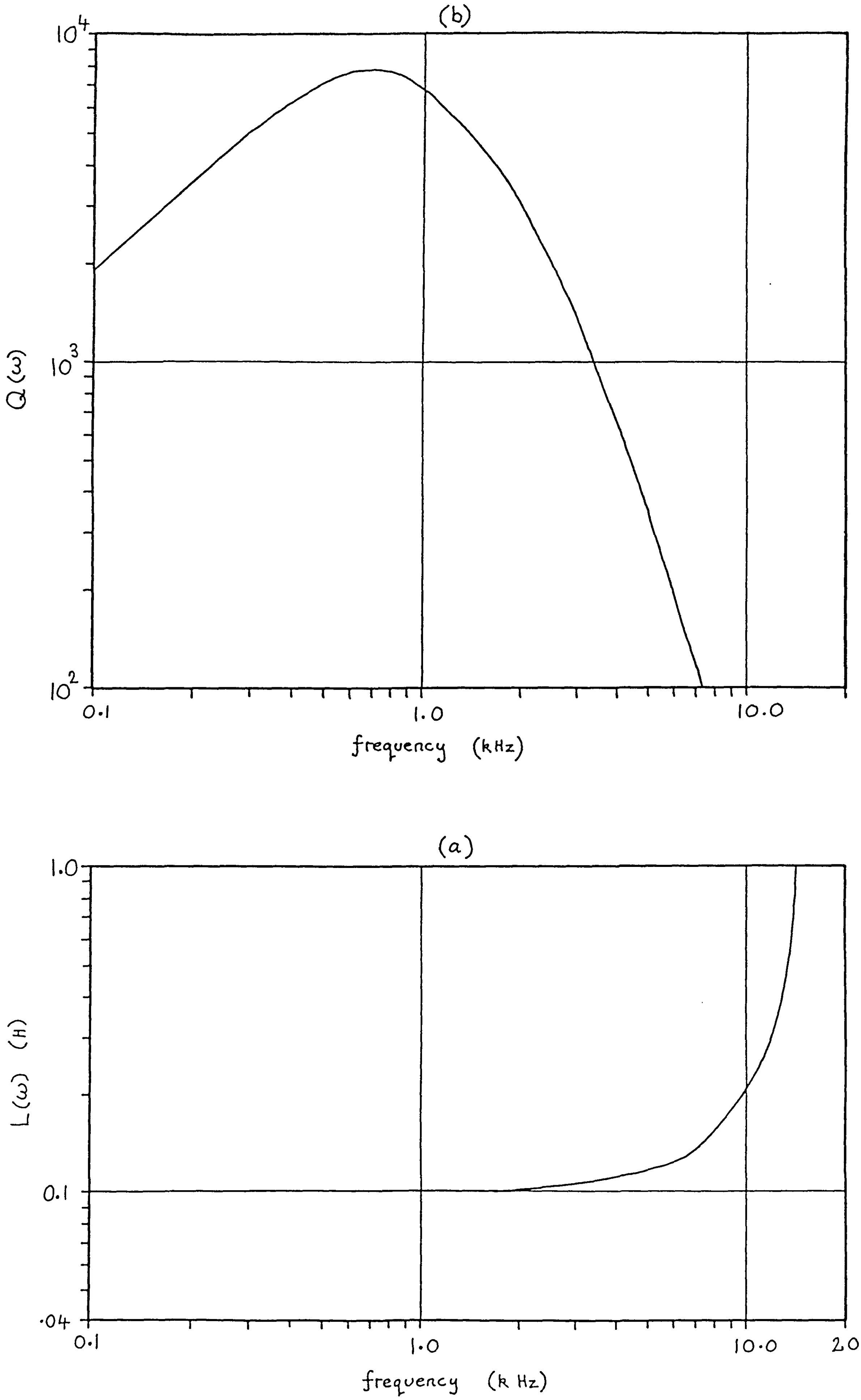

Fig. 4.9 $L(\omega)$ and $Q(\omega)$ behaviour for design having L_N = 100 mH and f_{op} = 1.0 kHz

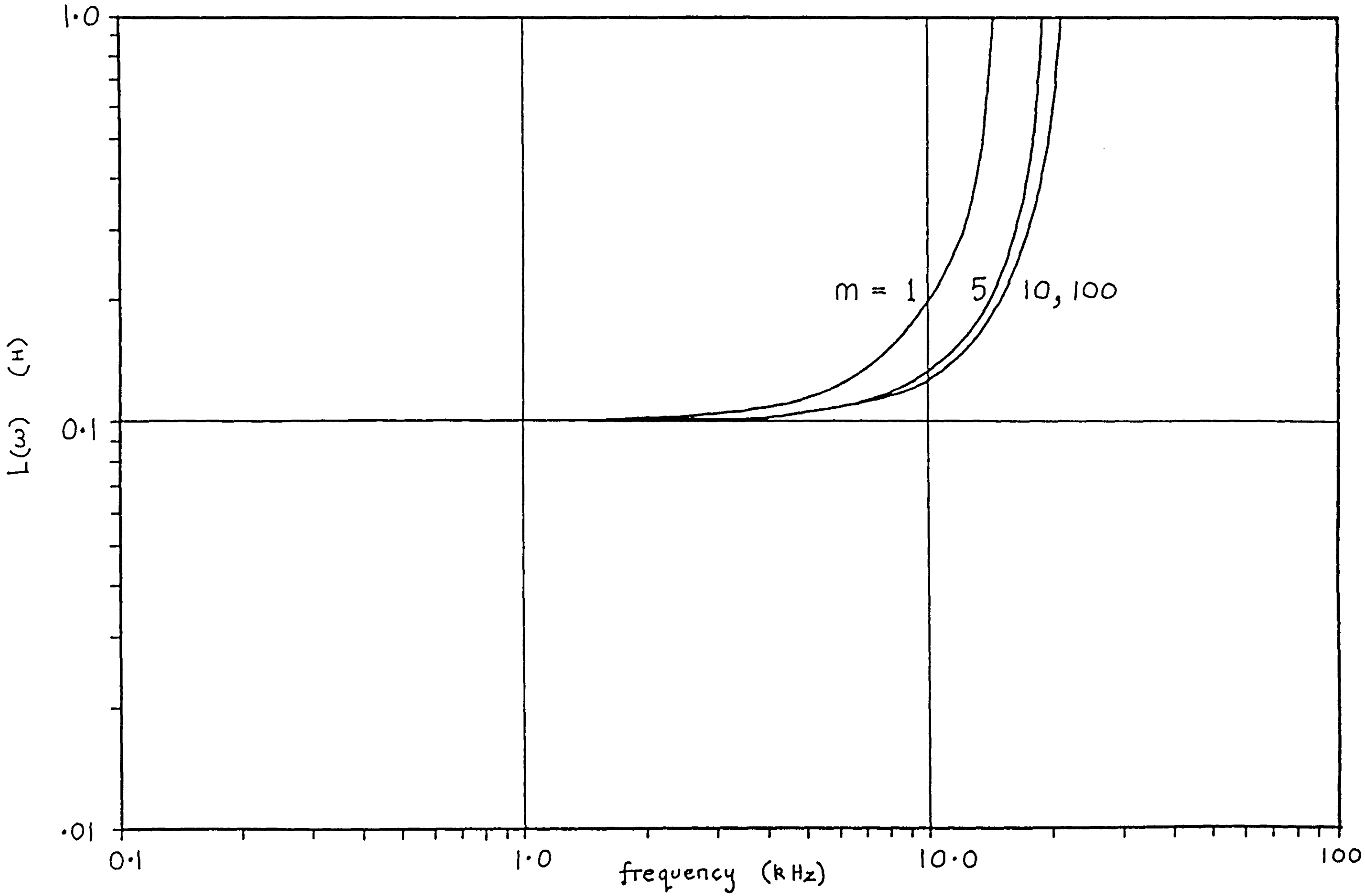

Fig. 4.10 L(ω) behaviour for different values of m

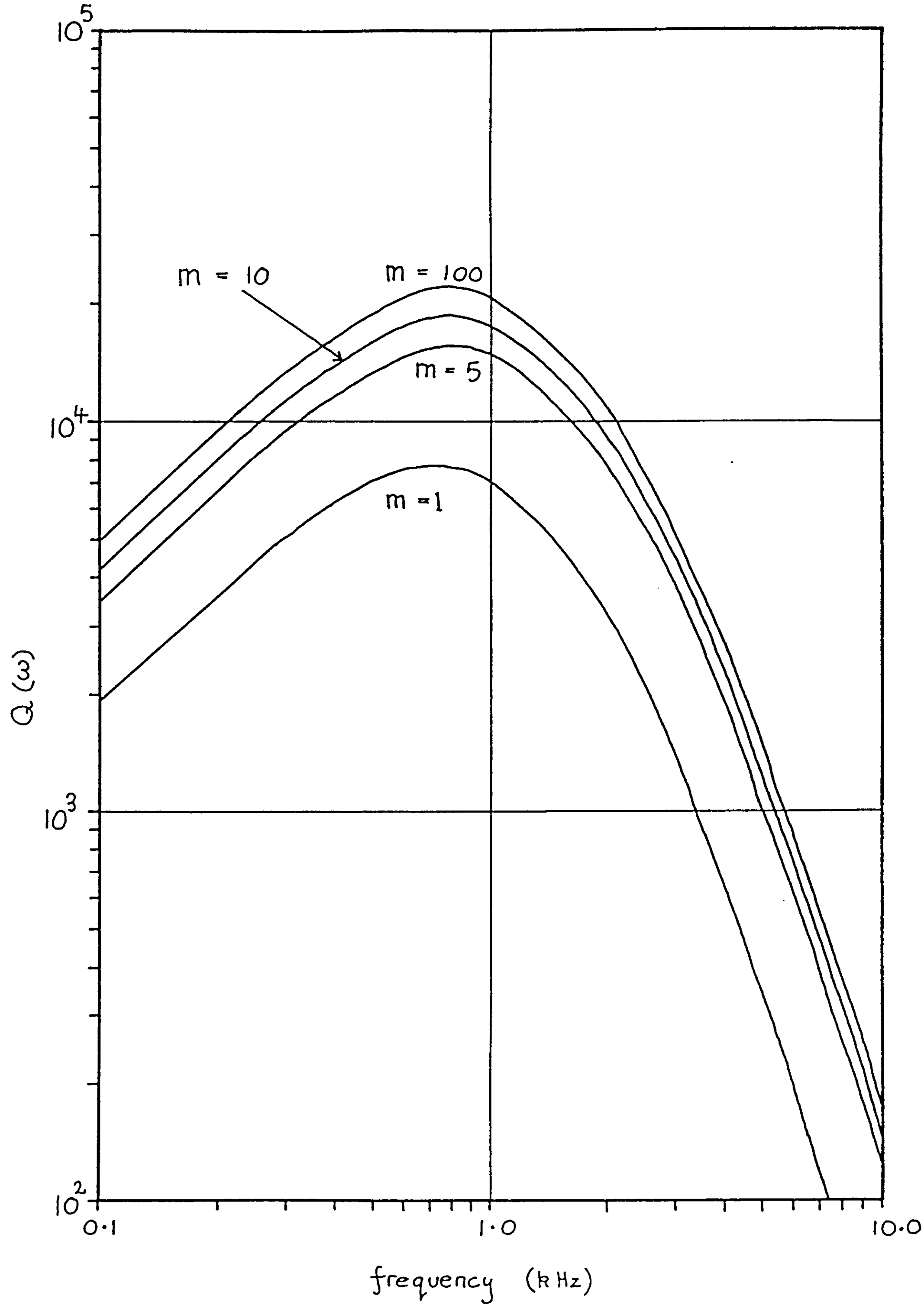

Fig. 4.11 Q(ω) behaviour for different values of m

component	values			
	m = 1	m = 5	m = 10	m = 100
R_1	1·64496 kΩ	1·08743 kΩ	1·01536 kΩ	0·947192 kΩ
R_2	0·909311 "	4·57501 "	9·2657 "	93·7845 "
R_3	2·03328 "	5·77057 "	10·4778 "	95·0327 "
R_4	2·03328 "	1·15411 "	1·04778 "	0·950327 "
R_5	2·03328 "	5·77057 "	10·4778 "	95·0327 "
R_6	1·64496 "	1·08743 "	1·01536 "	0·947192 "
C_0	156·55 nF	55·0506 nF	30·3795 nF	3·366 nF
spread factor	2·236	5·307	10·32	100·3

spread factor $\equiv R_{max}/R_{min}$

for amplifier gain : $\alpha = 10^{-5}$ and $f_T = 10^6$ Hz

L_N = 100 mH

f_{op} = 1·0 kHz

Fig. 4.12 Passive component values for different values for m

component	values		
	$f_{op} = 100$ Hz	$f_{op} = 1$ kHz	$f_{op} = 10$ kHz
R_1	0·101536 kΩ	1·01536 kΩ	10·1536 kΩ
R_2	0·925657 "	0·92657 "	92·5657 "
R_3	1·04778 "	10·4778 "	104·778 "
R_4	1·04778 "	1·04778 "	10·4778 "
R_5	1·04778 "	10·4778 "	104·778 "
R_6	0·101536 "	1·01536 "	10·1536 "
C_0	3·03795 μF	30·3795 nF	303·795 pF

$\alpha = 10^{-5}$, $f_T = 10^6$ Hz, $L_N = 100$ mH, $m = 10$

Fig. 4.13 Passive component values for different values for f_{op}

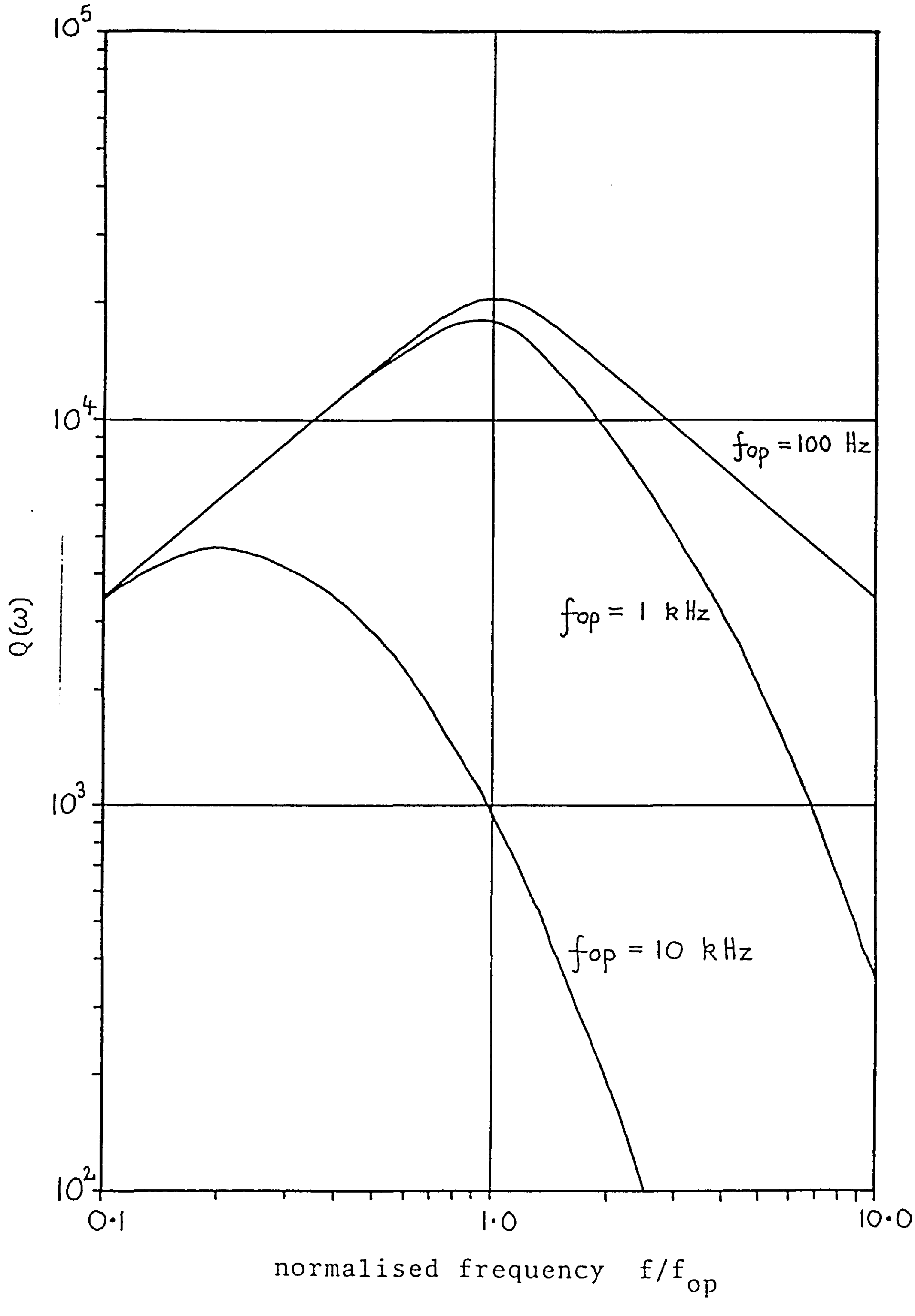

Fig. 4.14 $Q(\omega)$ behaviour for different values for f_{op}

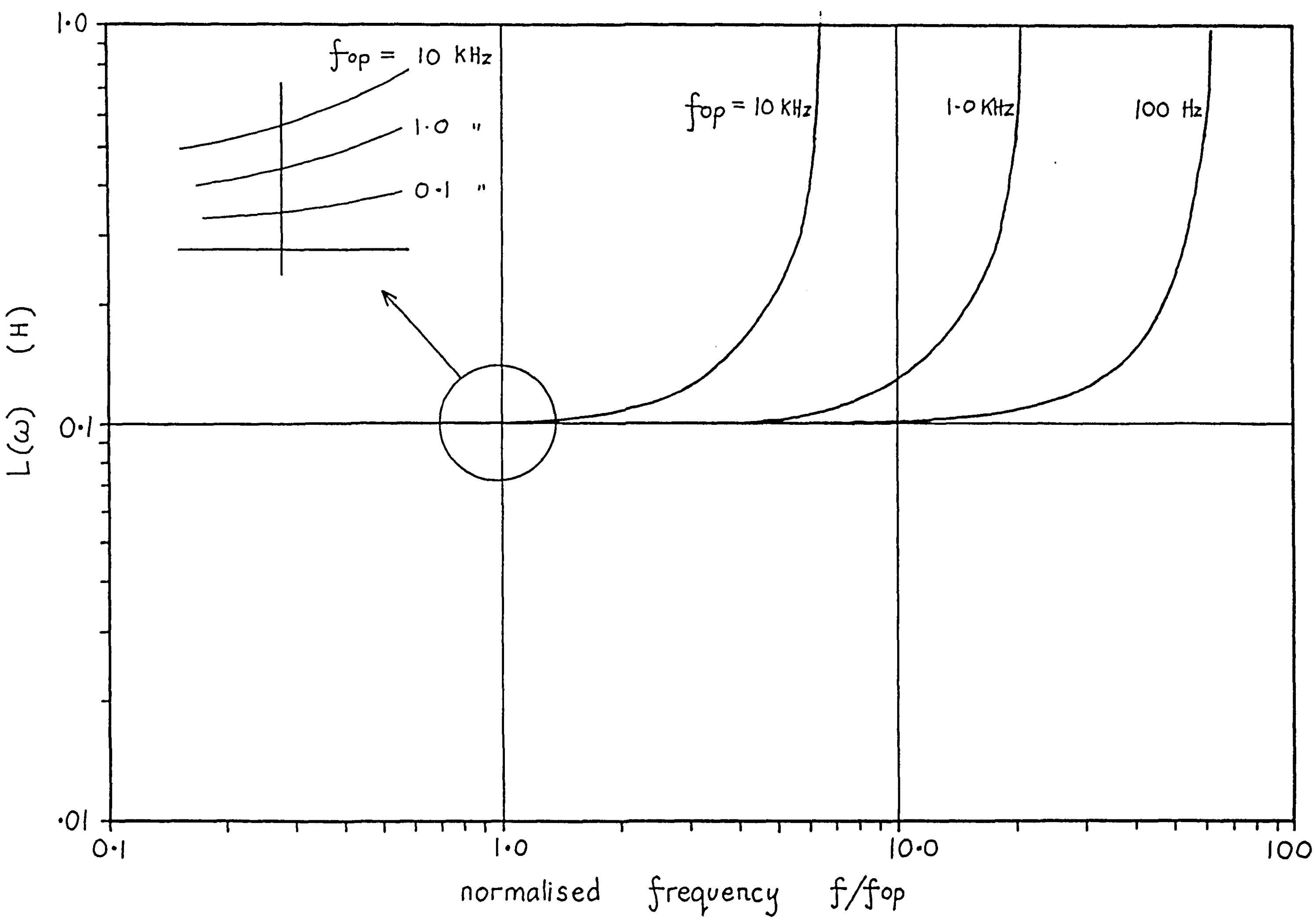

Fig. 4.15 L(ω) behaviour for different values for f_{op}

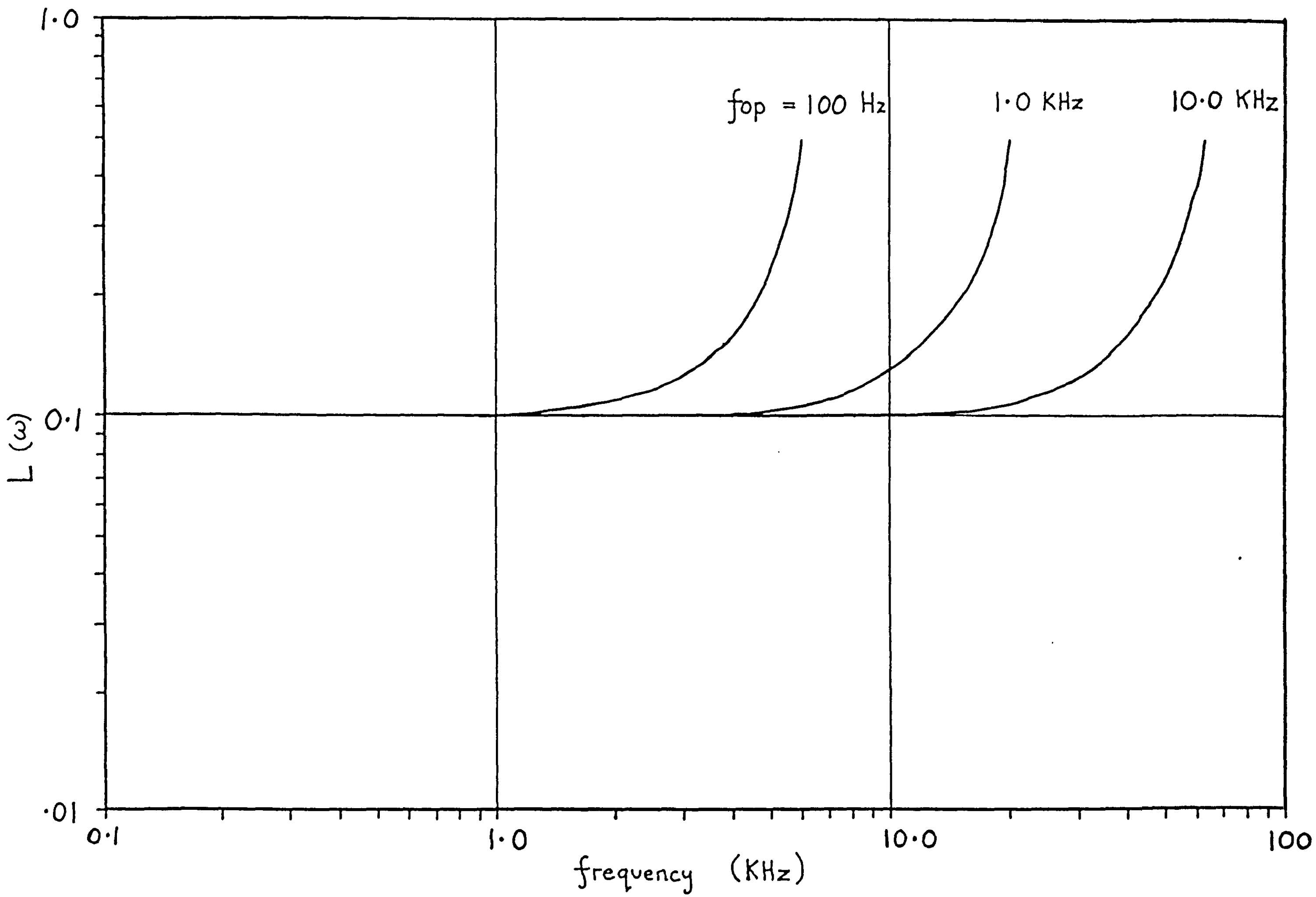

Fig. 4.16 L(ω) behaviour for different values for f_{op}

component	change in comp. value	change in $L(\omega)$ at 1.0 KHz
R_1	± 1.0 %	± 0.77 %
R_2	"	± 1.40 "
R_3	"	∓ 0.39 "
R_4	"	∓ 0.13 "
R_5	"	∓ 0.39 "
R_6	"	± 0.77 "
C_0	"	± 1.01 "

Fig. 4.17 Changes in $L(\omega)$ due to 1 % changes in the passive component values

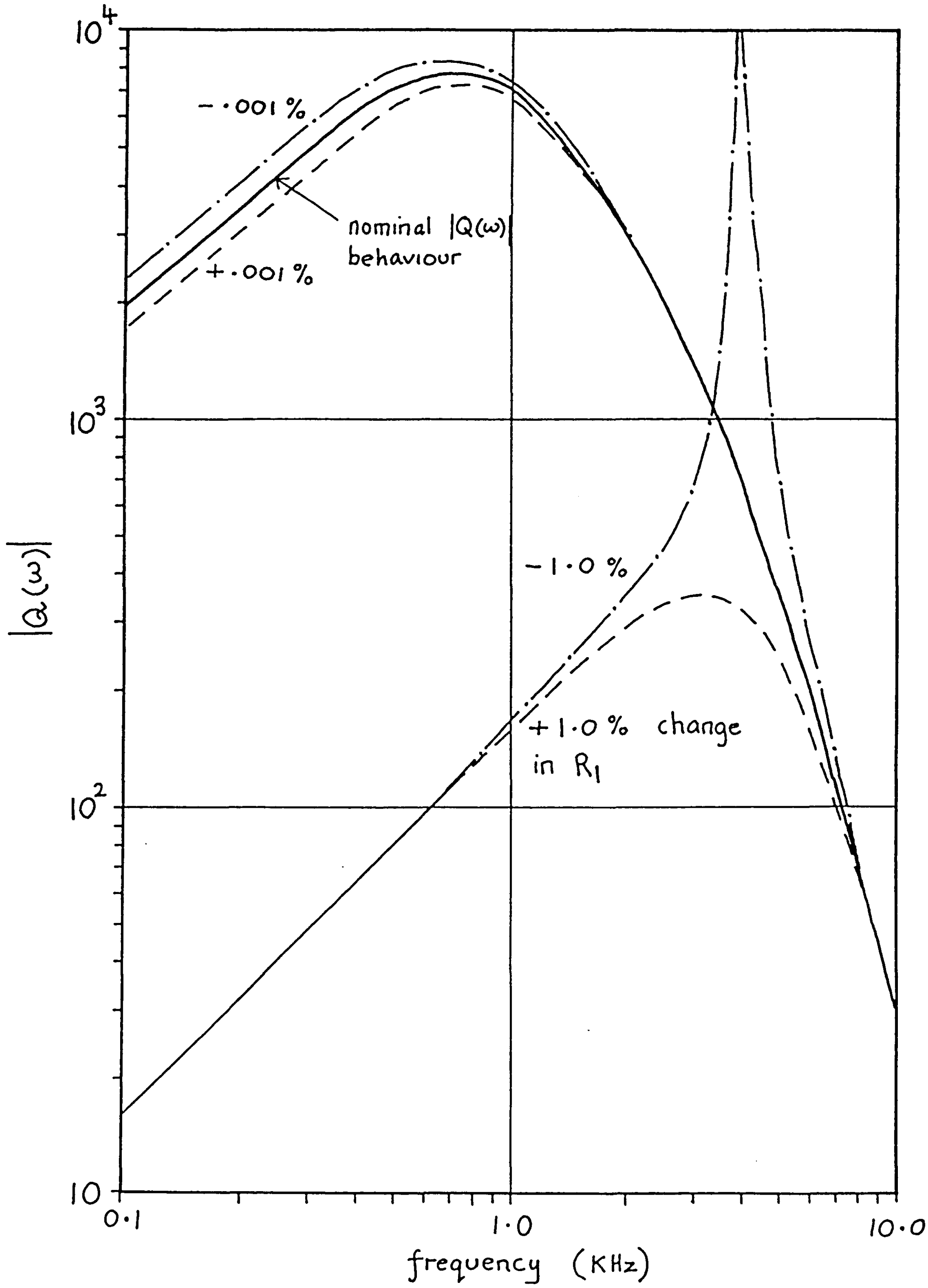

Fig. 4.18 (a) Changes in $|Q(\omega)|$ due to changes in R_1

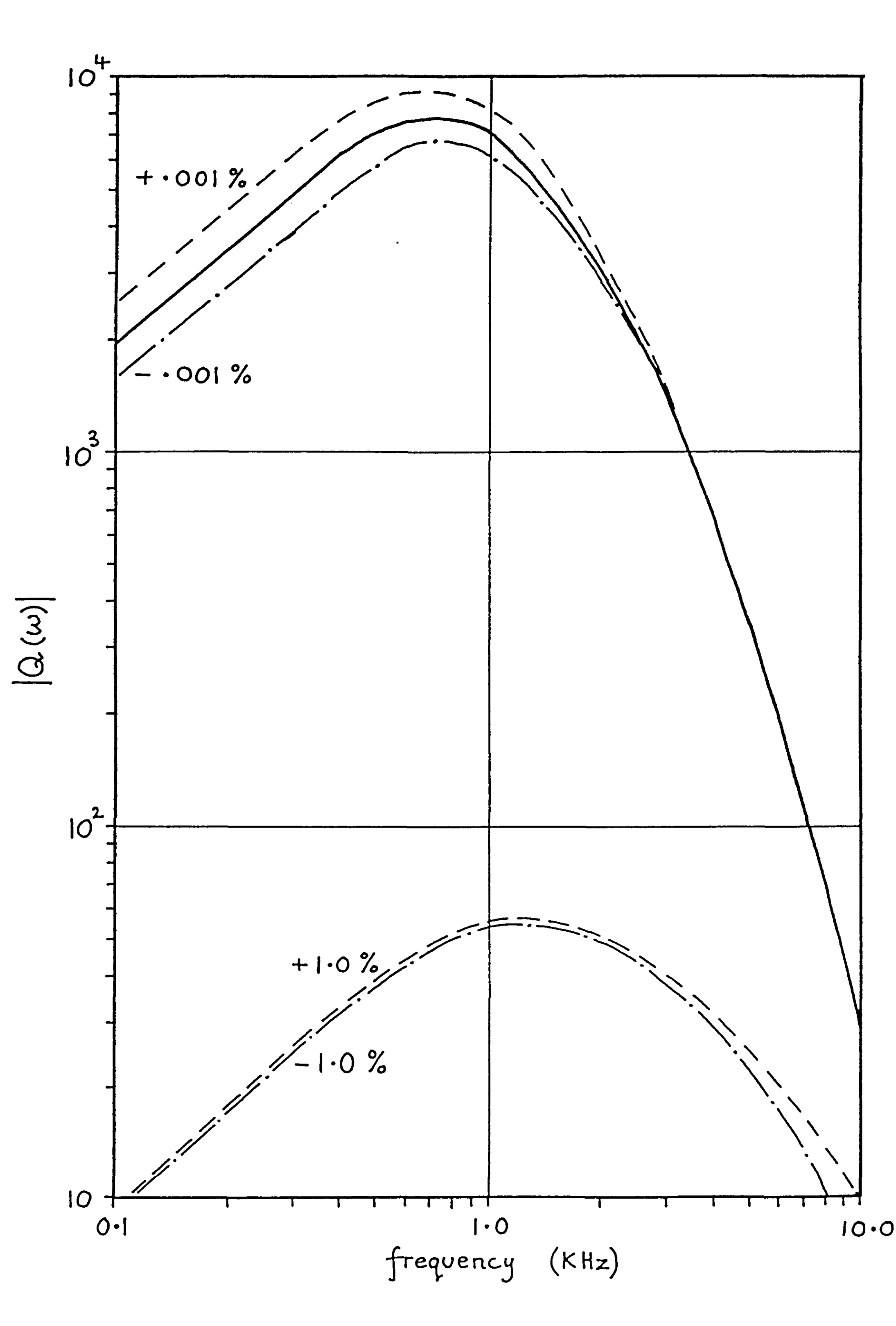

Fig. 4.18 (b) Changes in $|Q(\omega)|$ due to changes in R_2

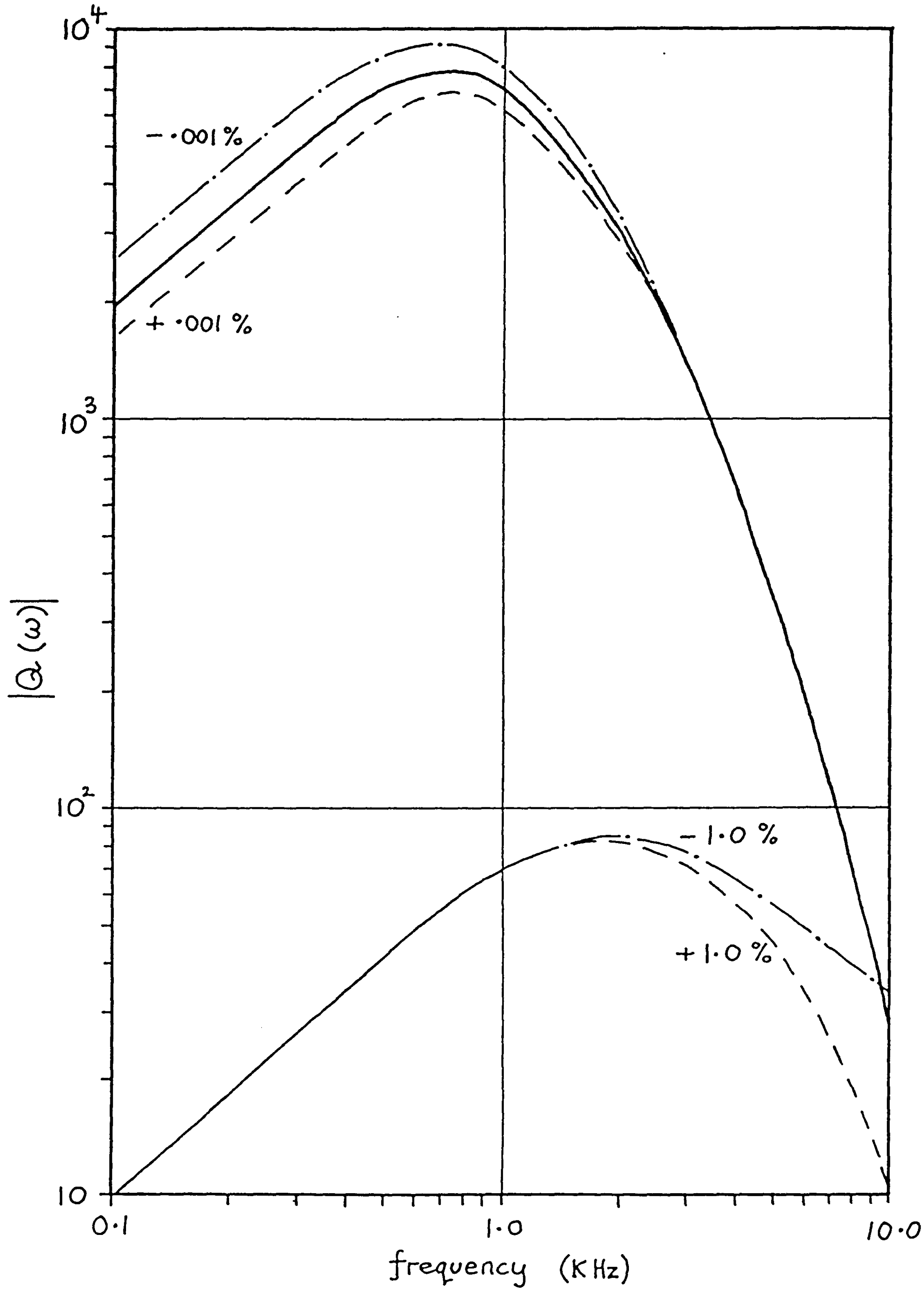

Fig. 4.18 (c) Changes in $|Q(\omega)|$ due to changes in R_3.

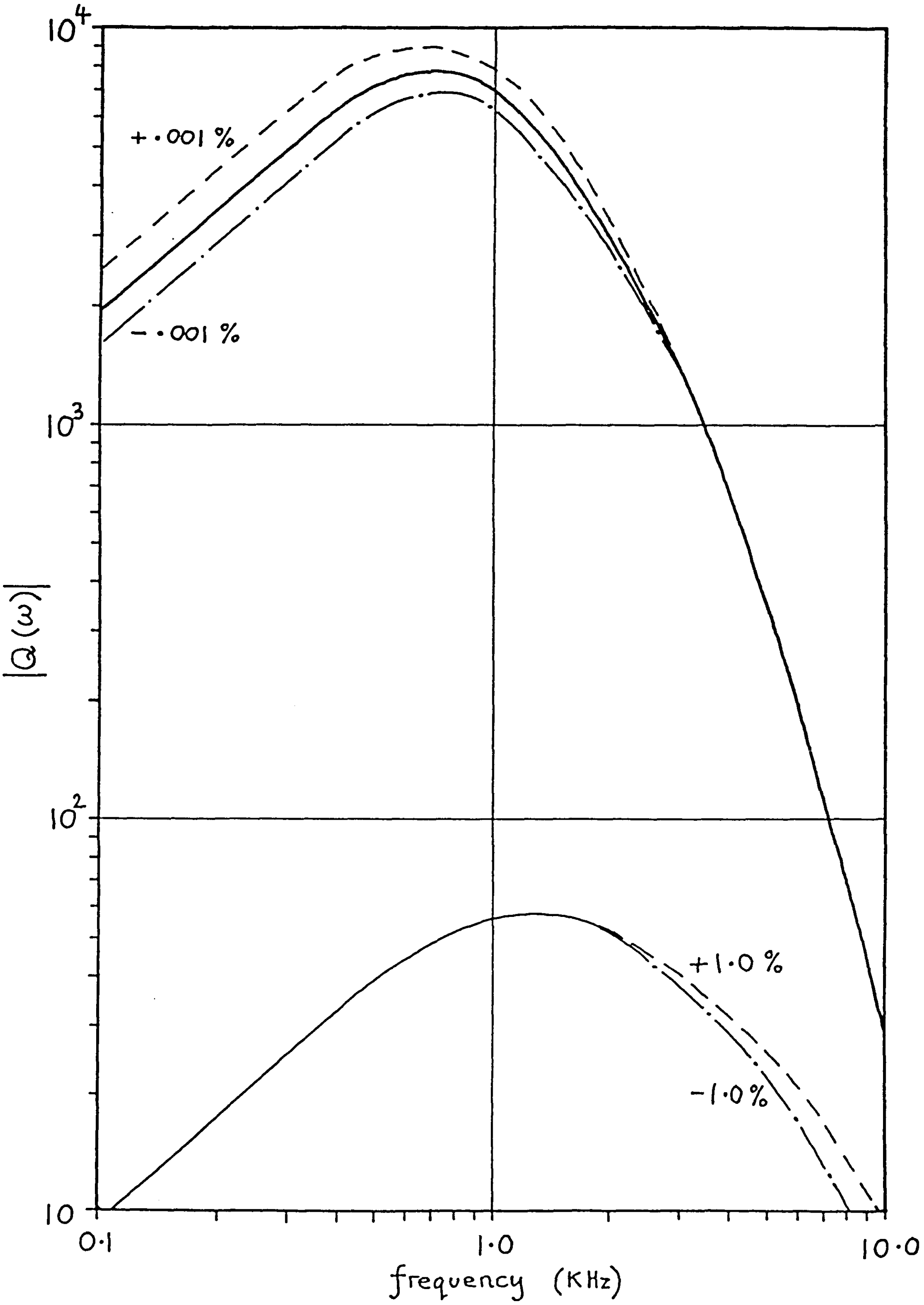

Fig. 4.18 (d) Changes in $|Q(\omega)|$ due to changes in R_4

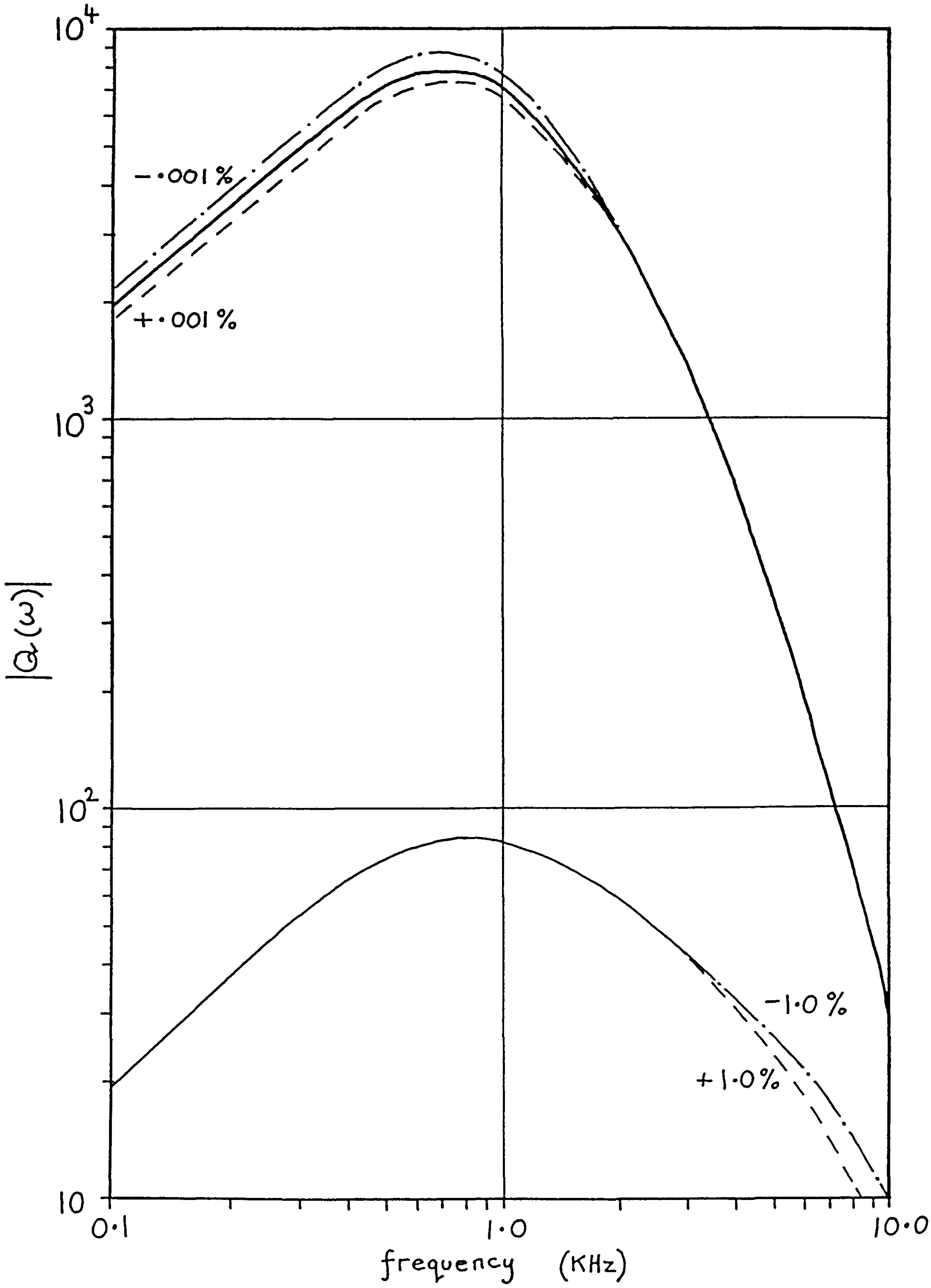

Fig. 4.18 (e) Changes in $|Q(\omega)|$ due to changes in R_5

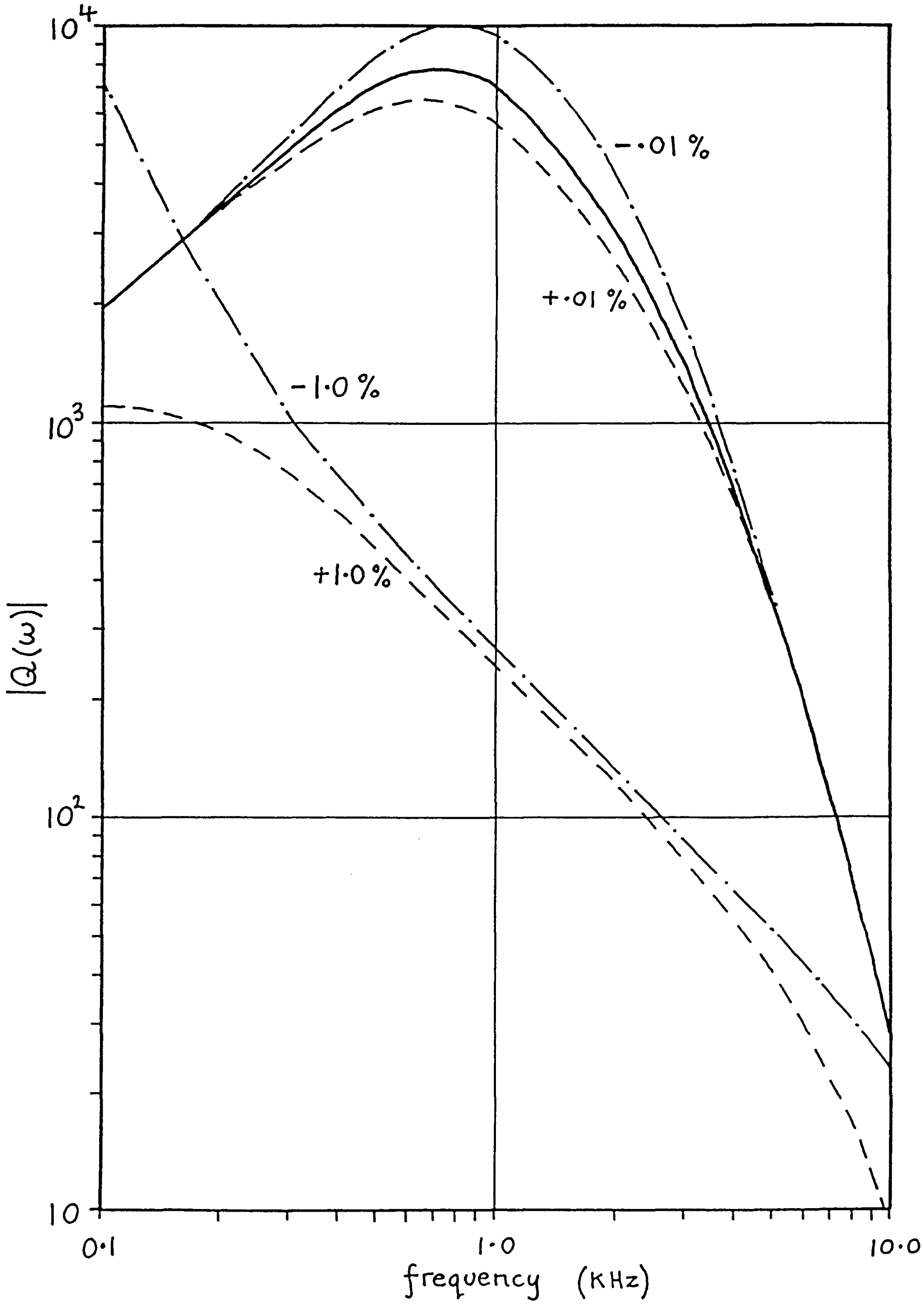

Fig. 4.18 (f) Changes in $|Q(\omega)|$ due to changes in R_6

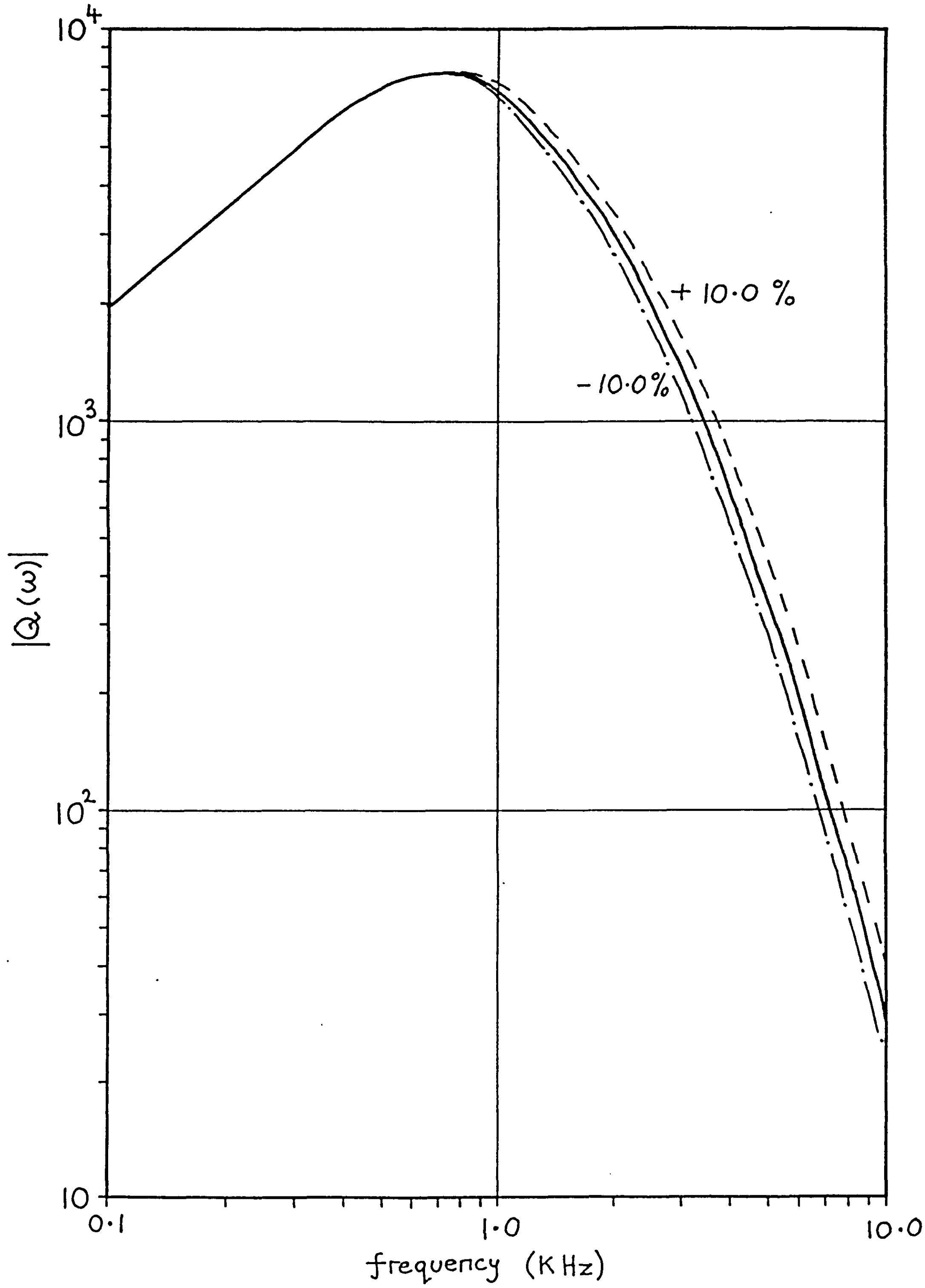

Fig. 4.18 (g) Changes in $|Q(\omega)|$ due to changes in C_0

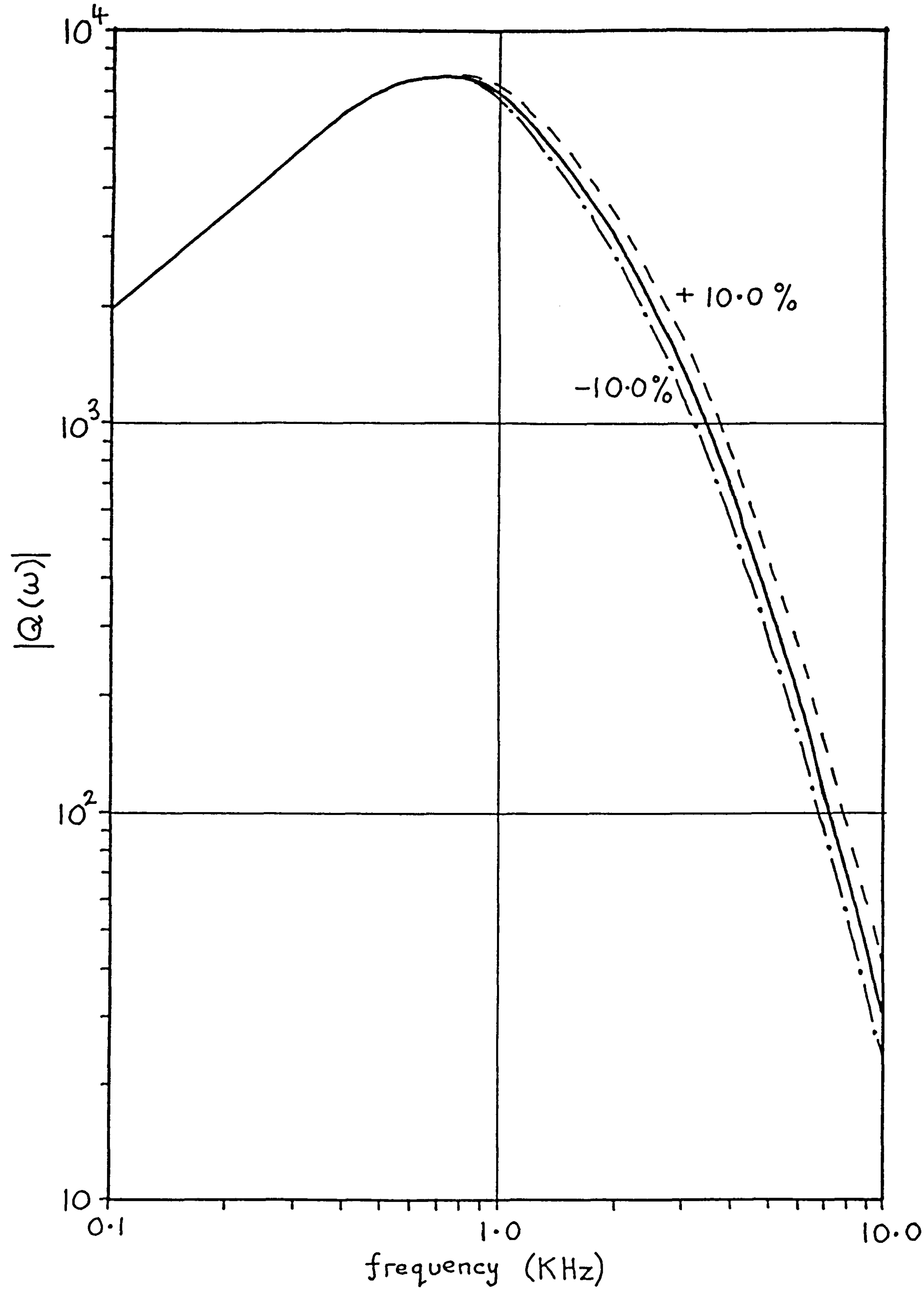

Fig. 4.18 (h) Changes in $|Q(\omega)|$ due to changes in f_T

component	value
R_1	0·352557 KΩ
R_2	3·17301 "
R_3	3·17301 "
R_4	28·5571 "
R_5	31·7301 "
R_6	0·317301 "
C_0	9·933 nF

Table (a) - values for the O/W S.I. circuit

component	value
R_1	628·319 Ω
R_2	628·319 "
R_3	628·319 "
R_4	628·319 "
C_0	0·2533 μF

Table (b) - values for the two-amplifier S.I. circuit

component	value
R_1	0·947192 KΩ
R_2	93·7845 "
R_3	95·0327 "
R_4	0·950327 "
R_5	95·0327 "
R_6	0·947192 "
C_0	3·366 nF

Table (c) - values for the S.I. circuit B

Fig. 4.19 Passive component values for the S.I. circuits

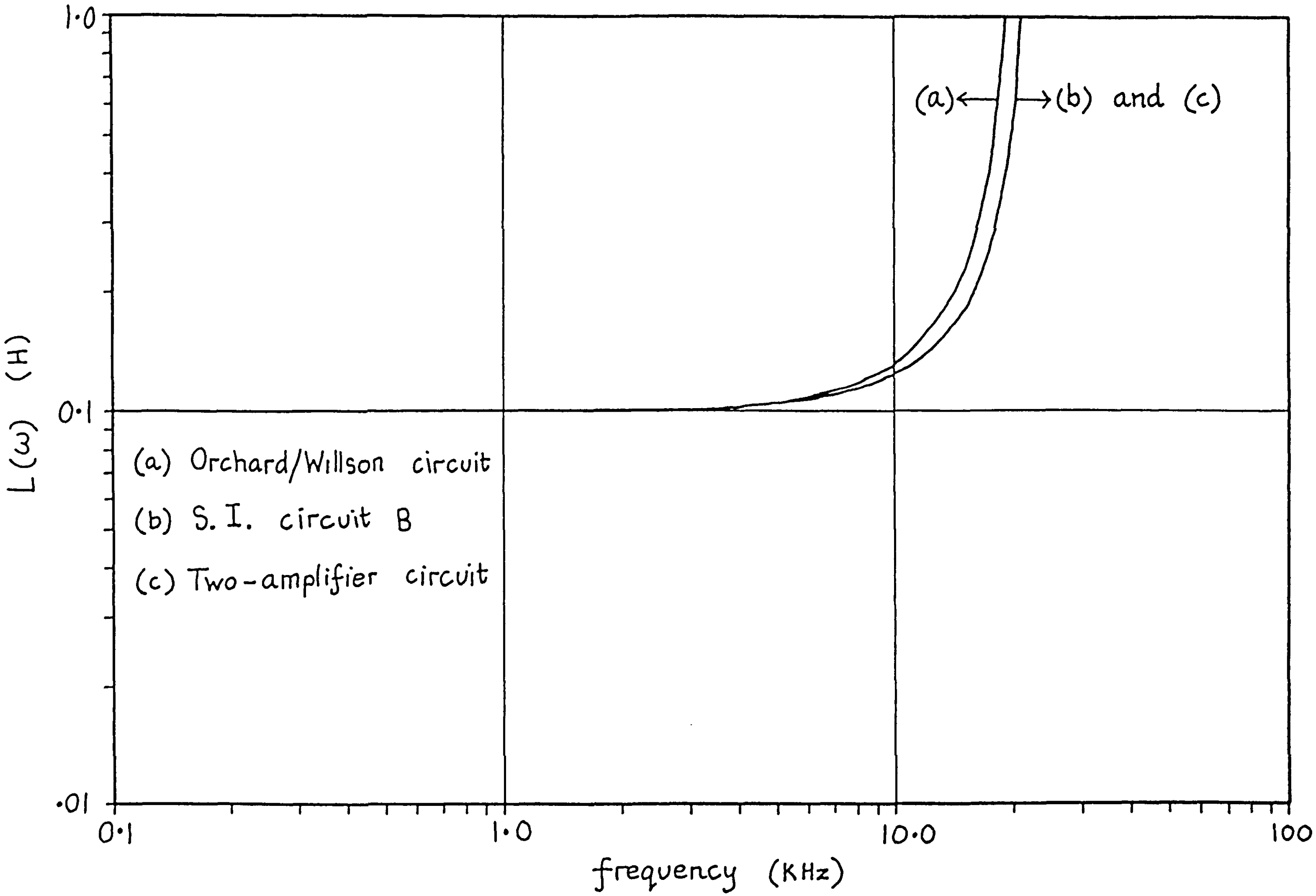

Fig. 4.20 Comparision of L(ω) behaviour

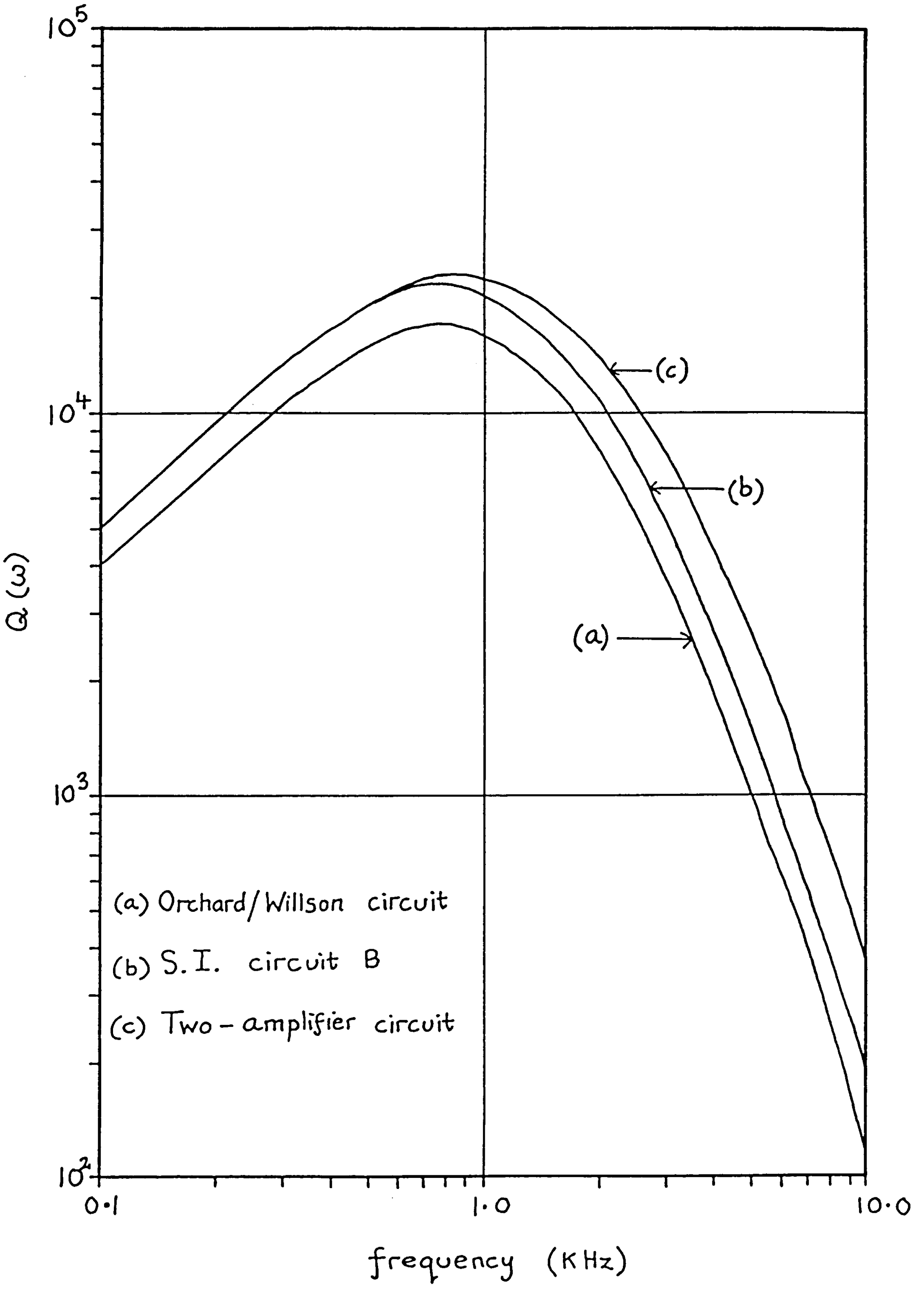

Fig. 4.21 Comparision of Q(ω) behaviour

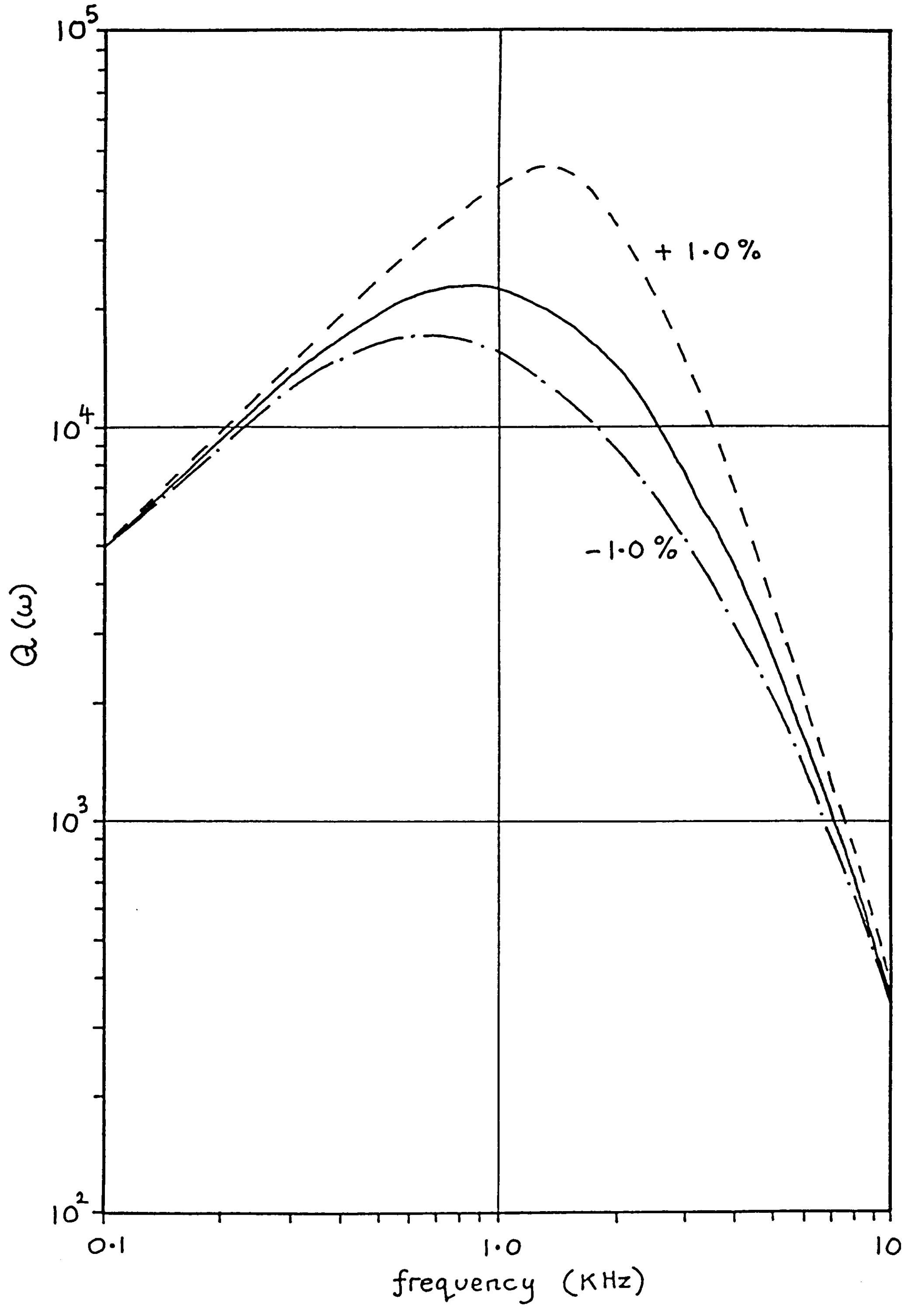

Fig. 4.22 (a) Effects of changes in R_2 on the $Q(\omega)$ behaviour for Antoniou's circuit

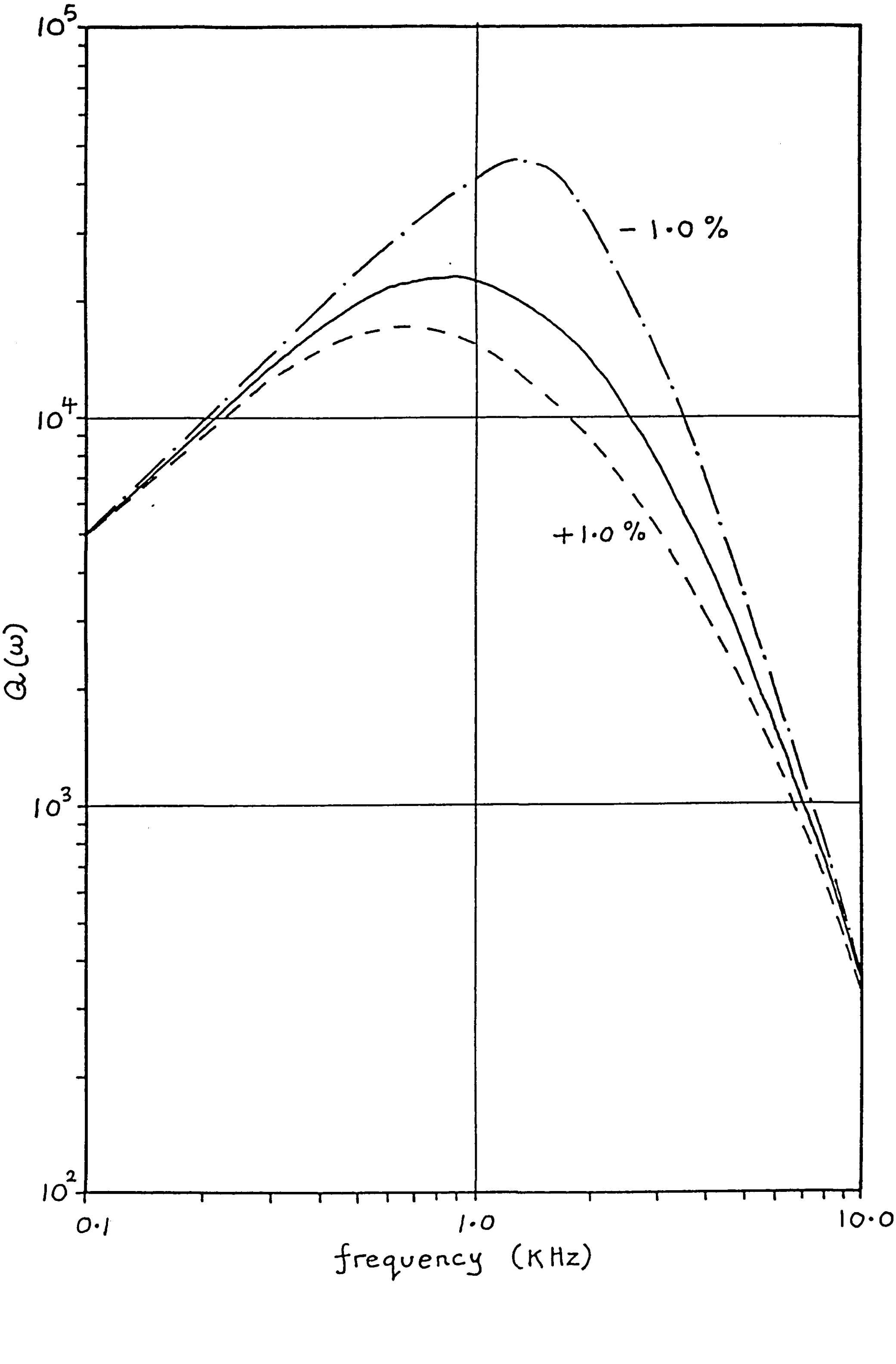

Fig. 4.22 (b) Effects of changes in R_3 on the $Q(\omega)$ behaviour for Antoniou's circuit

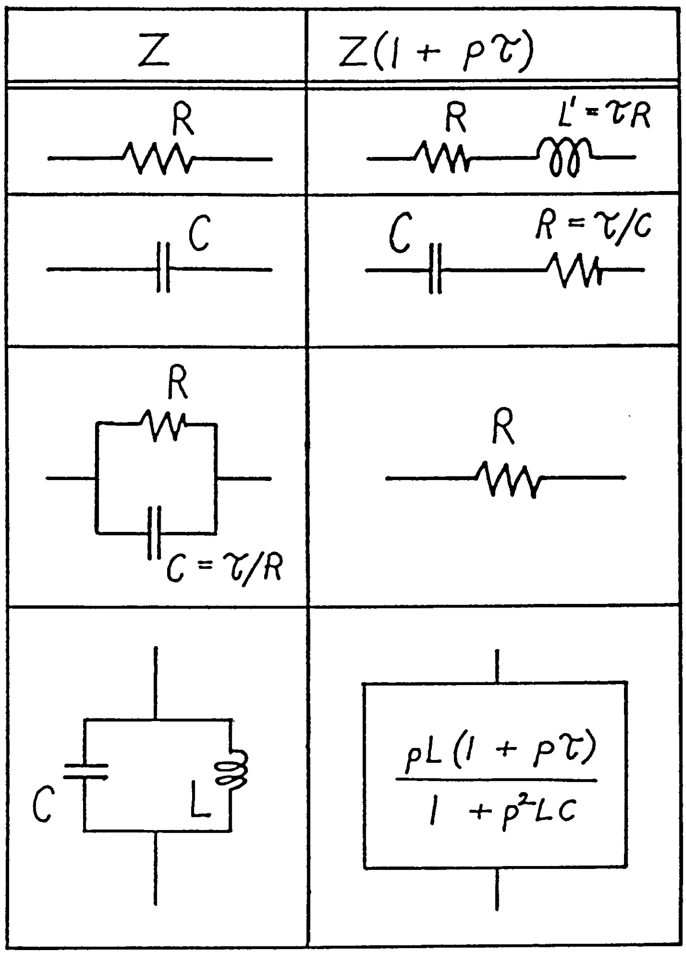

Fig. 5.1 Effects of impedance scaling by (1 + pτ)

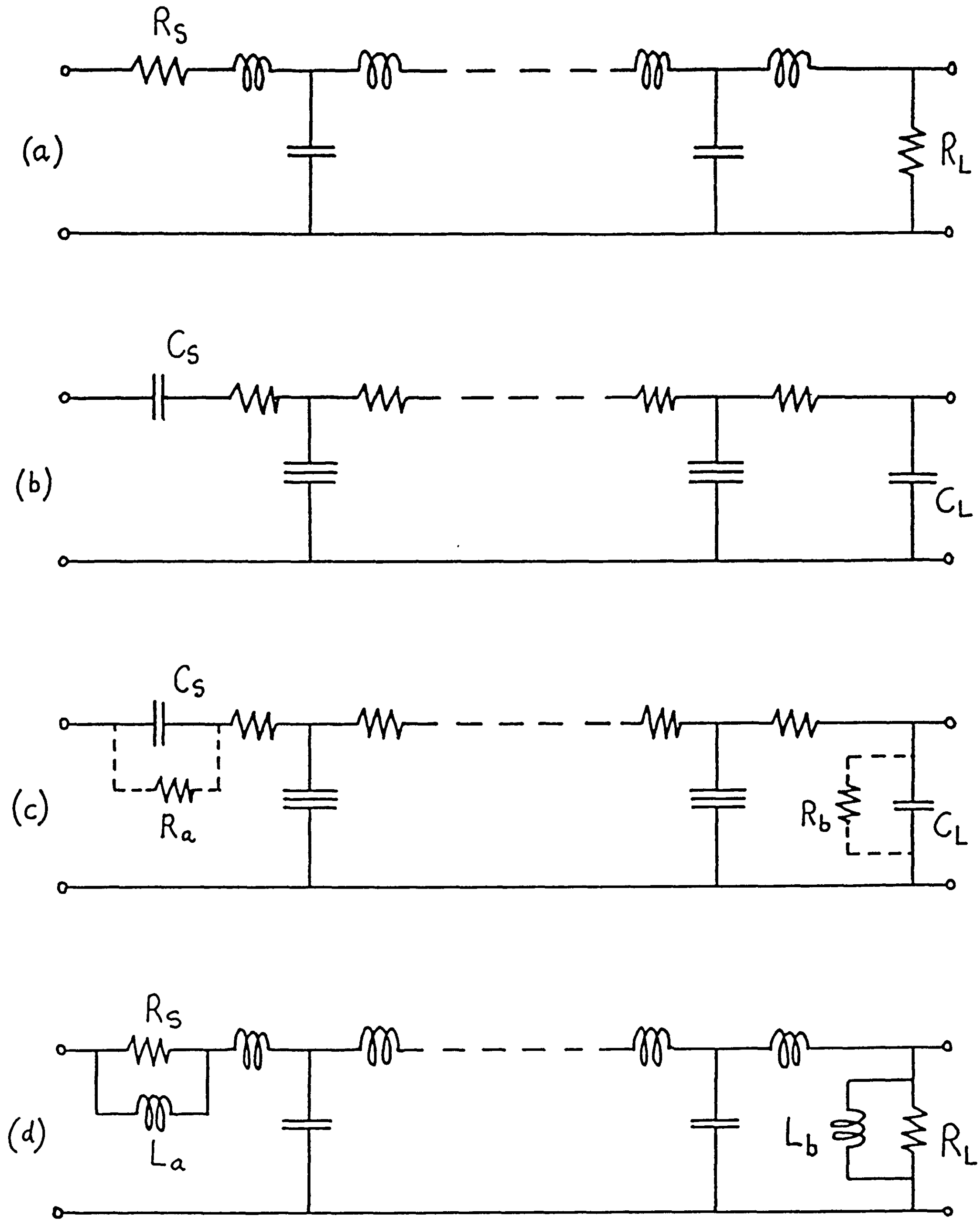

Fig. 5.2 Development of LC lowpass filters with parallel RL terminations

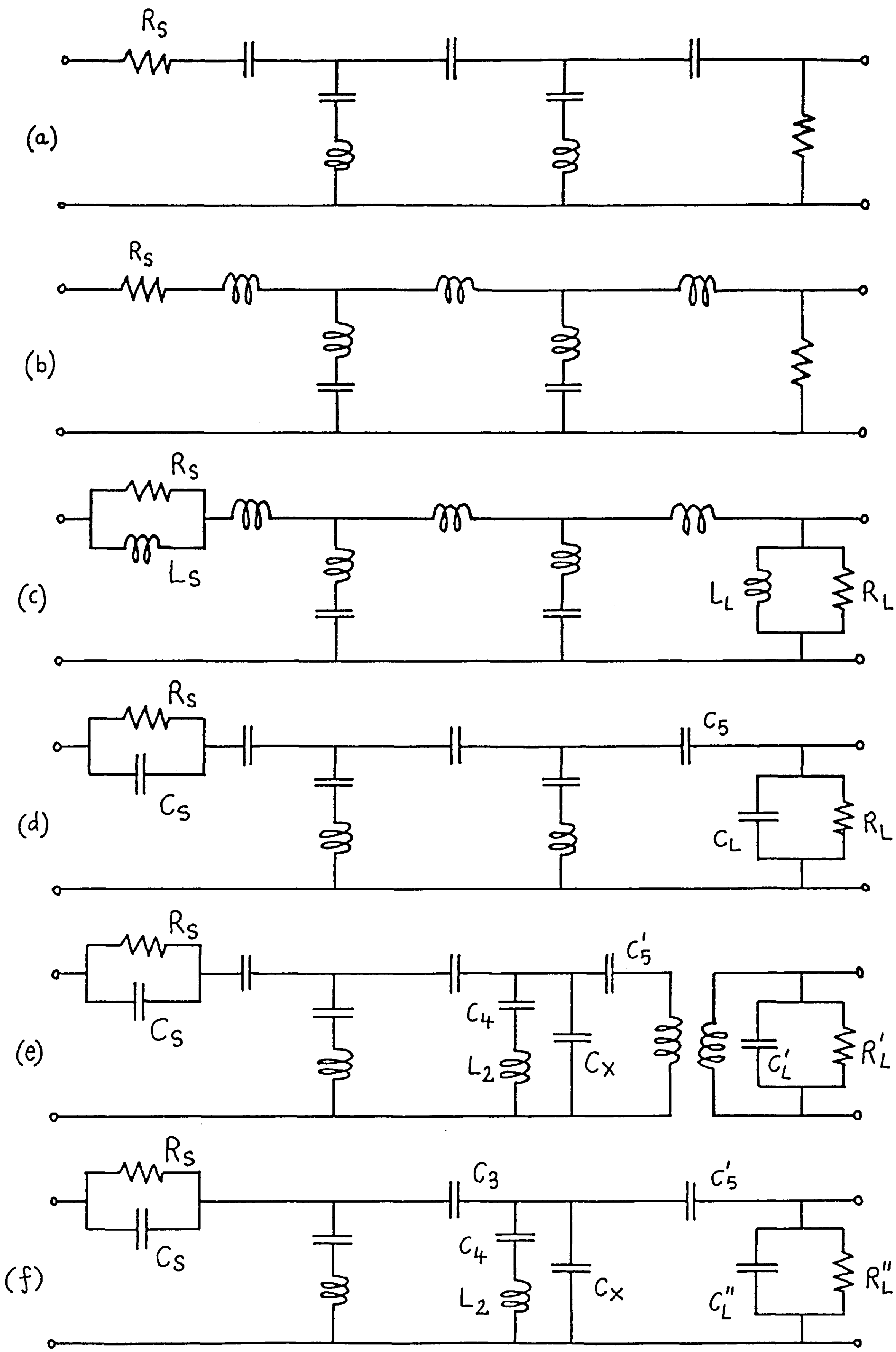

Fig. 5.3 Cauer type highpass filter design using S.B.I.s

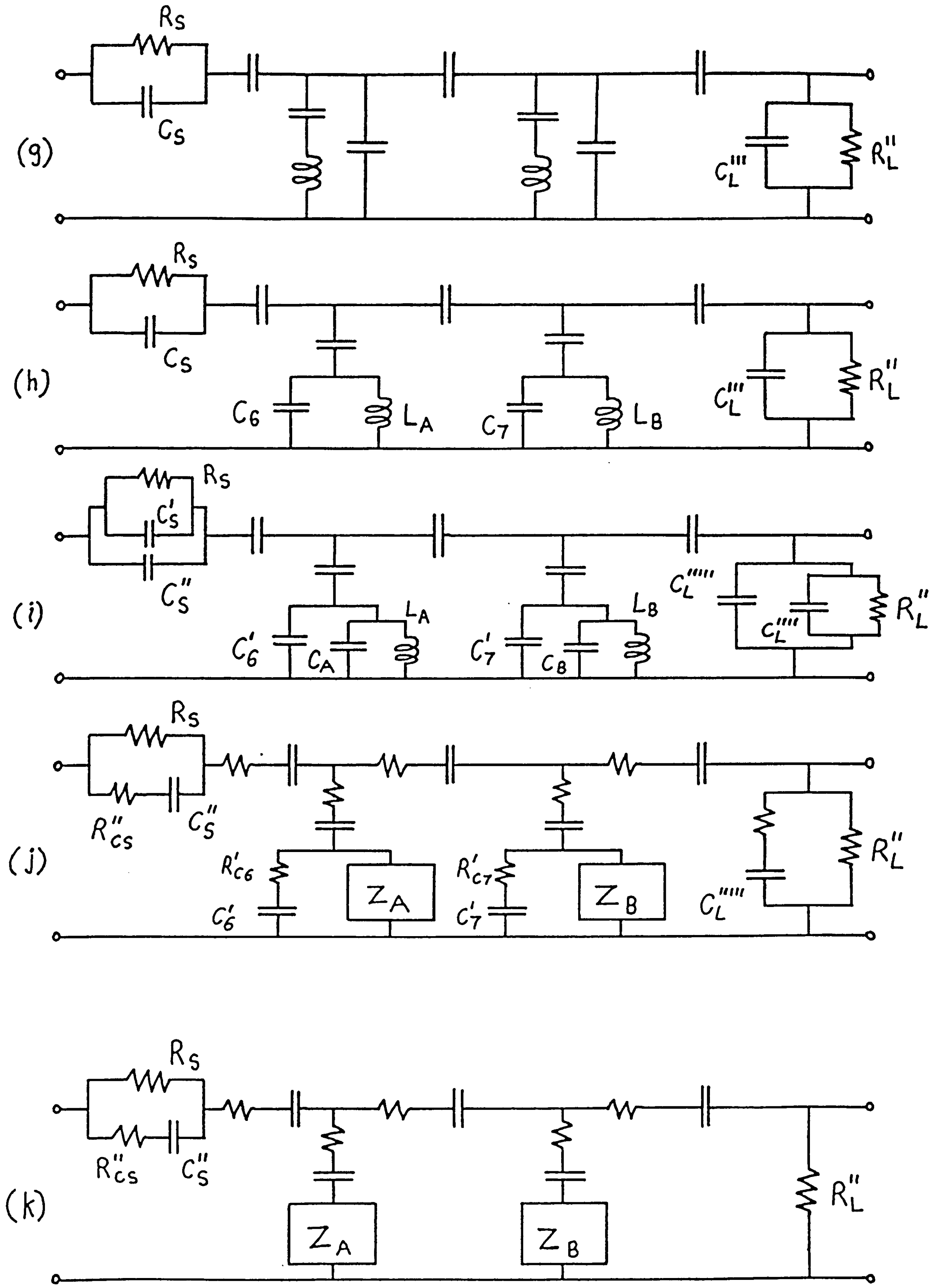

Fig. 5.3 Cauer type highpass filter design using S.B.I.s

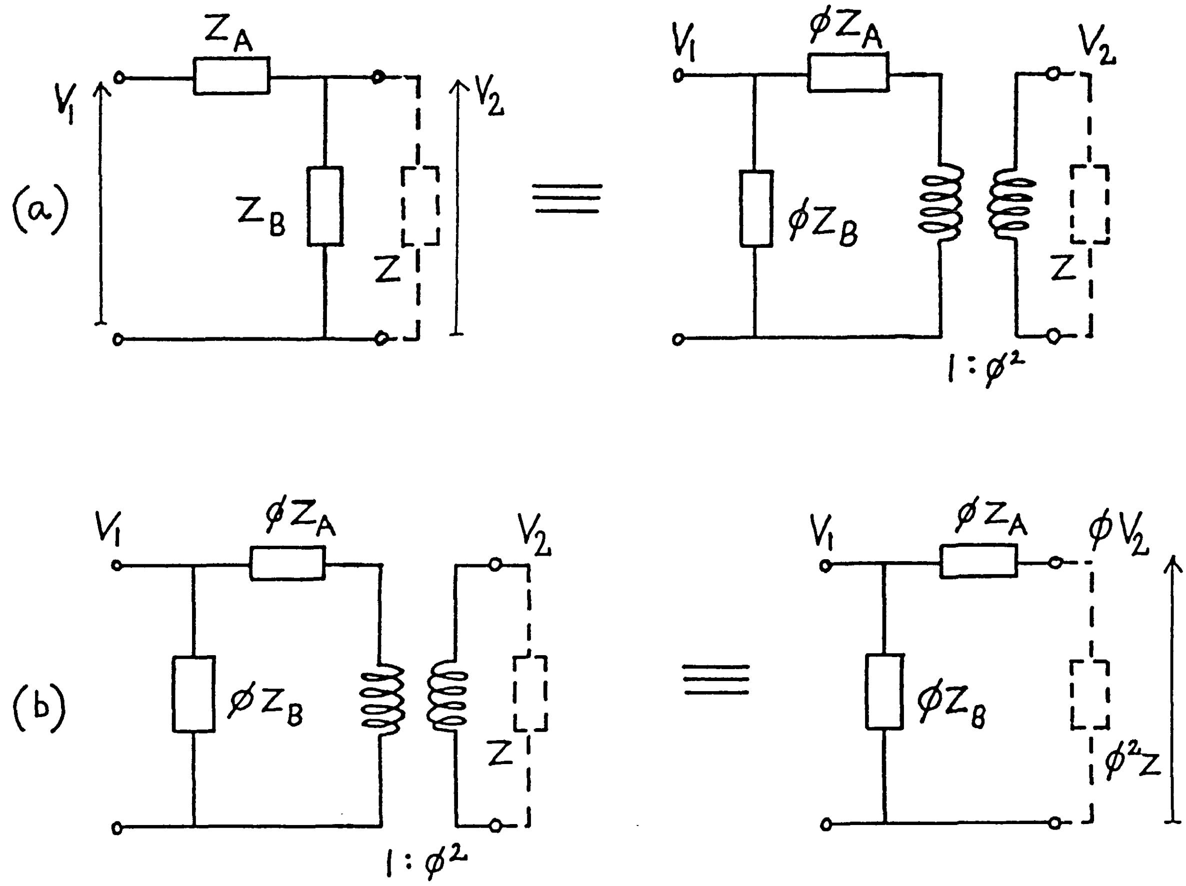

note $\phi = Z_B/(Z_A + Z_B)$

Fig. 5.4 (a) Norton transformation, (b) Elimination of the ideal transformer

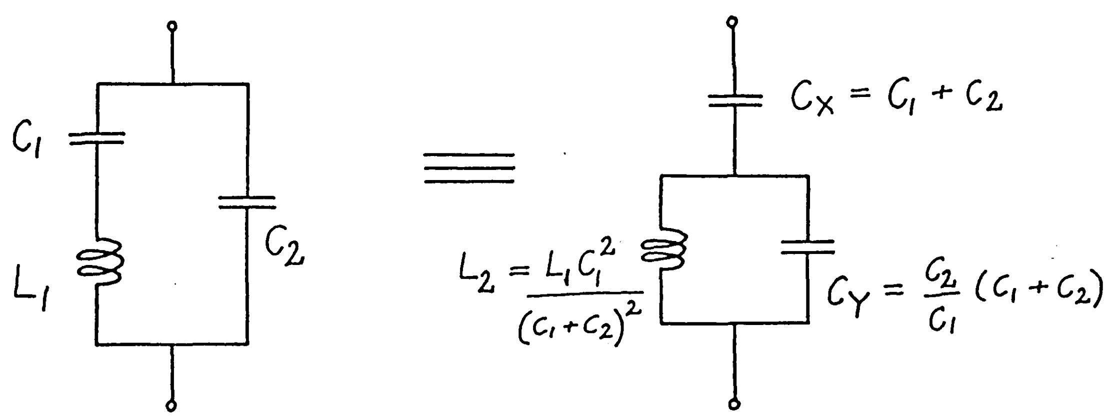

Fig. 5.5 Equivalence transformation

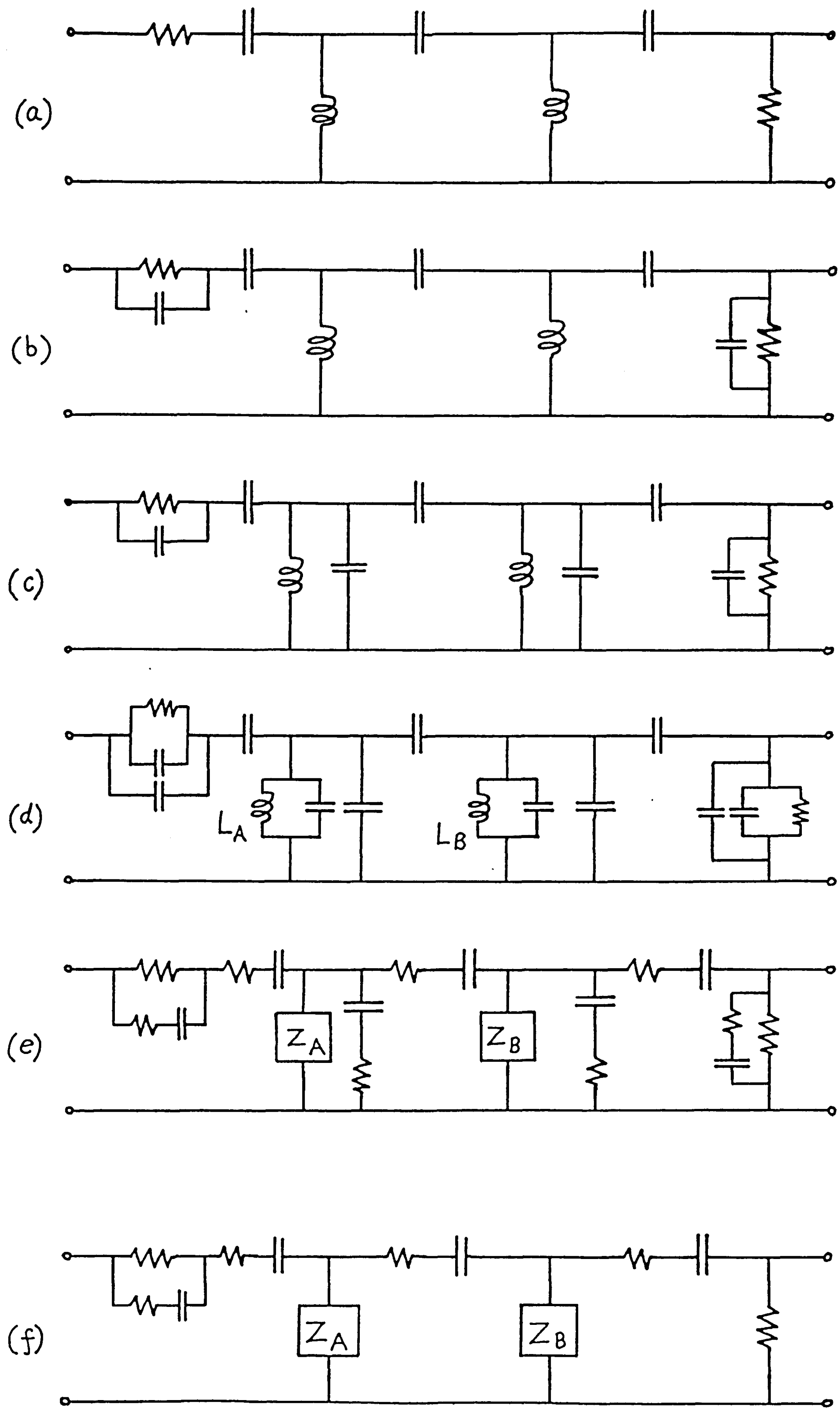

Fig. 5.6 Polynomial highpass filter design using S.B.I.s

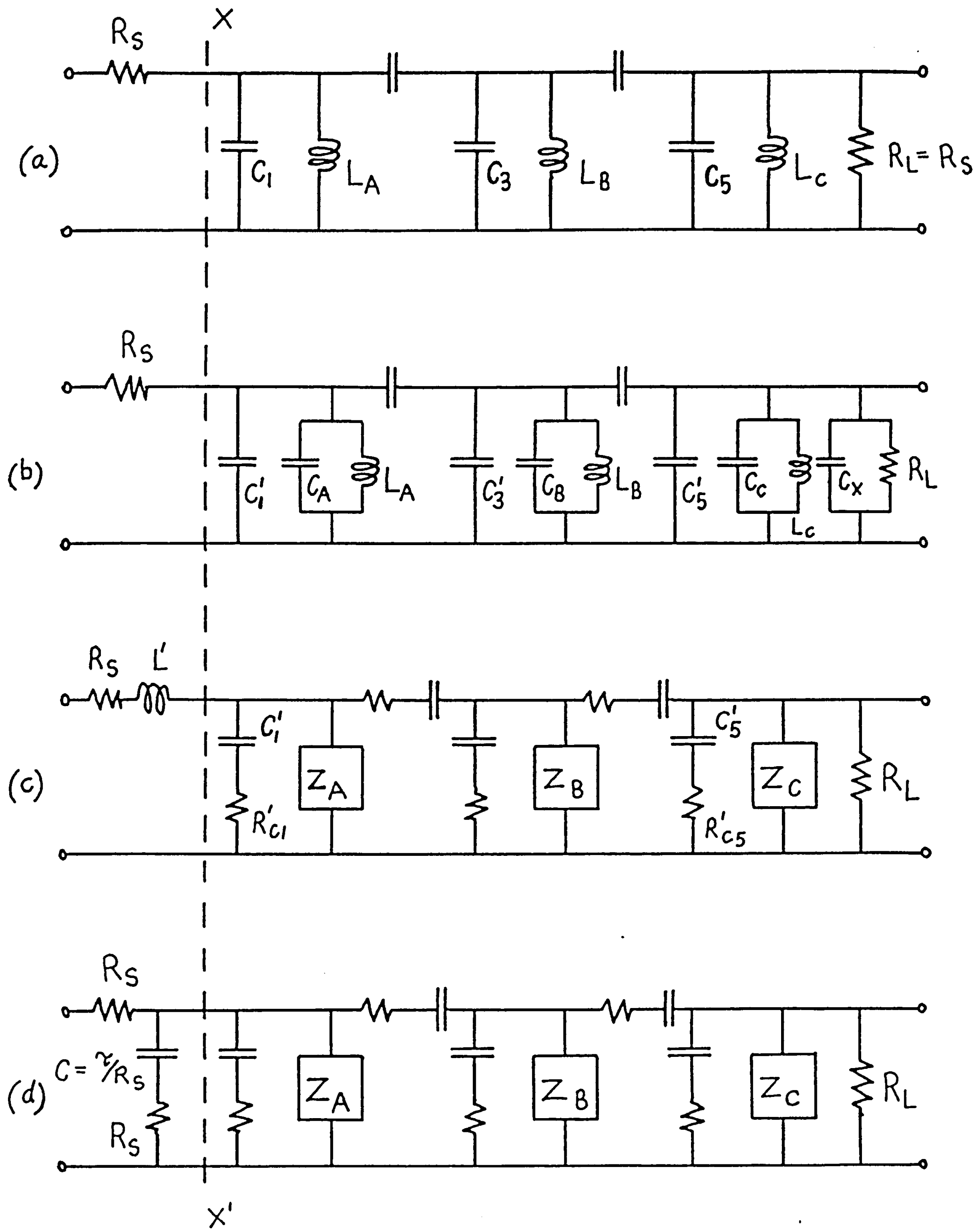

Fig. 5.7 Polynomial bandpass filter design using S.B.I.s

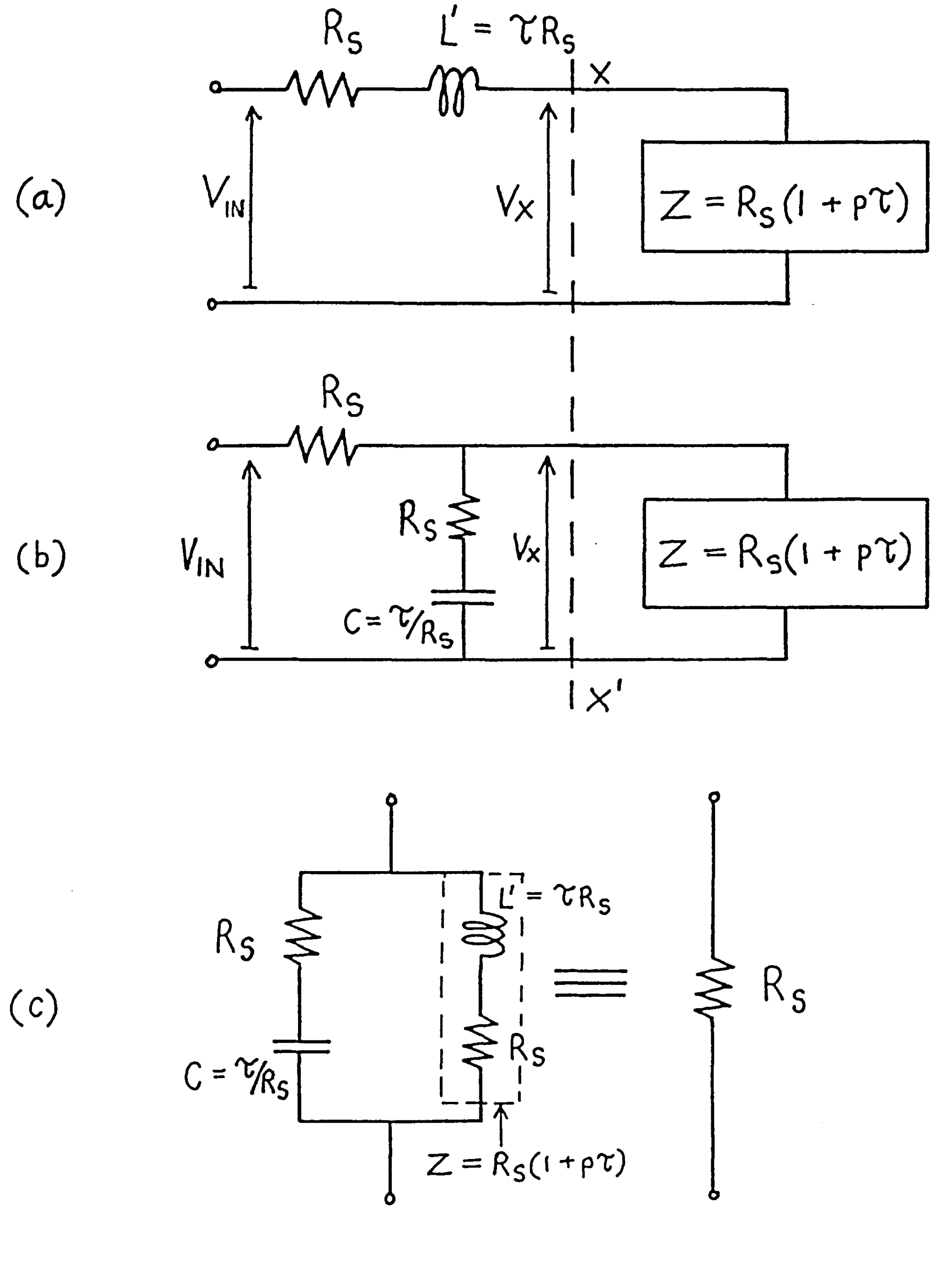

Fig. 5.8 Elimination of unwanted inductor

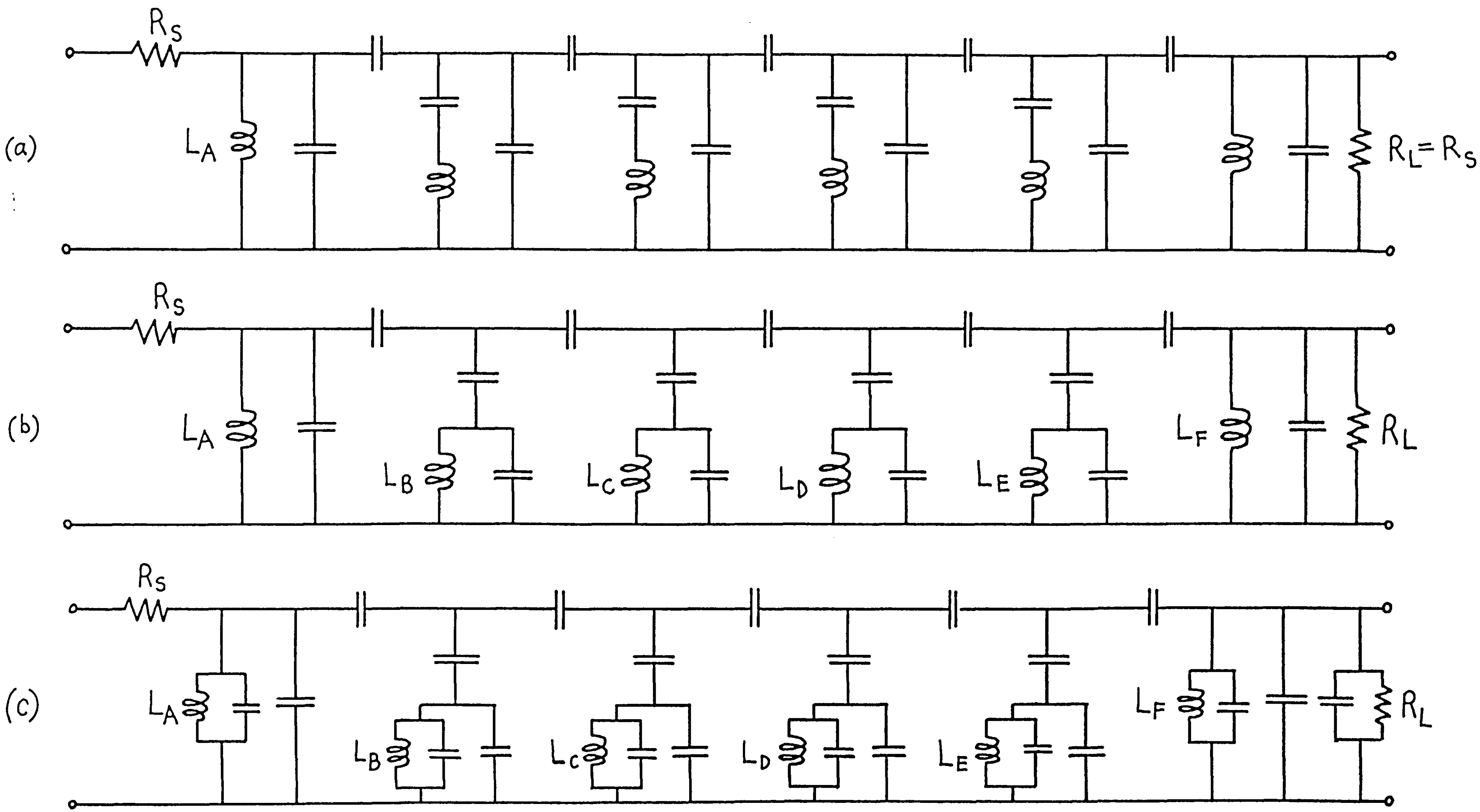

Fig. 5.9 Design procedure for bandpass filters with finite zeros

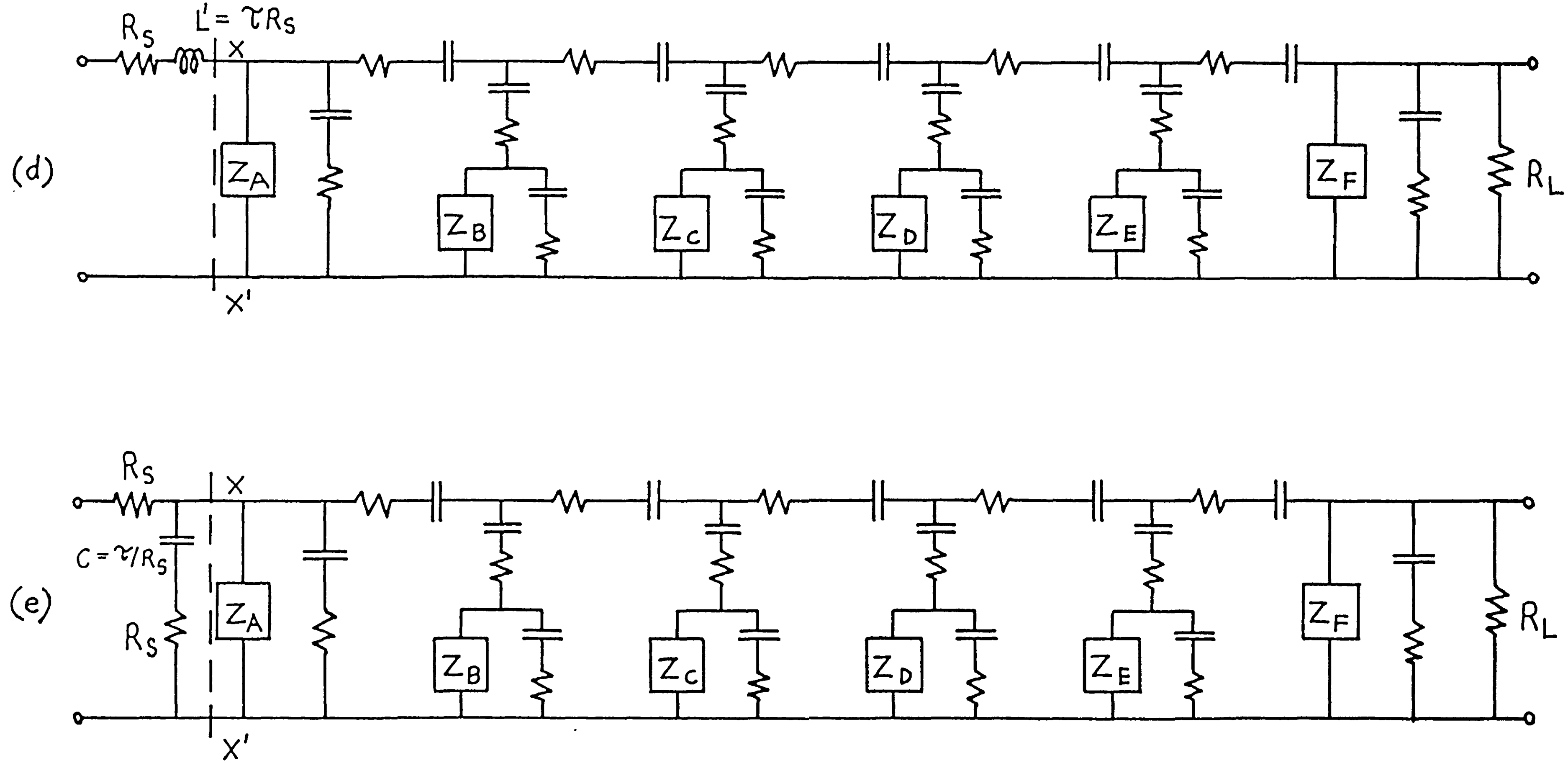

Fig. 5.9 Design procedure for bandpass filters with finite zeros

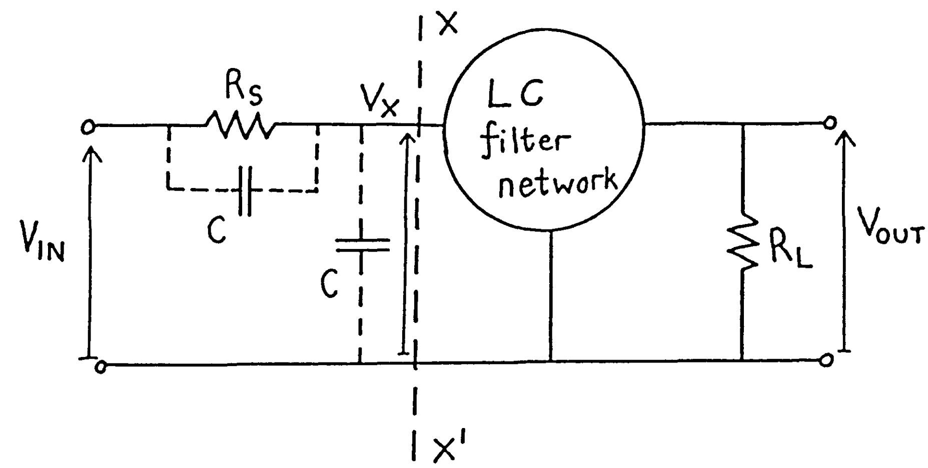

Fig. 5 10 Reinterpretation of design procedure for bandpass filters

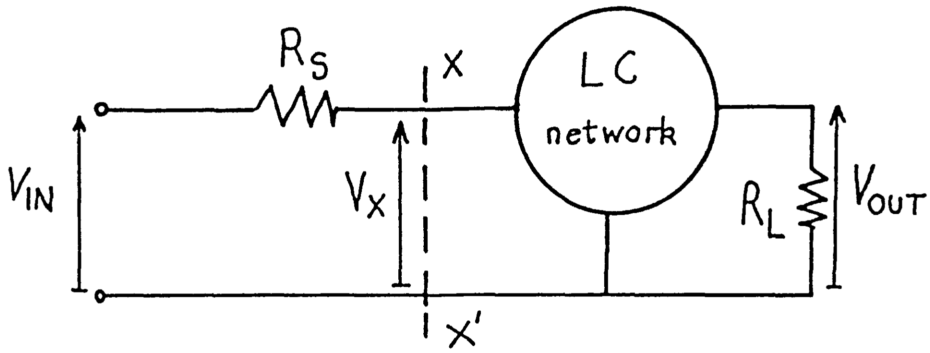

Fig. 6.1 Resistively terminated LC filter

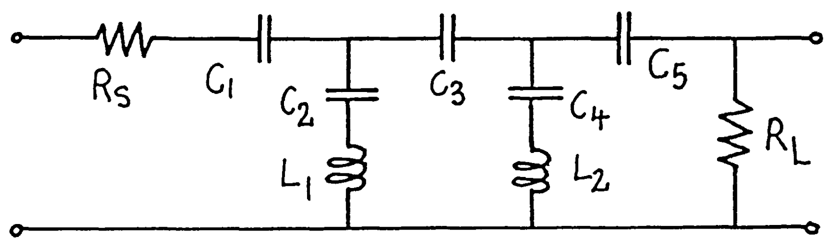

component	value
R_S	1·0000 KΩ
R_L	1·0000 "
C_1	0·1703 μF
C_2	0·5660 "
C_3	0·1118 "
C_4	0·1705 "
C_5	0·2733 "
L_1	0·1453 H
L_2	0·2407 "

Fig. 6.2 Highpass filter example

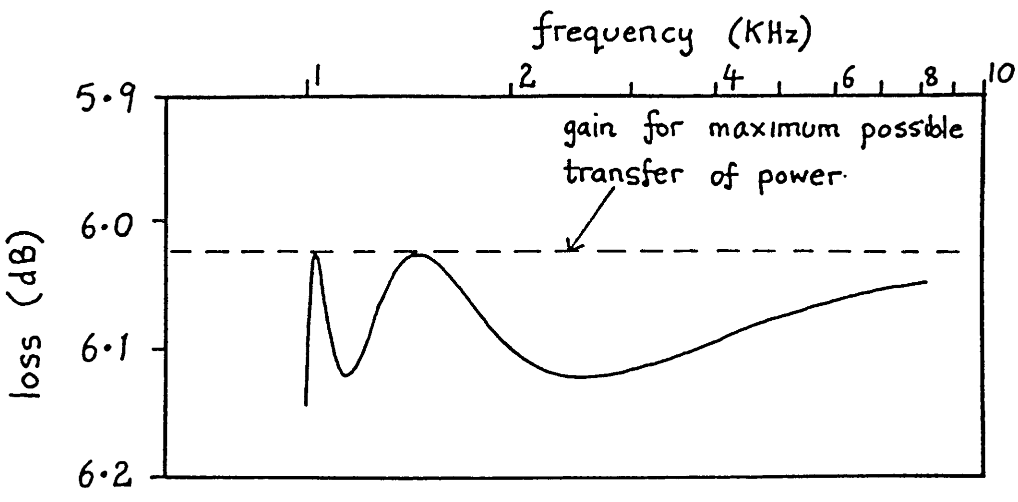

(a) Passband response

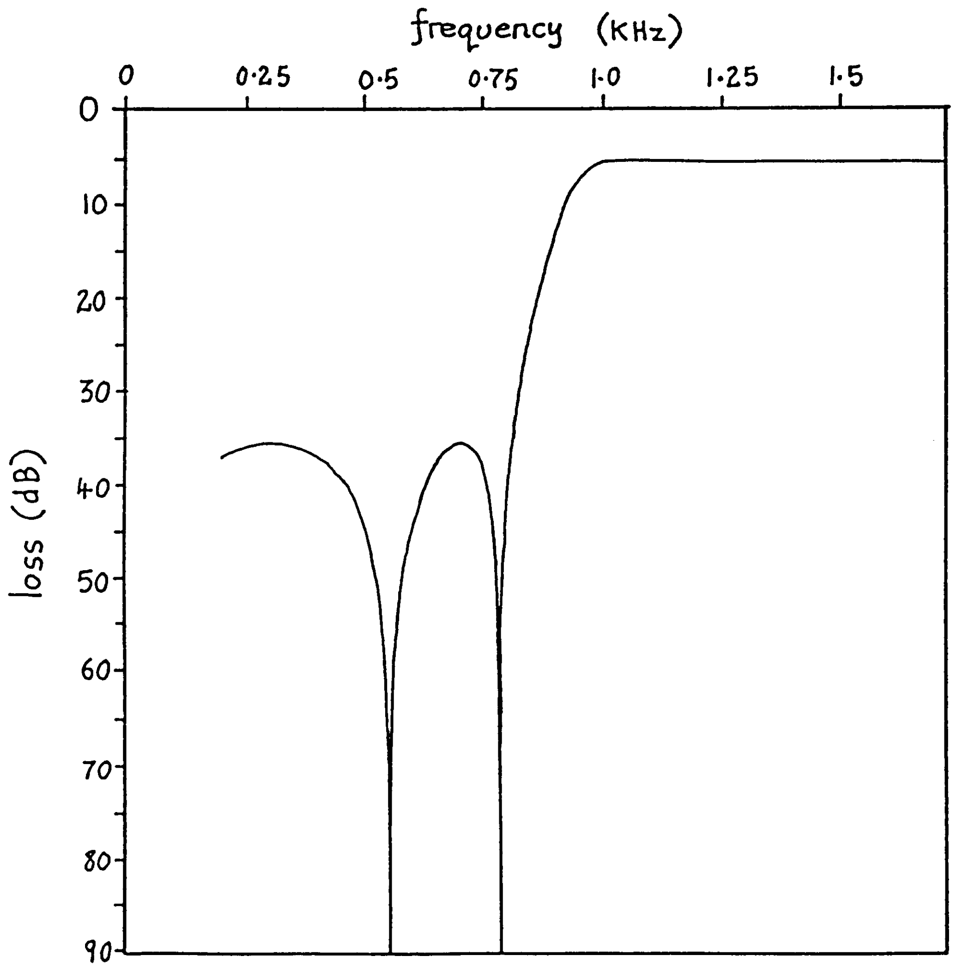

(b) Stopband response

Fig. 6.3 Loss/frequency behaviour for highpass filter

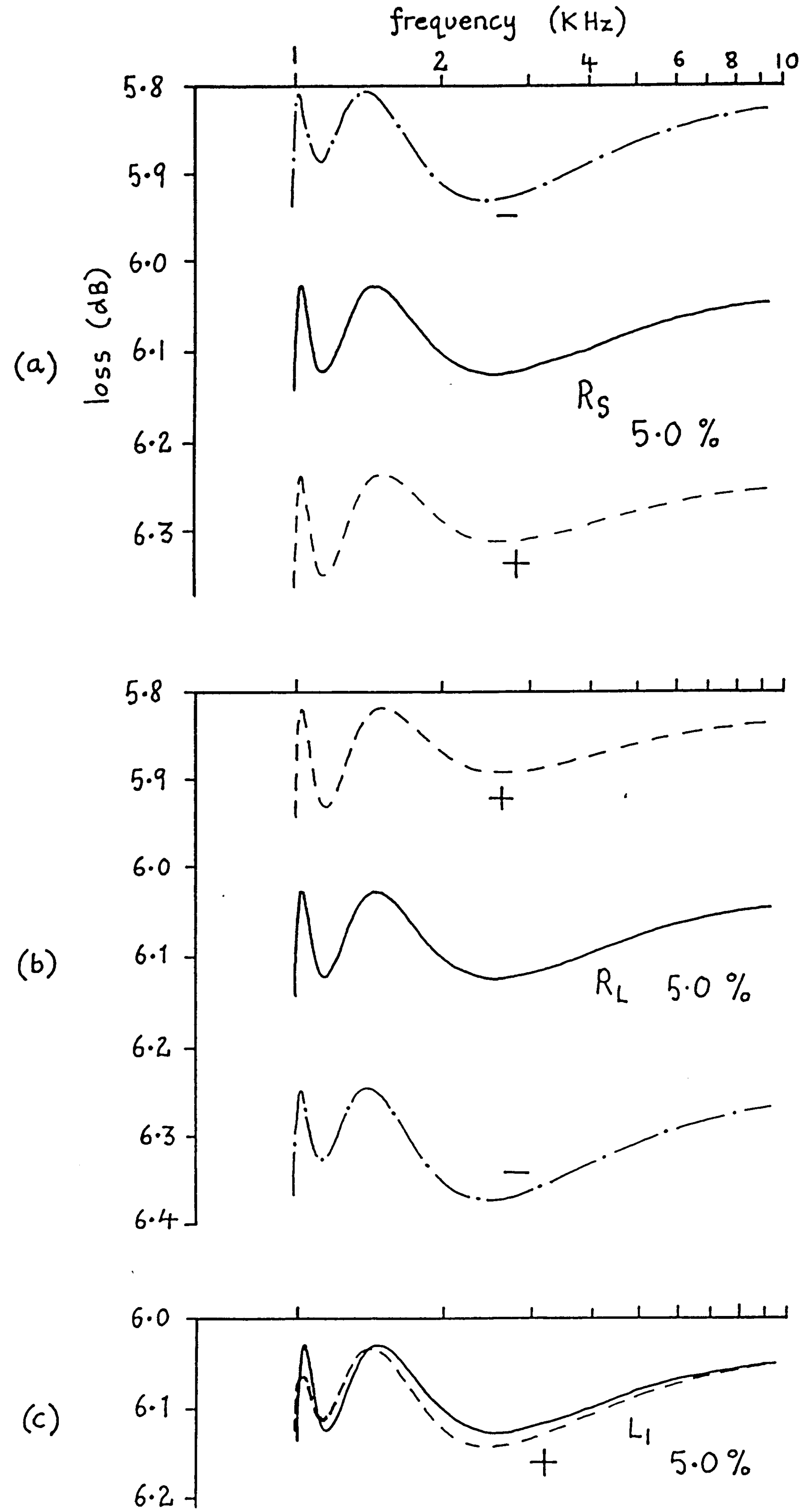

Fig. 6.4 Sensitivity investigation for highpass filter

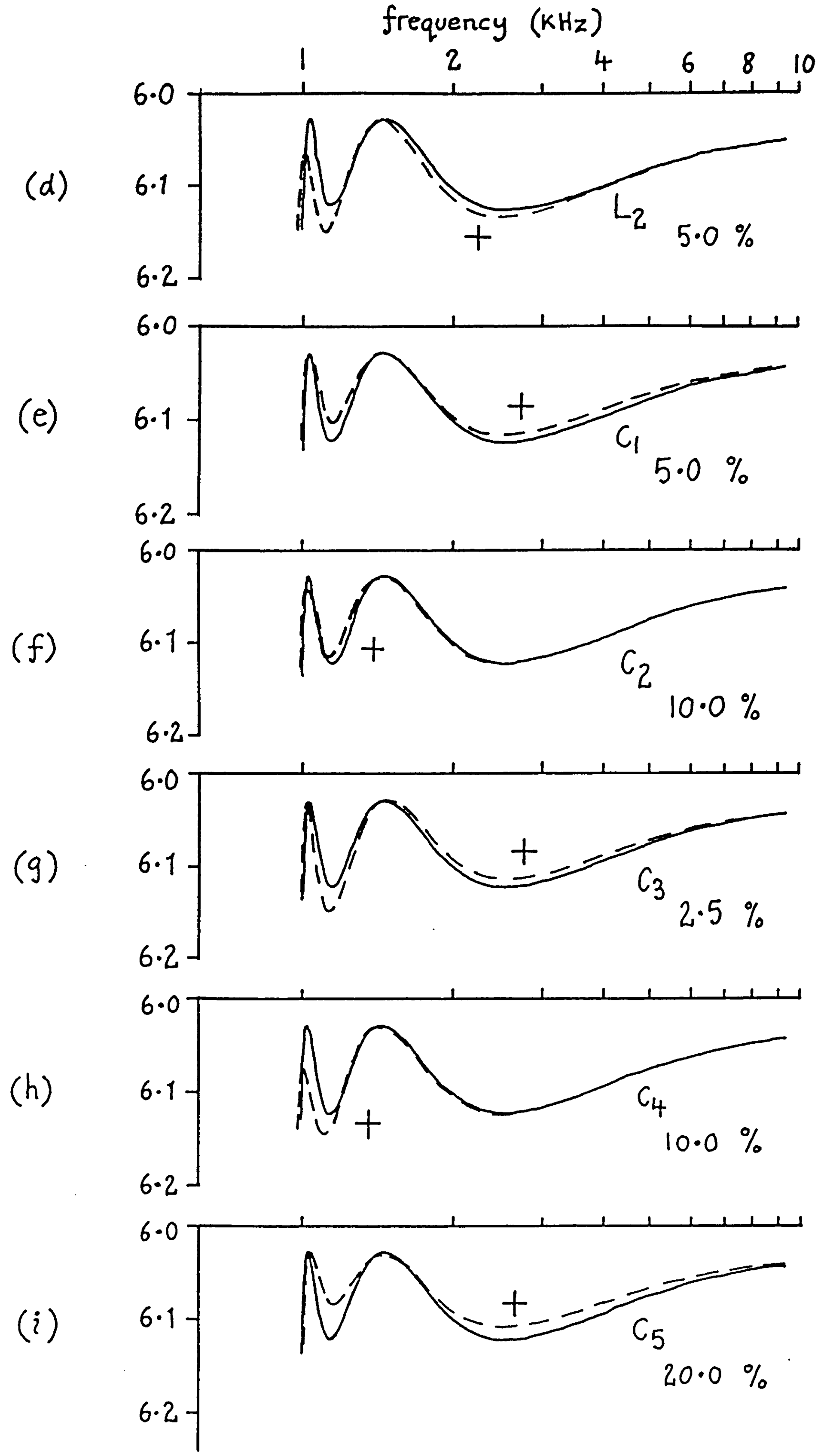

Fig. 6.4 (continued) Sensitivity investigation for highpass filter

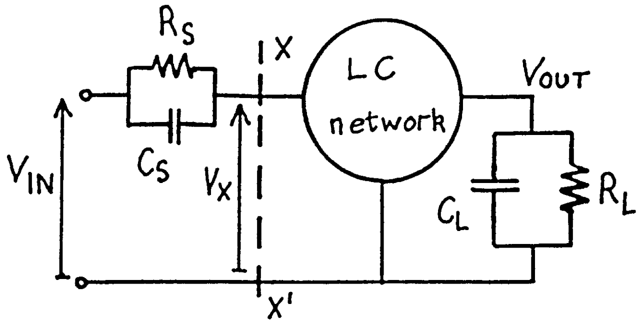

Fig. 6.5 LC filter with parallel RC terminations

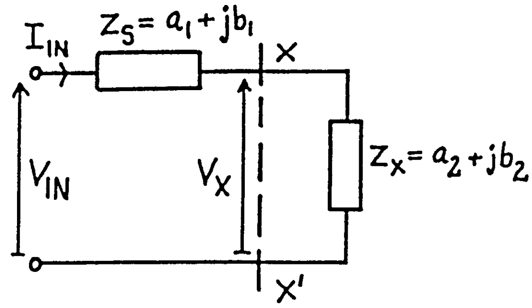

Fig. 6.6

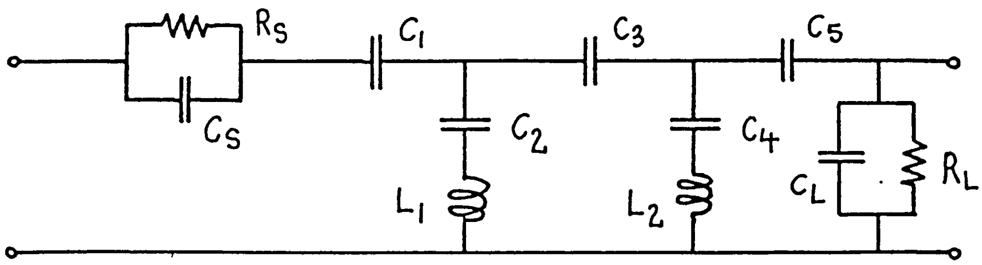

component	value	
R_S	1·0000	KΩ
R_L	0·6779	"
C_S	15·915	nF
C_L	20·370	"
C_1	96·096	"
C_2	0·6408	μF
C_3	0·1419	"
C_4	0·1919	"
C_5	1·3626	"
L_1	0·1285	H
L_2	0·2141	"

Fig. 6.7 Highpass filter with parallel RC terminations

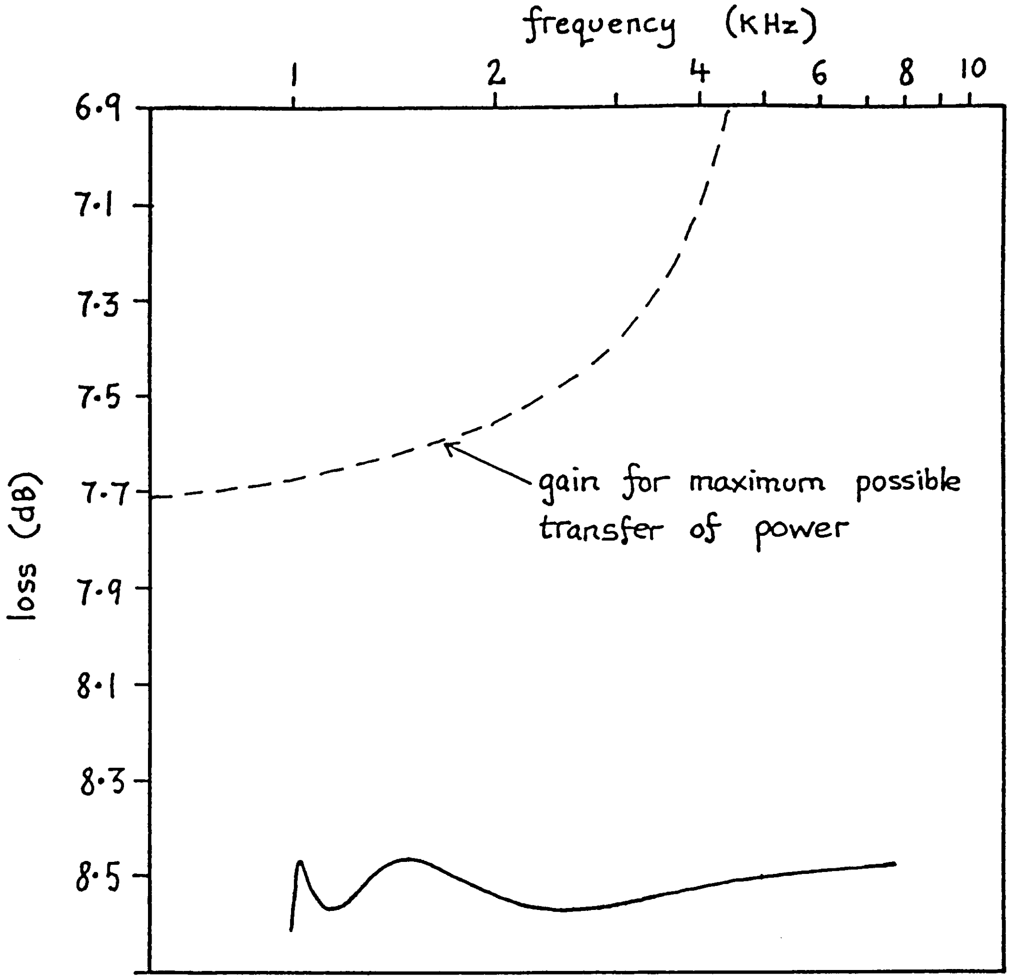

(a) Passband response

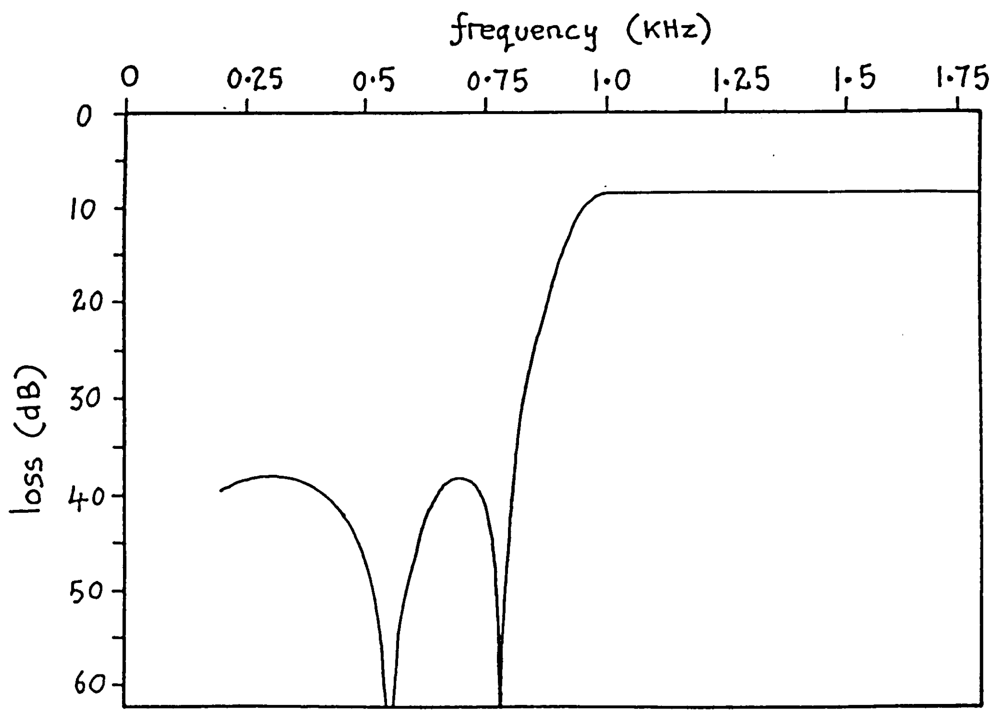

(b) Stopband response

Fig. 6.8 Loss/frequency behaviour for highpass filter with parallel RC terminations

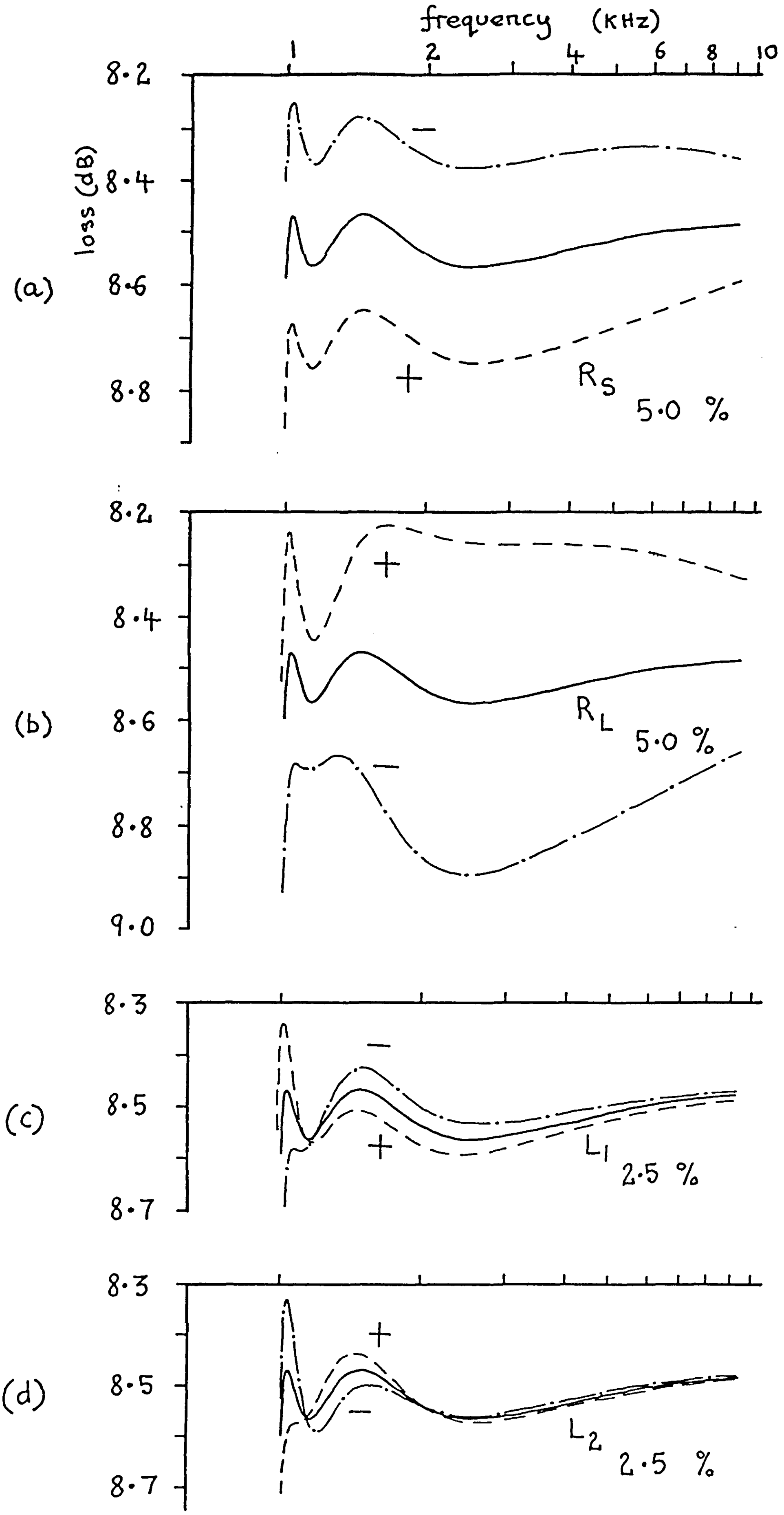

Fig. 6.9 Sensitivity investigation for highpass filter with parallel RC terminations

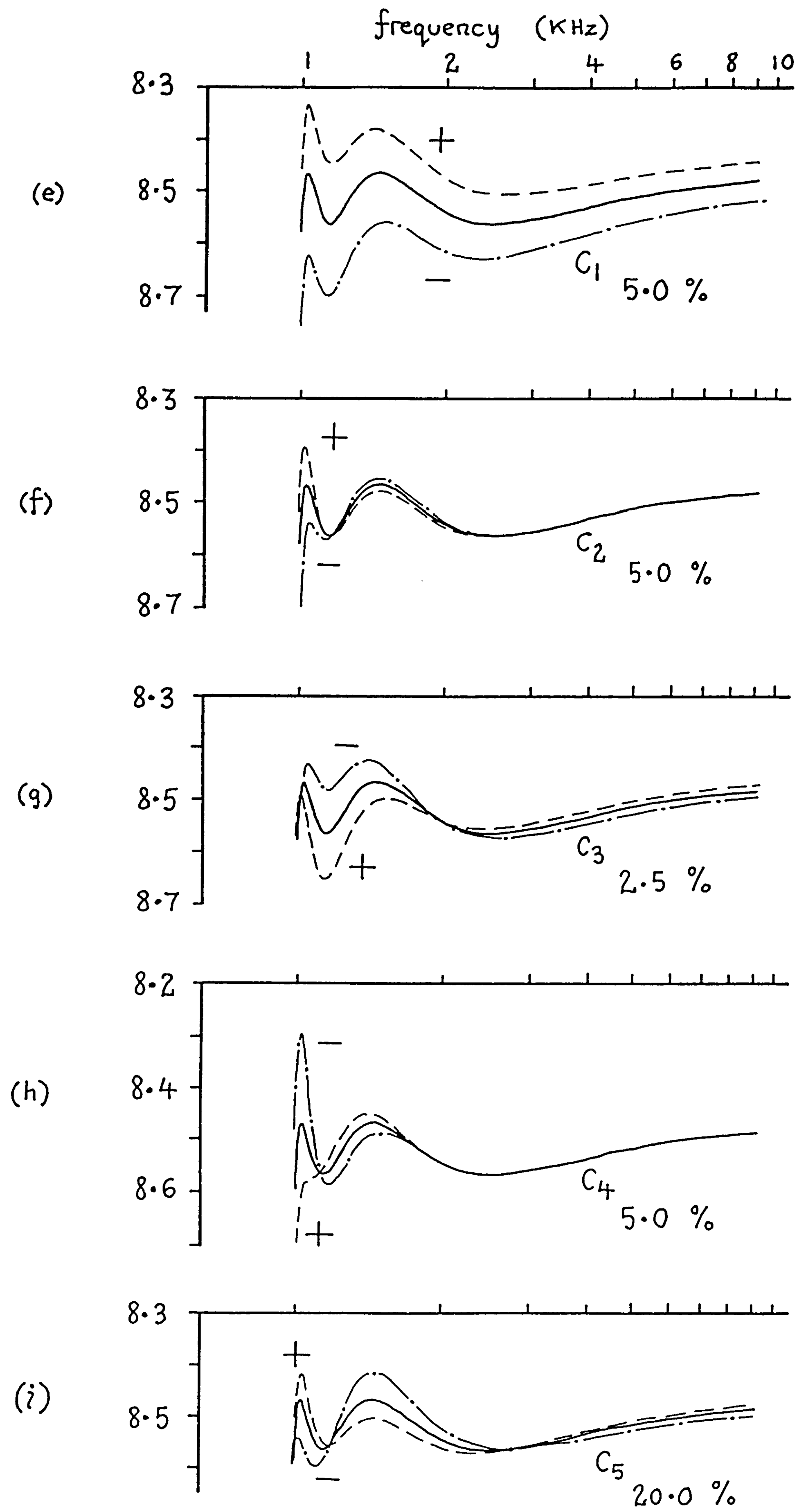

Fig. 6.9 (continued) Sensitivity investigation for highpass filter with parallel RC terminations

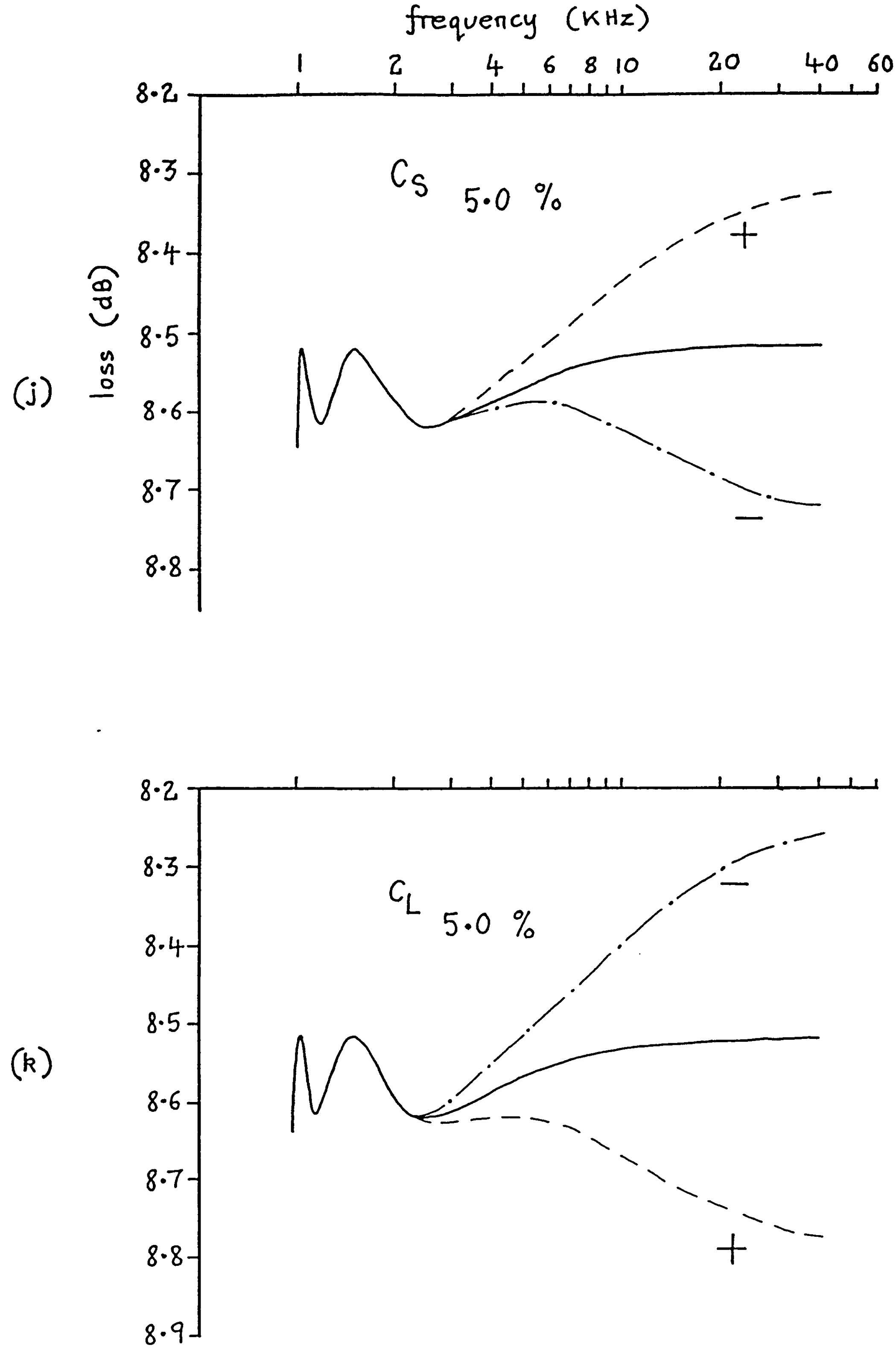

Fig. 6.9 (continued) Sensitivity investigation for highpass filter with parallel RC terminations

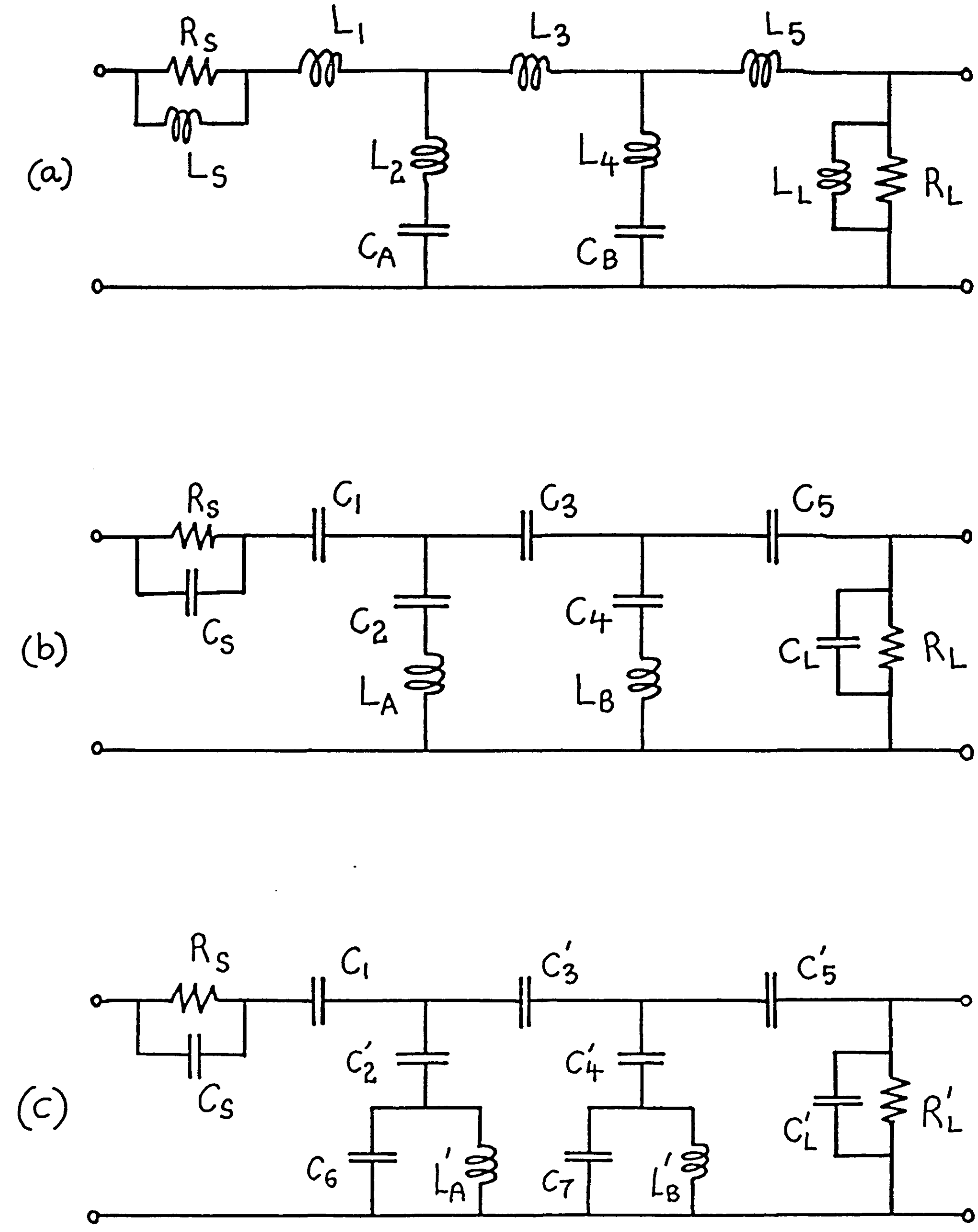

Fig. 7.1 Design of the active highpass filter

component	value
R_S	1.00000 Ω
R_L	0.6779 "
L_S	10.0000 H
L_L	7.81320 "
L_1	1.65622 "
L_2	0.248369 "
L_3	1.121599 "
L_4	0.829364 "
L_5	0.116803 "
C_A	1.23819 F
C_B	0.743552 "

(a)

component	value
R_S	2.0000 kΩ
R_L	1.3558 "
L_S	1591.55 mH
L_L	1243.51 "
L_1	263.595 "
L_2	39.5292 "
L_3	178.508 "
L_4	131.9974 "
L_5	18.5897 "
C_A	49.2662 nF
C_B	29.5850 "

(b)

component	value
R_S	2.00000 kΩ
R_L	1.3558 "
C_S	3.97887 nF
C_L	5.0925 "
C_1	24.0239 "
C_2	160.20 "
C_3	35.475 "
C_4	47.975 "
C_5	340.65 "
L_A	128.538 mH
L_B	214.047 "

(c)

component	values
R_S	2.0000 kΩ
R'_L	1.5760 "
C_S	3.97887 nF
C'_L	392.96 pF
C_1	24.0239 nF
C'_2	162.330 "
C'_3	33.364 "
C'_4	44.4614 "
C'_5	297.106 "
C_6	2.1485 "
C_7	2.1485 "
L'_A	125.202 mH
L'_B	220.3196 "

(d)

Fig. 7.2 Passive component values for the LC filters of Fig. 7.1

	(a)	(b)
component	values	
R_1	1·203 KΩ	2·117 KΩ
R_2	120·3 "	211·7 "
R_3	121·8 "	214·4 "
R_4	1·203 "	2·117 "
R_5	92·53 "	162·8 "
R_6	1·203 "	2·117 "
C_0	2·569 nF	1·460 nF

note for amplifiers : $\alpha = 10^{-5}$ $f_T = 1$ MHz

L	125·202 mH	220·3196 mH
C	404·787 pF	424·5437 pF
τ	$3{\cdot}197139 \times 10^{-7}$	$3{\cdot}197139 \times 10^{-7}$

Fig. 7.3 (a) Component values for the S.B.I. circuits

(b) L, C and τ values associated with the impedances for the S.B.I.s

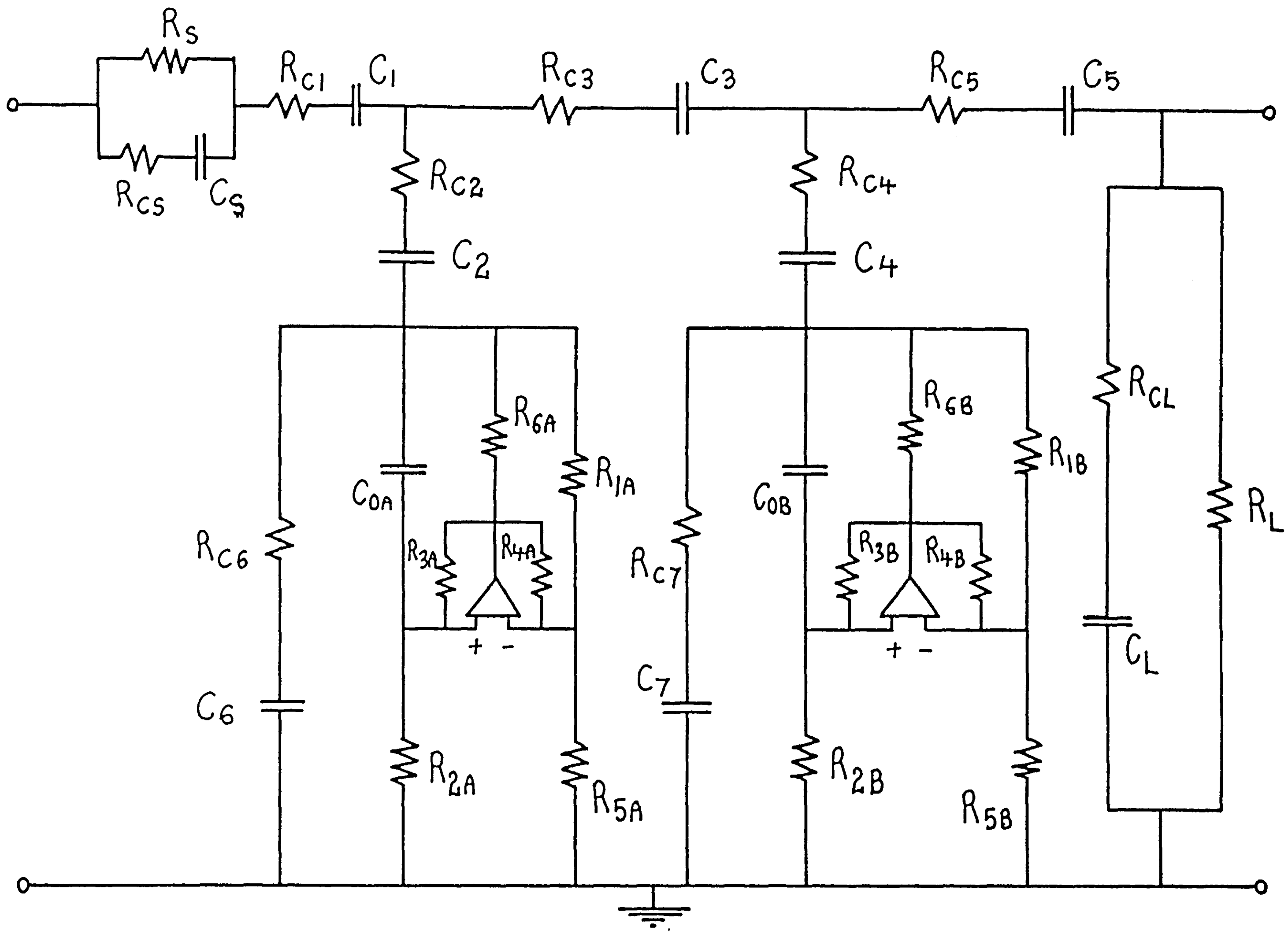

Fig. 7.4 (a) Active highpass filter using S.B.I. circuits B

component	value
R_S	2·000 KΩ
R_L	1·576 "
C_1	24·02 nF
C_2	162·3 "
C_3	33·36 "
C_4	44·46 "
C_5	297·1 "
C_{0A}	2·569 "
R_{1A}	1·203 KΩ
R_{2A}	120·3 "
R_{3A}	121·8 "
R_{4A}	1·203 "
R_{5A}	92·53 "
R_{6A}	1·203 "
C_{0B}	1·460 nF
R_{1B}	2·117 KΩ
R_{2B}	211·7 "
R_{3B}	214·4 "
R_{4B}	2·117 "
R_{5B}	162·8 "
R_{6B}	2·117 "
C_S	3·819 nF
C_6	1·744 "
C_7	1·919 "
C_L	0·1901 "
R_{CS}	83·72 Ω
R_{C1}	13·31 "
R_{C2}	1·970 "
R_{C3}	9·583 "
R_{C4}	7·191 "
R_{C5}	1·076 "
R_{C6}	183·3 "
R_{C7}	166·6 "
R_{CL}	1·682 KΩ

for amplifiers: $\alpha = 10^{-5}$

$f_T = 1{\cdot}0$ MHz

Fig. 7.4(b) Component values for active highpass filter

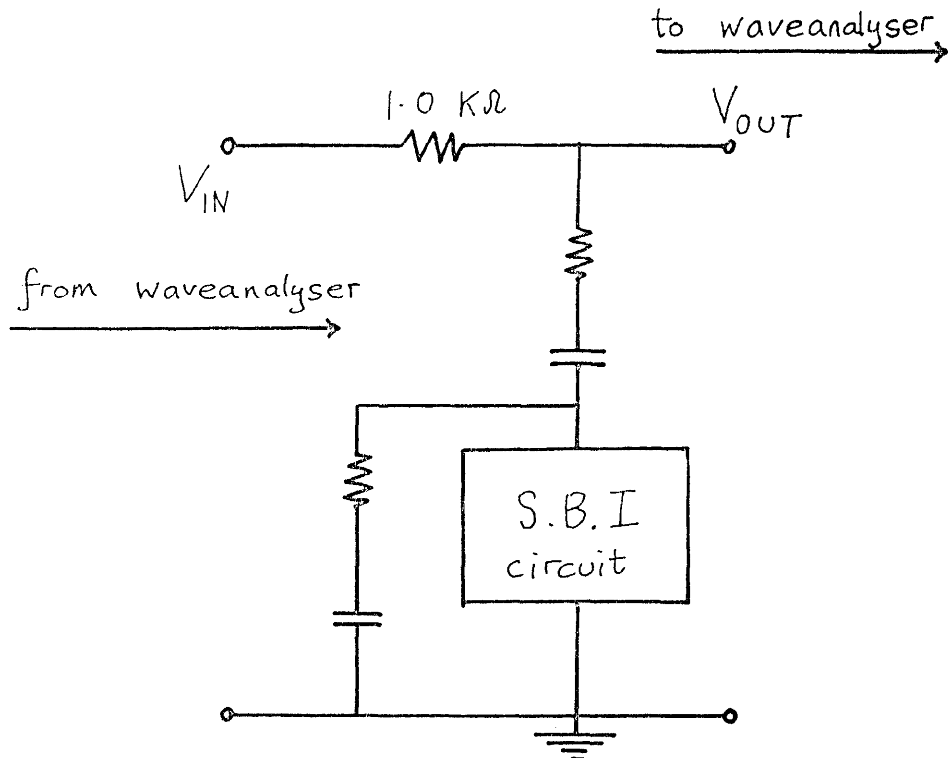

Fig. 7.5 Measuring setup for adjusting the series resonators

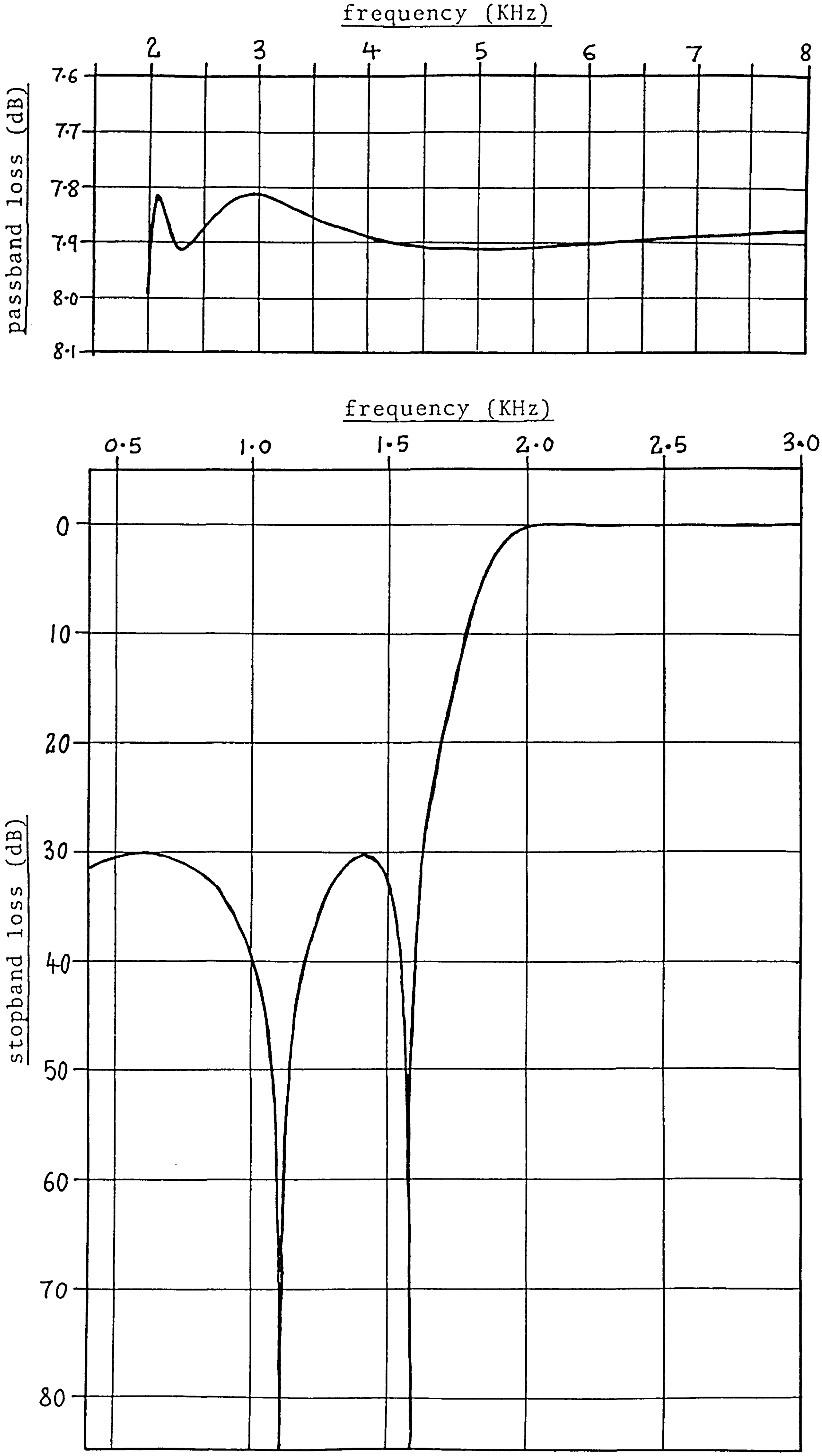

Fig. 7.6 Computed loss/frequency response for the active highpass filter

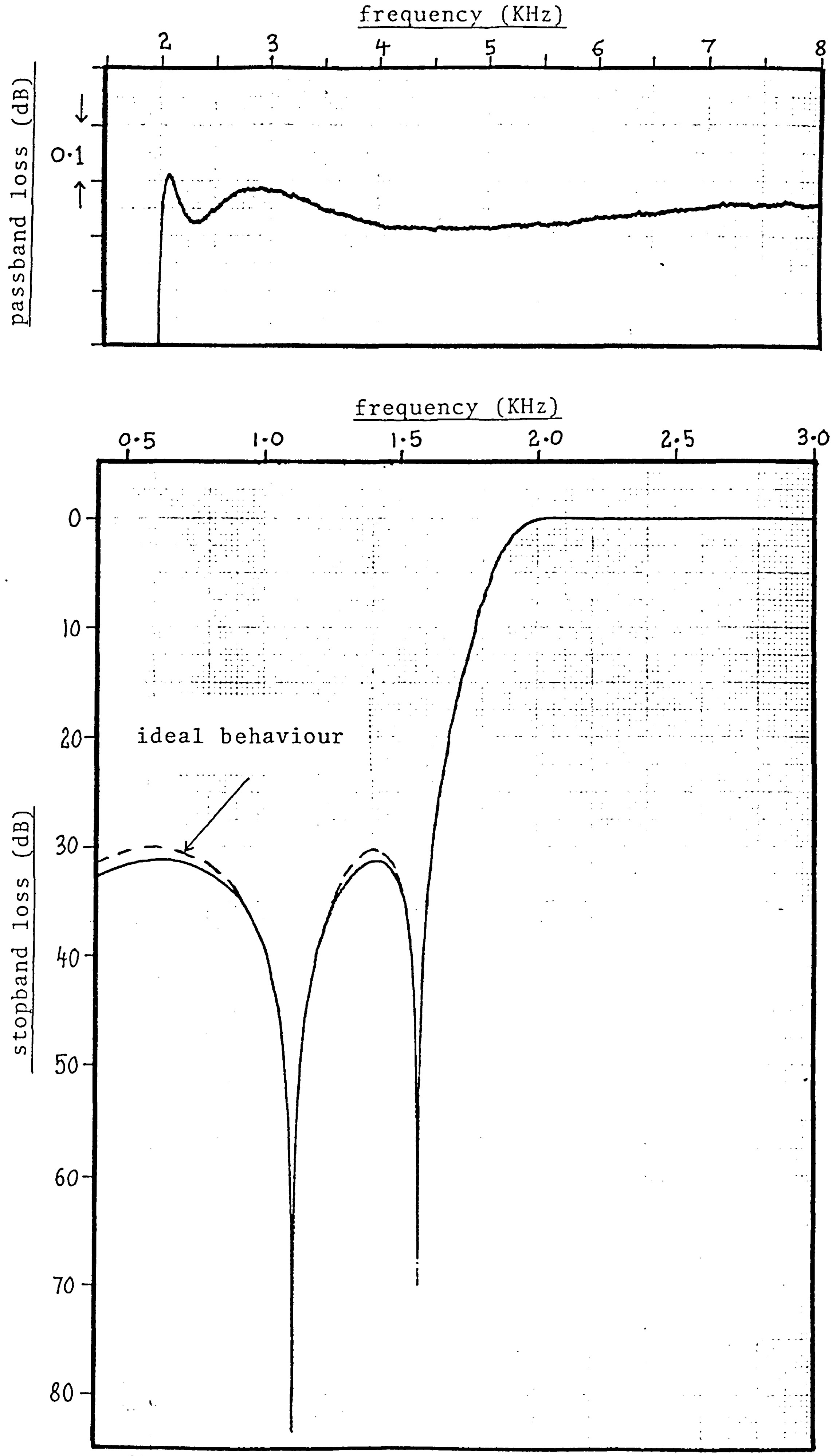

Fig. 7.7 Measured loss/frequency response for the active highpass filter

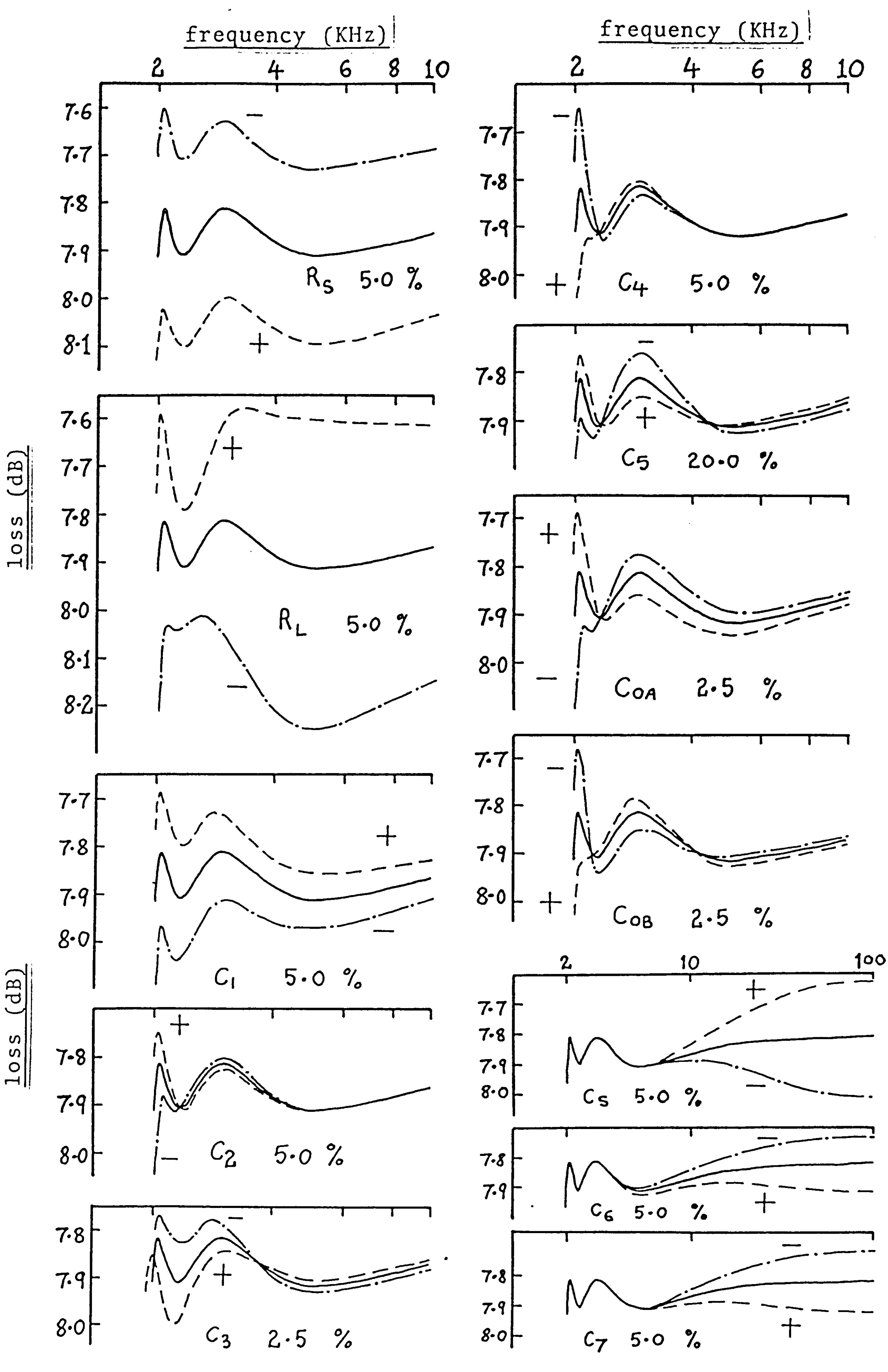

Fig. 7.8 (a) Sensitivity investigation for the active highpass filter

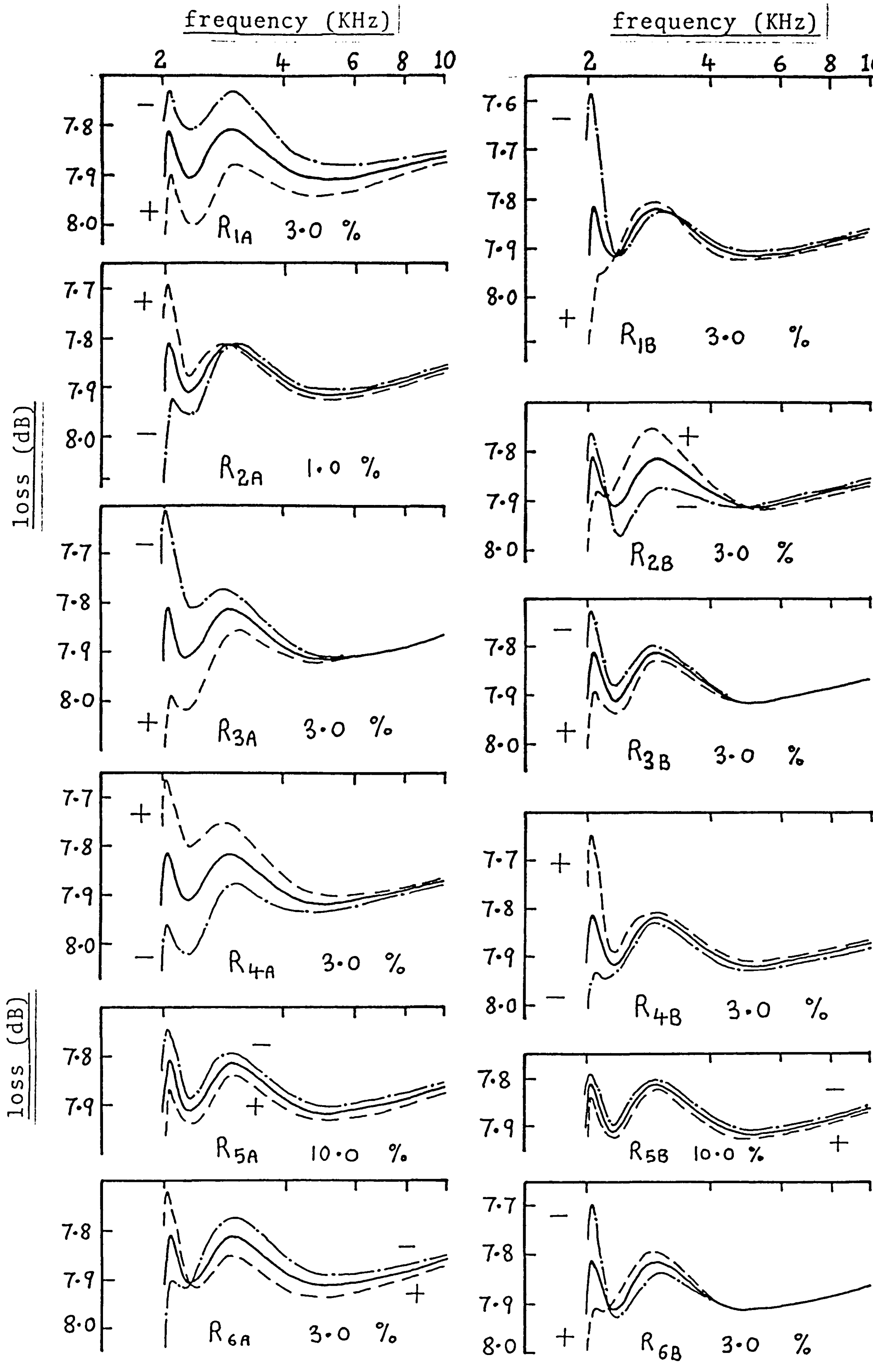

Fig. 7.8 (b) Sensitivity investigation for the active highpass filter

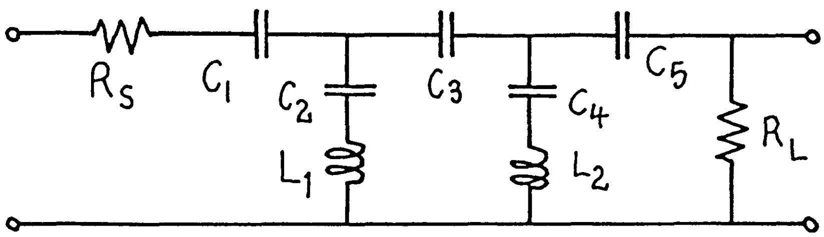

component	value
R_S	2·0000 kΩ
R_L	2·0000 "
C_1	42·58 nF
C_2	141·5 "
C_3	27·95 "
C_4	42·63 "
C_5	68·33 "
L_1	0·1453 H
L_2	0·2407 "

Fig. 7.9 Low sensitivity LC highpass filter example

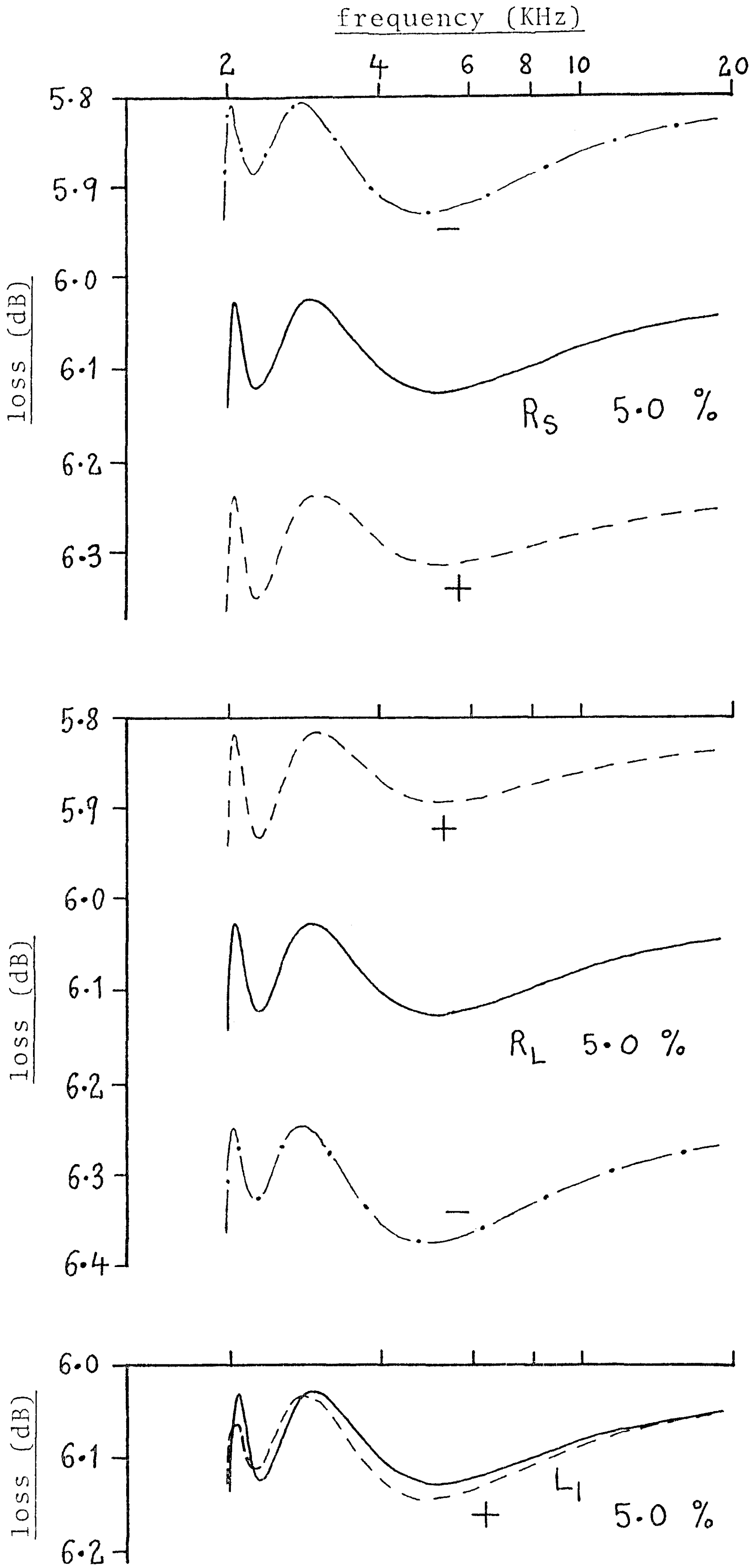

Fig. 7.10 (a) Sensitivity investigation for LC highpass filter

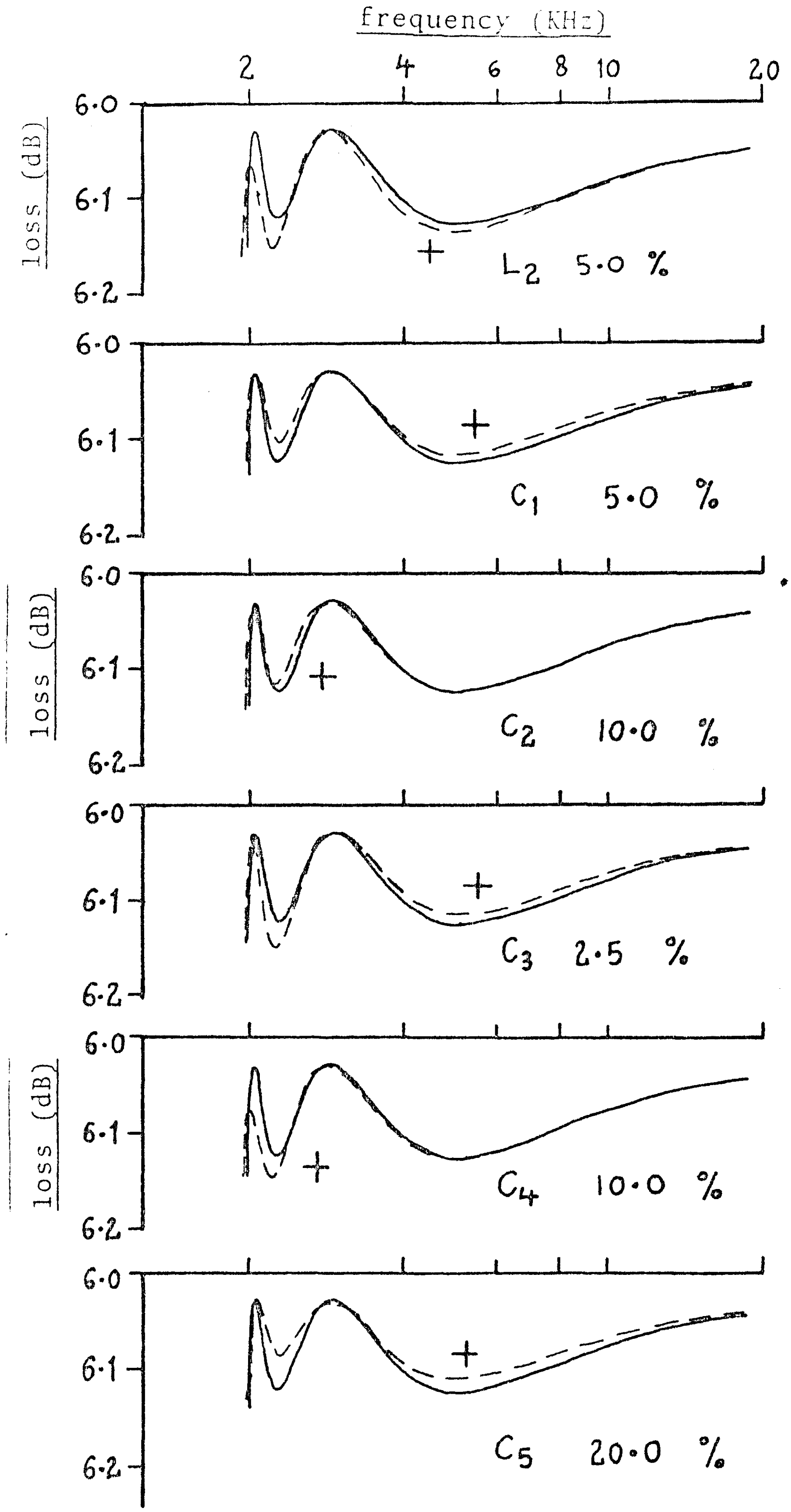

Fig. 7.10 (b) Sensitivity investigation for LC highpass filter

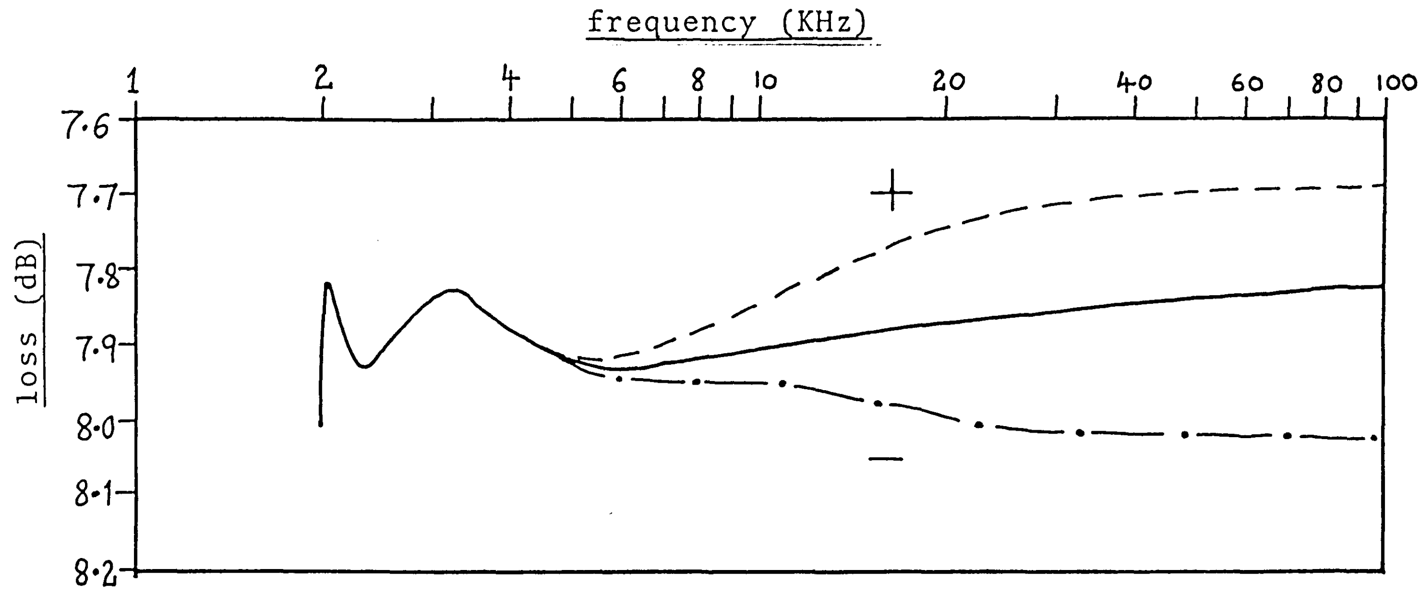

Fig. 7.11 Computed effects of ± 20.0 % simultaneous changes in the f_T values of both amplifiers

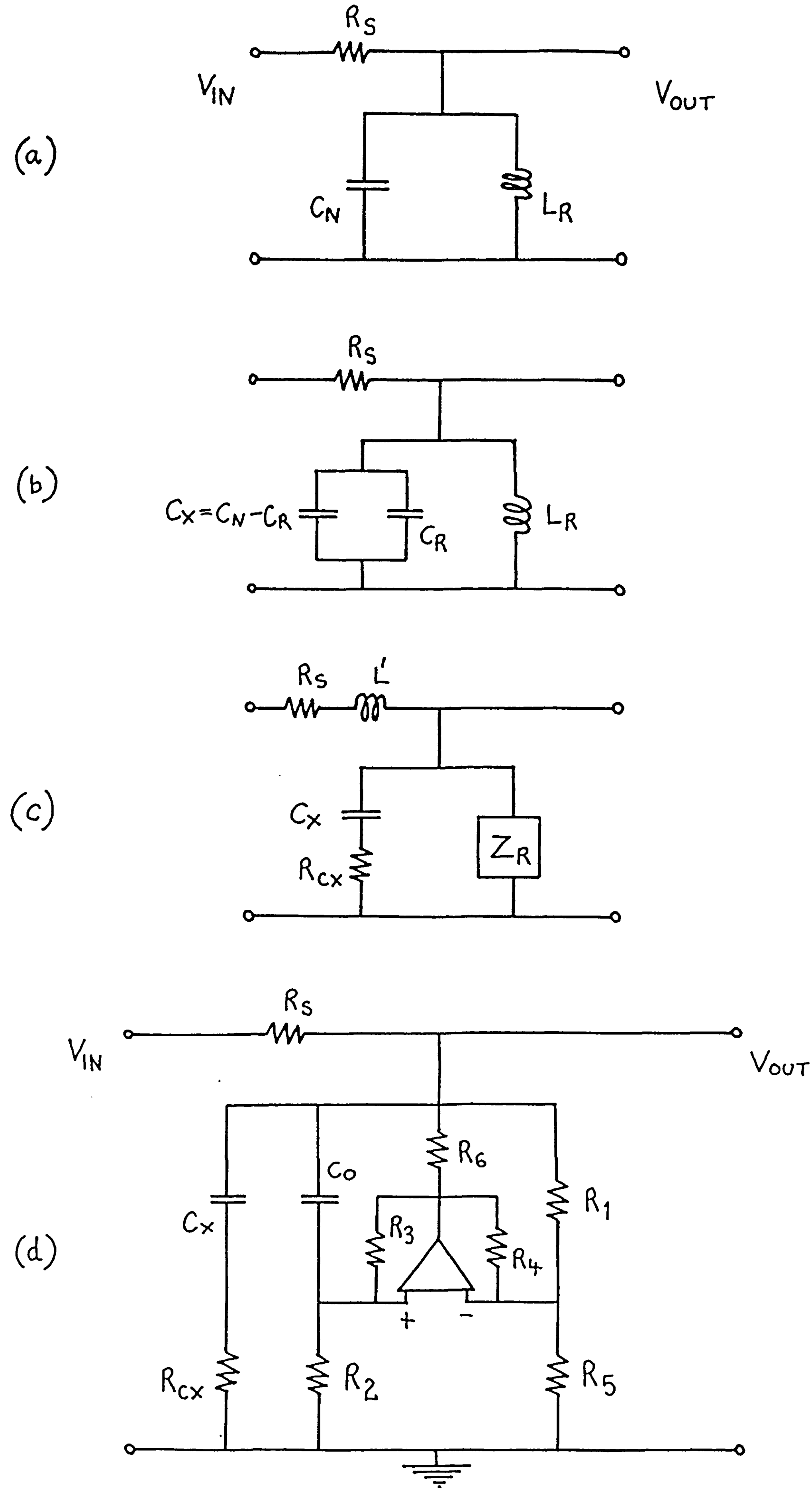

Fig. 7.12 Active resonator circuit using S.B.I. circuit B

component	value	
R_s	10·0000	KΩ
R_1	10·0000	"
R_2	10·0000	"
R_3	19·9992	"
R_4	10·0000	"
R_5	10·0000	"
R_6	18·4182	"
R_{cx}	2·8995	Ω
C_o	2·0203	nF
C_x	0·15903	μF

(a)

component	value	
R_s	10·0000	KΩ
R_1	10·0000	"
R_2	10·0000	"
R_3	20·0000	"
R_4	10·0000	"
R_5	10·0000	"
R_6	20·0000	"
R_{cx}	0	
C_o	1·98938	nF
C_x	0·15915	μF

(b)

component	value	
R_s	10·0000	KΩ
R_1	1·67985	"
R_2	100·000	"
R_3	100·367	"
R_4	1·65824	"
R_5	100·000	"
R_6	1·39353	"
R_{cx}	2·0039	Ω
C_o	3·1761	nF
C_x	0·158824	μF

(c)

Fig. 7.13 Passive component values for active resonator circuit

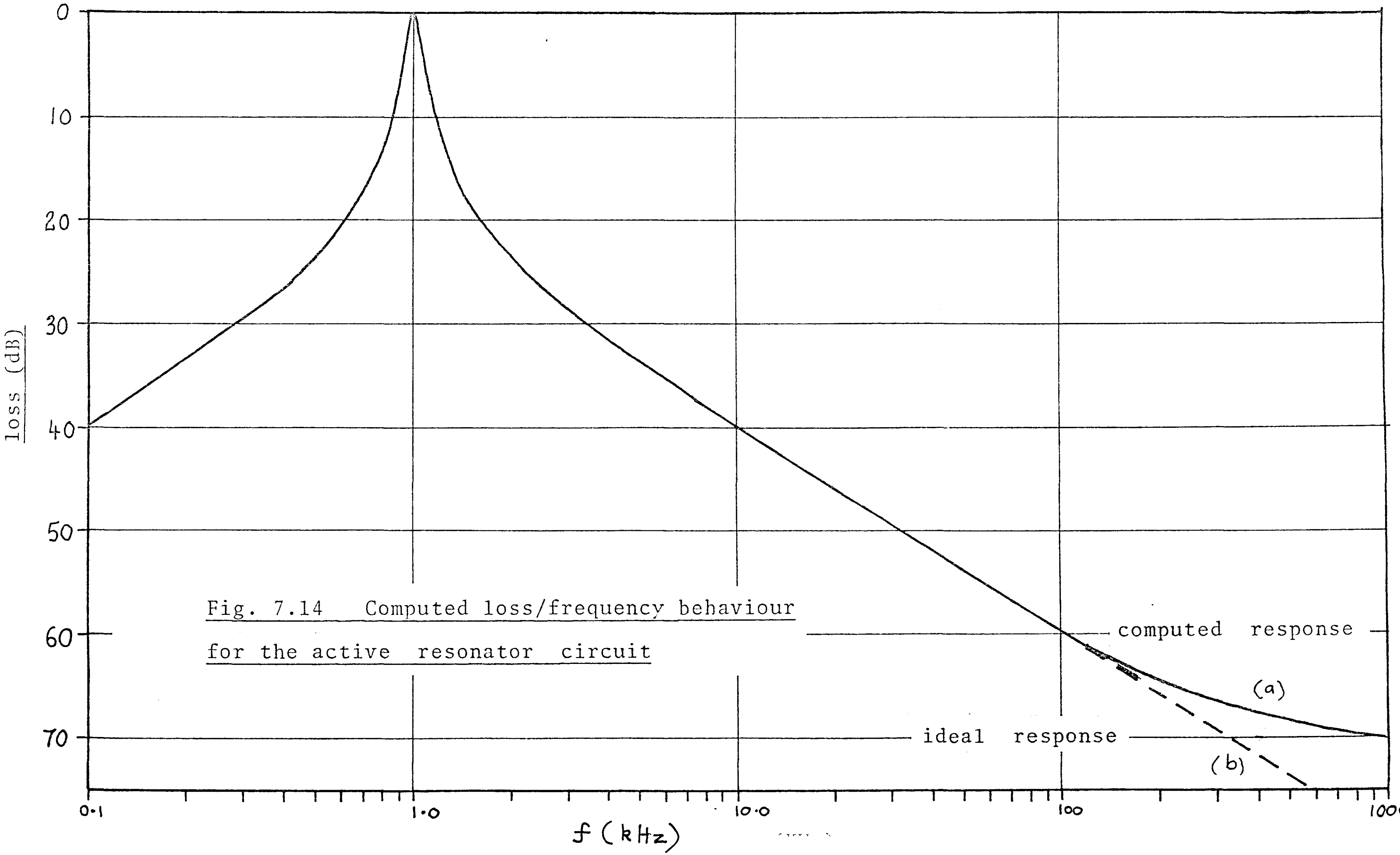

Fig. 7.14 Computed loss/frequency behaviour for the active resonator circuit

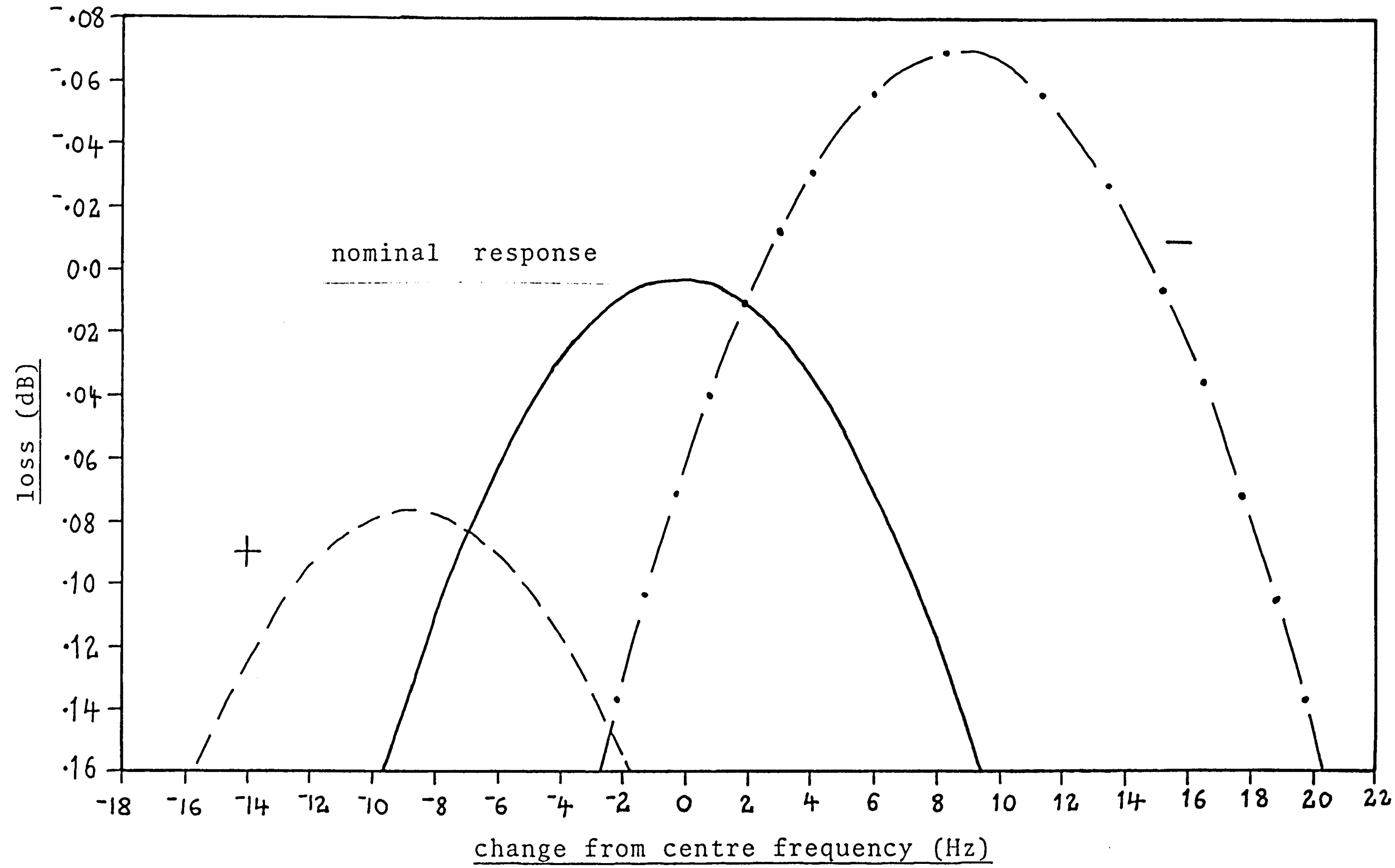

Fig. 7.15 Effects of changing $1/f_T$ by $\pm$ 50.0 %

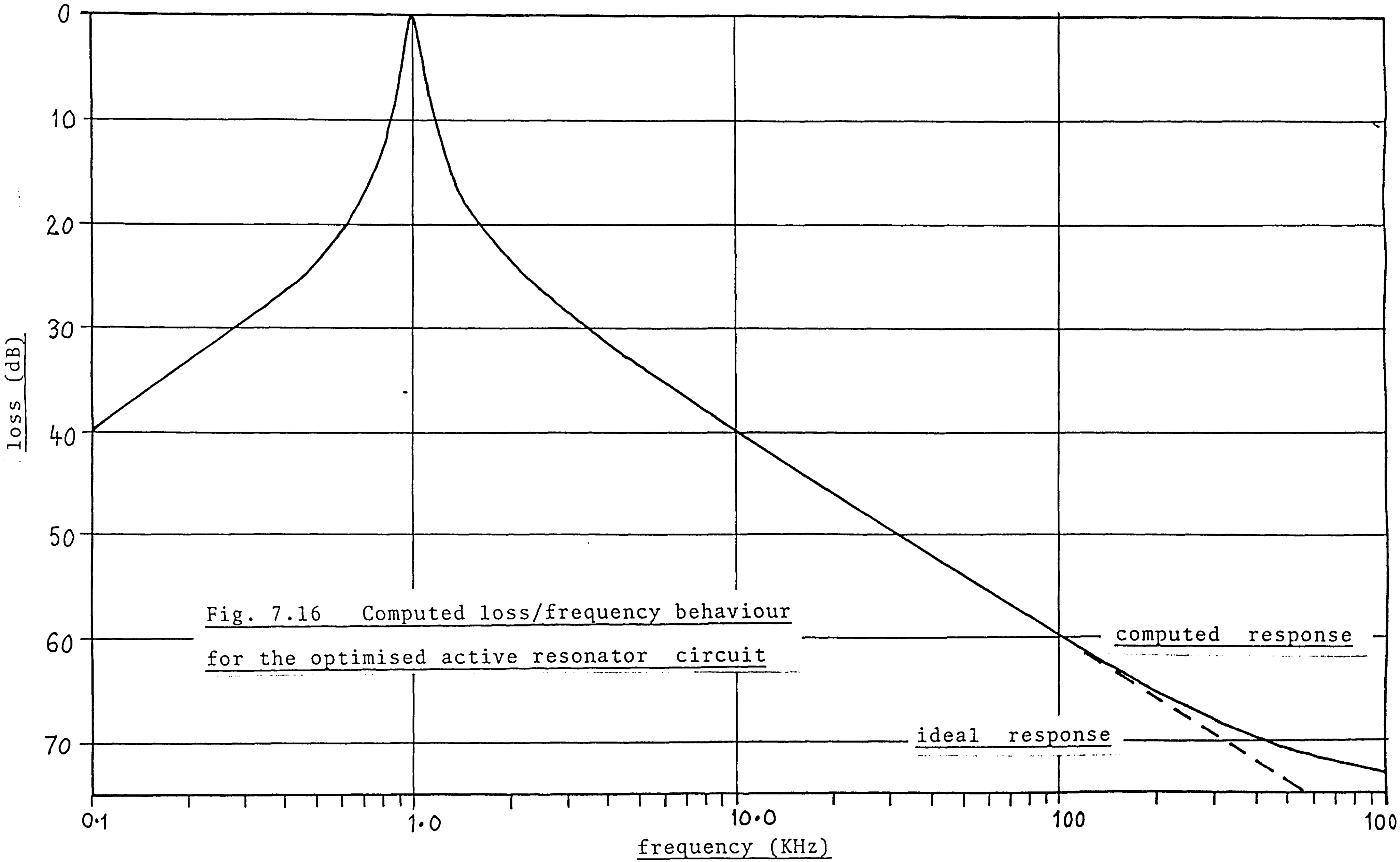

Fig. 7.16 Computed loss/frequency behaviour for the optimised active resonator circuit

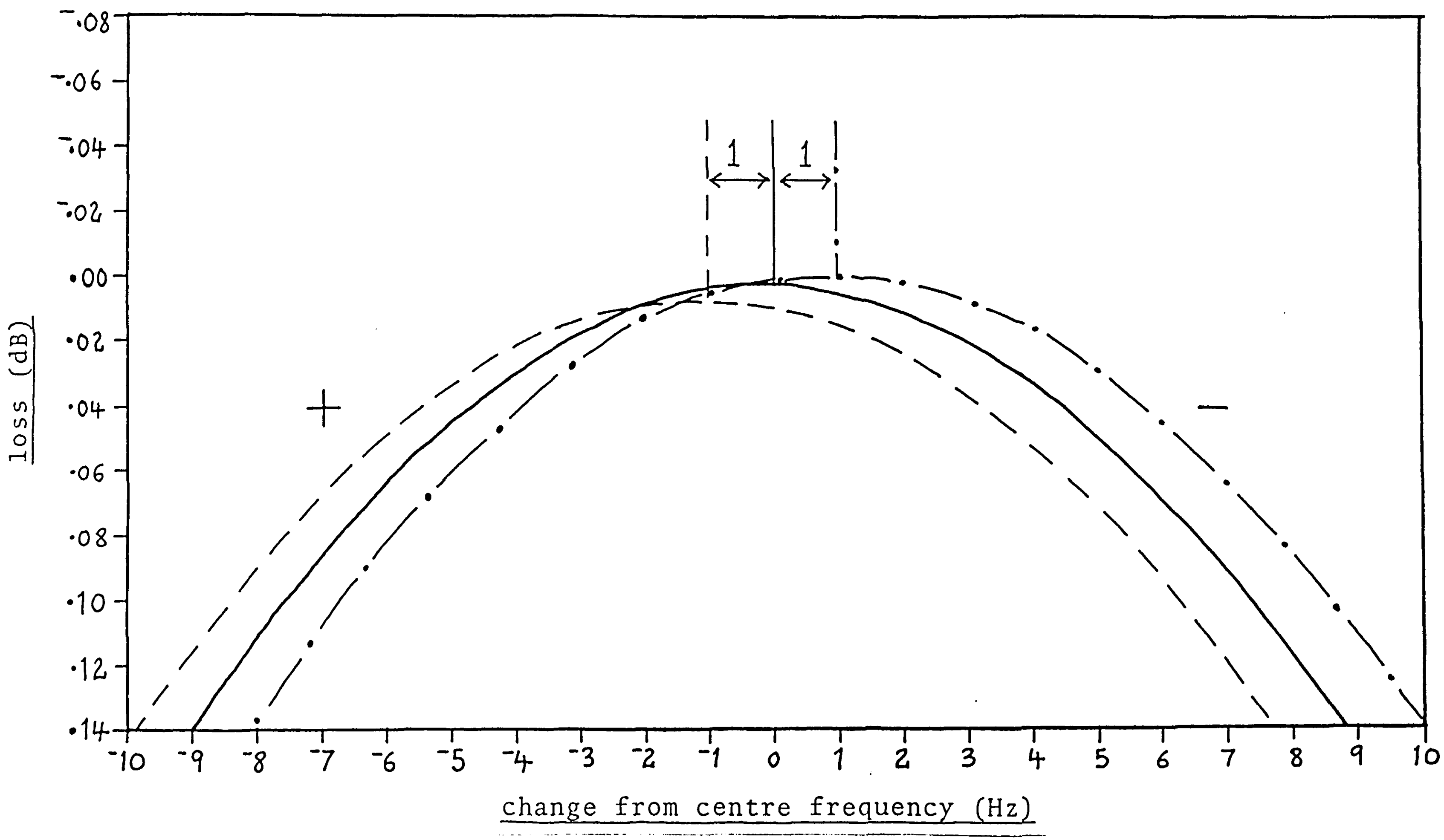

Fig. 7.17 Effects of changing $1/f_T$ by 50.0 % for the optimised resonator circuit

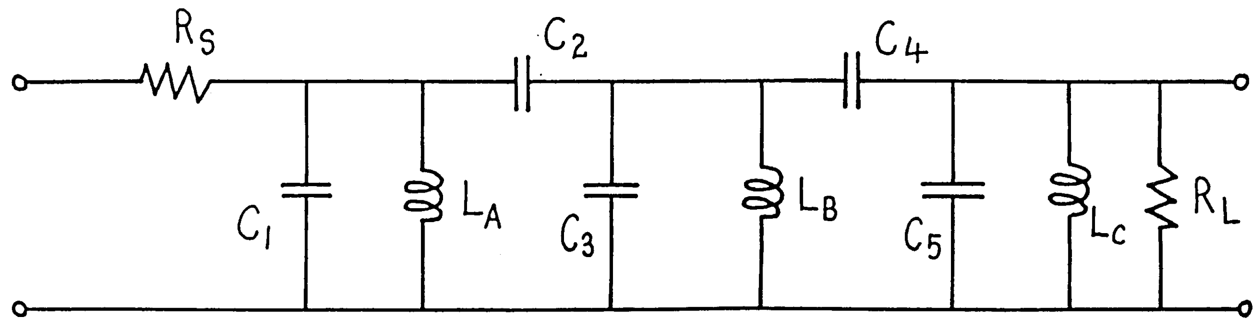

component	value
R_S	30.0000 KΩ
R_L	30.0000 "
C_1	16.3113 nF
C_2	640.068 pF
C_3	15.6826 nF

component	value
C_4	640.068 pF
C_5	16.3113 nF
L_A	14.9604 mH
L_B	14.9604 "
L_C	14.9604 "

Fig. 7.18 LC bandpass filter and component values

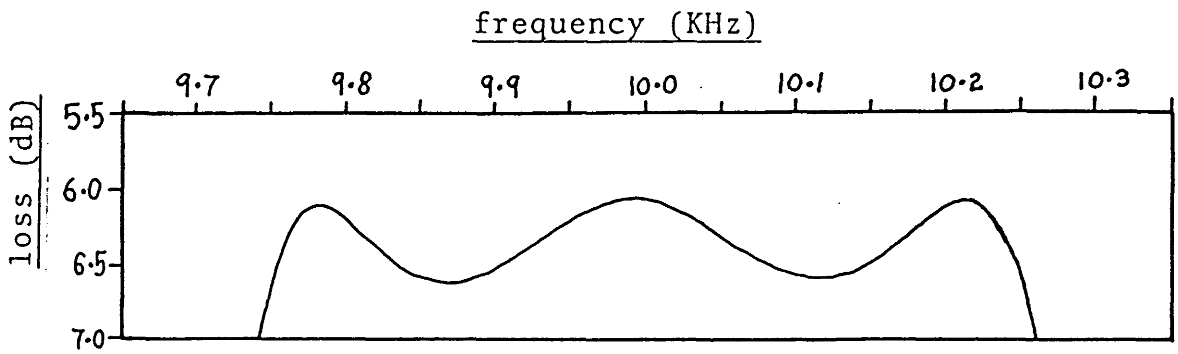

(a) passband response

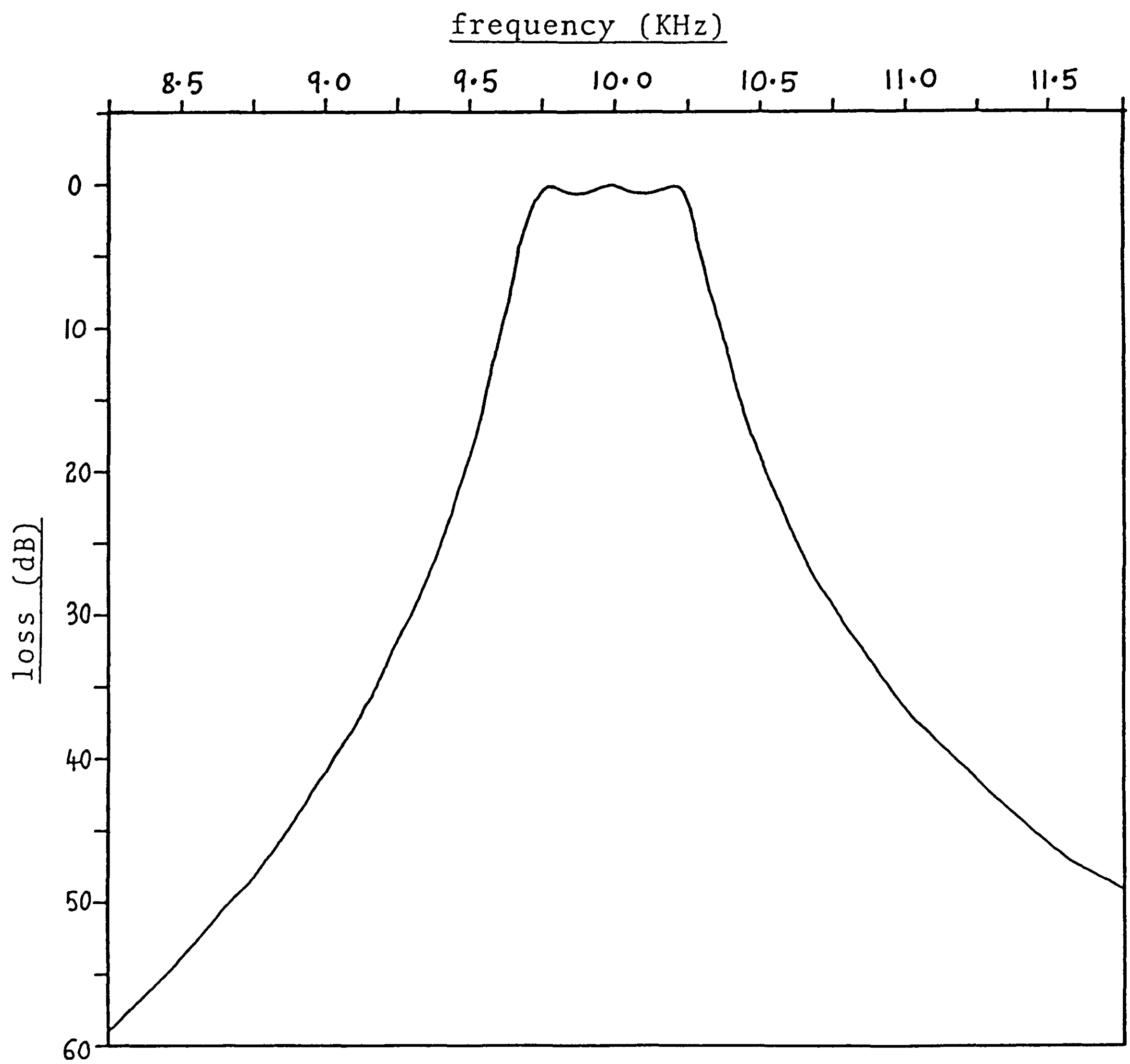

(b) stopband response

Fig. 7.19 Loss/frequency behaviour for passive LC bandpass filter frequency at which $S^{I(\omega)}_{1/\omega_T}$ was minimised

component values for the S.B.I. circuits

L, C and τ values associated with the impedance for the S.B.I.s

f_R	10·1884 KHz	10·3906 KHz	10·1884 KHz
R_1	1·99920 KΩ	2·03860 KΩ	1·99920 KΩ
R_2	100·000 "	100·000 "	100·000 "
R_3	101·112 "	101·133 "	101·112 "
R_4	1·98190 "	2·02061 "	1·98190 "
R_5	100·000 "	100·000 "	100·000 "
R_6	1·23426 "	1·25849 "	1·23426 "
C_0	310·538 pF	304·426 pF	310·538 pF
L	0·0149604 H	0·0149604 H	0·0149604 H
C	98·5319 pF	96·6731 pF	98·532 pF
τ	9·0919 $\times 10^{-8}$	9·0918 $\times 10^{-8}$	9·0919 $\times 10^{-8}$

note for amplifiers : $\alpha = 10^{-5}$ $f_T = 3\cdot5$ MHz

Fig. 7.20 Component values for the S.B.I.s in the active bandpass filter

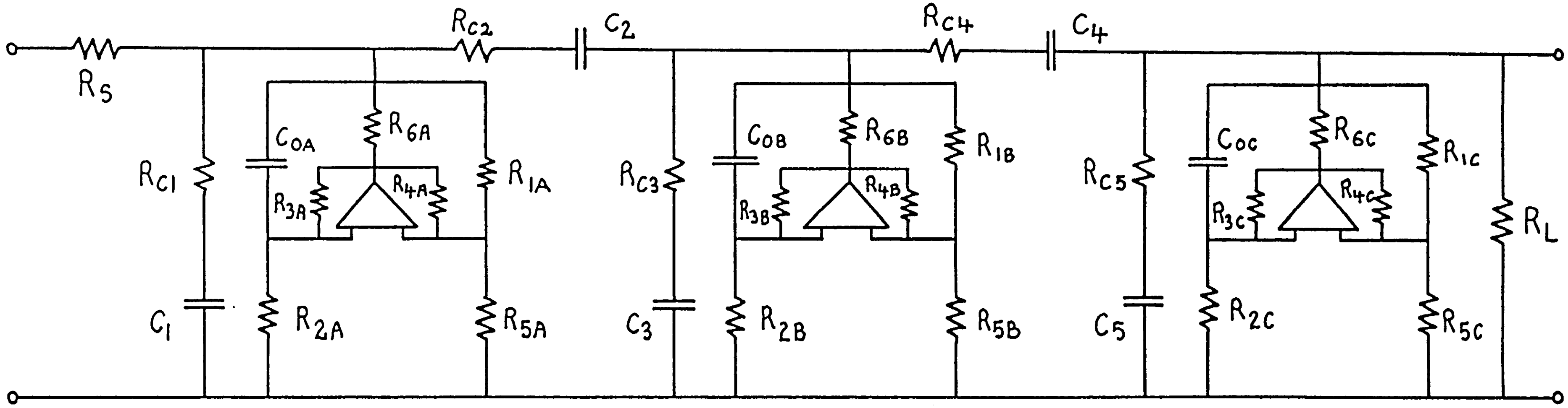

component	value	"	"	"	"	"	"
R_S, R_L	30.0000 kΩ	R_{2B}	100.000 kΩ	R_{4C}	1.98229 kΩ	C_1	16.2159 nF
R_{1A}	1.99920 "	R_{3B}	101.133 "	R_{5C}	100.000 "	C_2	640.068 pF
R_{2A}	100.000 "	R_{4B}	2.02061 "	R_{6C}	1.23452 "	C_3	15.5860 nF
R_{3A}	101.112 "	R_{5B}	100.000 "	R_{C1}	5.60677 Ω	C_4	640.068 pF
R_{4A}	1.98190 "	R_{6B}	1.25849 "	R_{C2}	142.046 "	C_5	16.2097 nF
R_{5A}	100.000 "	R_{1C}	1.99960 "	R_{C3}	5.83337 "	C_{OA}	310.538 pF
R_{6A}	1.23426 "	R_{2C}	100.000 "	R_{C4}	142.046 "	C_{OB}	304.426 "
R_{1B}	2.03860 "	R_{3C}	101.112 "	R_{C5}	5.60892 "	C_{OC}	310.479 "

for amplifiers : $\alpha = 10^{-5}$, $f_T = 3.5$ MHz

Fig. 7.21 and 7.22 Active bandpass filter and component values

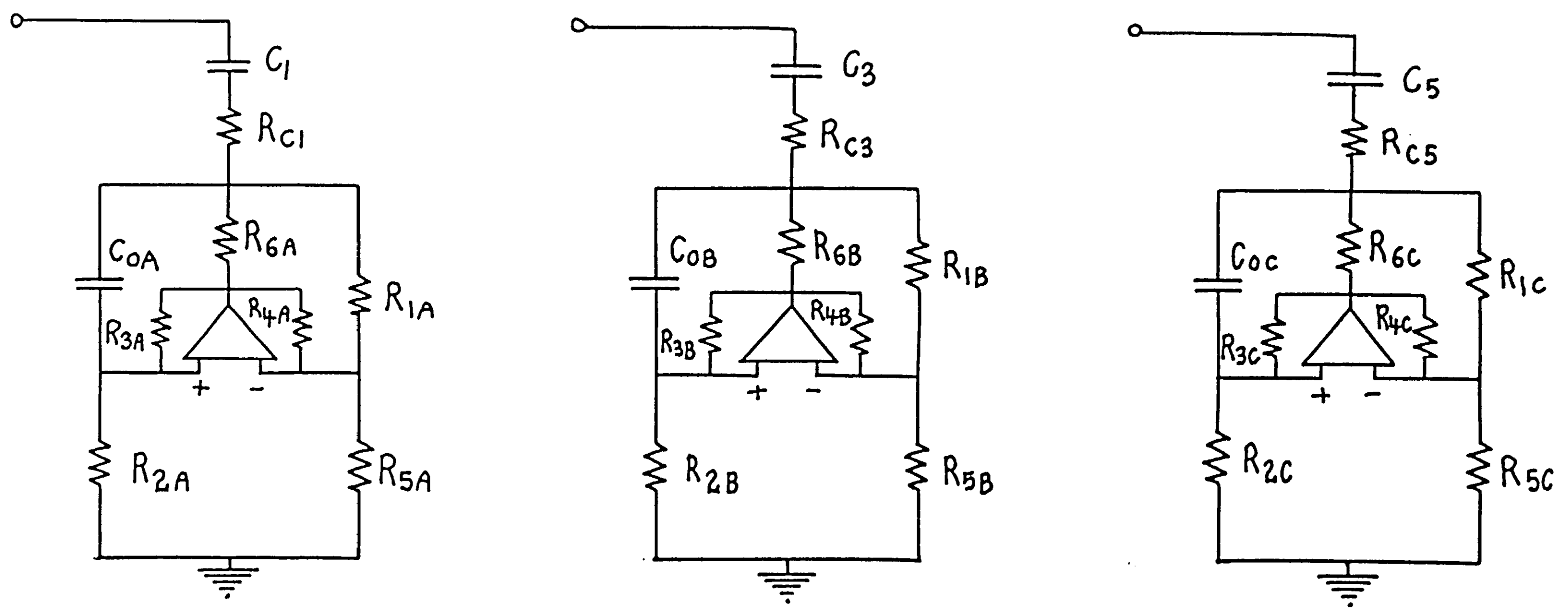

Fig. 7.23   Series resonator circuits for adjustment purposes

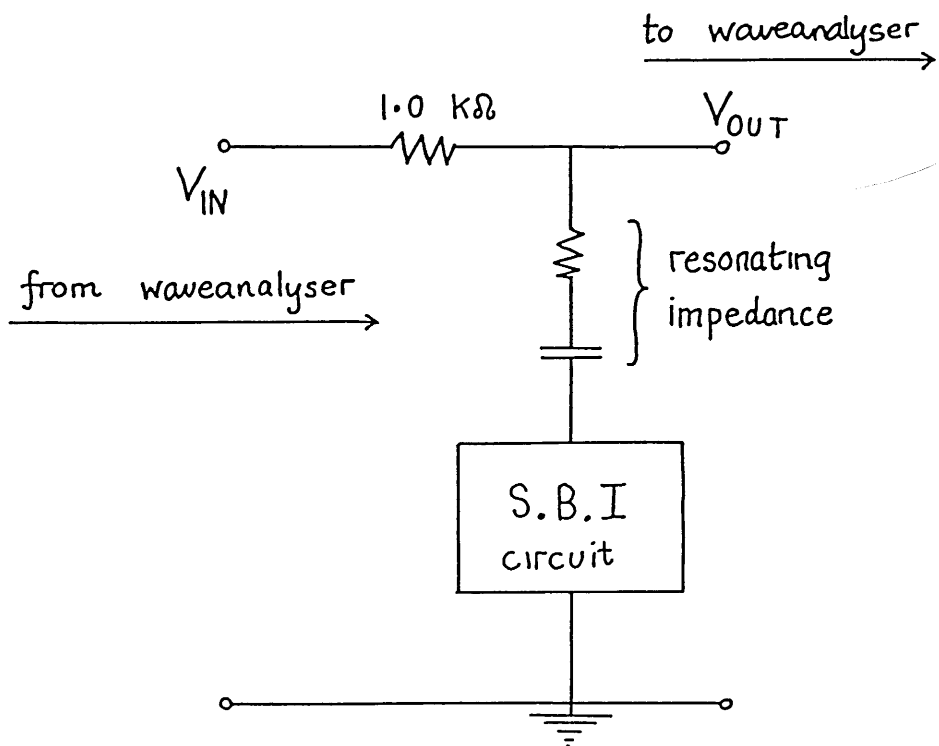

Fig. 7.24 Measuring setup for adjusting the series resonators

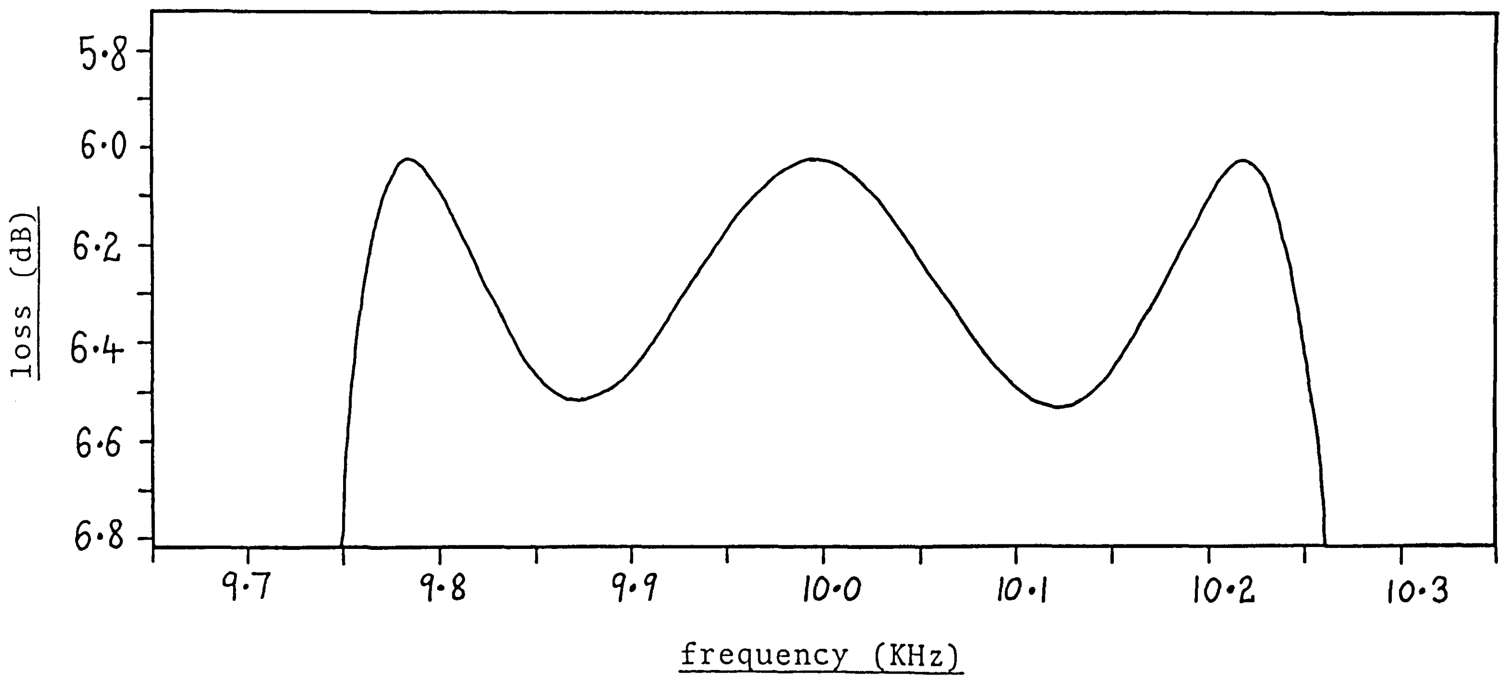

Fig. 7.25 (a) Computed passband response for the active bandpass filter

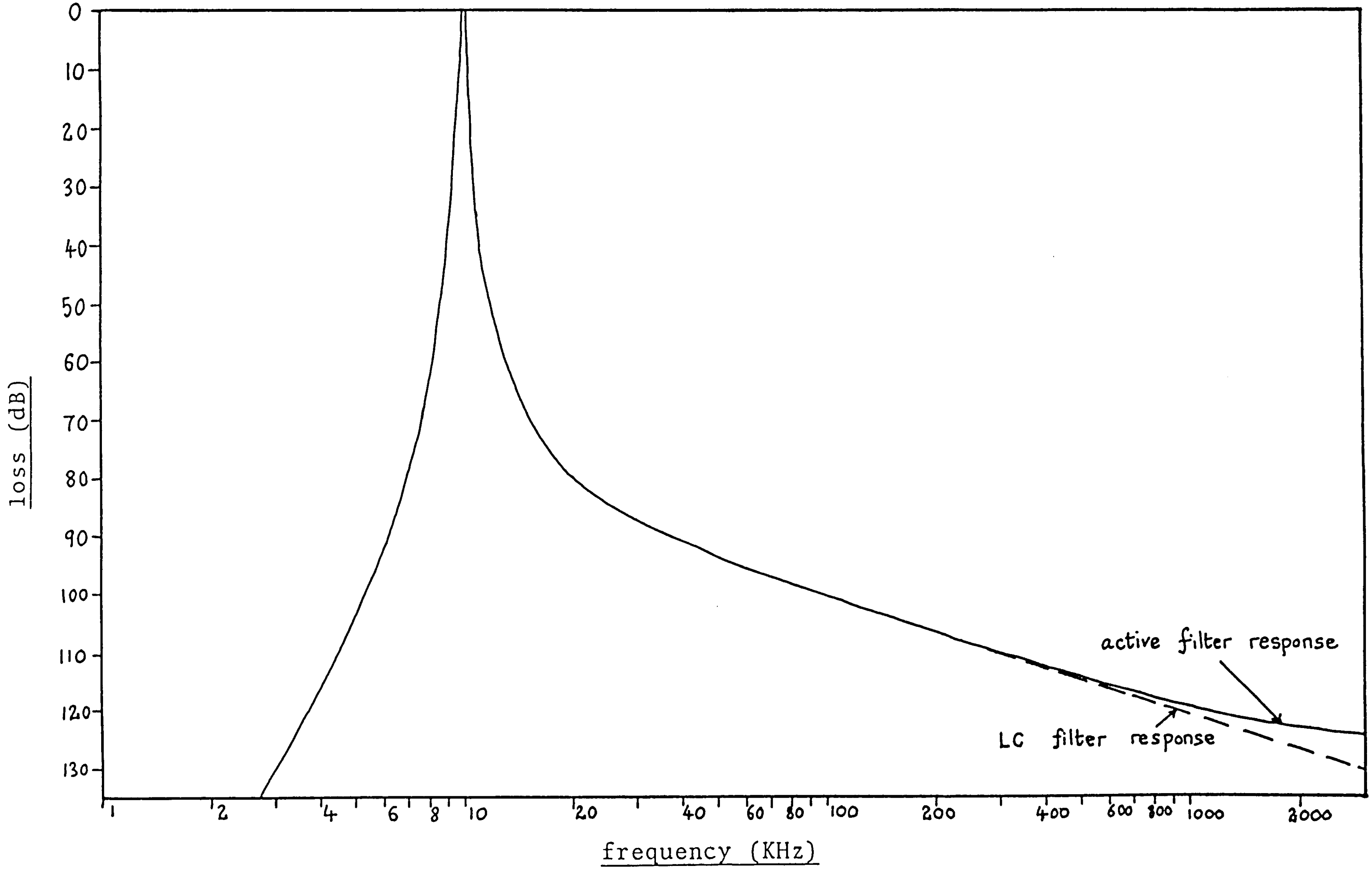

Fig. 7.25 (b) Computed stopband response for the active bandpass filter

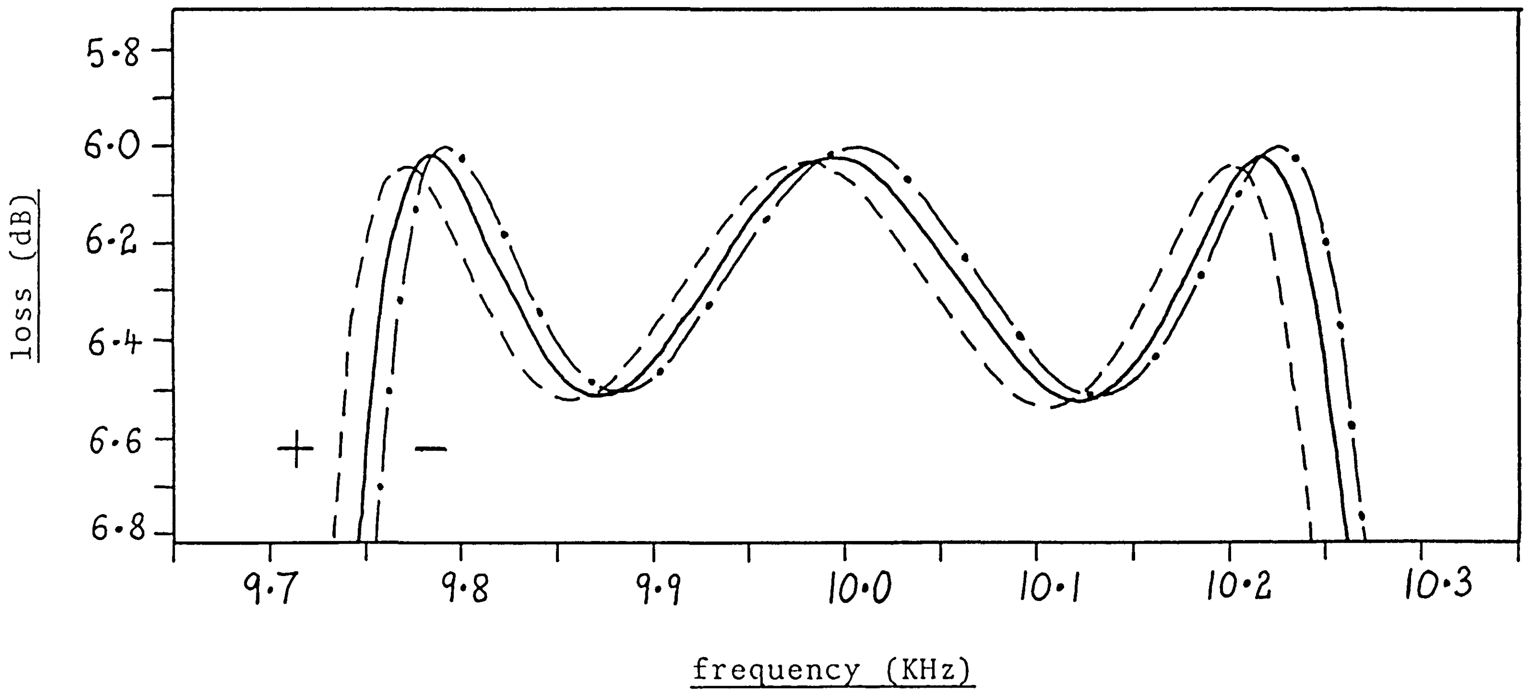

Fig. 7.26 Computed effects of ± 20.0 % simultaneous changes in the f_T values for the amplifiers

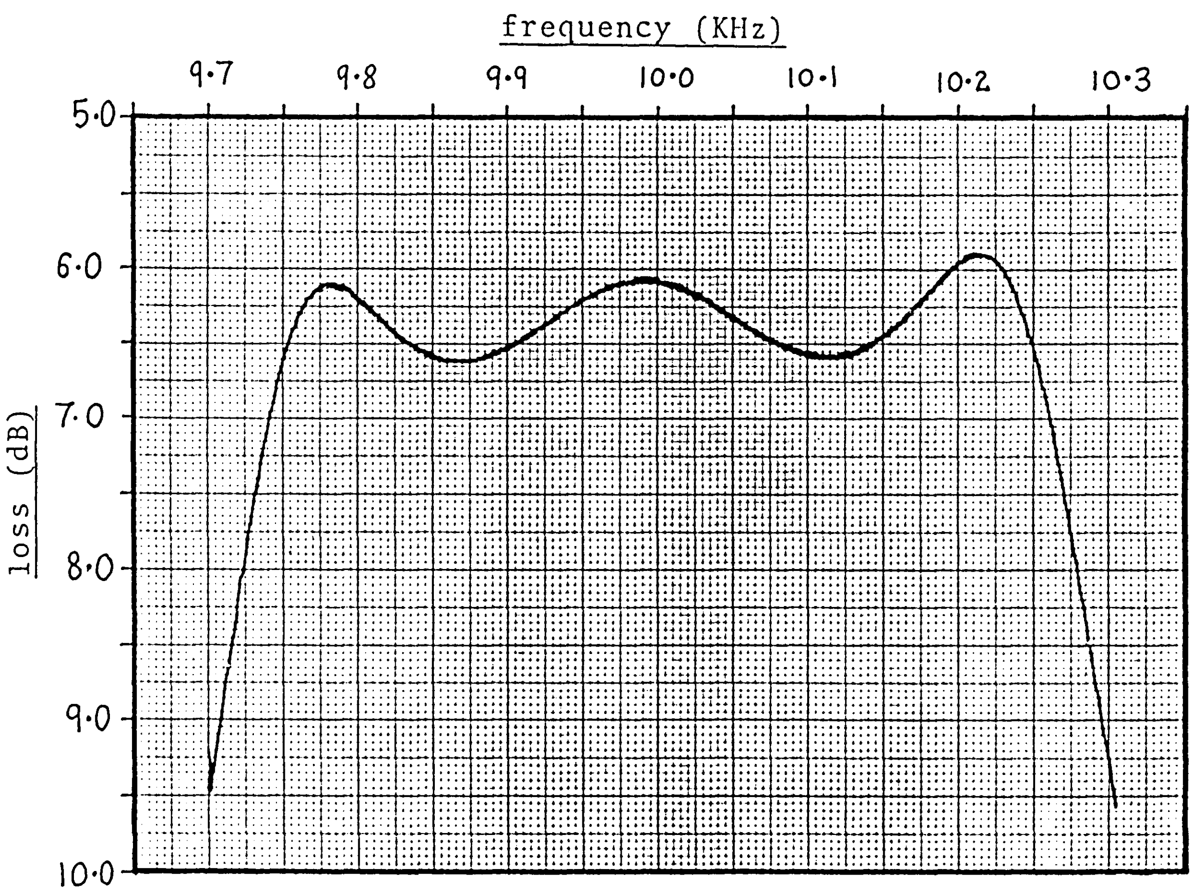

Fig. 7.27 (a) Measured passband response for active bandpass filter

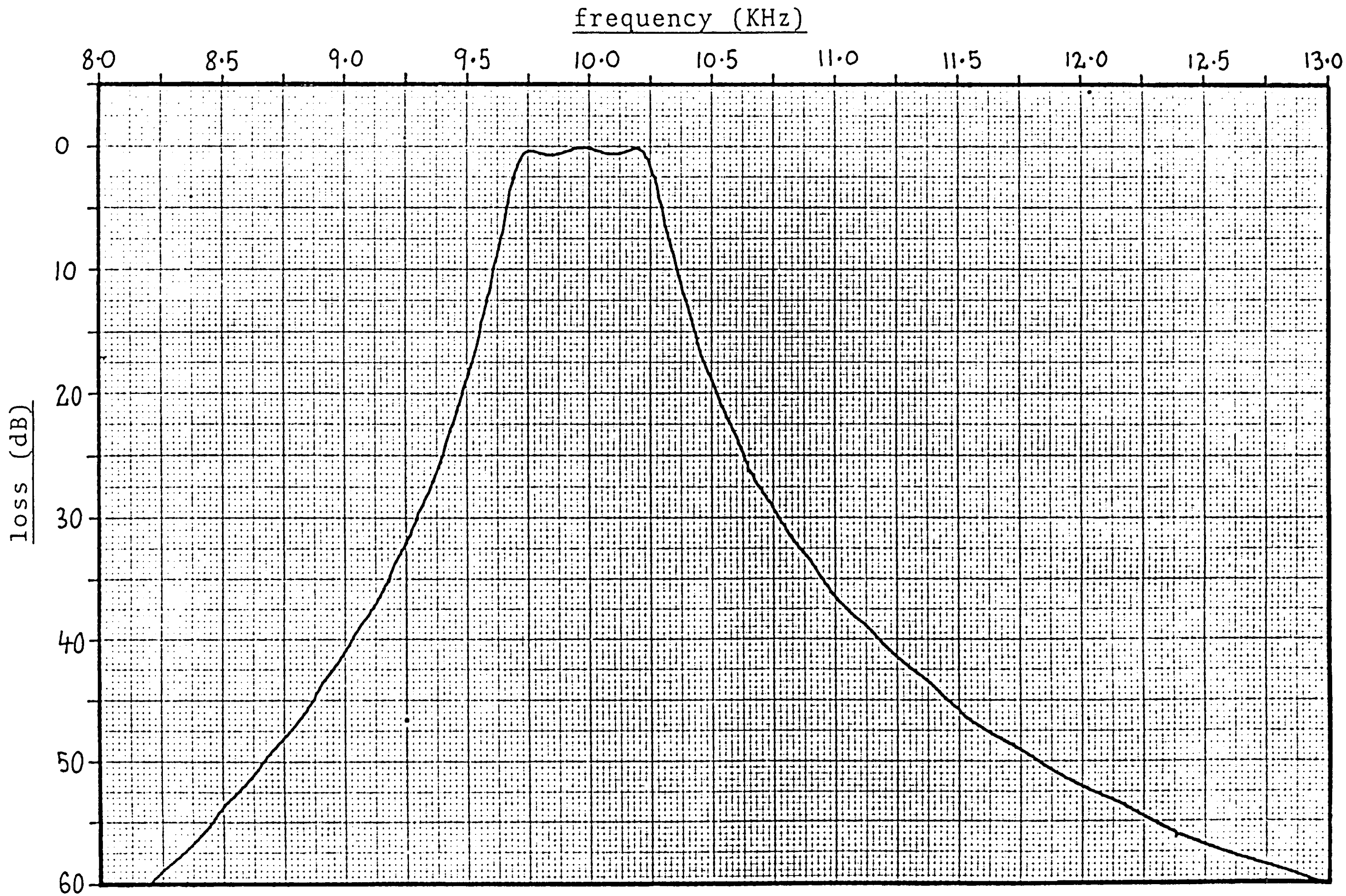

Fig. 7.27 (b) Measured stopband response for active bandpass filter

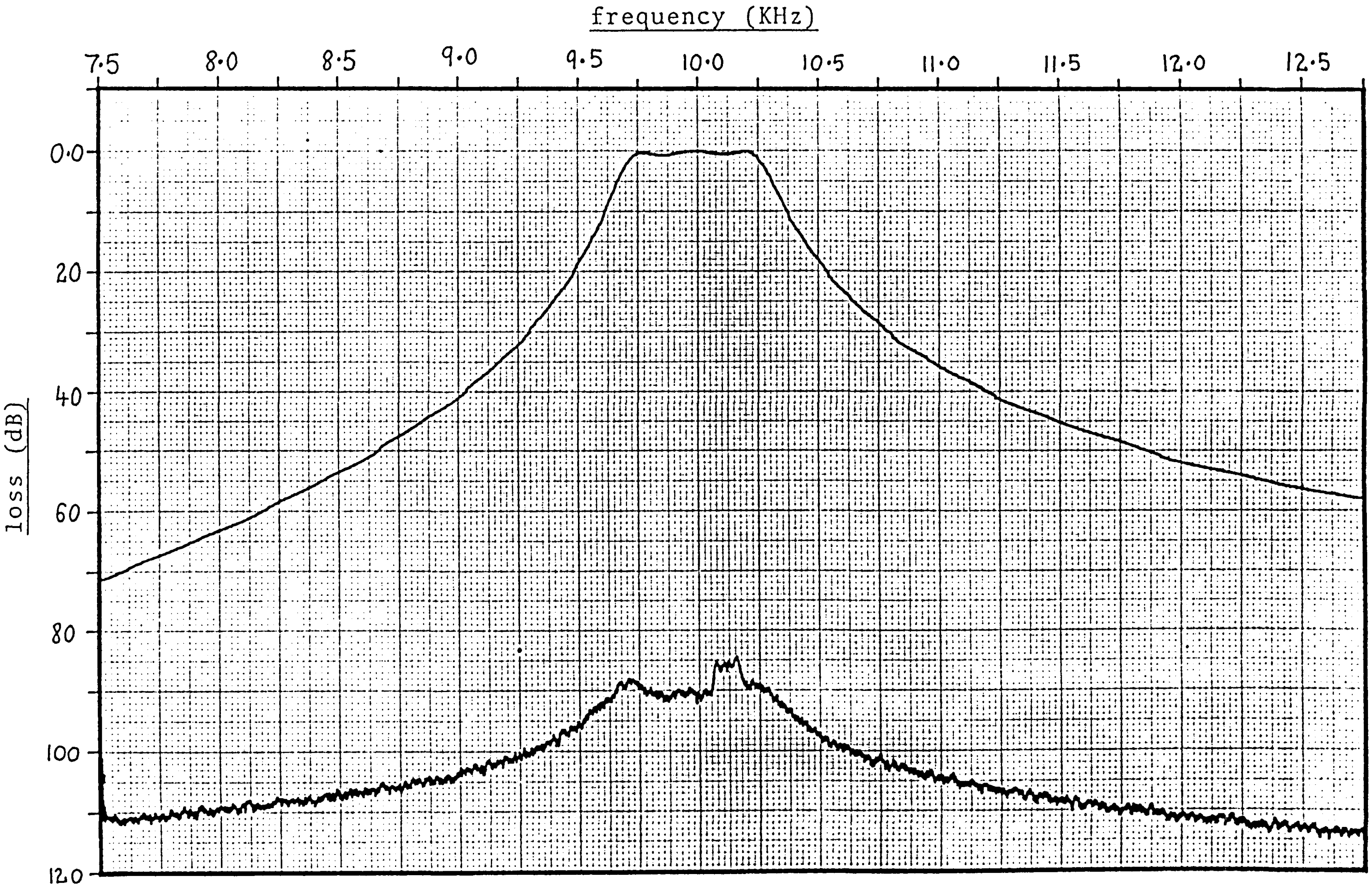

Fig. 7.28 (a) Noise level for measurement bandwidth of 100 Hz

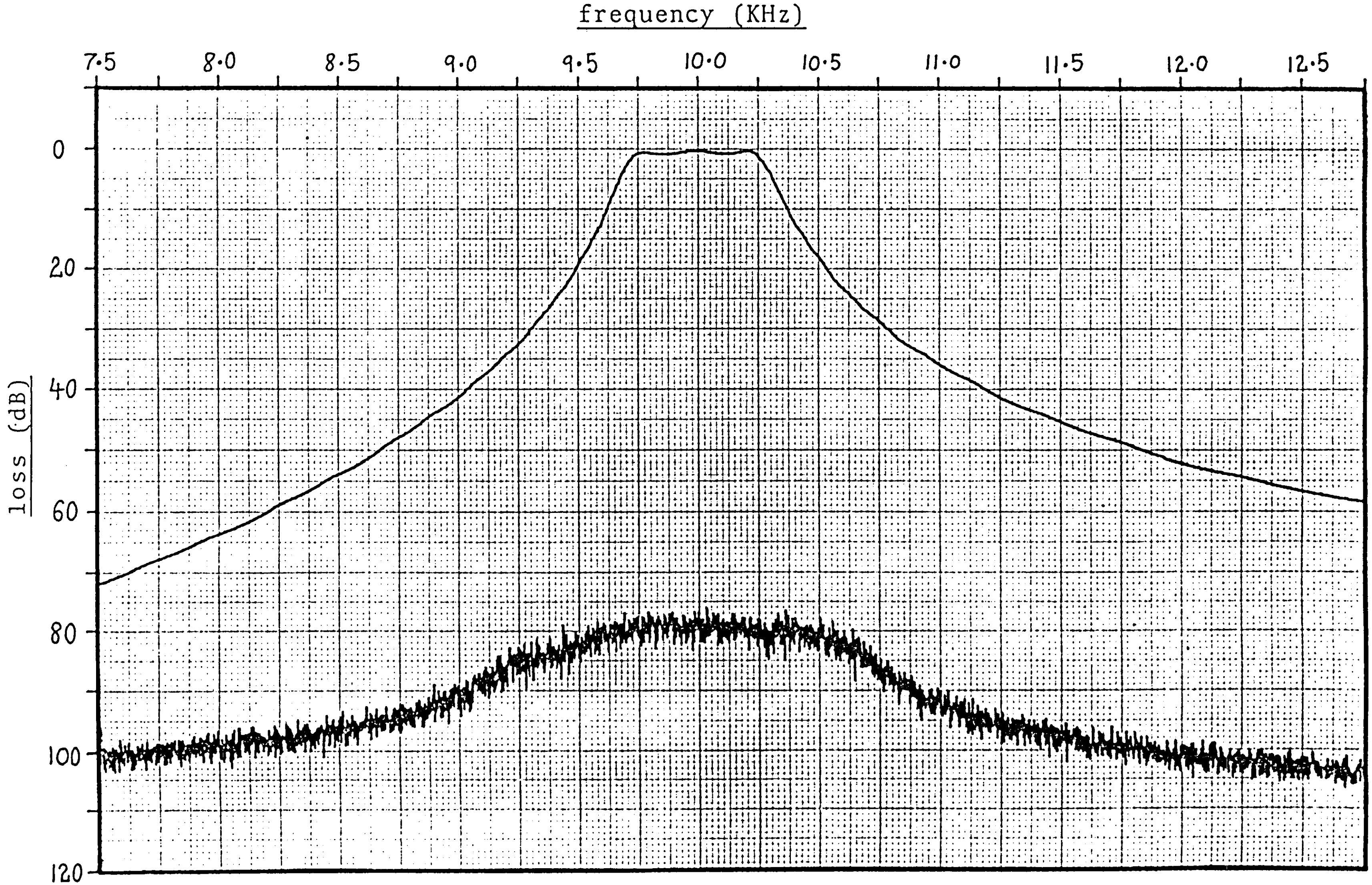

Fig. 7.28 (b) Noise level for measurement bandwidth of 1000 Hz

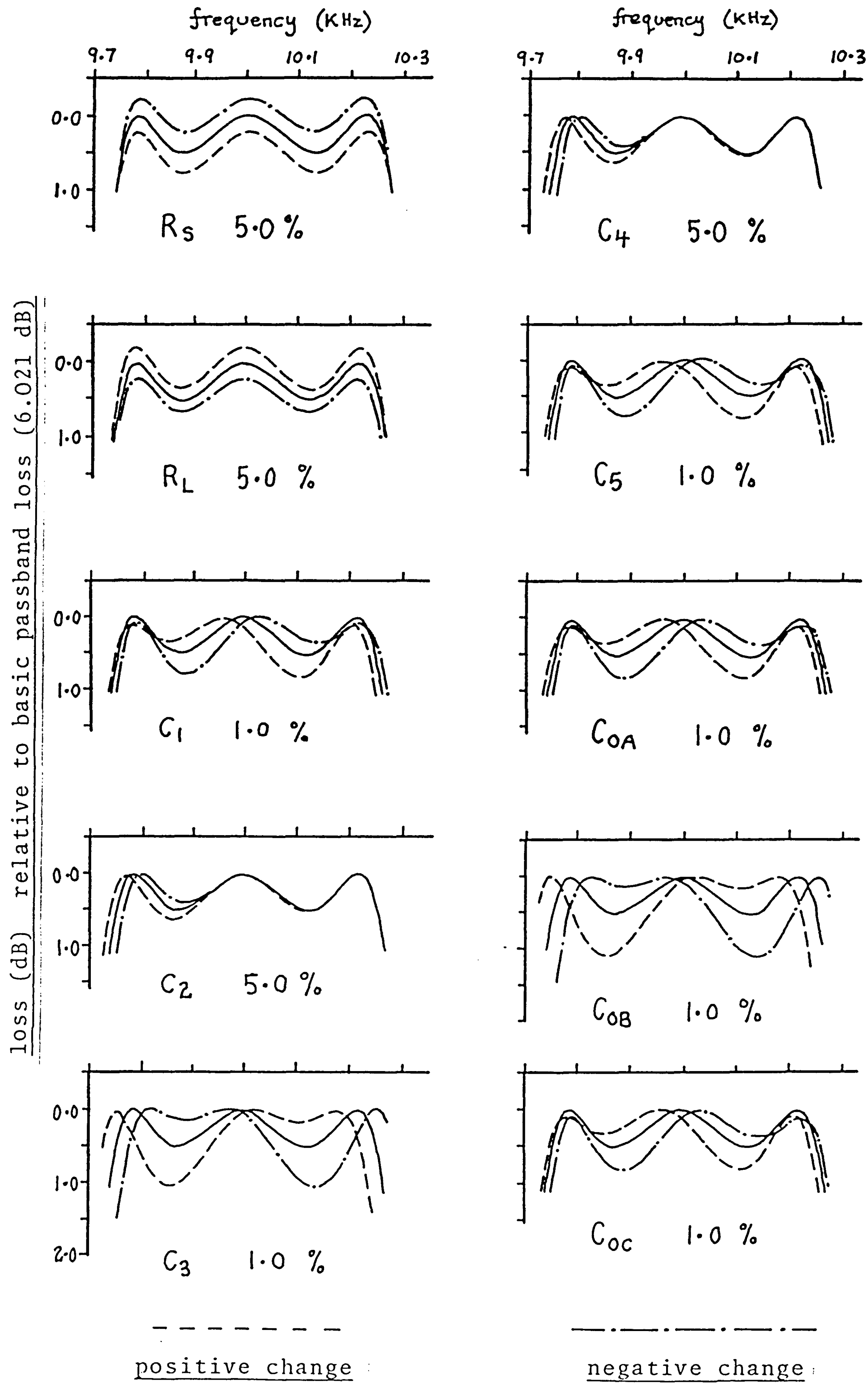

Fig. 7.29 (a) Sensitivity investigation for active bandpass filter

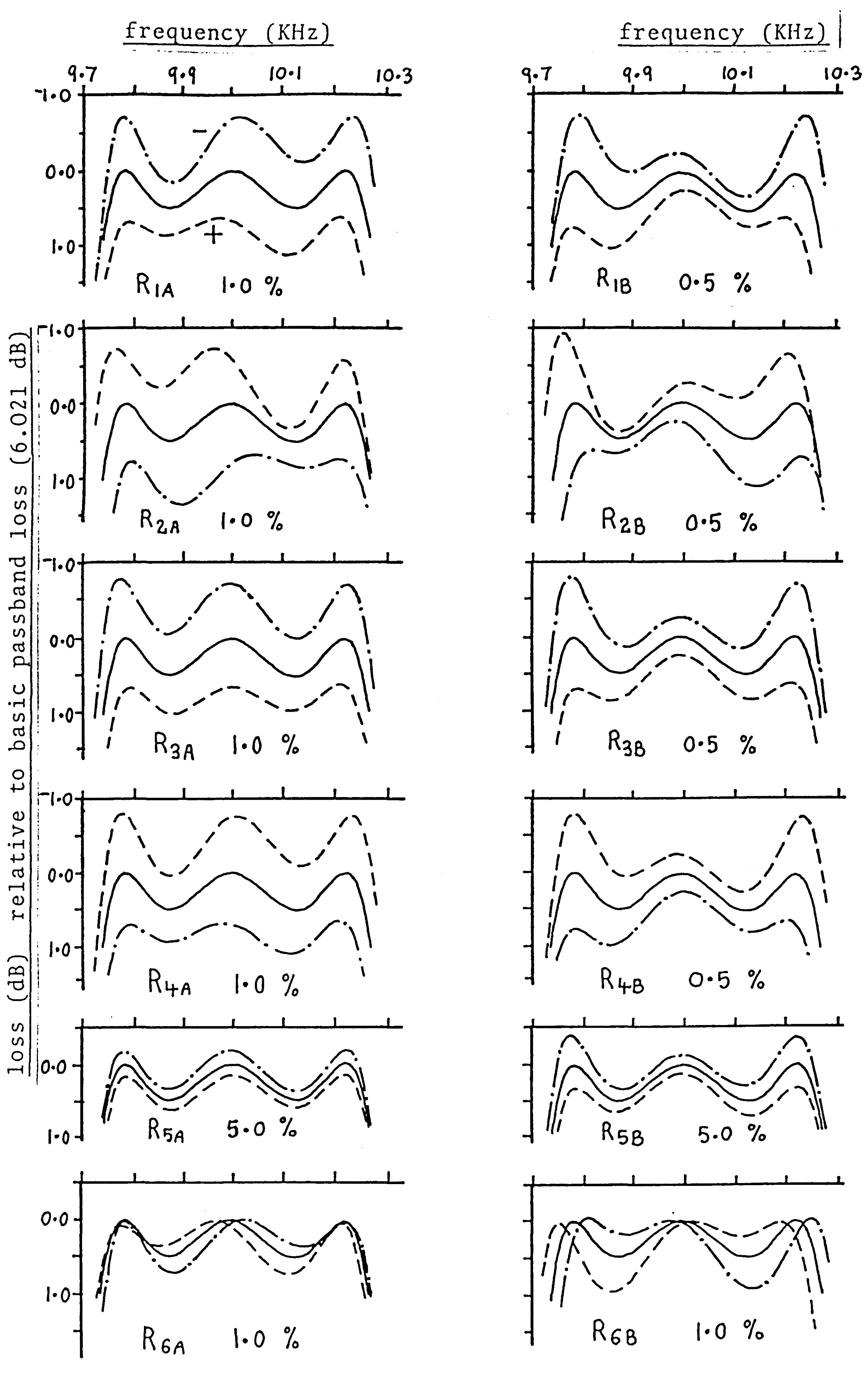

Fig. 7.29 (b) Sensitivity investigation for active bandpass filter

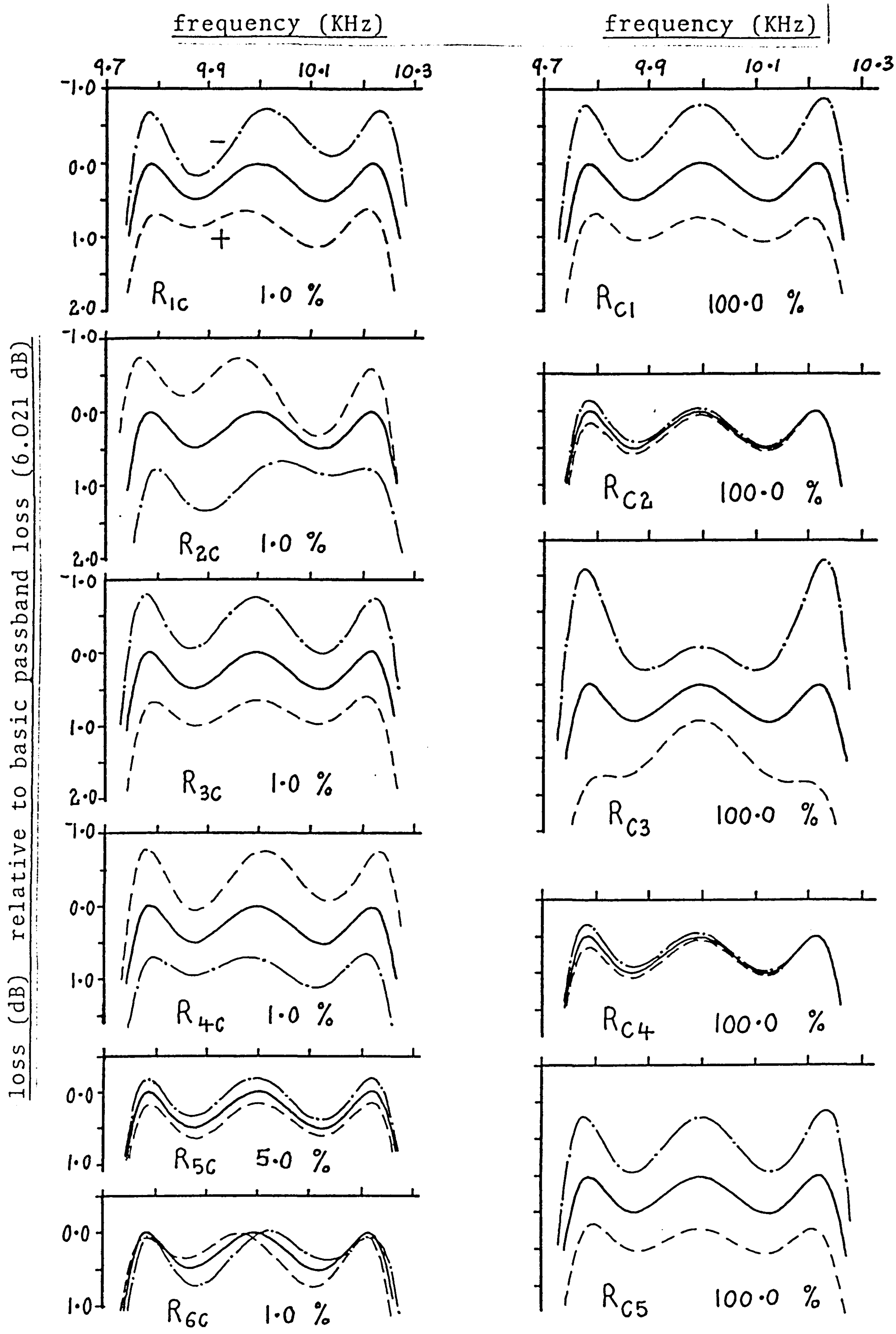

Fig. 7.29 (c) Sensitivity investigation for active bandpass filter

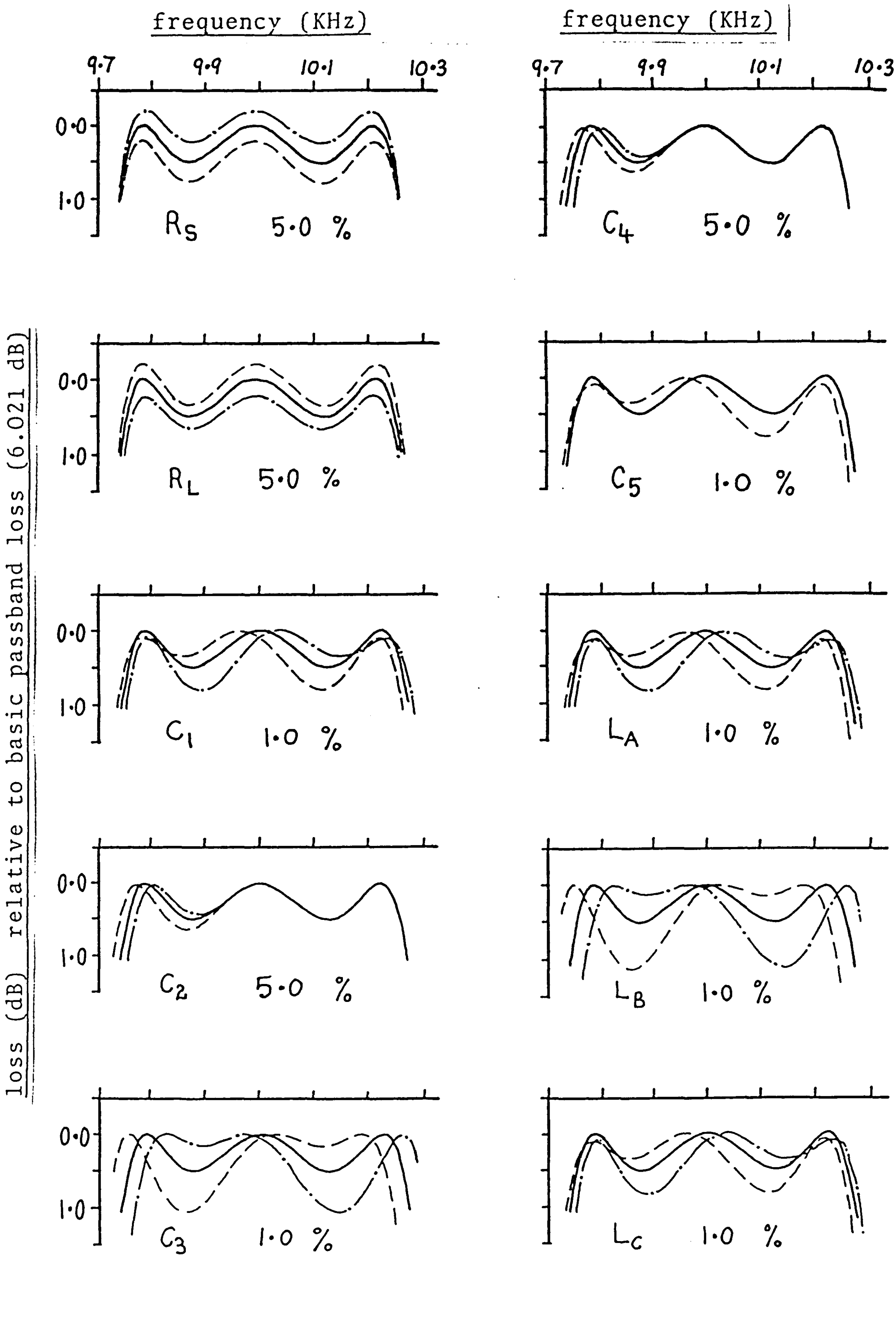

Fig. 7.30 Sensitivity investigation for passive LC bandpass filter

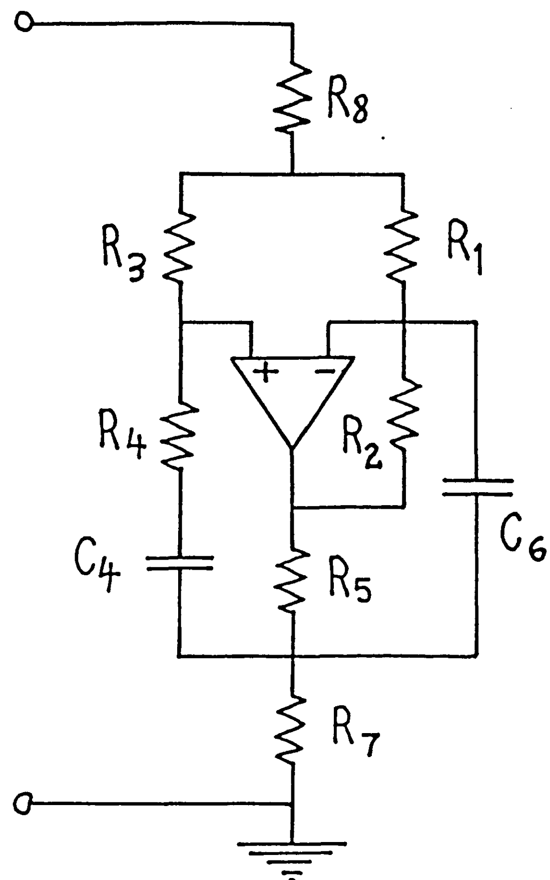

Fig. 8.1 Cheng/Lim circuit (Z = pL + 1/pC)

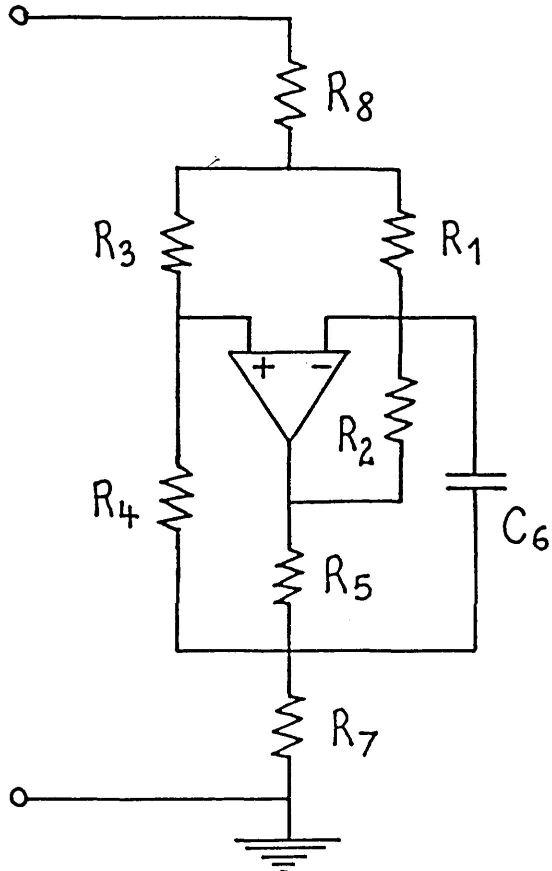

Fig. 8.2 New simulated inductor circuit

circuit	no. of amps.	no. of caps.	coeff. cancells.	pole/zero cancells.
Saraga (pL)	1	3	2	1
Sipress (pL)	1	2	2	1
Orchard/Willson (pL)	1	1	2	0
Schmidt/Lee (pL)	1	1	2	0
Cheng/Lim ($pL + 1/pC$)	1	2	1	0
Two-amp. (pL)	2	1	0	0
New S.I. circuit (pL)	1	1	1	0

Schmidt/Lee (Mp^2)	1	2	4	0
Schmidt/Lee (K/p^2)	1	2	3	0
Saraga (K/p^2)	1	3	2	1
Schmidt/Lee ($R + K/p^2$)	1	2	2	0
Cheng/Lim ($R + K/p^2$)	1	2	1	0
Two-amp. (K/p^2, Mp^2)	2	2	0	0

Fig. 8.3 Final classification of the single-amplifier simulation networks